

Aus dem  
Department für Anatomie Tübingen  
Klinische Anatomie und Zellanalytik

**The influence of two PAX7 splice variants on WNT  
signaling activity during embryonic development in the  
chicken midbrain.**

**Inaugural-Dissertation  
zur Erlangung des Doktorgrades  
der Medizin**

**der Medizinischen Fakultät  
der Eberhard Karls Universität  
zu Tübingen**

**vorgelegt von  
Neukum, Max Peter  
2026**

Dekanin: Professorin Dr. S. Y. Brucker

1. Berichterstatter: Professor. Dr. S. Liebau

2. Berichterstatter: Professor Dr. H. Lerche

Tag der Disputation: 06.03.2026

# I. Table of Contents

<b>I. TABLE OF CONTENTS</b>	<b>III</b>
<b>II. LIST OF FIGURES</b>	<b>IX</b>
<b>III. LIST OF TABLES</b>	<b>XII</b>
<b>IV. ABBREVIATIONS</b>	<b>XIV</b>
<b>V. ABSTRACT</b>	<b>XVI</b>
<b>1 INTRODUCTION</b>	<b>1</b>
<b>1.1 Chicken Development</b>	<b>1</b>
1.1.1 Early Chicken Development	1
1.1.2 Early CNS Formation	2
1.1.3 CNS Patterning	3
<b>1.2 PAX7 and PAX Gene Family</b>	<b>5</b>
<b>1.3 Wnt Signaling Pathway</b>	<b>8</b>
<b>1.4 HES Genes</b>	<b>10</b>
<b>1.5 Aim of the Project</b>	<b>12</b>
<b>2 MATERIALS</b>	<b>14</b>
<b>2.1 The Chicken as a Model Organism</b>	<b>14</b>
<b>2.2 Plasmids</b>	<b>15</b>
<b>2.3 Oligonucleotides</b>	<b>16</b>
<b>2.4 Antibodies</b>	<b>20</b>
<b>2.5 Bacterial Strains</b>	<b>21</b>
<b>2.6 Chemicals</b>	<b>21</b>
<b>2.7 Solutions</b>	<b>23</b>
2.7.1 Solutions for Bacteria Culture	23
2.7.2 Solutions for Electroporation	23
2.7.3 Solutions for Electrophoresis	24
2.7.4 Solutions for Western Blots	25
2.7.5 Solutions for Immunohistochemistry	27
<b>2.8 Enzymes</b>	<b>28</b>
<b>2.9 Kits and Master Mixes</b>	<b>28</b>

<b>2.10</b>	<b>Instruments and Consumables</b>	<b>29</b>
<b>2.11</b>	<b>Devices</b>	<b>30</b>
<b>2.12</b>	<b>Software</b>	<b>31</b>
<b>2.13</b>	<b>Online Tools and Software</b>	<b>32</b>
<b>2.14</b>	<b>Outside Services</b>	<b>32</b>
<b>3</b>	<b>METHODS</b>	<b>33</b>
<b>3.1</b>	<b>Plasmid Generation</b>	<b>33</b>
3.1.1	siRNA Sequence Selection	33
3.1.2	pSilencer1.0 Plasmid Digest	33
3.1.3	Agarose Gel Electrophoresis	34
3.1.4	Plasmid Dephosphorylation	35
3.1.5	siPAX7 Insert Phosphorylation	35
3.1.6	Ligation	36
3.1.7	Transformation	37
3.1.8	Colony PCR	37
3.1.9	Mini Preparation Plasmid Isolation	38
3.1.10	Glycerol Cryo Stocks	38
3.1.11	Midi Preparation Plasmid Isolation	39
3.1.12	DNA Concentration	39
<b>3.2</b>	<b>In-ovo Electroporation</b>	<b>40</b>
3.2.1	Embryo Staging and Egg Preparation	40
3.2.2	Electroporation	40
3.2.3	Tissue Preparation	41
3.2.4	TOP-dGFP Expression	41
3.2.5	Cell Counting for TOP-dGFP Experiments	42
<b>3.3</b>	<b>cDNA, RNA and Protein Isolation</b>	<b>42</b>
3.3.1	Isolations from Pooled Embryos	43
3.3.1.1	Phenol-Chloroform Protein Isolation	43
3.3.1.2	Phenol-Chloroform RNA Isolation	44
3.3.1.3	cDNA Synthesis	44
3.3.2	cDNA Synthesis Using the SyperScript IV CellsDirect Kit	45
3.3.3	QIAxcel Capillary Electrophoresis	46
<b>3.4</b>	<b>Quantitative Real-Time Polymerase Chain Reaction</b>	<b>46</b>

3.4.1 qPCR Primer Design and Validation	48
3.4.1.1 Primer Design	48
3.4.1.2 Primer Validation	49
3.4.2 Gene Expression Analysis	51
3.4.2.1 qPCR Using StepOne Plus Cyclers	52
3.4.2.2 qPCR Using Biomark	52
3.4.2.2.1 Pre-amplification	52
3.4.2.2.2 Exonuclease Digest	53
3.4.2.2.3 Chip Loading and Cycling	54
3.4.3 Data Analysis	54
3.4.3.1 Primer Efficiency Calculation	55
3.4.3.2 Comparative Expression Analysis	55
3.4.3.3 Statistical Analysis	56
3.4.3.4 RIN-Analysis	57
<b>3.5 Western Blot</b>	<b>57</b>
3.5.1 SDS-PAGE	58
3.5.2 Semi-Dry Blotting	58
3.5.3 Antibody Staining	59
3.5.4 Antibody Stripping	60
3.5.5 Whole Protein Stain	60
3.5.6 Image Analysis	60
3.5.7 Validation of Antibodies	61
<b>3.6 Cryosections, Immunohistochemistry and Microscopy</b>	<b>61</b>
3.6.1 Cryosections	61
3.6.2 Immunohistochemistry	62
3.6.3 Confocal Laser Scan Microscopy	62
3.6.4 Apotome Microscopy	63
3.6.5 Binocular Fluorescence Microscopy	63
<b>4 RESULTS</b>	<b>64</b>
<b>4.1 Wnt Signaling in Midbrain in Vivo</b>	<b>64</b>
4.1.1 Quantification of Canonical Wnt Signaling in Vivo Using Automated Cell Counting	66
4.1.2 Quantification of Canonical Wnt Signaling in Vivo by Manual Image Analysis	67
<b>4.2 Detecting PAX7 and Wnt Signaling on RNA Level Using qPCR</b>	<b>69</b>

4.2.1 qPCR Validation and Sample Preparation	70
4.2.1.1 RNA Isolation and cDNA Synthesis	70
4.2.1.1.1 cDNA Synthesis for Chip-Based qPCR	70
4.2.1.1.2 RNA Isolation and cDNA Synthesis for Well-Based qPCR	75
4.2.1.2 Quality Control	76
4.2.1.2.1 Good Sample Integrity for Chip-Based qPCR	76
4.2.1.2.2 Suboptimal RNA Integrity for Pooled Embryo Samples	76
4.2.1.3 Primer Validation	78
4.2.1.3.1 Primers Show Specific Amplification	78
4.2.1.3.2 PAX7 Primers Amplify Splice-Variants Specifically	80
4.2.1.3.3 Primers for Pooled-Embryo qPCR Have Good Efficiency	81
4.2.1.3.4 Primers for Single Embryo Analysis Have too High Efficiency	82
4.2.2 Short TA Splice Variant of PAX7 is Dominant in the Midbrain	85
4.2.3 ddCq Expression Analysis of Pooled Embryos	87
4.2.3.1 qPCR Quality	88
4.2.3.2 Reference Gene Expression Unaffected by Electroporations	89
4.2.3.3 PAX7 Expression Modifications Do Not Cause Expected Changes in PAX7 Expression	91
4.2.3.3.1 Midbrain	91
4.2.3.3.2 Hindbrain	94
4.2.3.3.3 Summary of PAX7 Expression Changes	96
4.2.3.4 PAX7 Knock-Down Does Not Reduce Wnt Signaling on an RNA Level	96
4.2.3.4.1 Midbrain	97
4.2.3.4.2 Hindbrain	100
4.2.3.4.3 LiCl Positive Control	102
4.2.3.4.4 Summary of Wnt Signaling Component Expression Changes	103
4.2.3.5 Effect of PAX7 Expression Modifications on CCND1 Expression	104
4.2.3.5.1 Midbrain at HH Stage 17	104
4.2.3.5.2 Mid- and Hindbrain at HH Stage 14	105
4.2.3.5.3 Hindbrain at HH Stage 17	105
4.2.3.6 Summary of Pooled Tissue qPCR	106
4.2.4 ddCq Expression Analysis of Tissue from Single Embryos	107
4.2.4.1 Disclaimer and Summary	108
4.2.4.2 Technical Summary and qPCR Performance	108
4.2.4.3 Reference Genes	109

4.2.4.4	PAX7 and PAX3 Expression Not Affected by siPAX7-pSilencer1.0	110
4.2.4.5	Expression of Wnt Signaling Pathway Components Not Affected by siPAX7-pSilencer1.0	112
4.4.6.4	Frizzled Receptor Expression Not Affected by siPAX7-pSilencer1.0	114
4.2.4.6	Expression of other Genes Active in Proliferating Cells Not Affected by siPAX7-pSilencer1.0	116
4.2.4.7	Potential siPAX7-pSilencer1.0 off-Target Genes Expression Not Affected by siPAX7-pSilencer1.0	118
<b>4.3</b>	<b>Detecting PAX7 and Wnt Signaling on Protein Level using Western Blot</b>	<b>120</b>
4.3.1	Difficulties	120
4.3.2	Validation of Antibodies for Western Blot	121
4.3.3	Expression Analysis	122
4.3.3.1	Summary	122
4.3.3.2	Whole Protein Stain	123
4.3.3.3	Quantification of PAX7 Expression and Canonical Wnt Signaling on a Protein Level	125
<b>4.4</b>	<b>New siRNA Constructs for PAX7</b>	<b>129</b>
4.4.1	Generation of New siPAX7 Plasmids	129
4.4.2	Size Reduction Caused by PAX7 Knock-Down	130
<b>4.5</b>	<b>Antibody Testing for IHC</b>	<b>131</b>
4.5.1	Detecting Canonical Wnt Signaling with IHC	131
4.5.2	Detecting HES Genes Using IHC	132
<b>5</b>	<b>DISCUSSION</b>	<b>134</b>
<b>5.1</b>	<b>Impact of PAX7 Targeting Transfections in Vivo</b>	<b>134</b>
5.1.1	PAX7 is Required for Canonical Wnt Signaling in Vivo	134
5.1.2	The Effects of the New siPAX7 Constructs Are Comparable to Old PAX7 Knock-Down in Vivo	136
<b>5.2</b>	<b>Detection of Wnt Signaling on a Protein Level</b>	<b>137</b>
5.2.1	Detection of Wnt Signaling in Cryosections	137
5.2.2	Detection of PAX7 and Canonical Wnt Signaling Using Western Blot	137
<b>5.3</b>	<b>Influence of PAX7 Transfections on Gene Expression on an RNA Level</b>	<b>139</b>

5.3.1 RNA Isolation for qPCR	140
5.3.1.1 RNA from Pooled Brain Tissue	140
5.3.1.2 RNA Isolation from Single Midbrain Halves	140
5.3.2 Primer Validation for qPCR	141
5.3.3 qPCR from pooled Brain Tissue	143
5.3.3.1 Reference Gene Expression Stability	143
5.3.3.2 PAX7 Expression in Wildtype Midbrain Tissue	143
5.3.3.3 Gene Expression Changes in Transfected Tissue	144
5.3.3.3.1 Pooled Tissue from Dorsal Midbrain	147
5.3.3.3.2 Hindbrain	149
5.3.4 Single Midbrain Tissue qPCR	149
<b>5.4 In-ovo Electroporation</b>	<b>150</b>
<b>6 CONCLUSION AND OUTLOOK</b>	<b>153</b>
<b>6.1 Zusammenfassung und Perspektiven</b>	<b>155</b>
<b>7 ERKLÄRUNG ZUM EIGENANTEIL</b>	<b>158</b>
<b>8 REFERENCES</b>	<b>159</b>
<b>9 APPENDIX</b>	<b>167</b>
<b>9.1 Canonical Wnt Signaling in Vivo</b>	<b>167</b>
<b>9.2 Detailed qPCR Results</b>	<b>169</b>
<b>9.3 Protein Expression Analysis</b>	<b>210</b>

## II. List of Figures

Figure 1-1: Structural elements of PAX genes in the human.	6
Figure 1-2: Overview of the three main Wnt signaling pathways.	9
Figure 3-1: Sequence used for siPAX7-pSilencer1.0 cloning.	33
Figure 3-2: Schematic drawing of a PCR reaction.	46
Figure 3-3: Schematic example of signal curves from qPCR.	47
Figure 4-1: Canonical Wnt signaling can be detected in vivo in the dorsal midbrain at HH stage 17 and is influenced by PAX7 knock-down.	65
Figure 4-2: PAX7 expression modifications did not affect canonical Wnt signaling in the midbrain, when images are analyzed automatically.	66
Figure 4-3: PAX7 expression modifications did not affect canonical Wnt signaling in the midbrain, when images are analyzed automatically.	67
Figure 4-4: gDNA contamination in cDNA isolated using the CellsDirect kit.	71
Figure 4-5: Mechanic lysis reduces gDNA contamination.	71
Figure 4-6: High differences in cDNA concentration between samples.	72
Figure 4-7: Samples used for final chip-based qPCR have similar cDNA concentrations.	73
Figure 4-8: Most samples for the final Biomark run contain cDNA.	74
Figure 4-9: Similar cDNA concentrations in samples used for final chip-based qPCR.	75
Figure 4-11: Exon-skipping primers are specific and cDNA selective.	79
Figure 4-10: The ES60PAX3-2 amplifies the intended PAX3 target gene.	79
Figure 4-12: Exon-skipping primers are specific and cDNA selective.	79
Figure 4-13: Exon-skipping primers are specific and cDNA selective.	80
Figure 4-14 PAX7 splice variant specific primers have off-target amplicons in the PAX7 gene.	81
Figure 4-15: Primers for pooled embryo qPCR show good efficiency.	82
Figure 4-16: Expression of PAX7 trans activation domain splice variants in the midbrain of wildtype chicken embryos between HH stage 17 and HH38.	87
Figure 4-17: Singular amplicon detected in all qPCRs, exemplary shown for qPCR from HH stage 17 midbrain tissue, electroporated with the pCAX plasmid.	88
Figure 4-18: qPCR quality control for samples with unexpected amplification curve shows only expected amplicon.	88
Figure 4-19: Low RNA input likely caused false reference gene expression measurements.	91
Figure 4-20: Only overexpression of the long PAX7 splice variant resulted in the expected PAX7 expression changes.	93
Figure 4-21: Overexpression of the short PAX7 splice variant greatly reduces PAX7 expression in the midbrain at HH stage 14.	94
Figure 4-22: PAX7 expression at HH stage 17 in the hindbrain is reduced by both PAX7 knock-down and overexpression.	95

Figure 4-23: Overexpression of the short PAX7 splice variant in the hindbrain at HH stage 14 reduces PAX7 expression.	96
Figure 4-24: The effects of PAX7 expression modifications on Wnt signaling in the midbrain are inconclusive.	99
Figure 4-25: No clear impact of PAX7 modifications on Wnt signaling in midbrains at HH stage 14.	100
Figure 4-26: Influence of PAX7 expression modifications on Wnt signaling in the hindbrain at HH stage 17.	101
Figure 4-27: Measurements of PAX7 overexpression impact on canonical Wnt signaling unusable.	102
Figure 4-28: LiCl does not show the expected increase in canonical Wnt signaling.	103
Figure 4-29: Changes in CCND1 expression at HH stage 17 in the midbrain, resulting from PAX7 expression modifications.	105
Figure 4-30: Overexpression of the short PAX7 splice variant caused strong reduction in CCND1 expression.	105
Figure 4-31: PAX7 modifications do not meaningfully impact CCND1 expression in the hindbrain.	106
Figure 4-32: PAX7 knock-down did not affect PAX3 expression.	112
Figure 4-33: PAX7 knock-down did not affect PAX7 expression.	111
Figure 4-34: PAX7 knock-down did not affect AXIN2 or CTNNB1 expression.	113
Figure 4-35: PAX7 knock-down did not affect LEF1 or WNT4 expression.	114
Figure 4-36: PAX7 knock-down did not affect FZD1 or FZD5 expression.	116
Figure 4-37: PAX7 knock-down did not affect FZD9 or FZD10 expression.	116
Figure 4-38: PAX7 knock-down did not affect NOTCH1 or HES1 expression.	117
Figure 4-39: PAX7 knock-down did not affect HES5A or HES5-like expression.	118
Figure 4-40: PAX7 knock-down did not affect HES6 or HEY1 expression.	118
Figure 4-41: PAX7 knock-down did not affect CHMP48 or ERMIN expression.	120
Figure 4-42: PAX7 knock-down did not affect MAP2 expression.	120
Figure 4-43: Good correlation between signal intensity and loaded protein.	122
Figure 4-45: Low amount of total protein loaded relative to E6 midbrain reference protein.	124
Figure 4-44: Low standard deviations in whole protein stain for protein isolated from whole body at HH stage 20.	124
Figure 4-46: PAX7 protein cannot be reliably quantified. Western blot results using the PAX7 antibody from DSHB.	127
Figure 4-47: High SDs undermine ability to draw conclusions about canonical Wnt signaling activity in HH stage 17 midbrain samples.	128
Figure 4-48: Positive control does not show expected increase in canonical Wnt signaling activity.	128
Figure 4-49: Successful recovery of the pSilencer1.0 backbone.	129

Figure 4-50: Successful ligation and transformation of new siPAX7-pSilencer1.0 constructs.	130
Figure 4-51: Successful generation of new siPAX7-pSilencer1.0 constructs.	130
Figure 4-52: IHC using the anti-active $\beta$ -catenin antibody (ABC antibody) from Upstate.	132
Figure 4-53: IHC using ant HES1 and anti HES4 antibodies on midbrain tissue.	133
Figure 5-1: The short PAX7 transactivation domain splice variant is the predominant one in the midbrain between HH stage 17 and 29.	143

### III. List of Tables

Table 1-1: Predicted isoforms of PAX7 in the chicken embryo.	8
Table 2-1 Hamburger and Hamilton stages (HH stage) of chicken development.	15
Table 2-2: List of plasmids used for electroporations.	16
Table 2-3: List of non-exon-skipping qPCR primers.	17
Table 2-4: List of exon-skipping primers for qPCR.	19
Table 2-5: List of primers used for cloning and gDNA detection.	19
Table 2-6: List of siPAX7-oligonucleotides for cloning in pSilencer1.0 plasmids.	20
Table 2-7: List of primary Antibodies.	20
Table 2-8: List of secondary antibodies.	21
Table 2-9: List of chemicals.	22
Table 2-10: List of enzymes. Enzymes included in kits are not listed separately. Manufacturer supplied buffers were used, if not specified otherwise.	28
Table 2-11: List of kits.	28
Table 2-12: List of master mixes for PCR applications.	28
Table 2-13: List of devices.	31
Table 4-1: PAX7 expression modifications did not affect canonical Wnt signaling in the midbrain, when images are analyzed automatically.	66
Table 4-2: PAX7 expression modifications did not affect canonical Wnt signaling in the midbrain, when images are analyzed automatically.	66
Table 4-3: PAX7 knockdown and enPAX7 expression reduce canonical Wnt signaling.	67
Table 4-4: Significance testing of Top-dGFP experiments.	68
Table 4-5: PAX7 knock-down reduces canonical Wnt signaling in the rhombencephalon.	69
Table 4-6: SuperScript IV CellsDirect cDNA Synthesis kit is the best kit for RNA isolation from midbrain halves.	70
Table 4-7: cDNA isolated using the CellsDirect kit also contains gDNA.	71
Table 4-8: CDNA concentration and not electroporation caused high C <sub>q</sub> variances.	73
Table 4-9: Electroporation has no impact on average reference gene expression in final Biomark run.	75
Table 4-10: Low RNA yields correlate with low RNA integrity.	77
Table 4-11: PAX7 splice variant specific primers are splice variant specific.	81
Table 4-12: Primers for pooled embryo qPCR show good efficiency.	82
Table 4-13: Too high primer efficiencies for primers used for single embryo analysis on the Biomark qPCR system.	84
Table 4-14: Preamplification process caused too high primer efficiencies.	85
Table 4-15: The short TA domain splice variant of PAX7 shows higher expression in the midbrain.	86
Table 4-16: Multiple PAX7 knock-downs in the midbrain.	87

Table 4-17: Overview of C <sub>q</sub> values, showing no impact of electroporation on reference gene expression.	90
Table 4-18: Overview of Expression Changes from PAX7 knock-downs, detected in qPCR in pooled midbrain tissue at HH stage 17.	106
Table 4-19: Overview of Expression Changes from PAX7 overexpressions, detected in qPCR in pooled midbrain tissue at HH stage 17.	107
Table 4-20: Reference gene expression in qPCR with tissue from single embryos.	110
Table 4-21: Group statistics for changes in expression (as $\Delta\Delta C_q$ -values) of PAX3 and the two PAX7 trans activation domain splice variants.	111
Table 4-22: Results from t-test for changes in expression of PAX3 and the two transactivation domain splice variants of PAX7.	111
Table 4-23: Group statistics for changes in expression (as $\Delta\Delta C_q$ -values) of canonical Wnt signaling components.	112
Table 4-24: Results from t-test for changes in expression of CTNNB1.	113
Table 4-25: Results from Mann-Whitney-U test for changes in expression of AXIN2, WNT4 and LEF1.	113
Table 4-26: FZD receptor expression. Comparison between C <sub>q</sub> -values of the control sample without reverse transcriptase in the cDNA synthesis reaction.	114
Table 4-27: Group statistics for changes in expression (as $\Delta\Delta C_q$ -values) of frizzled receptors (FZD).	115
Table 4-28: Results from t-test for changes in expression of frizzled receptors (FZD).	115
Table 4-29: Results from Mann-Whitney-U test for changes in expression of FZD9.	115
Table 4-30: Group statistics for changes in expression (as $\Delta\Delta C_q$ -values) of NOTCH 1 and multiple members of the HES gene family.	117
Table 4-31: Results from t-test for changes in expression of NOTCH and members of the HES gene family.	117
Table 4-32: Group statistics for changes in expression (as $\Delta\Delta C_q$ -values) of potential off-target genes of the siPAX7-pSilencer1.0 construct.	119
Table 4-33: Results from t-test for changes in expression potential off-target genes of the siPAX7-pSilencer1.0 construct.	119
Table 4-34: Anti PAX7 and Anti non-phospho $\beta$ -catenin antibodies show linear scaling.	122
Table 4-35: Whole protein stain shows low protein input relative to loading control, in Western Blots.	123
Table 4-36: PAX7 protein quantification of mid- and hindbrain tissue.	125
Table 4-37: Canonical Wnt signaling activity quantifiable in a few protein samples.	126
Table 4-38: PAX7 knock-down using the new siPAX7-pSilencer1.0 constructs does not reduce average midbrain size.	131

## IV. Abbreviations

APC	adenomatous-polyposis-coli
AU	Airy unit
AXIN	axis inhibition protein
BMP	bone morphogenic protein
bp	base pairs
cDNA	copy DNA
CKI $\alpha$	casein-kinase I $\alpha$
LSM	confocal-laser-scan microscope
CMV	cytomegalovirus
CNS	central nervous system
DAAM	dishevelled associated activator of morphogenesis
DI	diencephalon
DKK	dickkopf
dGFP	destabilized green fluorescent protein
DO	dorsal
DVL	dishevelled
EN1	ENGRAILED 1
eGFP	enhanced green fluorescent protein
FGF	fibroblast growth factor
FZD	frizzled receptor
GFP	green fluorescent protein
GPCR	G-protein coupled receptor
GSK3 $\beta$	glycogen synthase kinase 3 $\beta$
HB	hindbrain or rhombencephalon
HD	homeodomain
HES	hairy and enhancer of split
HEY	hairy ears, Y-linked
HH	Hamburger and Hamilton
HMG-box	high mobility group box gene
IHC	immunohistochemistry
IRES	internal ribosomal entry site
JNK	jun N-terminal kinase
IPAX7*	paired box domain protein 7, splice variant with long trans-activation domain
MASH	mammalian achaete-scute homolog
MB	midbrain
MCS	multi-cloning site
MHB	mid- hindbrain boundary
miRNA	microRNA
mRNA	messenger RNA
nt	nucleotide
PAX	paired-box domain protein

PCP	planar cell pathway
PCR	polymerase chain reaction
PFN	profilin
PMZ	posterior marginal zone
qPCR	quantitative real-time PCR
RE	rhombencephalon or hindbrain (HB)
RFP	red fluorescent protein
ROC	regulator of cullins
ROCK	rho kinase associated kinase
RT	reverse transcriptase
SD	standard deviation
SDS-PAGE	sodium dodecyl sulfate polyacrylamide gel electrophoresis
SHH	sonic hedgehog
SOX	SRY and HMG-box gene
SRY	sex-determining region Y protein
siRNA	short interfering RNA
sPAX7*	paired box domain protein 7, splice variant with short trans-activation domain – alternatively PAX7 <sup>ex9(-)</sup>
SV	splice variant
TCF/LEF	T-cell factor/lymphoid enhancer-binding factor
TD/TAD	transactivation domain
TE	telencephalon or forebrain
TLE	transducing-like enhancer
V	ventral
WB	Western blot
WNT	wingless integration site gene

\*In this thesis, only the presence or absence of the splice variant resulting from the in-/exclusion of the 66bp from PAX7 exon 9 were analyzed. Other alternate splice sites were not investigated. The terminology of long and short splice variant is preferred over the terminology used in the publication from Mao et al. in 2008. They used PAX7-1 to refer to the PAX7 variants that include the 9<sup>th</sup> exon, whereas PAX7-2 did not include it. As there now are six known splice variants of PAX7 (X1-X6) with their nomenclature not aligning with Mao et al., a different, more descriptive approach was taken, with the intent of preventing confusion.

## V. Abstract

PAX7 is a well-known transcription factor, that plays an important role in embryonic development and stem cell maintenance in adult organisms. It has been shown to regulate proliferation and differentiation during embryonic development in the dorsal midbrain. In the chicken (*Gallus gallus domesticus*), a splice variant in the transactivation domain of PAX7 has been found, that is exclusive to birds. In-vitro, this alternative splice variant impacts transcriptional activity. Furthermore, PAX7 has been previously found to interact with canonical Wnt signaling in the dorsal midbrain of chicken embryos.

Using an in vivo reporter gene and qPCR, it was possible to show that the pro-transcriptional activity of PAX7 is required for normal canonical Wnt signaling in the dorsal midbrain at HH stage 17. Expression of PAX7 on an RNA level correlates well with canonical Wnt signaling. Interestingly, PAX7 seems to partially regulate its own expression with differences in regulatory activities between the two transactivation domain splice variants.

# 1 Introduction

## 1.1 Chicken Development

### 1.1.1 Early Chicken Development

The chicken egg is one of the largest known cells, whereby yolk makes most of the egg cells cytoplasm. That leaves only a small space at the top of the cell free, called blastodisc. Whilst still inside of the hen, the egg cell undergoes its first discoidal meroblastic divisions, meaning the divisions are highly asymmetrical, creating new cells in the blastodisc whilst the yolk remains in a singular cell. By the time the hen lays the egg, the ovum is already in its late blastula stages forming the blastoderm with approximately 50000 cells (Sheng, 2014). Beneath the blastoderm the subterminal cavity is formed. Starting centrally, all cells except the outermost layer shed and die, leaving the epiblast, a one cell thick layer, the only cells giving rise to the embryo itself. In the area, where the epiblast touches the yolk, some cells survive and form the hypoblast. The area where only the epiblast remains is called area pellucida, the area where epi- and hypoblast overlap is called area opaca with the border being referred to as marginal zone (Gilbert, 2020).

After the egg is laid, the marginal zone thickens and forms Koller's sickle and the posterior marginal zone (PMZ), that later locates caudally of the forming embryo. The cranial-caudal axis is specified by gravity and the eggs rotation within the hen's reproductive tract. The upper side of the blastoderm will form the caudal end, or in other words: The head goes first (Wolpert, 1998). Starting from Koller's sickle, hypoblast cells start dividing and migrating across the zona pellucida. The hypoblast cells form the endoblast, that displaces the last remaining islands of hypoblast cells, resulting in a hollow two layered structure. The liquid filled space between the epi- and endoblast is called the blastocoel. Growing in the same direction as the endoblast, the primitive streak is formed. It progresses from the PMZ towards the center of the zona pellucida, where, at its anterior end, the first major organizer – Hensen's node – is formed (Boettger et al., 2001). The primitive

streak and Hensen's node enable gastrulation. Cells can pass through them into the blastocoel down to the endoblast. These cells replace the endoblast cells beneath the streak and form the endoderm, that for example later generates the digestive tube, lungs, and thyroid cells. The cells that stay in the blastocoel form the mesoderm, that gives rise to tissue like bones, blood, muscles, and the notochord. The epiblast gives rise to the third germ layer, the ectoderm giving rise to skin cells, the neural crest and – most important of all – the central nervous system (CNS) (Gilbert, 2020).

At this point, the cranial-caudal axis has been established along the primitive streak, the dorsal-ventral axis is also established with the epiblast/ectoderm as dorsal and the endoblast/endoderm as ventral side. The last axis to be established being the left-right axis. The exact mechanism defining left and right is yet unknown, however Hensen's node secretes sonic hedgehog (SHH) factors to the left side inducing Cerberus and fibroblast growth factor 8 (FGF8) to the right side, inhibiting Cerberus expression (Raya and Izpisua Belmonte, 2004).

Completion of germ layer formation occurs from cranial to caudal. Along with its completion, the primitive streak regresses back towards the PMZ, taking Hensen's node along with it towards the caudal end. With the regression of the primitive streak, the formation of a secondary organizer - the Notochord - begins, also in a cranial-caudal manner. Parallel to these processes, the ectoderm starts its epiboly, moving laterally and surrounding the yolk. During this 4-day long process, the cranial mesoderm already starts inducing CNS formation, whilst at the caudal end is still gastrulating (Gilbert, 2020, New, 1959, Spratt, 1963).

### **1.1.2 Early CNS Formation**

As my experiments primarily focus on the dorsal midbrain, the development of the CNS, especially the midbrain is of special interest. The ectoderm gives rise to the neural tube, a predecessor structure of the CNS, in a process called neurulation. In birds and mammals, there are two types of neurulation occurring simultaneously. Primary neurulation forms the neural tube cranial of the hindlimbs. The secondary neurulation occurs caudally and a large thoracal region where both forms overlap (Catala et al., 1996, Dady et al., 2014).

The midbrain is formed through primary neurulation. Here the neural tube is formed from the neural plate, a specialized part of the ectoderm above the notochord, where SOX transcription factors prevent epidermis formation by blocking BMP signaling. (Archer et al., 2011). The lateral ends of the neural plate start growing upwards out of the ectodermal plane and move towards each other, first forming a u-shaped indenture and later a tube. These movements are enabled by three hinge points where the ectoderm bends. The medial hinge point above the notochord allows for indenture formation, whilst the dorsolateral hinge points allow for convergence of the lateral neural folds. The 'hinging' in both cases is achieved by displacing the nucleus to the outside (or basal side) of the cells whilst simultaneously the central (or apical) side is constricted through actin-myosin interactions (Schoenwolf and Smith, 1990). Once the lateral sides of the neural plate come into contact and connect, turning the groove into a tube. The first point of tube closure in the chicken is usually in the midbrain, around Hamburger and Hamilton stage 8 (HH8). From here, the tube closes in both directions in a zipper like fashion, leaving cranial and caudal openings, called neuropores. Failure to close the neural tube can result, depending on the position, in a spina bifida (caudal) or lethal anencephalia (cranial). With the closure of the neural tube, it separates from the ectoderm. This separation is done by switching from E- to N-cadherin expression in the neural tube, whilst the ectoderm keeps expressing E-cadherin, weakening the attachment between them. A small population, located at the junctional area between neuro- and ectoderm does express neither E- nor N-cadherin and leaves the epithelial structures. These cells, alongside with other cells, leaving later the neural tube, form the neural crest cells, giving rise to the peripheral nerves, melanocytes and craniofacial cartilage and bones (Detrick et al., 1990, Fujimori et al., 1990, Gilbert, 2020, Kuphal and Bosserhoff, 2012) .

In secondary neurulation cells derived from both ecto- and mesoderm, cluster together into a medullary cord, later undergoing cavitation to form a central lumen (Schoenwolf and Delongo, 1980).

### **1.1.3 CNS Patterning**

In chicken, at HH9, shortly after cranial neural tube closure, the primary vesicles of the brain become visible: the forebrain, the midbrain and the hindbrain. By the

time, the caudal end of the neural tube has closed the primary vesicles have formed further substructures, the secondary vesicles. The forebrain divides in dien- and telencephalon, that later forms the cerebral hemispheres. The hindbrain will split into the metencephalon, growing to become the pons and cerebellum and caudally of it the myelencephalon forming the medulla. Only the midbrain (mesencephalon) stays a singular vesicle. Whilst the midbrain continues to grow and stays the largest of the vesicles until around HH stage 29-30, the hindbrain starts forming the rhombomeres that, together with their neural crest cells, will form most of the cranial nerves (Lumsden and Keynes, 1989, Lumsden, 2004, Gilbert, 2020).

The foundation for this cranial-caudal differentiation is already induced prior to neural tube closure in the neural plate. The exact mechanisms aren't fully understood yet, it's known that the inhibition of BMPs is relevant for generation of cells with cranial properties (Zimmerman et al., 1996) and that retinoic acid can induce posterior cell and regulates rhombomere formation (Shawlot and Behringer, 1995, Marshall et al., 1992). Relevant organizers for these initial patterning steps seem to be the prechordal ectoderm and Hensen's node, known to secrete retinoic acid during its regression (Simeone et al., 1995, Lumsden and Krumlauf, 1996).

Later, patterning steps are orchestrated by regionalized organizers, like the mid-hindbrain boundary (MHB, or isthmus) that controls mid- and hindbrain development. The MHB secretes FGF8 amongst other morphogens, creating a gradient with concentration decreasing both cranially and caudally. In the midbrain, the transcription factor ENGRAILED1 (EN1) is expressed, an early midbrain marker protein and mandatory for the formation of the tectum. As transplant experiments have shown, from HH stage 20 (E3) on, cells are committed to tectum formation under the influence of EN1 (Hanks et al., 1995, Martinez et al., 1991, Lumsden and Krumlauf, 1996).

Dorsal – ventral patterning in the neural tube is orchestrated by the roof and floor plate. The dorsally located roof plate is induced by BMP4 and BMP7, secreted from the ectoderm and starts in turn secreting BMP4 (Liem et al., 2000). Similarly, the floor plate is induced on the ventral side by SHH, secreted from the notochord.

The floor plate itself also starts secreting SHH. These two secondary signaling centers now generate two opposing gradients, with BMP4 concentration decreasing from the dorsal to the ventral side and SHH concentration increasing at the same time. Depending on the intricate balance of SHH and BMP4 exposure, different transcription factors become activated, determining the fate of individual cell populations based on their location. In the later spinal cord for example, PAX6 and NKX2.2 form a pair of transcription factors, inhibiting each other's expression. Whilst PAX6 expression is inhibited by SHH, NKX2.2 is induced by it, resulting in PAX6 being less and less expressed the closer to the floor plate you get (Briscoe et al., 1999). PAX7 is being expressed on the dorsal side, within the roof plate from HH stage 10 onwards (Kawakami et al., 1997b).

Whilst the midbrain, shares BMP and SHH as morphogens for dorsal-ventral patterning with other brain regions, like the spinal cord, WNT1 joins BMP as an additional morphogen from the roof plate, resulting in an altered gene expression and later differentiation compared to other brain compartments. It has been shown, that the longer cells are exposed to these morphogens, the more determined their cell fates are (Li et al., 2005). The ventral side, giving rise to the tegmentum expresses NKX2.2 and NKX6.1, whilst PAX7 is expressed in the dorsal midbrain, where the tectum is later formed (Moreno-Bravo et al., 2012, Martinez-Lopez et al., 2015, Bayly et al., 2007).

Later, in the adult, the tectum is an important relay station for the chicken's visual system, whilst the tegmentum houses essential motoric systems, like the substantia nigra (Mey and Thanos, 2000, Bayly et al., 2007).

## **1.2 PAX7 and PAX Gene Family**

The paired box (PAX) gene family consists of nine different, highly conserved transcription factors, playing a major role in embryonic development acting as "master regulators" determining tissue specific cell fate (Shaw et al., 2024).

Based on structural elements, the PAX genes can be differentiated in four sub-groups. All PAX genes share the name giving paired domain consisting of two helix-turn-helix motives for DNA binding and a transactivation (TAD) domain allowing for interaction with other proteins. These protein-protein interactions

include chromatin remodeling complexes, which make condensed chromatin accessible for transcription. Facilitating the opening of chromatin allows for their function as pioneer transcription factors (Mayran et al., 2015). The octapeptide allows for outside regulation of transcriptional activity through protein-protein interaction and post-transcriptional modification. The homeodomain is another helix-turn-helix DNA binding domain, involved in interaction with other homeodomains or the paired domain (Eberhard et al., 2000).

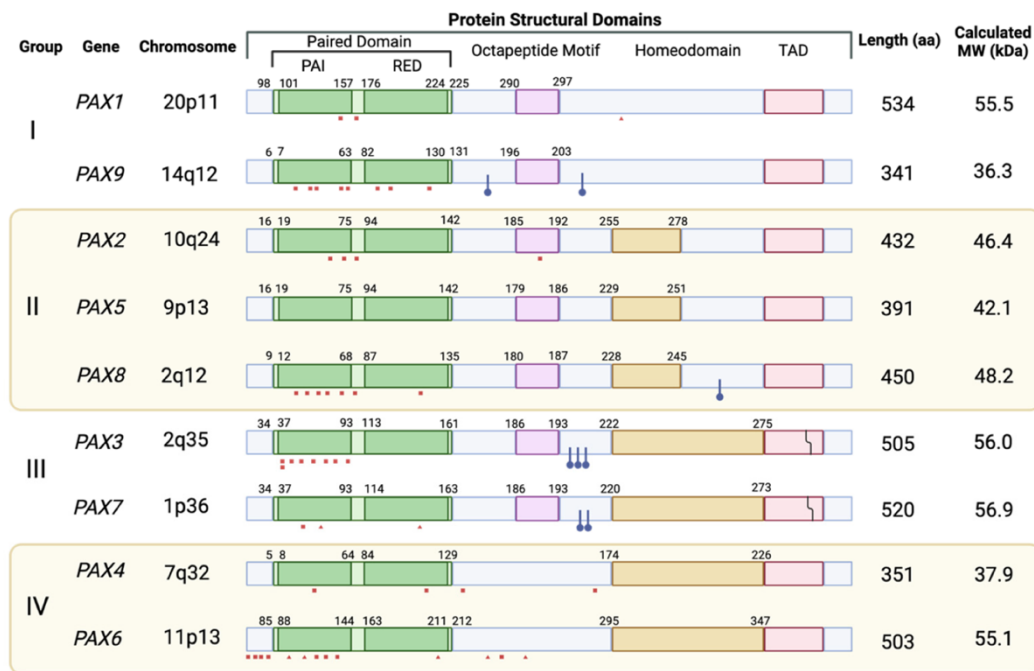


Figure 1-1: **Structural elements of PAX genes in the human.** *PAX7* and *PAX3* belong to subgroup three. They both contain paired and homeodomain mediate DNA binding. TAD mediates protein-protein interactions. After (Shaw et al., 2024)

My work primarily focuses on *PAX7*, forming subgroup 3 alongside *PAX3*. Both are involved in development of skeletal muscles, neural crest cells and the central nervous system, especially in the dorsal mid-, hindbrain and spinal cord. Both genes are potential oncogenes in alveolar rhabdomyosarcoma by forming fusion proteins with FOXO1 (Davis et al., 1994). *PAX3* defects can result in Waardenburg syndrome or craniofacial-deafness-hand syndrome whereas *PAX7* defects can result in congenital myopathy-19. Expression of both genes is often overlapping, and mouse knockouts revealed partial functional redundancies (Mansouri et al., 1996, Shaw et al., 2024).

In chicken, a total of three alternative splice sites of PAX7 have been described but only partially analyzed so far. Two splice variants are located in the paired box domain, and one is located in the transactivation domain. The paired box domain splice variants are present in mice or humans and result in the in- or exclusion of a glycine and leucine (GL) or a singular glutamine (Q), and influence binding to different DNA sequences, with the GL+ variants shown to be more myogenic. The specific difference in activity on a molecular level have not been understood so far (Ziman and Kay, 1998, Du et al., 2005).

The primary focus for this thesis was the splice variant in the transactivation domain, with the long splice variant including a complete 66bp exon, that seems to be exclusive to birds (Internal, Lim, 2016, unpublished). Mao et al. showed that, at most Hamburger Hamilton stages the long splice variant showed higher expression. Findings of our own group (Ulrike Kohler and Kiona Lim, unpublished) indicate that the short splice variant, that is skipping this 9<sup>th</sup> exon entirely, has a higher expression in the dorsal midbrain. Naixin Li found this splice variant to promote proliferation of the dorsal midbrain around HH stage 10 (Li, 2007). It has been shown that the long splice variant has higher transcriptional activity using a luciferase assay in CHO cells (Mao 2008).

Looking at the reference genome assembly (bGalGal1.mat.broiler.GRCg7b) for chicken available today (March 2024), four predicted splice variants exist – non containing the splice variant in the transactivation domain. These can only be found in the alternative assembly (bGalGal1.pat.whiteleghornlayer.GRCg7w), which is from a different breed of chicken. This could be the result of differences between breeds or from methodical differences as the genomic sequence of the intron and splice sites is identical between assemblies.

Splice Variant	Broiler (Reference)	White Leghorn Layer (alternative)	Q (CAG)	GL (GTTTAG)	66bp TA (Exon 9)
X1	XM_015296830.4	XM_046931153.1	+	+	-
X2	XM_015296831.4	XM_046931154.1	-	+	-
X3	XM_015296832.4	XM_046931155.1	+	-	-
X4*	XM_025142486.3	XM_046931156.1	-	-	-
X5		XM_046931151.1	+	+	+
X6*		XM_046931152.1	-	-	+

Table 1-1: **Predicted isoforms of PAX7 in the chicken embryo.** Only the alternative genomic assembly contains the isoforms containing the transactivation domain splice variant. \* marks splice variants used for electroporations. + sequence present, - sequence absent.

PAX7 expression in chicken embryos can be detected as early as HH5 in the ectoderm of the primitive fold and stays highly expressed in the dorsal side of the neural tube, where it is required for cell differentiation and in cooperation with PAX3 involved in neural tube closure. PAX7 is also required for formation of neural crest cells (Goulding et al., 1991, Walther et al., 1991, Basch et al., 2006).

Outside of the neural tube, PAX7 is expressed from HH8 on in somites, the muscle precursor cells and stays actively expressed in satellite cells, where it is required to maintain stem cell character (Otto et al., 2006, Chi and Epstein, 2002, Halevy et al., 2004).

### 1.3 Wnt Signaling Pathway

Tight coordination and signaling between cells is mandatory for embryogenesis, tissue formation, growth and later homeostasis and regeneration, with of the evolutionarily highest conserved forms of cell-cell signaling being the Wnt pathway. The different 19 secreted Wnt (from *D. melanogaster*'s Wingless and mouse int-1) proteins typically bind to membrane bound frizzled (FZD) receptors forming heterodimers with low-density lipoprotein-related protein 5/6(LRP5/6) coreceptors, but they have also been shown to bind a variety of other receptors, including some GPCRs and tyrosine kinase receptors (Lu et al., 2004, Katanaev, 2010).

Depending on the secreted WNT proteins, the receptor and associated proteins and coreceptors, three different pathways have been described: the canonical  $\beta$ -catenin pathway, the planar cell pathway (PCP) involved in cytoskeletal rearrangements and the WNT/Ca<sup>2+</sup> regulating phospholipase C (Hayat et al., 2022).

In  $\beta$ -catenin based canonical signaling, the binding of WNT inhibits the destruction complex through interaction with dishevelled (DVL) proteins. The destruction complex consisting of APC, AXIN, CK1 $\alpha$  and GSK3  $\beta$  that usually cause degradation of the cytoskeletal protein  $\beta$ -catenin (CTNNB1) by inducing ubiquitination through phosphorylation. If the complex is inhibited, concentrations of non-phosphorylated  $\beta$ -catenin rise allowing for translocation into the nucleus, where it associates with members of the T cell factor/lymphoid enhancer factor (TCF/LEF) family promoting transcription of various genes regulating proliferation and differentiation. As negative feedback mechanism the expression of AXIN2 is increased. (Jho et al., 2002)

In the absence of  $\beta$ -catenin TCF/LEF proteins are bound by groucho (TLE) proteins, strong transcriptional inhibitors (Hayat et al., 2022, Huelsken and Behrens, 2002). Besides AXIN2, the destruction complex and TLE other proteins also inhibit canonical Wnt signaling, like secreted FZ associated proteins (SFRP) or the family of dickkopf (DKK) proteins inhibiting signal transduction at the cell membrane by binding LRP5/6 (Hayat et al., 2022).

The different Wnt signaling pathways have been shown to play an important role in CNS, both during embryonic development and adulthood (Inestrosa and Varela-Nallar, 2015). The PCP pathway is involved in neural tube closure and gradients of Wnt ligands are important for the specification of the anterior-posterior axis (Kiecker and Niehrs, 2001, Wen et al., 2010). Depending on developmental stage and brain region, canonical Wnt signaling has been shown to promote differentiation or proliferation of neural progenitor cells (Hirabayashi et al., 2004, Mutch et al., 2010).

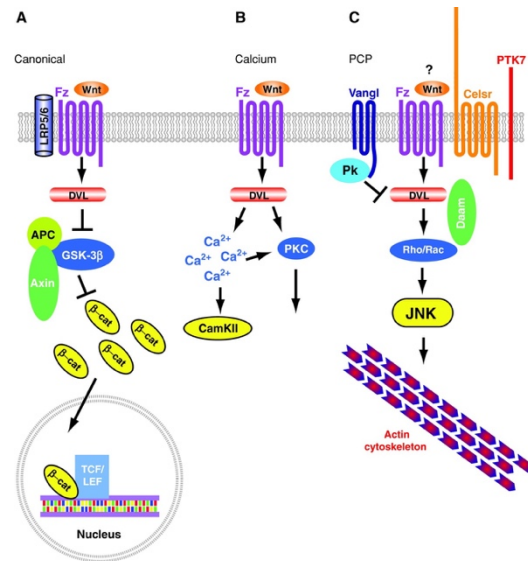


**Figure 1-2: Overview of the three main Wnt signaling pathways.** **A** canonical Wnt signaling: WNT binds FZD receptor, inhibiting the destruction complex.  $\beta$ -catenin no longer gets phosphorylated, translocates into the nucleus and promotes transcription. **B**: Wnt/ $Ca^{2+}$  signaling: WNT interacts with FZD/G-protein complexes activating phospholipase C resulting in intracellular  $Ca^{2+}$  increase. **C**: Planar cell pathway (PCP): WNT/FZD interaction activates jun N-terminal kinases (JNK), ROCK and PFN (not shown) through DAAM, ROC and RAC, regulating migration and polarization by altering the cytoskeleton. Image: (Montcouquiol et al., 2006)

## 1.4 HES Genes

The hairy and enhancer of split (HES) genes are a family of basic helix-loop-helix transcription repressors working either by inhibiting transcription factors through heterodimerization with them or as homo-/heterodimers with other HES family proteins. These HES dimers recruit chromatin remodeling factors through TLE proteins (Buscarlet et al., 2008). Even though they play an important role in development, HES genes aren't as conserved across species as for example transcription factors from the PAX family (Kobayashi and Kageyama, 2014). So far, there are 10 different HES genes described in the chicken, most predicted, some validated (March 2024, NCBI Gene Database). The homologs of HES3 and HES7, both found in humans and mice, haven't been found in chicken yet. No ortholog sequences in birds have been annotated for HES3 so far and for HES7 only five sequences in falcons and parrots were found. (April 2024, NCBI Orthologs) For HES5, the three different genes HES5A (HES5), HES5B (HES5L) and HESC (HESL) exist, with orthologs in other birds, but not in Humans or mice (April 2024, NCBI Gene Database).

Overall, the nomenclature of HES genes in the chicken is somewhat ambiguous, varying between publications and genomic assemblies. For example, the Geisha gene expression database shows RNA in-situ hybridization results for HES7 but blasting the probe used retrieves HES5-like (RefSeq: XM\_015302395.4) (April 2024, NCBI Gene Database, NCBI BLAST and GEISHA). Some publications also mention HES7, like Ku et al. in 2014, where it was part of a transcriptome analysis, but no sequence or RefSeq ID were given (Ku et al., 2014).

In mice, HES1 and HES3 play a major role in maintaining the stem cell character of neuroepithelia cells, radial glia cells and cells in boundary regions of the developing CNS. They are expressed from the beginning of neural plate formation. HES1 stays active in radial glia cells, where it is joined by HES5 whilst HES3 is no longer being expressed. By repressing its own transcription HES1 acts as a biological clock, with a cycle of 2h also inducing cyclic expression of other genes, like its pro-neurogenic counterpart MASH1, allowing for a balance of stem cell renewal and differentiation into neurogenic precursor cells. In cells with organizer

functions, like in the MHB, HES1 is constantly expressed preventing differentiation (R. Kageyama, 2006, Kageyama et al., 2008).

Besides CNS development, the cyclic expression of HES1 and HES5 is also crucial for stem cell maintenance in many organs, like the lungs, digestive tract and hematopoietic stem cells (Kobayashi and Kageyama, 2014). HES1 has been shown to interact with Jak-Stat signaling to maintain its own oscillation (Yoshiura et al., 2007). Many pathways, like Wnt (Kobayashi and Kageyama, 2014) and Notch signaling induces HES5 expression in the radial glia cells and it regulates HES1 expression promoting stem cell maintenance. Outside of the neural tube, HES7 also seems to be a target of Notch signaling (Ohtsuka et al., 1999, Kageyama et al., 2008, Niwa et al., 2007).

HES6 is the only HES gene lacking DNA binding capabilities, acting as an inhibitor of other HES genes, as it still forms dimers with them (Bae et al., 2000).

Like HES1, HES7 shows cyclic expression in mice. It works as a *segmentation clock* in somite formation, with every cycle of HES7 expression resulting in formation of another same sized somite (Bessho et al., 2001). The cycle time varies between species, with a cycle taking 8h in humans, 2h in mice and 1.5h in chicken (Kobayashi and Kageyama, 2014).

Other HES genes, like HES2 and HES4 are also involved in the development of various organs, including the CNS or neural crest cells, however their function isn't as well understood as the function of HES1, HES3, HES5 or HES7 (Pla and Monsoro-Burq, 2018).

HEY1 has been implied in cochlear development (Tateya et al., 2011) whilst HEY2 is required for development of the organ of Corti (Doetzlhofer et al., 2009).

Most of the functions HES genes have only been described so far were discovered in mouse embryos or cell culture and can't be taken for granted in the chicken. The fact, that not all HES genes are present/described in all organisms studied, like Hes4 is missing in mice or HES3 and HES7 missing in chicken (April 2024, NCBI Gene Database) show that more research is required and once again highlight the difference between species.

## 1.5 Aim of the Project

The aim of my work was the investigation of the influence of the transcription factor PAX7 on dorsal midbrain development. Unpublished results by Li showed that overexpression of the short PAX7 splice variant in the dorsal midbrain resulted in enlarged midbrains, whereas a PAX7 knock-down resulted in smaller midbrains (Li, 2007). Internal, also yet to be published experiments, using a reporter plasmid, showed the PAX7 knock-down reducing canonical Wnt-signaling activity. Since Wnt-signaling is known to be involved in proliferation and differentiation, this might be a possible pathway causing the size changes observed by Li, and that the overexpression of PAX7 might result in an increase of canonical Wnt-signaling.

Only few PAX7/WNT interactions have been studied so far. Canonical Wnt signaling involving WNT1 and FZD10 is known to be required for dorsalization of neural tube cells, inducing PAX7 expression (Alrefaei et al., 2020, Otto et al., 2006) and in muscular stem cells, called satellite cells, Wnt-signaling promotes differentiation, for example after muscle injury. On the other hand, in the same cells, PAX7 is required for cell survival, self-renewal, and maintenance of stem cell characteristics, by blocking Wnt-signaling. PAX7 and Wnt-signaling antagonize each other, which is the contrary of our hypothesis, of PAX7 promoting Wnt-signaling (Hulin et al., 2016, Zhuang et al., 2014, Cui et al., 2019). In addition to these findings, WNT3A has been shown to influence gene expression through a more direct interaction with PAX3 and PAX7, not going through one of the three traditional Wnt pathways (Pan et al., 2015).

Notch signaling has been shown to induce and regulate PAX7 expression in satellite cells, both during embryonic development and during muscle injury recovery. (Wen et al., 2012) Further expanding upon this, Wnt signaling is involved in regulation of Notch signaling, forming a complex network, regulating proliferation and differentiation of satellite cells.

Unfortunately, preliminary experiments using the same reporter system with PAX7 being overexpressed were inconclusive (Zhu et al., 2017).

Various PAX7 splice variants, exclusive to the chicken, with different transcriptional activities further complicated the matter, (Mao et al., 2008) which led to the

decision to move to real time quantitative PCR (qPCR) and Western blotting, in an effort to quantify the impact of our *in-ovo* electroporations on the individual PAX7 splice variants and on canonical Wnt signaling.

Establishing these two methods, which hadn't been used in our work group so far, ended up being the main task of this project.

## 2 Materials

### 2.1 The Chicken as a Model Organism

For all in vivo experiments eggs and embryos from the common chicken (*Gallus gallus*) were used. This organism was selected, as it is commonly used for neurodevelopmental research, allows easy transient genetic modification through electroporation and the embryos can be easily accessed inside their eggs.

The experiments conducted do not fall under animal experiment regulations (TierSchVersV §14 and TierSchG), as the embryos were harvested prior to formation of complex synaptic structures.

The development of chicken embryos can be microscopically assessed using the stages of normal chicken development, published by Hamburger and Hamilton in 1951 (Hamburger and Hamilton, 1951).

HH Stage	Incubation time	Description
1		Preprimitive streak
2	6-7h	Initial primitive streak
3	12-13h	Intermediate primitive streak
4	18-19h	Definitive primitive streak
5	19-22h	Head process
6	23-25h	Head fold
7	23-26h	1 somite
8	26-29h	4 somites
9	29-33h	7 somites
10	33-38h	10 somites
11	40-45h	13 somites
12	45-49h	16 somites
13	48-52h	19 somites
14	50-53h	22 somites
15	50-55h	24-27 somites; visceral arch III
16	51-56h	26-28 somites; wing bud
17	52-64h	29-32 somites; leg bud
18	E 3	30-36 somites; allantois
19	E 3-3.5	37-40 somites; maxillary process
20	E 3-3.5	40-43 somites; eye pigment
21	E 3.5	43-44 somites; visceral arch IV
22	E 3.5-4	Somites extend to tip of tail
23	E 4	Dorsal contour from hindbrain to tail is curved
24	E 4.5	Toe plate
25	E 4.5-5	Elbow and knee joints
26	E 5	3 toes
27	E 5-5.5	Beak

28	E 5.5-6	3 digits, 4 toes
29	E 6-6.5	Rudiment of 5th toe
30	E 6.5-7	Feather germs
31	E 7-7.5	Web between 1st and 2nd digits
32	E 7.5	Mandible has reached beak
33	E 7.5-8	Web on radial margin of wing
34	E 8	Nictitating membrane
35	E 8.5-9	Phalanges in toes
36	E10	Length of 3rd toe = $5.4 \pm 0.3$ mm
37	E11	Length of 3rd toe = $7.4 \pm 0.3$ mm

Table 2-1 **Hamburger and Hamilton stages (HH stage) of chicken development.** After (Hamburger and Hamilton, 1951)

## 2.2 Plasmids

A variety of plasmids was used for in-ovo electroporation or as templates in PCR. All plasmids used contained a bacterial replication origin and an open reading frame coding for an ampicillin resistance, allowing for easy expansion in *E.coli*. The variants of the PAX7-pMES plasmids, as well as the pSilencer1.0 constructs were generated by (former) members of the AG Wizenmann. The siPAX7-506-pSilencer, siPAX7-1105-pSilencer and siPAX7-2307-pSilencer constructs were newly generated for this study.

Plasmid	Function	Promoter	Enhancer
pCAX	eGFP expression, used as negative control for electroporations	Chicken ACTB	CMV
sPAX7-pMES	Overexpression of PAX7 (SV), co-expresses eGFP using an IRE-site	Chicken ACTB	CMV
IPAX7-pMES	Overexpression of PAX7 (SV), co-expresses eGFP using an IRE-site	Chicken ACTB	CMV
sPAX7-pMES- $\Delta$ GFP	Overexpression of PAX7 (SV), no eGFP expression	Chicken ACTB	CMV
IPAX7-pMES- $\Delta$ GFP	Overexpression of PAX7 (SV), no eGFP expression	Chicken ACTB	CMV
enPAX7-pMIW	Overexpression of PAX7-EN1-fusion protein, represses expression of genes usually activated by PAX7	Chicken ACTB	CMV
siPAX7-pSilencer1.0	First siRNA for PAX7 knockdown, sequence: GAAAGAGGAAGAGGAGGAC	Mouse U6	-
siPAX7-506-pSilencer1.0	PAX7 knockdown, sequence: TCCTCTGCAGGTACCAAGA	used together as 3x	Mouse U6
siPAX7-1105-pSilencer1.0	PAX7 knockdown, sequence: CCAACTCGCAGCATTCAAC		Mouse U6

siPAX7-2372-pSilencer1.0	PAX7 knockdown, sequence: GACCTATGGACCAAACATA		Mouse U6	-
PAX3-pMIW	Overexpression of PAX3		Chicken ACTB	CMV
TOPdGFP	Reporter for canonical WNT signaling using d2eGFP		Mouse cFos	4x LEF binding site
2A-lyn-Cherry	RFP with nuclear localization, used to detect electroporated cells alongside TOPdGFP plasmid		Chicken ACTB	CMV

Table 2-2: List of plasmids used for electroporations.

## 2.3 Oligonucleotides

Oligonucleotides were used as primers for PCR and qPCR applications as well as inserts for cloning of siRNA plasmids. All oligonucleotides were synthesized by Eurofins Genomics.

The Primers used for the first qPCR on the Biomark were designed using DNASTAR Primer Designer, aiming at around 450bp amplicon length. All primers were designed for an annealing temperature of 60°C, indicated by the prefix 60. The ACTB, CCND1, CCND2 and PAX3 primers had been previously designed by other members of the AG Wizenmann. The PAX7 splice variant specific primers (P7, P8, P9 and P10) were designed and published by Mao et al. in 2008. The EGFP primers used were published by Schüle et al. in 2006. Primer efficiencies aren't listed, as the required data wasn't acquired, and they were replaced by their exon skipping counterparts (Mao et al., 2008, Schule et al., 2006).

Gene	Primer Name	Sequence	Amplicon
ACTB	Beta-Actin-Fwd1	GTGCGTGACATCAAGGAGAAGC	426bp
	Beta-Actin-Rev1	GGACAGGGAGGCCAGGATAGA	
GAPDH	60GAPDH5'-F	GCGAGATGGTGAAAGTCGGA	196bp
	60GAPDH5'-R	TTCCCGTTCTCAGCCTTGAC	
GAPDH	60GAPDH3'-F	CTCCACCTTTGATGCGGGT	214bp
	60GAPDH3'-R	CAGAACTGAGCGGTGGTGAA	
AXIN1	60Axin1-F	GCAGTGCATCCGTGGGTGAGTG	435bp
	60Axin1-R	GAAGATGGGCAG-GATGGTGTGTCGTC	
AXIN2	60Axin2-F	CTCCACCGGGGTCATCTCCTTG	432bp
	60Axin2-R	GGCTACCTGCCGACCTTGAACG	
WNT1	60Wnt1-F	GGATGCGCCTGCCACCTTC	231bp

	60Wnt1-R	TCCCCGCCGTCCCCATCTTC	
WNT4	60Wnt4-F	GTGCTGGTGCCGAAAACTCCCAG	433bp
	60Wnt4-R	TCCTCCGGGGCTCTGTCTCTGTAT	
LEF1	60Lef1-F	GCCATACAGCACATCGAGGAATG	405bp
	60Lef1-R	CATGGCTACTGACCAGCTGACTGT	
CCND1	Cyclin D1-F	TCAAGTGC GTGCAGAAGGAAA	439bp
	Cyclin D1-R	GTAGCGCACAGAGCCACAAAAGT	
CCND2	Cyclin D2-F	ACAATTCCATCAAACCCCAAGA	282bp
	Cyclin d2-R	ATCTGTCCCCATCATCAAGC	
PAX3	cPax3-fo2	TGCCGACTCTGCCGACATACC	347bp
	cPax3-rev2	AGGGGACAGGGCATAATCAGTTTG	
PAX7	P7	AATGGCCTCTCTCCGCAGGTGA	196bp
	P8	ACTGCGAGGTTCGGGAGGCTGT	
PAX7	P9	CAAAACAAGATGCAGTGCTCCAG	184bp
	P10	CGGACTTGATGGAGTCACTCCG	
EGFP	EGFP-F	CGTCCAGGAGCGCACCATCTTCTT	373bp
	EGFP-R	ATCGCGCTTCTCGTTGGGGTCTTT	
NEUROG1	60NEUROG1-F	TAGCCCTGCCCGTGCGTGTC	509bp
	60NEUROG1-R	CCAGTGGCTCAATACCCCGTGTG	

Table 2-3: List of non-exon-skipping qPCR primers. PAX7 primers from (Mao et al., 2008). EGFP primers from (Schule et al., 2006)

In the further qPCRs exon skipping primers, thus cDNA specific, were used. These primers were designed using NCBI Primer Blast, with an annealing temperature of 60°C. They share the prefix ES60. Exceptions to this are the PAX7 forward primers, as the primers P7 and P9 published by Mao et al. in 2008 were used with an exon skipping reverse primer and the primers for FZD1 and FZD10, as these genes only have a singular exon. (Mao et al., 2008)

Gene	Primer Name	Sequence	Amplicon
ACTB	ES60ACTB-F	CAGCCAGCCATGGATGATGA	150bp
	ES60ACTB-R	CATACCAACCATCACACCCTGA	
ATP5B	ES60ATP5B-F	CGCAAGATCCAGCGCTTTTT	133bp
	ES60-ATP5B-R	GGTGGTCGTATTACCTGCC	
AXIN2	ES60AXIN2-F	CGACAGAAGATCACAAA-GAGCC	214bp
	ES60AXIN2-R	CAGTCAAACCTCGTCGCTTGC	
CCND1	ES60CCND1-F	CCGACGAGTTACTGCAAATGG	128bp
	ES60CCND1-R	CTGTTTGGTGTCTCTGCCA	
CHMP4B	ES60CHMP4B-F	CCATCAAAGCCAGCCAAGAAG	100bp
	ES60CHMP4B-R	CAGCCGATTACTGCTGTGGT	
CTNNB1	ES60CTNNB1-F	CAATGGCTTGGAACGAGACAG	129bp

	ES60CTNNB1-R	CCAAGGCATCCTGACCGTAT	
FDZ1	60FDZ1-F	TTCTGGATCTGGTCGGGGAA	181bp
	60FDZ1-R	CCCCAAGTCTGTCCAAGC	
FZ10	60FDZ10-F	ATCCCAGCCTGTAGGGTCAT	164bp
	60FDZ10-R	TCATCTGACCCGTTGTTGGG	
ERMIN	ES60ERMIN-F	AGAGGAGCAATGCGGAGAAAA	87bp
	ES60ERMIN-R	TGGGGCTCAGTCGTATCCTG	
GAPDH	ES603'GAPDH-F	CAAGCTTGTTTCCTGG- TATGACA	196bp
	ES603'GAPDH-R	GGAACAGAACTGGCCTCTCA	
GAPDH	ES605'GAPDH-F	AGTCGGAGTCAACGGATTTGG	216bp
	ES605'GAPDH-R	AAGATAGTGATGGCGTGCCC	
HES1	ES60HES1-F	GCCGACCTGATGGAGAAGAG	212bp
	ES60HES2-R	GAGTGCCGCGAACTATCCTT	
HES5-like	ES60HES5like-F	CCGTGACCGGATTAACAGCA	165bp
	ES60HES5-like-R	TTGTGAATGAATGCTGGCTCC	
HES5A	ES60HES5A-F	CCTGAAATACAGCCGAGCTTTT	270bp
	ES60HES5A-R	TACCAAGGCCTCCAGAGGTT	
HES6	ES60HES6-F	ACAAGCTGTCCAGCACCAA	222bp
	ES60HES6-R	CCACTTTGGAATCAGCCATCA	
HESX1	ES60HESX1-F	TGCTTTCACTAGAAAC- CAGATTGA	499bp
	ES60HESX1-R	ACACAACCCAGAACTTAC- GGTT	
HEY1	ES60HEY1-F	GGCCGGAGGGAAAGGTTATT	249bp
	ES60HEY1-R	TGAGGGTGATGTCCAAAGGC	
HMBS	ES60HMBS-F	CCTCTGCTTTGAGATTGTT- GCC	77bp
	ES60HMBS-R	TCTCCCAATCTTAGAAAGCG	
LEF1	ES60LEF1-F	AAGCGCAGCTATCAACCAGA	205bp
	ES60LEF1-R	TCTGGGGCCTGTACCTGAT	
MAP2	ES60MAP2-F	TTCTGCAGGGGGAGGAAATG	111bp
	ES60MAP2-R	CGTCCACCTCCTGGCTTG	
NOTCH1	ES60NOTCH1-F	GGCGGCCTCCGGATCTAT	199bp
	ES60NOTCh1-R	GCACTGCTGCACTGGCAC	
PAX3	ES60PAX3-2F	AGCTCGAGTTCAGGTTTGGT	165bp
	ES60PAX3-2R	GTGGGCTGATAGGATGGCTC	
PAX7	P7	AATGGCCTCTCTCCG- CAGGTGA	282bp
	ES60PAX7-R	CAAATAATCAACAGCAGTTT- GTCCA	
PAX7	P9	CAAAACAAGATGCAG- TGCTCCAG	318bp

	ES60PAX7-R	CAAATAATCAACAGCAGTTT-GTCCA	
TCF7L1	ES60TCF7L1-F	ATGAACGCCTCCATGTCCAG	178bp
	ES60TCF7L1-R	TGATGGGGGATTTCGAGCTG	
TCF7L1-2	ES60TCF7L1-2R	GCGATCCTGTAAGGGAAGGG	341bp
	ES60TCF7L1-2R	GCTGTCGTCTGACCACTTCA	
WNT1	ES60WNT1-F	GATCGTTAACAGGGGGTGCC	409bp
	ES60WNT1-R	GTCGAAGCGGTCTTTGAGGA	
WNT3a	ES60WNT3A-F	TTACCTGGTCGGGTCGAGTT	304bp
	ES60WNT3A-R	CAATCGCCAAGGACCACCA	
WNT4	ES60WNT4-F	AGGTGGTAACACAAGGGACG	219bp
	ES60WNT4-R	GGACGTCGACAAAGGACTGT	
YWATZ	ES60YWATZ-F	TCGGCCATGAAGTCGGTAAC	166bp
	ES60YWATZ-R	CCAGCTTCTTCTCGTTCCA	
ZEB1	ES60ZEB1-F	AAGGAGCCATGTTTTCCAATCT	237bp
	ES60ZEB1-R	GTTATTGTAATT-GGTGACTCACAGG	

Table 2-4: List of exon-skipping primers for qPCR. Forward PAX7 primers from (Mao et al., 2008).

In addition to the qPCR primers, pSilencer primers were used for colony PCR. 60Chr1Centromere primers were used for the detection of the genomic DNA, by amplifying the untranscribed centromere region of chromosome 1. The centromere primers were designed using NCBI Primer BLAST. The pSilencer primers had been previously designed by other members of the AG Wizenmann.

Primer Name	Sequence	T <sub>a</sub>	Amplicon
pSilencer-F	GGAAACTCACCTAACTGTAAA	56°C	229bp (with 66bp insert)
pSilencer-R	CGCGCAATTAACCCTCAC		
60Chr1Centromere-F	GATACCGTTCCACCGGAAA	60°C	104bp
60Chr1Centromere-R	AAATGCCACGTACTGGGGAG		

Table 2-5: List of primers used for cloning and gDNA detection.

For knockdown experiments, siRNA targeting PAX7 was designed using GeneScrips siRNA Target Finder.

The design of the full oligonucleotide used for cloning derived from the manufacturer's instructions. A loop segment was flanked by the sense (5' side) and the antisense (3' side) sequence for the siRNA. The 5' end has a full Apal site, the 3' end a full EcoRI site, allowing for removal of the insert, if needed.

Name	Sequence
siPAX7 506 S	CTCCTCTGCAGGTACCAAGATTCAAGAGATCTTGGTACCTG- CAGAGGATTTTTAG
siPAX7 506 A	AATTCTAAAAAATCCTCTGCAGGTACCAAGATCTCTTGAATCTT- GGTACCTGCAGAGGAGGGCC
siPAX7 1105 S	CCCAACTCGCAGCATTCAACTTCAAGAGAGTT- GAATGCTGCGAGTTGGTTTTTAG
siPAX7 1105 A	AATTCTAAAAAACCAACTCGCAGCATTCAACTCTCTTGAAGTT- GAATGCTGCGAGTTGGGGGCC
siPAX7 2372 S	CGACCTATGGACCAACATATTCAAGAGATATGTTTGGTCCA- TAGGTCTTTTTTAG
siPAX7 2372 A	AATTCTAAAAAAGACCTATGGACCAACATATCTCTTGAA- TATGTTTGGTCCATAGGTCGGGCC

Table 2-6: List of siPAX7-oligonucleotides for cloning in pSilencer1.0 plasmids. The underlined sequences mark the siRNA sequences.

## 2.4 Antibodies

Antibodies were used for western blotting and fluorescence immunohistochemistry (IHC).

Antibody	Manufacturer	Type	Application (dilution)
anti active- $\beta$ -catenin (ABC) antibody, clone 8E7	Upstate	mouse IgG1 $\kappa$	IHC: 1:100 WB: 1:1000
anti $\beta$ Catenin non-phospho(active) S45 antibody	Abcam	rabbit IgG	WB 1:1000
anti GAPDH antibody	Abcam	mouse IgG2b	WB 0.1 $\mu$ g/ml
anti GFP antibody	MoBiTec	rabbit IgG	IHC: 1:1000
anti HES1 antibody (E-5)	Santa Cruz Biotechnology	mouse IgG2b	IHC 1:100
anti HES4 antibody (D12)	Santa Cruz Biotechnology	mouse IgG1	IHC 1:100
anti PAX7 antibody	DSHB	mouse IgG1 $\kappa$	IHC: 2-5 $\mu$ g/ml WB: 0.5 $\mu$ g/ml

Table 2-7: List of primary Antibodies. Used for Western blot and IHC.

Antibody	Manufacturer	Chemistry	Application (dilution)
Affinipure goat anti mouse, IgG (H+L), F(ab') <sub>2</sub>	Jackson Immuno Research	Cy3	IHC 1:200
Affinipure goat anti rabbit IgG (H+L) F(ab') <sub>2</sub> Fragment	Jackson Immuno Research	Alexa488	IHC 1:200
ECL Anti-Rabbit IgG, whole donkey antibody	Amersham	HRP	WB 1:250

Table 2-8: **List of secondary antibodies.** Used for Western blot or IHC. The secondary antibody for Western blots using mouse primary antibodies is not listed, as it was part of the Pierce Fast Kit (see Table 2-11).

## 2.5 Bacterial Strains

For cloning, transformation and plasmid expansion DH5 $\alpha$  competent *E.coli* from NEB (C2987) were used. This is commonly used strain of bacteria allows for high transformation efficiency and easy selection using plasmids encoding an ampicillin resistance gene.

## 2.6 Chemicals

Name	Manufacturer
10x Buffer A+ATP	Fermentas
10x DreamTaq Buffer	Thermo Fischer Scientific
10x DreamTaq Buffer (green)	Thermo Fischer Scientific
10x Exonuclease Reaction Buffer	Thermo Fischer Scientific
1Kb Plus DNA Ladder	Thermo Fischer Scientific
20x DNA Binding Dye Sample Loading Reagent	Fluidigm
20x Bolt™ MES SDS Running Buffer	Thermo Fischer Scientific
2x Assay Loading Reagent	Fluidigm
2x Quick Ligase Buffer	NEB
5x RT Buffer	Thermo Fischer Scientific
6x Loading Dye	Fermentas
Ampicillin Sodium Salt	Carl Roth
10x Antarctic Phosphatase Buffer	New England Biolabs
Boric Acid	Carl Roth
Bromophenol Blue	Carl Roth
Chloroform	AppliChem
Control Line Fluid	Fluidigm
Color Prestained Protein Standard	NEB
CutSmart Buffer	New England Biolabs
Disodium Phosphate	Carl Roth
DRAQ5	Invitrogen
dNTP-mix	Invitrogen
Dithiothreitol (DDT)	Carl Roth

Ecosurf SA-9	Carl Roth
Ethylenediaminetetraacetic acid (EDTA)	Carl Roth
Ethanol	IWT reagents
Fast Green	Sigma Aldrich
Fetal Calf Serum (FCS)	Sigma Aldrich
Gel Green	Biotium
Glacial Acetic Acid	Merck
Glycerol	Merck
Glycine	AppliChem
Immersol Immersion Oil	Carl Zeiss
Isopropanol	Sigma Aldrich
LB-Agar (Luria/Miller)	Carl Roth
LB-Medium	MP Biomedicals
Methanol	VWR
3-(Morpholin-4-yl)propane-1-sulfonic acid (MOPS)	Carl Roth
Oligo dT-Primers	Carl Roth
PageRuler Plus Prestained Protein Ladder	Thermo Fischer Scientific
Penicillin/Streptomycin Solution	Gibco BRL, Karlsruhe
Polysorbate 20 (Tween20)	Sigma Aldrich
PonceauS Reagent	Thermo Fischer Scientific
Potassium Chloride	Carl Roth
Potassium Phosphate	Sigma Aldrich
Proteinase Inhibitor	AppliChem
2x Quick Ligase Buffer	New England Biolabs
Revert™ 700 Total Protein Stain	Licor
Ringer Solution	Fresenius Kabi GmbH
SeaKem LE Agarose	Lonza Group Ltd.
Sodium Dodecyl Sulfate (SDS)	AppliChem
SOC Broth	NEB
Sodium Acetate	Carl Roth
Sodium Chloride	Carl Roth
Tris-EDTA buffer pH8	Invitrogen
Tissue Tek	Sakura
TritonX	AppliChem
TrisBase	Sigma Aldrich
Trisodium Citrate	Merck
PeqGold TriFast Extraction Reagent	VWR
Water, RNase free	Invitrogen

Table 2-9: *List of chemicals.*

## 2.7 Solutions

### 2.7.1 Solutions for Bacteria Culture

For liquid culture, LB-broth was prepared and autoclaved. Ampicillin was added to a final concentration of 100µg/ml.

#### LB Broth

25g	LB medium, powder
1l	H <sub>2</sub> O

LB agar plates were prepared in batches from autoclaved, previously dissolved LB agar, by heating the gel using a microwave. Ampicillin was added prior to casting at 100µg/ml.

#### LB Agar

40g	LB agar, powder
1l	H <sub>2</sub> O

Cryo-stocks of transformed *E.coli* were prepared using a 1:1 mixture of autoclaved LB broth and glycerol.

### 2.7.2 Solutions for Electroporation

To compensate for evaporation during electroporation and to prevent infection of the egg, a few drops of Ringer solution with Pen/Strep were added to each egg.

#### Ringer Solution with Pen/Strep

8ml	Ringer Solution
8µl	Penicillin/Streptomycin Solution

The plasmid DNAs were mixed with FastGreen to visualize injection prior to electroporation. The final concentration of each individual plasmid was approximately 1 µg/µl.

#### Injection Solution

20µg	Plasmid DNA, per plasmid
1µl	FastGreen
x µl	RNase free H <sub>2</sub> O
<hr/>	
20µl	

### 2.7.3 Solutions for Electrophoresis

For agarose gel electrophoresis a 10x Tris-Borate-EDTA (TBE)-buffer was prepared. Diluted down to 1x TBE, it was used as chamber solution and to cast the gels.

#### 10x TBE buffer

108g	Tris base
55g	Boric acid
40ml	0.5M Na <sub>2</sub> EDTA (pH 8.0)
X ml	H <sub>2</sub> O
<hr/>	
1l	

Depending on the size of the electrophoresis chamber, different sized agarose gels were prepared, usually at 1% w/w. TBE was heated using a microwave solubilizing the agarose. GelGreen was added after heating. Evaporated volume was adjusted using water.

#### 1% Agarose gel

Agarose	0.4g	0.8g	2g
1x TBE buffer	40ml	80ml	200ml
GelGreen	0,4µl	0,8µl	2µl
<hr/>			
total volume	40ml	80ml	200ml

## 2.7.4 Solutions for Western Blots

Proteins were initially dissolved and stored in 1% SDS solution.

### 1% SDS solution

1g	SDS
100ml	H <sub>2</sub> O

For SDS-PAGE, the protein was then mixed with 2x SDS probe buffer.

### 2x SDS probe buffer

0.24g	Tris base
6g	SDS
0.02g	Bromophenol blue
3.08g	DTT
x $\mu$ l	H <sub>2</sub> O
<hr/>	
100ml	
+12ml	Glycerol

Some western blots were ran using MOPS-SDS running buffer, prepared as a 20x stock. Later blots used a pre-mixed MES-SDS running buffer. Both buffers were diluted 1+19 with water.

### 20x MOPS-SDS Running Buffer

104.6g	MOPS
60.6g	Tris base
10g	SDS
3g	EDTA
x $\mu$ l	H <sub>2</sub> O
<hr/>	
500ml	

For blotting the protein onto the nitrocellulose membrane, a semi-dry blot buffer was used.

#### Semi-Dry Blot Buffer

2.9g	Tris base
0.185g	Glycine
0.185g	SDS
100ml	Methanol
<u>x <math>\mu</math>l</u>	<u>H<sub>2</sub>O.</u>
500ml	

Stripping buffer was used to remove primary and secondary antibodies from nitrocellulose membranes previously stained. HCl was added until pH2.

#### Stripping Buffer

0.94g	Glycine
5g	SDS
5ml	TritonX
<u>x <math>\mu</math>l</u>	<u>H<sub>2</sub>O</u>
500ml	

The membranes were washed post stripping, using Tris-Buffered-Saline (TBS) and TBST (TBS+Tween) buffers. The TBS was prepared as 10x TBS stock and diluted down 1+9 with water when needed. Its pH was adjusted to pH7.6 using HCl.

#### 10x TBS

12g	Tris base
<u>44g</u>	<u>Sodium chloride</u>
500ml	

1xTBST

100ml	10x TBS
900ml	H <sub>2</sub> O
1ml	Tween20

For whole protein stains a wash solution and destaining solution were prepared.

Wash Solution

33.5ml	Glacial acetic acid
150ml	Methanol
to 500ml	H <sub>2</sub> O

### 2.7.5 Solutions for Immunohistochemistry

Cryosections were washed using Phosphate-Buffered-Saline (PBS), prepared as a 10x stock. Antibody solution, derived from PBS was used to dilute antibodies and to block unspecific binding sites. 1x PBS was obtained by mixing it 1+9 with water.

10x PBS

17.8g	Disodium Phosphate
2.4g	Potassium Phosphate
80g	Sodium Chloride
2g	Potassium Chloride
<u>x ml</u>	<u>H<sub>2</sub>O</u>
1l	

Antibody Solution

900ml	1x PBS
100ml	FCS
<u>1ml</u>	<u>Ecosurf</u>

A mixture of 9 parts glycerol with 1 part PBS was used as cover media for slides.

## 2.8 Enzymes

Name	Manufacturer
10x Antarctic Phosphatase (5U/μl)	New England Biolabs
Apal	NEB
EcoRI-HF (20U/μl)	NEB
Exol	Thermo Fischer Scientific
DNaseI	Fermentas
DNaseI	NEB
DreamTaq DNA Polymerase (5U/μl)	Thermo Fischer Scientific
Maxima H Minus Reverse Transcriptase (200U/μl)	Thermo Fischer Scientific
Quick Ligase	NEB
Murine RNase Inhibitor (40U/μl)	NEB
T4 Polynucleotide Kinase (10U/μl)	Fermentas

Table 2-10: **List of enzymes.** Enzymes included in kits are not listed separately. Manufacturer supplied buffers were used, if not specified otherwise.

## 2.9 Kits and Master Mixes

Name	Manufacturer
Extract Me Total RNA kit	Blirt
NEBNext Single Cell/Low Input cDNA Synthesis & Amplification Module	NEB
peqGold TRIfast	Peqlab
Pierce Fast Western Blot, Super Signal West Femto Mouse kit	Thermo Fischer Scientific
Plasmid Plus Midi Kit	Qiagen
QIAzol/Maxtract/RNeasy,	Qiagen
QuantiNova SYBR Green PCR Kit	Qiagen
Qubit Protein Assay kit	Thermo Fischer Scientific
RNeasy Plus Micro Kit	Qiagen
SyberScript IV CellsDirect cDNA Synthesis kit	Thermo Fischer Scientific

Table 2-11: **List of kits.**

Name	Manufacturer
PreAmp Master Mix	Fluidigm
SsoFast EvaGreen Supermix with low ROX	BioRad

Table 2-12: **List of master mixes for PCR applications.**

## 2.10 Instruments and Consumables

- 0.5ml, 1.5ml and 2ml DNase/RNase free reaction tubes (Eppendorf)
- 1.4/2.8mm ceramic bead lysis tubes (OMNI international)
- 15ml and 50ml DNase/RNase free reaction tubes (Falcon)
- 200µl PCR reaction tubes (Biorad)
- Bolt™ Bis-Tris Plus acrylamide gels, as 4-12%, 8% and 12% gels (Thermo Fischer Scientific)
- Cover slides for microscope slides, 24x50mm
- Curves, sharp-pointed scissors
- Egg stools, cut from water pipe insulation
- Filtered Micropipette tips 10µl, 200µl, 1000µl (Starlab)
- Fine watchmaker's forceps
- Glass capillary TW100-3 (WPI) inside  $\varnothing$  0.75 mm, outer  $\varnothing$  1 mm
- Ice bucket
- Micropipette tips 10µl, 200µl, 1000µl (Starlab)
- Micropipettes, 0.1-2.5µl, 1-10µl, 2-20µl, 10-200µl, 100-1000µl (Gilson and Eppendorf)
- Microscope slides SuperFrost® plus (R. Langenbrinck)
- Nitrocellulose membrane 0.2µm (Amersham)
- Octa channel micropipette (Eppendorf)
- Parafilm, size M (Bemis)
- Petri dishes, sterile  $\varnothing$  6 cm and  $\varnothing$  10 cm
- Platinum electrode (self-made)
- Pure tungsten wire
- Reaction tube stands
- Scalpel blade and handle
- Sellotape and thick plastic canvas tape
- Serological pipettes, 5ml, 10ml, 25ml, 50ml (Thermo Fischer Scientific)
- Sous vide tube
- Stainless steel spatula, 5-8 mm wide tip
- Syringes (20 ml) and needles  $\varnothing$  0,1 mm, sterile

- ultrafine scissors
- Vannas spring scissors
- QIAxcel Cartridge (Qiagen)

## 2.11 Devices

Device	Model	Manufacturer
Agarose Electrophoresis Chamber	GH202	Biostep
Agarose Electrophoresis Chamber	40-2314-N	Peqlab
Agarose Electrophoresis Power Supply	Consort E844	Merck
Autoclave	VX100	Systec
Capillary electrophoresis device	QiAxcel Advanced System	Qiagen
Centrifuge	5415D	Eppendorf
Centrifuge	Heraeus Fresco 17	Thermo Scientific
Centrifuge	Heraeus Megafuge 16R	Thermo Scientific
Centrifuge	MiniSpin	Eppendorf
Chip loader	IFC controller HX	Fluidigm
Chip loader	IFC controller MX	Fluidigm
CLSM	LSM 510 Meta	Zeiss
Egg incubator	Bertha 56	Campo24
Electric pulse source	Intracel TSS	Intracel
Fluorescence source	HXP 120C	Zeiss
Fluorescent microscope	Observer Z1	Zeiss
Fluorometer	Qubit 2.0	Thermo Fischer Scientific
Gel Visualizer	Pharmacia Biotech Image Master VDS	Amersham Biosciences
Incubator Block/Shaker	Thermomixer Comfort	Eppendorf
Incubator/Shaker	GFL 3031	Gesellschaft für Labortechnik mbH
Micropipette Puller	PUL-1	World Precision Instrument
Microwave	NN-E205W	Panasonic
PCR cycler	My Cycler	Bio Rad
PCR cycler	Primus 96	MWG-Biotech
PCR cycler	peqStar, 96 Universal Gradient	Peqlab
Plate centrifuge	Perfect Spin P	Peqlab
Petri dish incubator	Heratherm	Thermo Fischer Scientific

Pipettboy	Pipetus	Hirschmann Laborgeräte
Pulse Stimulator	Intracel TSS10	Intracel Ltd.
qPCR cycler, 96well	StepOne Plus	Applied Biosystems
qPCR cycler, chip format	Biomark	Fluidigm
Reaction Tube Rotor	-	H Saur Laborbedarf
Scale	ABJ 220-4NM	Kern & Sohn
Scale	-	Sartorius
Vacuum Sealer	vacuplus	Petra Electronic
SDS-PAGE Chamber	XCell SureLock Mini-Cell	Thermo Fischer Scientific
SDS-PAGE Chamber	ECO-Maxi EBC	Biometra
SDS-PAGE Power Supply	-	Biometra
Shaker	Vibrax-VXR	IKA
Spectrophotometer	Nanophotometer Pearl	Implen
Steam cooker	FS300	Braun
Tissue Lyser	Minilys	Bertin
Western blot imager	Odyssey FC	Licor
Western Blot, blotting cassette	Fastblot B43	Jena Analytik
Apotome	Observer.Z1	Zeiss
Binocular microscope (Imaging)	MZFLIII	Leica
Binocular microscope (Preparation)	Stemi 2000-C	Zeiss
Light source	KL1500 electronic	Schott
Cryotome	CM3050 S	Leica
pH meter	WTW Series	InoLab

Table 2-13: *List of devices.*

## 2.12 Software

Adobe Photoshop CS6  
 DNASTar Lasergene 15  
 Fiji 2.16  
 Fluidigm BioMark Software Suit  
 IBM SPSS Statistics 29.0.2.0  
 Licor Empiria 3.0.0.173  
 Microsoft Excel 2011  
 Microsoft Excel 365

Microsoft Word 2011

Microsoft Word 365

Qiagen QIAxcel ScreenGel

Thermo Fischer Scientific StepOne™ Software

Zeiss ZEN blue/black

## **2.13 Online Tools and Software**

<http://biotools.nubic.northwestern.edu/OligoCalc.html>

<https://blast.ncbi.nlm.nih.gov/Blast.cgi>

<https://www.ncbi.nlm.nih.gov>

<https://www.genscript.com/tools.html>

<https://www.google.com>

<http://geisha.arizona.edu/geisha/>

## **2.14 Outside Services**

Eurofins Genomics was used as the only outside service. They supplied custom oligonucleotides, and their Light Run sanger sequencing service was used.

## 3 Methods

### 3.1 Plasmid Generation

Plasmids are small, circular DNA constructs that are commonly used in molecular biology, due to their stability and easy expandability in bacteria they are a great vehicle to deliver genes into cells and tissues.

While most plasmids had already been generated for previous studies a new set of three siRNA plasmids was generated, with the aim of more efficiently repressing the expression of PAX7 *in-ovo*. The idea was, that three siRNAs targeting the same PAX7 mRNA would result in a stronger and more specific knock-down than the singular siRNA used in previous experiments. siRNAs are short (19-23nt) fragments of RNA, that inhibit translation and induce degradation of complementary mRNA by associating with the RISC complex.

#### 3.1.1 siRNA Sequence Selection

19nt long siRNA sequences were selected using GeneScrips online siRNA Target Finder and checked for off target binding using BLAST. The sequences selected were combined with ligation adapters and a loop sequence, allowing for easy cloning and generation of the required hairpin loop dsRNA when being expressed *in-ovo*, and ordered alongside their antisense sequence from Eurofins.

5' C N(19) TTCAAGAGA N*(19) TTTTITAG 3'
3' CCGG N*(19) AAGTTCTCT N(19) AAAAAATCTTAA 5'

*Figure 3-1: Sequence used for siPAX7-pSilencer1.0 cloning. Backbone sequence results in sticky ends, compatible with Apal and EcoRI digested pSilencer1.0 plasmid. N(19): sense si-sequence, 19bp length, N\*(19) antisense si-sequence, 19bp length.*

#### 3.1.2 pSilencer1.0 Plasmid Digest

The pSilencer1.0 plasmid was used as backbone for cloning. It was obtained by digesting the preexisting siPAX7-pSilencer with EcoRI-Hf and Apal in CutSmart buffer using the following reagents:

2µl (1µg)	pSilencer-siPAX7 plas- mid
10µl	10x CutSmart buffer
5µl	EcoRI-HF
5µl	Apal
78µl	RNase free H <sub>2</sub> O
<hr/>	
100µl	

Initially only EcoRI-HF was added and incubated for 20min at 37°C, then Apal was added and incubated for 20min at 25°C. The enzymes were inactivated at 65°C for 10min. Negative controls without restriction enzymes were carried along.

### 3.1.3 Agarose Gel Electrophoresis

Agarose gel electrophoresis is a simple method for size analysis of DNA fragments. The DNAs backbone consists of 2-desoxyribose and a phosphate group, which carries a negative electric charge. This charge causes DNA to migrate towards the cathode in an electric field, which is used in gel electrophoresis. Here the DNA fragments migrate through an agarose gel in an electric field, resulting in a size separation, as smaller fragments encounter less resistance from the gel, thus migrating faster.

The DNA fragments can be visualized using intercalating dyes, like GelGreen, which can be added to the liquid gel prior to casting or after DNA separation by bathing the gel for a few minutes. The latter one results in an overall better separation of bands, as the dyes interfere with the migration, but also adds additional steps.

Gel electrophoresis allows for the separation of single and double stranded DNA, as well as RNA, but their migration characteristics differ, requiring different size markers, voltages and run times.

For this study, all gels were self-cast, usually using 1% w/w of Agarose in the final gel. Total volume was scaled for the different sized chambers. GelGreen was always added prior to casting, as gels were just used as spot-checks and weren't used for quantification.

Agarose and TBE buffer were heated using a microwave until fully dissolved. GelGreen was added afterwards, if strong evaporation occurred during heating, the total volume was adjusted using water. The liquid gel was poured bubble-free on the trays, combs were added, and the gel was left on the bench for 15min, before being chilled to 4°C to harden.

Electrophoresis chambers were filled using 1xTBE buffer. Combs were removed inside the chamber, to prevent gel pockets from collapsing. Depending on the upstream application, various amounts of DNA were loaded. Voltage and runtime were adjusted, depending on the expected fragment size and the chamber used. The fragments were visualized using UV light.

A few µl of the siPAX7-pSilencer1.0 digest product were mixed in a 5+1 ratio with 6xDNA loading dye and loaded on a 1% agarose gel containing GelGreen, alongside the native siPAX7-pSilencer and a 1kb+ ladder for size comparison. The gel was run for 60min at 120V.

### 3.1.4 Plasmid Dephosphorylation

The digested plasmid was dephosphorylated using Antarctic phosphatase. This prevents self-ligation during cloning, as ligases require 5' phosphates to ligate two DNA strands. Dephosphorylation was achieved by heating the following mix to 37°C for 30min:

51µl	digested siPAX7-pSilencer
6µ	10x Antarctic phosphatase buffer
3µl	Antarctic phosphatase
<hr/>	
60µl	

The reaction was terminated by heating to 90°C for 2min.

### 3.1.5 siPAX7 Insert Phosphorylation

Sense and antisense strand were mixed equimolar (100pmol/l) in 1xDreamTaq buffer and annealed by heating to 95°C for 3min and to 37°C for 30min prior to 5' phosphorylation. This is required, as ligases generally require a 5' phosphate

group when ligating DNA strands. Phosphorylation was performed using T4 kinase using following reaction mix:

8µl	annealed DNA insert (45pM)
4µl	buffer A
0.4µl	ATP (100pM)
2µl	T4 polynucleotide kinase
25.6µl	RNase free H <sub>2</sub> O
<hr/>	
40µl	

The reaction mix was incubated for 20min at 37°C.

### 3.1.6 Ligation

The digested and dephosphorylated plasmids and the phosphorylated siPAX7-inserts were ligated in an approximated molar plasmid to insert ration of 1:4 using quick ligase. The complementary sticky ends produced by the digest facilitated insertion and ligation in the desired direction. The required amount of insert was calculated using this formula:

$$n_{insert} = \frac{n_{plasmid} * size_{insert}}{size_{plasmid}}$$

The inserts had a size of 56bp and the digested pSilencer1.0 plasmid had a size of approximately 3300bp. In combination with the 49ng of plasmid used, this resulted in an ideal amount of 830pg of phosphorylated insert per reaction:

5.8µl	digested and dephosphorylated pSilencer1.0 plasmid (5.8ng/µl)
1µl	phosphorylated siPAX7 insert (400 to 600 pg/µl)
10µl	2x quick ligase buffer
1µl	quick ligase
2.2µl	RNase free H <sub>2</sub> O
<hr/>	
20µl	

The reactions were incubated for 30min at room temperature and then directly used for transformation.

### 3.1.7 Transformation

To amplify the amount of freshly ligated plasmid, it was transformed into NEB DH5 $\alpha$  competent *E.coli* using a heat shock.

The cells were thawed on ice for half an hour and then mixed with equal amounts of ligation product. After another 30min on ice, the cells were heat shocked at 42°C for 30sec, causing them to incorporate the plasmids. The cells were incubated on ice for another final 5min, then 25 $\mu$ l of cells were mixed with 475 $\mu$ l of SOC broth and incubated for 60min, at 37°C and 250rpm in a heat block.

The entire 500 $\mu$ l were plated using plastic beads, on self-cast LB-agar plates containing ampicillin at 100 $\mu$ g/ml. The ampicillin prevents all bacteria, that didn't absorb ligated plasmid containing an ampicillin resistance gene to die. The plates were incubated for 20h at 37°C.

### 3.1.8 Colony PCR

A master mix for 20 reactions was prepared as follows:

50 $\mu$ l	10x green DreamTaq buffer
40 $\mu$ l	dNTP-mix
20 $\mu$ l	pSilencer-F primer
20 $\mu$ l	pSilencer-R primer
2 $\mu$ l	DreamTaq polymerase
348 $\mu$ l	RNase free H <sub>2</sub> O
<hr/>	
500 $\mu$ l	

Individual reactions of 25 $\mu$ l were prepared, alongside 15 liquid cultures of 5ml LB-broth, once again containing 100 $\mu$ g/ml of ampicillin. Five colonies per plate were selected, marked on the plate and the picked up using a 10 $\mu$ l pipet. The pipets tip was initially dipped into a PCR mix, pipetted up and down three times and then dropped into one of the liquid cultures.

The liquid cultures were incubated for 18h at 37°C in an incubator-shaker combination with 250rpm. The PCR reactions were cycled using this protocol:

95°C	2min	1x
<hr/>		
95°C	30sec	
56°C	30sec	
72°C	15sec	40x
<hr/>		
72°C	2min	1x
8°C	∞	

The PCR products were analyzed using gel electrophoresis in an 1.2% agarose gel, using 5µl reaction product, running for 40min at 120V.

### 3.1.9 Mini Preparation Plasmid Isolation

For each different insert, depending on the results of the colony PCR, three liquid cultures containing the insert were selected for plasmid isolation. 2ml of culture were used for isolation using the Monarch Plasmid Miniprep Kit from NEB. The concentration of the DNA obtained was measured using a spectrometer at 260nm wavelength. The 260/280nm ratio was used to determine the purity, with a ratio of approximately 1.8 correlation with pure DNA. The concentration was calculated automatically by the spectrometer.

150ng of plasmid DNA was sent out for sanger sequencing using Eurofins Light Run services. The pSilencer-F primer was as sequencing primer.

### 3.1.10 Glycerol Cryo Stocks

Long term storage of transformed cells at -80°C requires bacteria to be suspended in a mixture of glycerol and LB broth. The glycerol prevents ice crystals from forming and penetrating the bacterial cell membrane and wall. Bacteria stored in form of glycerol stocks can be regrown by simply scratching some ice from the top of the stock and resuspending it in LB broth, allowing the isolation of fresh plasmid decades after it has initially been transformed into bacteria.

For the preparation of glycerol stocks, the remaining 3ml of the liquid cultures were pelleted for 3min at 6000g and then simply resuspended in 1.5ml 1:1

mixture of glycerol and LB broth. For each insert, one stock, for which the sequencing confirmed the desired insert, was stored at -80°C.

### 3.1.11 Midi Preparation Plasmid Isolation

As electroporation requires larger quantities of plasmid DNA, 100ml LB broth cultures, with 100µg/ml of ampicillin were grown for 14h at 37°C and 250rpm in an incubator-shaker. The cultures were grown from the glycerol stocks. The plasmids were then isolated using the Qiagen Plasmid Plus Midi Kit, following the steps of the high-yield protocol, but still using the full 100ml of culture. The plasmid DNA isolated was quantified using a spectrometer and sent out for sequencing using the same primer as before.

### 3.1.12 DNA Concentration

*In-ovo* electroporation is typically conducted using plasmid concentrations between 1µg/µl and 6µg/µl per plasmid in the injection solution. As the three new siPAX7-pSilencer constructs also required an eGFP expressing pCAX plasmid to be electroporated alongside them, a final concentration of at least 4µg/µl was required. This high of a concentration is typically not achieved when isolating plasmids from bacteria, so the DNA needs to be concentrated by precipitation.

DNA was precipitated by mixing 200µl of isolated plasmid with 140µl of isopropanol and 20µl of 3M sodium acetate at a pH of 5.4. The DNA in this mixture was pelleted by centrifugation for 30min at 16000g and 4°C. The supernatant was removed and replaced with 1.5ml of pure ethanol, followed by another 20min of centrifugation under the same conditions. The ethanol was removed afterwards and the pellet air dried for 10min at 37°C in the heat block.

The DNA pellet was resuspended using RNase free water. The volume used was calculated using the following formula, aiming for a final concentration of 6µg/µl to have some headroom for DNA losses during prior steps.

$$V_c = \frac{C_i * V_i}{V_c}$$

The concentration obtained was measured using a spectrometer.

## **3.2 In-ovo Electroporation**

*In-ovo* electroporation is one of the easiest and most reliable methods for the genetic modification of chicken embryos, using once again the property of DNA to move towards the positive electrode in an electric field because of its negatively charged phosphate groups. Injecting plasmid DNA into the neural tube and applying a series of electrical pulses temporarily perforates the cell membranes, allowing DNA to enter the cells following the electric field. This results in a transient, genetic modification of the neural epithelium cells one sided of the brain, whilst the other side remains as an internal negative control.

### **3.2.1 Embryo Staging and Egg Preparation**

Upon postal arrival, the fertilized chicken eggs were laid sideways, and the top was marked as the most likely position for the embryo to grow. 1-2ml of the egg's albumin was removed from the egg using a syringe and an egg picker, poking a hole at the bottom side of the egg, where the air chamber is localized. The eggs were then incubated at 37°C and 65% humidity for 1.5 days using the Berta 56 incubator. The eggs shells were then cut open using a forceps, scissors, and adhesive film. The adhesive film was first applied to the previously marked location, preventing debris from falling on the embryo during the process of cutting. The age of embryonic development was assessed under a binocular microscope using the Hamburger and Hamilton (HH) stages of chicken development.

### **3.2.2 Electroporation**

Chicken embryos at HH stage 9-11 were selected for electroporation. Under a binocular microscope the vitellin membrane was cut open using a sharpened tungsten wire, after a few drops of Ringer solution containing penicillin and streptomycin were added into the egg. This was done to prevent the egg from drying out or getting infected during the further procedures.

A mixture of plasmids, usually around 1µg/µl each, were injected into the neural tube using a micropipette pulled from glass capillaries. The injection mixture also contained 0.05% FastGreen allowing visual tracking of the injection.

After the injection, two electrodes were placed lateral on both sides of the embryo's midbrain. Five to eight electric pulses with a voltage of 20V and duration of 50ms were applied.

The electroporated eggs were sealed back off using tape and put back in the incubator until reaching HH stage 14 or 17.

The growth and electroporation success were monitored and documented using a microscope equipped with a fluorescent light capable of exciting the eGFP encoded on the electroporated plasmids.

### **3.2.3 Tissue Preparation**

Under a binocular microscope, using a sharpened forceps and micro scissors the embryos were removed from their eggs and placed in a petri dish filled with ringer solution. Both sides of the dorsal midbrains of the embryos were isolated and transferred into 1.5ml reaction tubes using a pipet. The supernatant was removed after a centrifugation at 16000g for 1min and the tissue was stored at -20°C or directly processed into RNA, cDNA, or protein. Hindbrains, that by chance sometimes were electroporated as well, were also isolated for further analysis.

A few embryos, electroporated with the three new siPAX7-pSilencer plasmids, had their midbrains imaged as an open book preparation prior to the final tissue isolation, with the idea of measuring potential differences in midbrain size under a microscope. For this special preparation technique, the midbrain is removed from the embryo, and then cut open ventrally, resulting in a flat, butterfly shaped preparation that can be imaged using a conventional microscope.

### **3.2.4 TOP-dGFP Expression**

A TOP-dGFP construct was used to assess canonical Wnt signaling in-ovo. The TOP-dGFP plasmid contains a d2eGFP gene, coding a GFP protein with a short half-life time, under the control of 4 TCF/LEF binding sites. When Wnt signaling is active, CTNNB1 ( $\beta$ -catenin)/TCF complexes bind to the TCF/LEF site, resulting in GFP expression. Due to the short lifespan of the GFP, canonical Wnt signaling can be observed in real time. A plasmid encoding for an RFP protein was electroporated alongside the TOP-dGFP plasmid as an electroporation control. PAX7 expression was modified using pMES- $\Delta$ GFP or pSilencer plasmids, not encoding

any fluorescent proteins. As a baseline, embryos only electroporated with the TOP-dGFP and 2A-lyn-Cherry plasmids were used.

Electroporated embryos were incubated until HH stage 17-18. The electroporated side of the embryo was prepared and imaged quickly, as the fluorescence of proteins isn't as stable as the fluorescence of synthetic dyes.

### **3.2.5 Cell Counting for TOP-dGFP Experiments**

Microscope images were analyzed using Fiji for automated cell counting. In a first step the RFP and GFP channels were turned into a binary image using the threshold function. These binaries were then overlaid and once again turned into a binary, leaving only signal, where RFP and GFP overlapped. The individual cells were then separated using the watershed tool on the RFP and merged binary. Using the analyze particles tool, particles larger than 45 pixels<sup>2</sup>. The ratio of the merged to RFP cell number and area were calculated and compared between different PAX7 expression modifications.

## **3.3 cDNA, RNA and Protein Isolation**

RNA extraction, especially for the analysis of individual dorsal midbrains, presented a challenge.

The quantification of tissue used for RNA isolation using scales wasn't reliable, as the residual ringer solution from tissue preparation had a higher mass than the tissue itself. Most common commercial RNA isolation kits (RNeasy Plus/Micro, peqGold TriFast) couldn't be scaled down sufficiently and even if RNA is isolated, detection and quantification wasn't possible outside of PCR reactions, as neither spectroscopic nor dye-based systems (Qubit, RNA High Sensitivity Kit) had a low enough detection threshold.

Ultimately, a traditional phenol-chloroform extraction was performed, using Peqlabs peqGold TriFast, for the analysis of pooled embryos, as this method also allowed for protein isolation. For the individual analysis of embryos, cDNA was directly synthesized from tissue lysates using SuperScript IV CellsDirect cDNA Synthesis kit from ThermoFischer.

For both methods, the amount of tissue used was controlled by careful and symmetric tissue preparation. For pooled embryo analysis, the amount of RNA used

for cDNA synthesis was measurable and thus controlled. For the remaining variations in concentrations, multiple reference genes were used in qPCR, and whole protein stains were used for western blot normalization.

### **3.3.1 Isolations from Pooled Embryos**

The mid- and hindbrains of embryos at the same Hamburger and Hamilton stage, electroporated with the same plasmids were pooled and their RNA and proteins were extracted using a modified protocol of the peqGold TriFast kit. The RNA was later used for cDNA synthesis prior to qPCR, and the protein was used for western blot analysis.

Pooled tissue was suspended in 1m TriFast reagent and transferred into 1.4/2.8mm ceramic lysis tubes. Tissue lysis was done using a Bertin Minilys system on the medium setting for three times 10s, letting the tubes chill on ice for 1-2min between runs. This step was added to improve yields and reduce genomic DNA contaminations.

The lysates were then transferred into a 2ml reaction tubes, where 200µl of chloroform were added. Tubes were inverted three times, incubated at room temperature for 10min and the centrifuged for 5min at 12000g, separating the clear aqueous phase containing the RNA from the DNA and protein, contained in the interphase and the red phenolic phase.

#### **3.3.1.1 Phenol-Chloroform Protein Isolation**

After separating the aqueous phase from the red phenolic phase and the interphase, the latter two were mixed by with 300µl of pure ethanol. The ethanol caused DNA precipitation during centrifugation for 15min at 2000g and 4°C, after an initial incubation for 2min at room temperature. The supernatant was removed and mixed with 1.5ml of isopropanol, incubated for 10min at room temperature followed by centrifugation for 10min at 12000g, once again at 4°C. The supernatant was discarded, the pellet obtained air dried for 30min at 40°C and resuspended in 1% SDS at 75°C.

The protein obtained was quantified using a spectrometer at 280nm or using the Qubit with its Qubit Protein Assay. For Qubit assays, the manufacturer's

instructions were followed, and new standards were always prepared, prior to quantification.

For short term, the protein was stored at -20°C, for storage longer than a week, samples were kept at -80°C.

### 3.3.1.2 Phenol-Chloroform RNA Isolation

The RNA in the aqueous phase was precipitated by adding 500µl of isopropanol, incubating the mixture on ice for 15min and a 10min centrifugation at 12000g and 4°C. The pellet obtained was washed twice by removing the supernatant and replacing it with 75% ethanol followed by 20s of vortexing and 10min centrifugation under the same conditions.

The pellet obtained was air dried for 20min, resuspended using water at 55°C and quantified using a spectrometer at 260nm. The 260/280 ratio was used for assessment of RNA purity, with ratios of 1.8-2.1 indicating pure RNA. The RNA integrity was measured using a QIAxcel capillary electrophoresis device.

For short term, the RNA was stored at -20°C, for storage longer than a week, samples were kept at -80°C.

### 3.3.1.3 cDNA Synthesis

To be used in PCR and qPCR reactions, RNA needs to be transcribed into cDNA. This is accomplished by reverse transcription using enzymes derived from RNA viruses, like the Maxima H Minus reverse transcriptase.

cDNA synthesis was done in two steps, in the first step, secondary structures in the RNA were dissolved, and oligo dT primer were annealed. This was accomplished by heating the following reaction to 65°C for 10min.

1330ng	total RNA
2µl	dNTP-mix
2µl	oligo dT primers
	RNase free H <sub>2</sub> O
<hr/>	
29µl	

After the first heating step, the reaction was cooled on ice, and following buffers and enzymes were added:

8 $\mu$ l	5x RT buffer
2 $\mu$ l	Maxima H Minus reverse transcriptase
1 $\mu$ l	RNase inhibitor
<hr/>	
40 $\mu$ l	

The reaction containing the enzymes, was now once again heated to 65°C for 30min, followed by heat inactivation for 10min at 85°C.

cDNA was stored at -20°C and used for qPCR within 24h.

### 3.3.2 cDNA Synthesis Using the SyperScript IV CellsDirect Kit

Individual midbrains of embryos electroporated, with mainly the siPAX7-pSi-lencer1.0 and a pCAX plasmids, were used for direct cDNA synthesis with the SyperScript IV CellsDirect cDNA Synthesis kit.

Following the manufacturer's instructions, a lysis master mix was first prepared.

per reaction:

25.61 $\mu$ l	SyperScript IV CellsDirect Lysis Solution
0.26 $\mu$ l	100x Lysis Enhancer
0.53	50x DNase I
<hr/>	
26.4 $\mu$ l	

24 $\mu$ l of lysis mix were added to each individual midbrain half in a 1.5ml reaction tube. Tissue was mechanically lysed using a sterile pestle. After an incubation of 10min 3 $\mu$ l of SyperScript IV CellsDirect Stop Solution were added, mixed, and incubated for another 2min. Both incubations were done at room temperature.

The final step was the reverse transcription itself. For this 8 $\mu$ l of SuperScript IV RT Master Mix were added and the tubes were transferred into a heat block. A master mix without reverse transcriptase was used as negative control.

25°C	10 min	primer annealing
50°C	10min	reverse transcription
85°C	5min	heat inactivation

After the heat inactivation, the cDNA was stored at -20°C.

### 3.3.3 QIAxcel Capillary Electrophoresis

Both, dsDNA and ssRNA capillary electrophoresis was done. DNA electrophoresis was used for quality control spot checks of qPCR products and in primer testing. PCR product was directly loaded, alongside a 15-500bp marker.

## 3.4 Quantitative Real-Time Polymerase Chain Reaction

To analyze the effects of the electroporated plasmids on gene expression on an mRNA level quantitative real-time polymerase chain reaction (qPCR) was used. qPCR is a method derived from regular polymerase chain reaction (PCR). In a PCR, DNA is repeatedly heated up to 95°C to separate its strands. The temperature is then dropped down to usually around 60°C, allowing short oligonucleotides - called primers – to bind to the DNA. In most PCRs two primers per reaction are used specifically binding to opposing strands of the same gene of interest. After the primers are annealed to their DNA template, the reaction temperature is increased to 72°C allowing the Taq-Polymerase to synthesize the complementary strands of DNA starting from the primers. This process is repeated multiple times, theoretically doubling the amount of newly synthesized DNA with every cycle.

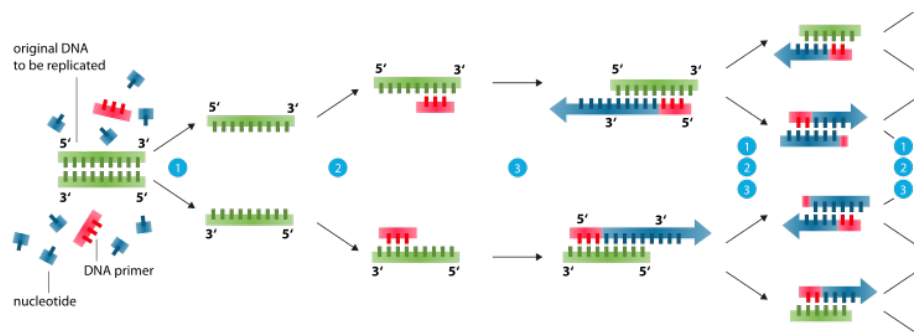


**Figure 3-2: Schematic drawing of a PCR reaction.** If primers are available, the amount of targeted DNA doubles with each cycle, resulting in exponential amplification. **1: Denaturation.** DNA strands separate at 95°C. **2: Annealing.** DNA primers bind template DNA, temperature variable, usually 60°C. **3: Elongation.** The DNA polymerase synthesizes complementary DNA strand, starting at the primers 3' end. Usually at 72°C. Image after (Enzoklop, 2014)

To observe the amplification of DNA with every cycle, an intercalating dye (CYBR-/EVA-Green) can be added to the reaction. These dyes reversibly bind to double strand DNA, allowing the quantification of the total PCR product after each cycle using fluorescence. With the DNA molecules, that the primers bind to, doubling with every cycle the signal intensity from the dyes increases exponentially. This phase, that allows for the quantification of the amount of DNA of the gene of interest, is typically flanked by an initial phase of only background signal caused by the other DNA present in the reaction and a plateau phase in the later cycles caused by the polymerase running out of nucleotides for further DNA synthesis.

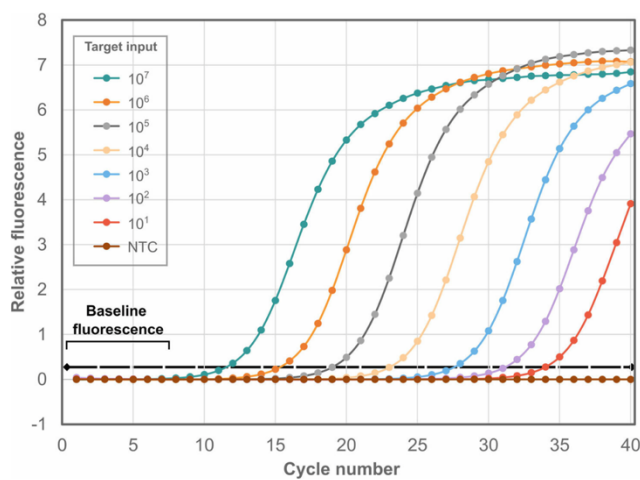


Figure 3-3: **Schematic example of signal curves from qPCR.** Curves have a sigmoid shape. The central, linear part represents the exponential amplification of DNA and is used for quantification. The lower the DNA input, the higher the number of cycles needed for the fluorescence signal to cross the baseline and to show detectable amplification. Image: (Mészáros, 2022)

Using the fluorescence curves, a signal threshold can then be defined. All reactions using the same primers within a run share the same threshold allowing for comparisons of the number of cycles needed to cross it, commonly referred to as  $C_t$  (cycle of threshold crossing) or  $C_q$  (cycle of quantification) value. A threshold as low as possible, whilst still intersecting all signal curves during the phase of exponential amplification is optimal. Most cyclers and software automatically set the thresholds and only in a few instances manual adjustment was needed.

Once the cycling itself is completed, melting curves were obtained. This was done by reducing the temperature of the reactions down to 20°C and then slowly increasing it back up to 95°C while measuring the fluorescence every 0.7°C. The increase of temperature leads to a denaturation of the DNA double strands, causing a reduction in fluorescence. As the sequence of the DNA determines the temperature at which the strands separate, a drastic reduction in signal can be detected at a specific temperature when the PCR product denatures. The change

in fluorescence was blotted against the temperature. A singular peak corresponds to a singular product being produced in the PCR (See figure 4-15).

The experiments were performed using a 96 well format StepOne Plus cycler for pooled embryo analysis or on a Biomark with a 48.48 or 96.96 chip format for single embryo analysis.

### **3.4.1 qPCR Primer Design and Validation**

Primers are one of the key components for stable qPCR reactions. For gene expression analysis primers must bind specifically to the intended cDNA target (=specificity) and show linear (exponential) amplification over a large range for target concentrations (=efficiency).

#### **3.4.1.1 Primer Design**

Initially PCR primers were designed using DNASTAR PrimerSelect. The design criteria were a PCR product length of about 400-600bp, a location close to the 3' end of the mRNAs sequence and a melting temperature of around 60°C. After initial testing these primers were discarded as they also amplified the residual genomic DNA in the cDNA samples.

The primers finally used for qPCR experiments were designed using Primer BLAST. Annealing temperatures of 60°C, the maximum PCR product length of less than 400bp and the RefSeq accession number were used as inputs, as well as the requirement of primers skipping an exon-exon junction to avoid amplification of residual genomic DNA.

For the detection of the two splice variants of the transactivation domain of PAX7 the forward primers P7 and P9 published by Mao et al. were combined with an exon skipping reverse primer. (Mao et al., 2008)

Predicted off target PCR products, using the Gallus gallus mRNA RefSeq library within Primer BLAST, of a length greater than 1500bp with only partial primer binding were accepted and their absence was validated both in regular PCR as well as in the qPCR reactions.

### 3.4.1.2 Primer Validation

All primers were initially tested using regular PCR and agarose electrophoresis. This was done to ensure the primers only amplified the intended gene and only worked on cDNA as a template.

For the PCR reactions a master mix containing cDNA, genomic DNA or plasmid DNA was prepared on ice. Primers were added individually afterwards.

X $\mu$ l	Template (2.5 $\mu$ l cDNA or 50ng plasmid DNA)
2.5 $\mu$ l	10x green DreamTaq buffer
2 $\mu$ l	dNTP-mix
0.1 $\mu$ l	DreamTaq polymerase
Y $\mu$ l	RNase free H <sub>2</sub> O
<hr/>	
23 $\mu$ l	

1 $\mu$ l of forward and 1 $\mu$ l of reverse primer (both 10 $\mu$ mol/l) were added to each reaction for a total reaction volume of 25 $\mu$ l. PCR grade water was used as no primer control.

The genomic DNA was used as a control for cDNA specific amplification. The reactions containing cDNA were used to determine the gene specificity of the primers by analyzing the length of the PCR product produced. Plasmid DNA was used to check the splice variant selectiveness of the P7 and P9 primer combinations, as in most tissues both splice variants seem to be expressed.

sPAX7-pMES- $\Delta$ GFP and iPAX7-pMES- $\Delta$ GFP were used as plasmid DNA.

Reactions were performed using the Primus 96 cycler. A total number of 40 cycles was used to amplify weakly expressed genes and have a higher chance of detecting unintended amplification products.

95°C	5min	1x
<hr/>		
95°C	1min	
60°C	45sec	
72°C	1min	40x
<hr/>		
72°C	5min	1x
20°C	∞	

Initially some temperature gradient PCRs were performed, with the intend of optimizing annealing temperatures. This idea was soon discarded, as both qPCR cyclers only supported one annealing temperature per plate or chip.

The PCR products were analyze using agarose gel electrophoresis, as described in 3.1.3. PCR products were loaded onto the gel, alongside with a 1kb+ DNA ladder for size comparison of the products. If only one band, at the expected size was detected in the reactions containing cDNA and no band in the reaction containing genomic DNA the primer was assumed to be specific. For the reactions containing plasmid DNA, the P7 primer was expected to only amplify the short TA splice variant of PAX7, and the P9 primer was expected to only amplify the long TA splice variant of PAX7.

In a second step the primer efficiency was tested using a dilution series of cDNA, derived from wildtype spinal cord RNA of HH stage 29 chicken embryos. The efficiency describes the ability of a PCR reaction to consistently double a template each cycle. The efficiency depends on the primers; the other chemicals present in the reaction and the surrounding reaction conditions. As a result of this it is important to test for primer efficiency using conditions as close to the final experimental conditions as possible, hence the efficiency was tested individually for the qPCRs on the StepOne Plus cycler and on the Biomark. The efficiency testing for the latter one was done alongside the samples that is being further described in its own section.

The efficiency of a reaction can be determined by running a dilution series under the same conditions as the later experiments themselves. A primer efficiency between 90% and 110% is commonly considered to be acceptable.

For the qPCRs performed on the StepOne Plus cycler a 96 well plate format was used, allowing for a total of 32 reactions when using triplicates of each reaction. A total of eight 1:1 dilutions were used, ranging from 400ng to 3.125ng of RNA equivalents of cDNAs, allowing for four primers being tested simultaneously. For each concentration of cDNA an individual master mix for 15 reactions (12 + 3 overage) was prepared. The QuantiNova SYBR Green PCR Kit was used.

150µl	SYBR Green PCR Master Mix
15µl	QN ROX Reference Dye
15µl	cDNA
93.75µl	RNase free H <sub>2</sub> O
<hr/>	
273.75µl	

Forward and reverse primers were mixed at a concentration of 10µmol/l each and 1.75µl/well were loaded onto the 96 well plate. 18.25µl of master mix were added afterwards for a total reaction volume of 20µl per well. All preparation, mixing and loading steps were performed on ice.

The plates were sealed with adhesive film, spun down using a plate centrifuge, vortexed and spun down again before being placed in the cycler. The qPCR was conducted using the following protocol, including a melting curve.

95°C	10min	1x
<hr/>		
95°C	10sec	
60°C	1min	40x
<hr/>		
20°C	∞	1x

### 3.4.2 Gene Expression Analysis

The gene expression analysis experiments were performed on two different systems, using different reagents, methods of cDNA generation and sample pretreatments. Pooled embryos were analyzed in a 96 well format on the StepOne Plus cycler using cDNA from RNA previously isolated using phenol-chloroform precipitation. Individual embryos were analyzed using 48.48 or 96.96 chips on the Fluidigm using cDNA isolated using the SuperScript IV CellsDirekt cDNA Synthesis Kit.

For both instances the non-electroporated sides functioned as control groups and were always ran alongside the GFP positive electroporated samples, allowing for expression comparisons.

#### **3.4.2.1 qPCR Using StepOne Plus Cyclers**

The effect of the plasmids electroporated of gene expression was analyzed using relative quantification. Pooled cDNA from chicken embryos was analyzed using the QuantiNova SYBR Green PCR Kit in a 96 well format. Like for the primer efficiency qPCRs, three master mixes were prepared for each plate, one from the control side, one from the electroporated GFP positive side and a negative control containing water instead of cDNA. For each region of the brain, each Hamburger Hamilton stage and each plasmid electroporated an individual plate was run.

280µl	SYBR Green PCR Master Mix
28µl	QN ROX Reference Dye
28µl	cDNA
175µl	RNase free H <sub>2</sub> O
<hr/>	
511µl	

One master mix allowed for reactions in triplicates of eight primers and still have the volume of four reactions as pipetting overage. The plate loading, preparation and cycling were performed identical to the reactions described under 3.4.1.2.

#### **3.4.2.2 qPCR Using Biomark**

cDNA from single embryos was used for chip-based qPCR on the Biomark. This specialized cyclers uses low reaction volumes and allows for the parallel analysis of up to 96 samples with 96 different primer pairs. The reaction and the data obtained is the same as in any regular qPCR, but a preamplification of the samples is needed to ensure acceptably low C<sub>q</sub>-values. In the following, sample preparation and loading are described for a 96.96 IFC. Volumes were scaled down for smaller chips during initial testing.

##### **3.4.2.2.1 Preamplification**

Preamplification was done using 12 cycles of regular PCR with a master mix containing all primers used for the later qPCR. The low number of cycles and ensures

an excess of reagents and allows for an even amplification of all target sequences.

First, 1 $\mu$ l primers, forward and reverse, all at 100 $\mu$ mol/l were mixed and the total volume was adjusted to 200 $\mu$ l using TE-buffer at a pH8.

Using the primer mix, the following master mix for 96 reactions, including overage was prepared:

110 $\mu$ l	PreAmp Master Mix
55 $\mu$ l	pooled primer mix
247.5 $\mu$ l	RNase free H <sub>2</sub> O
<hr/>	
313.5 $\mu$ l	

1.25 $\mu$ l of cDNA were mixed with 3.75 $\mu$ l of master mix and amplified as a 2-step-PCR in the StepOne Plus cycler.

95°C	2min	1x
<hr/>		
95°C	15sec	
60°C	4min	12x
<hr/>		
8°C	5min	1x

#### 3.4.2.2.2 Exonuclease Digest

Prior to loading the preamplification product on the qPCR chip, remaining primers and single stranded cDNA was removed by digest using Exol. For this purpose, another master mix was prepared.

154 $\mu$ l	RNase free H <sub>2</sub> O
22 $\mu$ l	10x Exonuclease Reaction Buffer
44 $\mu$ l	Exol Exonuclease
<hr/>	
220 $\mu$ l	

2 $\mu$ l of master mix were added to the product of each preamplification reaction, the mixture was heated to 37°C for 30min, followed by heat inactivation at 80°C for 15min.

### 3.4.2.2.3 Chip Loading and Cycling

Prior to loading of the chip, the products of the Exol digest were diluted 1+9 with TE-buffer at pH8. 3.3µl of these dilutions were mixed with Sample Pre-Mix, vortexed for 20sec and then centrifuged at 1000g for 30sec. The Sample Pre-Mix was freshly prepared by adding 36µl of 20x DNA Binding Dye to 360µl of 2x Sso-Fast EvaGreen Supermix with low ROX.

The primer assays were prepared using following ingredients:

9µl	2x Assay Loading Reagent
0.45µl	forward primer
0.45µl	reverse primer
8.1µl	RNase free H <sub>2</sub> O
<hr/>	
18µl	

The primer assays were also mixed by vortexing and then centrifuged at 1000g for 30sec.

The 96.96 chip was primed following the manufacturer's instructions and using the HX IFC Controller, program Prime (136x), after injecting 150µl of control line fluid and removing the cover sticker from the chip.

The chip was then loaded by adding 5µl of each sample into the sample inlets. The primer assays were loaded in triplicates, using 5µl per assay inlet. The samples in primers were then injected into the chip itself using the Load Mix (136x) protocol on the HX IFC Controller.

The fully loaded chip was then run on the Biomark, using the GE 96x96 PCR+Melt v2 protocol, provided by Fluidigm.

### 3.4.3 Data Analysis

As described previously, the most common way to analyze amplification curves from qPCR reactions, is the comparison of C<sub>q</sub> values – the instruments software of both, the StepOne Plus and the Biomark, automatically set the thresholds for quantification and directly report C<sub>q</sub> values.

For all reactions, the amplification curves and thresholds were inspected individually, checking for exponentiality of amplification and whether the threshold was within the cycles of exponential amplification and sufficiently above the background signal. In addition to this, the melting curves for reactions using the same primers were compared – if all reactions showed one distinctive peak at the same temperature and the amplification curves showed clean amplification, the  $C_q$  values were included for downstream analysis.

As all reactions were conducted in triplicates, the averages and standard deviations were calculated. If the  $C_q$  value of one of the reactions differed strongly from the others, that reaction was omitted and only two values were used for further calculations. All calculations, except statistical testing were done using Excel.

### 3.4.3.1 Primer Efficiency Calculation

Primer efficiency reflects a primer pairs ability to duplicate the template DNA present each cycle. It was determined using the  $C_q$  values from dilution series experiments.

The average of the  $C_q$  values obtained were blotted against the logarithmic RNA concentrations. Using the slope of a linear fit, the primer efficiency was calculated using following formula:

$$efficiency = \left(10^{\frac{-1}{slope}} - 1\right) * 100\%$$

An efficiency of 100% corresponds to a perfect doubling of DNA templates. Efficiency values between 90%-110% were considered acceptable.

### 3.4.3.2 Comparative Expression Analysis

The effects of electroporation on gene expression were analyzed using the  $\Delta\Delta C_q$  method, which allows the calculation of relative differences between two samples, in this case, between the non-electroporated wild type side and the electroporated, GFP expressing side.

In a first step, the geometric mean of the expression of all reference genes was calculated, alongside its standard deviation and standard error.

$$\bar{C}_{qgeom} = \sqrt[n]{C_{q1} * C_{q2} * \dots * C_{qn}}$$

$$SD_{geom} = \frac{\bar{C}_{qgeom}}{n} * \sqrt{\left(\frac{SD_1}{C_{q1}}\right)^2 + \left(\frac{SD_2}{C_{q2}}\right)^2 + \dots + \left(\frac{SD_n}{C_{qn}}\right)^2}$$

$$SE_{geom} = \frac{SD_{geom}}{\sqrt{n}}$$

The expression of the genes of interest was normalized by subtracting the just calculated geometric mean from the  $C_q$  values of the genes of interest. Alongside the normalized gene expression, its standard error was calculated.

$$\Delta C_q = C_{qGOI} - \bar{C}_{qgeom}$$

$$SE_{\Delta C_q} = \sqrt{SE_{GOI}^2 + SE_{geom}^2}$$

Using the normalized expression, the relative expression between the different sides of the brain was calculated by another subtraction step. This time subtracting the wildtype side from the electroporated side. The standard error of this difference was calculated alongside, ultimately allowing for the calculation of the standard deviation of expressional difference between the two sides.

$$\Delta\Delta C_q = \Delta C_{qGFP} - \Delta C_{qWT}$$

$$SE_{\Delta\Delta C_q} = \sqrt{SE_{\Delta C_{qGFP}}^2 + SE_{\Delta C_{qWT}}^2}$$

$$SD_{\Delta\Delta C_q} = SE_{\Delta\Delta C_q} * \sqrt{n}$$

The fold change of gene expression was then calculated from the  $\Delta\Delta C_q$  value.

$$FC = 2^{-\Delta\Delta C_t}$$

### 3.4.3.3 Statistical Analysis

All statistical analysis was done using SPSS. The tests were selected based on scale level and sample distribution. For nominal scaled data, a Mann-Whitney-U test was performed. Interval scaled data was tested for distribution using the Kolmogorov-Smirnov test. Based distribution t-test for equality of means was used for data with a normal distribution. For data with skewed distribution, Lavene's test for equality of variances was performed.

#### 3.4.3.4 RIN-Analysis

As the SyperScript IV CellsDirect cDNA Synthesis kit, as the name indicates, directly synthesizes cDNA from tissue, the RNA integrity couldn't be measured using traditional capillary electrophoresis. To get at least some insight into the quality of cDNA used, two primers were designed. The ES603'GAPDH and the ES605'GAPDH primers were not only used for reference gene detection, but the difference of their  $C_q$  values also correlates with RNA/cDNA integrity. A  $\Delta C_{q3'-5'} < 3$  correlates to a RIN > 7.

### 3.5 Western Blot

One of the most common techniques to assess gene expression on a protein level is western blotting. This technique combines the size separation of proteins by SDS poly acrylamide gel electrophoresis (SDS-PAGE) with the specificity of antibodies in on a bolt.

In the first step, protein is denatured in the presence of SDS and DTT using heat, then loaded onto a poly acrylamide gel and separated by size using an electric field.

As proteins vary in the composition of amino acids, they don't have an electric charge proportional to their mass, like for example DNA has. SDS helps to compensate for this, by not only acting as a detergent, but by surrounding the proteins, it also contributes the negative charges of its sulfate groups, resulting in evenly negatively charged proteins. This negative charge now causes the proteins to migrate towards the cathode, with larger proteins migrating a shorter distance in the gel, as the encounter a higher resistance.

After electrophoresis, the poly acrylamide gel is then transferred on top of a nitrocellulose membrane and the proteins are transferred out of the gel, onto the membrane, once again using an electric field. This step is reoffered to as the blotting itself.

Protein on the membrane is very stable and allows for a large variety of detection methods, like full protein stains or specific protein detection by antibodies. Both methods can be, depending on the chemistry used, be done in a way, that allows for quantification of the protein on the membrane.

### **3.5.1 SDS-PAGE**

Prior to loading the protein on the precast Bolt-Bis-Tris gels, it was mixed 1:1 with 2x SDS probe buffer, 1% v/v proteinase inhibitor was added, and the mixture was heated to 95°C for 10min.

The electrophoresis chamber was filled using MES or MOPS buffer, the comb was removed from the gels and up to 40µl of protein in SDS probe buffer were loaded alongside protein standards. Depending on the gel, chamber and power supply, the gels were run for different durations and at different voltages, usually starting at a lower voltage for the collection of the protein in the gel, prior to separation. The electric field was turned off, once the blue band from the bromophenol blue had just left the gel. The final runs, used for quantification were done using the XCell system, 8% Bolt Bis-Tris gels, MES buffer and ran for 10min at 100V followed by 17min at 200V.

### **3.5.2 Semi-Dry Blotting**

The gels were removed from the electrophoresis chamber; the shells were prodded open using a large spatula. Nitrocellulose membranes were rinsed using semi-dry blot buffer and placed on top of three sheets of Whatman paper soaked in the same buffer. This stack was transferred into the blotting chamber. The collection gel and the lower end of the gel were removed and discarded; the center piece of the gel was placed on the nitrocellulose membrane and cover with another three sheets of soaked Whatman paper. With the stack completed, the blotting chambers lid was closed and pressed down using two full one-liter glass flasks. 15V were applied for 1h, with the positive electrode being at the bottom of the stack. A maximum of two gels were blotted simultaneously.

The success of blotting was tracked by whole protein staining. The blots were submerged in PonceauS reagent for 5min, rinsed twice using water and then imaged. After Imaging, the membranes were trimmed using a scalpel and labeled using a pencil.

### 3.5.3 Antibody Staining

All antibody stains on western blots were done using the Pierce Fast Western Blot, Super Signal West Femto Mouse kit. This kit uses a modified luminol reagent and horseradish peroxidase coupled secondary antibody to generate chemiluminescence. As the stream of light emitted correlates with the amount of peroxidase coupled antibody, it ultimately allows for the quantification of individual proteins on the nitrocellulose membrane.

The antibodies were diluted, as recommended by their manufacturers using the Antibody Dilutant contained within the kit. A final volume of 1.5-2ml was used per blot. Blots were sealed in sous vide bags for antibody incubations. A maximum of two blots was stained within the same bag. The blots were incubated for 10-16h over night at 4°C.

The next morning, the blots were transferred into individual 50ml reaction tubes. For primary antibodies from mice, 1ml of Optimized HRP Reagent, provided in the kit, was mixed with 9ml of Antibody Dilutant. For primary antibodies from rabbits, 40µl of Amersham HRP anti rabbit antibody was mixed with 10ml of Antibody Dilutant. Either way, 10ml of diluted secondary antibody was added to the western blot membrane and incubated for 15min at room temperature on a rotor.

After removing the secondary antibody, the membrane was washed four times for 5min using 20ml of the Wash Buffer provided in the kit. Washes were also conducted on the rotor system at room temperature.

The final step of staining was adding 10ml of SuperSignal West Femto Working solution, freshly prepared from even parts of SuperSignal West Femto Luminol/Enhancer Solution and SuperSignal West Stable Peroxide Solution. This solution was incubated for 5min under the same conditions as in the prior steps.

Once the final incubation was done, the membrane was sealed in a sous vide bag, to prevent drying, and imaged using the Odyssey Fc system, with 10min exposure on the chemiluminescence channel, and 30sec on the 600nm and 700nm channels. The latter ones imaged the protein standard, whilst the protein stained by the antibodies was visualized in the chemiluminescence channel.

### 3.5.4 Antibody Stripping

As multiple different proteins were to be detected, the antibodies used for each staining needed to be removed before a membrane could be probed again with a different antibody. This was done using stripping buffer, in which the membranes were incubated for 10min. The remainders of the strip buffer were removed by three times 5min in TBST buffer and a final 5min in TBS buffer. All five incubations were done on in trays on a shaker.

### 3.5.5 Whole Protein Stain

For normalization of protein loaded, whole protein staining using the Revert 700 Total Protein Stain from Licor was used.

After detecting the individual antibodies, blots were stripped and incubated with 10ml of Revert 700 Total Protein Stain in a 50ml reaction tubes on a rotor for 10min, followed by two 30sec washes in self-prepared Revert Wash Buffer in trays on an orbital shaker. Prior to being sealed in plastic the blots were rinsed in water.

The stain was detected using the 700nm channel on the Odyssey FC system for 10min.

### 3.5.6 Image Analysis

Fiji was used for analysis of concentration gradients for antibody validation and Empiria was used for the final expression analysis, as it allowed for automatic normalization using the whole protein staining.

In Fiji, images were first cropped and rotated. The image type was adjusted to 8-bit greyscale. Only the chemiluminescence channel was used. The individual bands (ROI) were marked, and using the measuring function (cmd+m) the mean intensity was measured. Individual background measurements per lane were taken as well. The final signal intensity was calculated using following formula:

$$signal = (255 - ROI) - (255 - background)$$

Calculated signal intensities were blotted against the amount of protein loaded and a liner fit was calculated using Excel.

The amount of protein detected using antibodies was analyzed using Empiria and its function for quantitative western blots. Where possible, the functions for automatic detection of lanes and bands were used. As many blots suffered from low protein input, manual adjustments were necessary in many cases.

The individual signals measure were exported to Excel, which was used to calculate means, standard deviations and generate diagrams.

### **3.5.7 Validation of Antibodies**

Antibodies were validated, like qPCR primers, by dilution series. This allowed to check for proportional increase in signal, when increasing the protein on the blot. Dilutions from 5 $\mu$ l to 40 $\mu$ l of protein obtained from wild type E9 midbrain tissue were blotted, stained and imaged. The signal intensity was blotted against the volume of protein used. The  $r^2$  value of a liner fit with a  $y=0$  intersect was calculated. Values of  $>0.85$  were considered acceptable.

The specificity of antibodies could unfortunately not be fully analyzed, as no purified protein of interest was available. Only the location of the signal from the blot could be compared with the protein standard and correlated with the expected weight of the target protein.

## **3.6 Cryosections, Immunohistochemistry and Microscopy**

Microscopy and antibody-based stains are one of the foundations of gene expression analysis in tissues. They allow the correlation of anatomic structures with the qualitative expression of genes within that tissue. Genetically modified tissues themselves can also express genes, like GFP that can be directly detected under a fluorescence microscope.

### **3.6.1 Cryosections**

Tissue, like for example whole midbrains, was prepared and snap frozen in molds filled with Tissue Tek using dry ice. The block was kept at  $-20^{\circ}\text{C}$  and further processed inside the cryotome. Excess Tissue Tek was removed using a razor blade and the trimmed down block was mounted using a few drops of Tissue Tek. Using

the trim function, the block was further cut down, until the desired region of the tissue was reached. Consecutive cryosections were then performed, usually between 15-20 $\mu$ m thickness. The sections were air dried overnight and stored at -20°C.

### **3.6.2 Immunohistochemistry**

Like the antibody stains on western blots, proteins in tissue can be detected and their expression anatomically localized. A primary antibody binds to its epitope on the protein of interest. A secondary antibody, that is labeled with a fluorescent dye, now binds the primary antibody, visualizing the location of the protein of interest. Multiple different antibodies can be used on the same slide, allowing for colocalization of expression of multiple proteins.

For this, cryosection were taken from the freezer, thawed for 15min and then rehydrated using BPS buffer. The tissue was circled using a hydrophobic pap pen, preventing liquids from spilling of the slide.

For some antibodies, the slides were incubated in boiling 3mol/l citric acid at a pH6 using a steam cooker. Three rinses using PBS were done to remove the remaining acid.

Sections were then blocked and permeabilized using antibody solution for 60min. Primary antibody incubation was done overnight at 4°C using antibody diluted in antibody solution.

The next day, slides were washed three to four times for 10min at room temperature using PBS, before adding the secondary antibodies in antibody solution and incubating for 2h in the dark at room temperature.

The sections were washed for an additional 3 times for 15min, using PBS, with the second rinse also containing the DRAQ5 nuclear stain at 1:5000. Using 24x50mm cover slide and 9+1 glycerol and PBS, the sections were covered and stored at 4°C for imaging.

### **3.6.3 Confocal Laser Scan Microscopy**

Cryosections stained using immunohistochemistry were imaged using Z stacks on a Zeiss confocal laser scan microscope. Using the 488nm, 543nm and 633nm lasers, the Cy3, Cy5, Alexa dyes and DRAQ5 were visualized using appropriate

filters to exclude exciter frequencies. The pinhole size was set to 1 AU; the gain was individually adjusted for each section and the averaging was set to 4x.

### **3.6.4 Apotome Microscopy**

A Zeiss inverted microscope with an apotome unit was used to image the unstained open book preparations of midbrains electroporated with pSilencer-siPAX7 plasmids. The microscope was only used as a conventional fluorescence microscope with tile scan function, allowing for the imaging of the relatively large open book preparations. Slides were imaged in 488nm fluorescence and bright-field mode.

### **3.6.5 Binocular Fluorescence Microscopy**

Some embryos electroporated with Top-Flash plasmid constructs had been imaged using the Leica binocular microscope, equipped with a mercury arc lamp and filters, capable of exciting GFP and RFP proteins expressed in-ovo. Exposure times for individual channels had been adjusted manually.

This microscope was also used to check for electroporation success.

## 4 Results

The influence of PAX7 and its transactivation domain splice variants on canonical Wnt signaling were analyzed using various approaches:

- Initial testing was done using in vivo reporter assays. (Chapter 4.1)
- These were later expanded upon, with RNA expression analysis using qPCR. (Chapter 4.2)
- And complemented with protein expression quantification using Western blots. (Chapter 4.3)

As the quantitative methods (qPCR and Western blot) had not been done in our lab previously, establishing these techniques took up a lot of time. The findings of this process are presented at the beginning of each individual chapter.

Results from testing methods, that were not used in final testing as well as results from cloning new siRNA constructs can be found at the end of the results section.

### 4.1 Wnt Signaling in Midbrain in Vivo

The initial experiments using the TOP-dGFP plasmids done by Martin Zeeb in our lab indicated a reduction of canonical Wnt signaling in the midbrain, when PAX7 expression was knocked down using the siPAX7-pSilencer1.0 plasmid. Building on these experiments, chicken embryos were electroporated with TOP-dGFP reporter gene constructs alongside different plasmids overexpressing the individual PAX7 splice variants, PAX3 or the PAX7/ENGRAILED fusion protein. For PAX7 knock-downs, the newly made siPAX7-pSilencer1.0 plasmids (chapter 4.5) were used.

As shown in figure 4-1, the transfections were successful. Canonical Wnt signaling appears to be active in the dorsal midbrain as well as in the hindbrain, indicated by the expression of GFP.

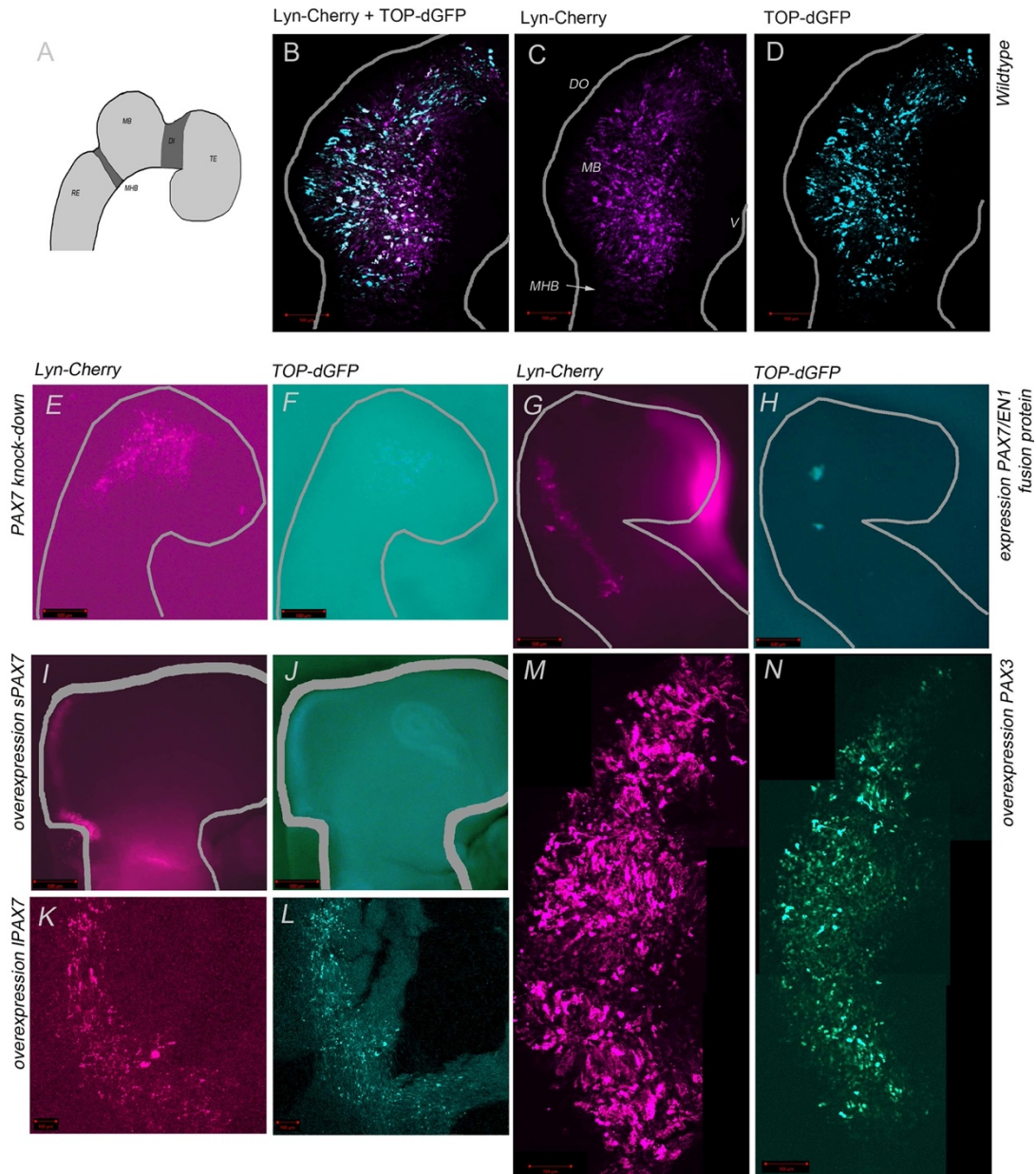


**Figure 4-1: Canonical Wnt signaling can be detected in vivo in the dorsal midbrain at HH stage 17 and is influenced by PAX7 knock-down.** Without PAX7 expression modification (**B-D**), canonical Wnt signaling is active in the dorsal midbrain. Both, the PAX7 knock down (**E and F**) and the expression of the PAX7/EN1 fusion protein (**G and H**), that represses genes usually promoted by PAX7, reduce canonical Wnt signaling in the midbrain. The overexpression of the short (**I and J**) or the long PAX7 splice variant (**K and L**) as well as the overexpression of PAX3 (**M and N**) did not impact canonical Wnt signaling. **A** schematic overview of the chicken brain anatomy at HH stage 17. RE rhombencephalon (hindbrain), MB midbrain, DI diencephalon, TE telencephalon (forebrain), MHB mid-hindbrain-boundary, DO dorsal, V ventral. Scale bar equals 100 $\mu$ m. GFP expression (encoded by TOP-dGFP reporter plasmid) indicates canonical Wnt signaling (**B, D, F, H, J, L and N**). RFP (encoded by Lyn-Cherry) functions as transfection baseline (**B, C, E, G, I, K and M**). Images **B-D** and **K-N** imaged using an LSM. Scale bar in these images: 100 $\mu$ m. Images **E-J** acquired using a binocular microscope, scalebar in these: 500 $\mu$ m.

### 4.1.1 Quantification of Canonical Wnt Signaling in Vivo Using Automated Cell Counting

When using automated image analysis in Fiji, cell counting (table 4-1 and figure 4-5) did not show any relevant changes in canonical Wnt signaling. Images of 26 embryos electroporated with the TOP-dGFP reporter system and PAX7 expression modifying plasmids were analyzed.

	WT (n=11)	siPAX7-pSi-lencer1.0 (n=2)	enPAX7-pMIW (n=2)	sPAX7-pMES-ΔGFP(n=3)	IPAX7-pMES-ΔGFP (n=8)
mean	0,335	0,488	0,181	0,451	0,395
SD	0,117	0,321	0,244	0,212	0,387

Table 4-1: **PAX7 expression modifications did not affect canonical Wnt signaling in the midbrain, when images are analyzed automatically.** Number of cells with canonical Wnt signaling relative to all electroporated cells, in embryos at HH stage 17 electroporated with the TOP-dGFP reporter system and PAX7 expression modifications, counted using Fiji. SD: standard deviation, WT: wildtype – in this instance only electroporated with the TOP-dGFP reporter system. Data visualized in figure 4-5.

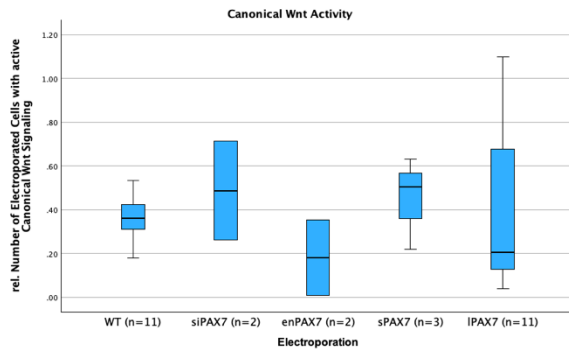


Figure 4-2: **PAX7 expression modifications did not affect canonical Wnt signaling in the mid-brain, when images are analyzed automatically.** Number of cells with canonical Wnt signaling relative to all electroporated cells, in embryos at HH stage 17 electroporated with the TOP-dGFP reporter system and PAX7 expression modifications, counted using Fiji. WT: wildtype, siPAX7: PAX7 knock-down, enPAX7: repression of the pro-transcriptional activity of PAX7, s/IPAX7: overexpression of the short or long PAX7 TA splice variant. Visualization of table 4-1.

The image quality varied significantly, as most images were taken using a binocular microscope system from whole mounted embryos at a <10x magnification whilst others were flat mounted and imaged using a LSM system and magnifications of 100x or 200x. Especially in images with lower magnification, the software struggled to identify individual cells.

An attempt to circumvent this issue, by analyzing the fluorescent areas of the same images failed to show significant changes in canonical Wnt signaling too (table 4-2 and figure 4-6).

	WT (n=11)	siPAX7-pSi-lencer1.0 (n=2)	enPAX7-pMIW (n=2)	sPAX7-pMES-ΔGFP(n=3)	IPAX7-pMES-ΔGFP (n=8)
mean	0,315	0,263	0,140	0,220	0,294
SD	0,099	0,215	0,191	0,178	0,278

Table 4-2: **PAX7 expression modifications did not affect canonical Wnt signaling in the midbrain, when images are analyzed automatically.** Fluorescent areas analyzed using Fiji, in embryos at HH stage 17 electroporated with the TOP-dGFP reporter system and PAX7 expression modifications. SD: standard deviation, WT: wildtype – in this instance only electroporated with the TOP-dGFP reporter system. siPAX7:

PAX7 knock-down, enPAX7: repression of the pro-transcriptional activity of PAX7, s/IPAX7: overexpression of the short or long PAX7 TA splice variant Data visualization in figure 4-6.

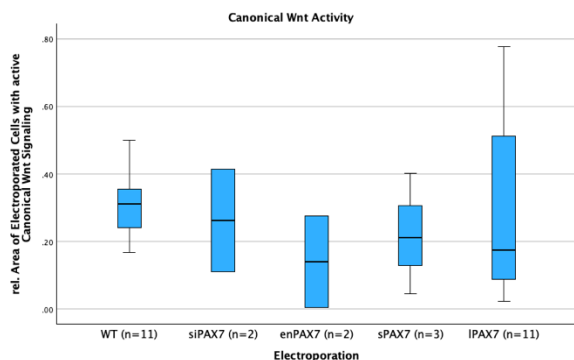


Figure 4-3: **PAX7 expression modifications did not affect canonical Wnt signaling in the mid-brain, when images are analyzed automatically.** Fluorescent areas analyzed using Fiji, in embryos at HH stage 17 electroporated with the TOP-dGFP reporter system and PAX7 expression modifications. SD: standard deviation, WT: wildtype – in this instance only electroporated with the TOP-dGFP reporter system. siPAX7: PAX7 knock-down, enPAX7: repression of the pro-transcriptional activity of PAX7, s/IPAX7: overexpression of the short or long PAX7 TA splice variant. Visualization of table 4-2.

The results of the cell counting and area analysis were inconclusive, due to the varying quality of images and low number of replicates, especially for siPAX7, enPAX7 and sPAX7, resulting in high standard deviations.

Previous experiments from other members of the lab had similar problems. Attempts to improve image quality by only using flat mounted embryos and the LSM system struggled with fluorescent protein degradation. Attempts to amplify the fluorescent signal using dye coupled antibodies failed due to poor antibody specificity. Further complicating attempts to recreate what had already been done in our lab, the original images and documentation of the cell counting experiments conducted by Martin Zeeb could not be found and reanalyzed, due to a hard drive failure.

#### 4.1.2 Quantification of Canonical Wnt Signaling in Vivo by Manual Image Analysis

Because of the difficulties with software-based image analysis, we settled for visual analysis and categorization, based on the perceived expression of GFP relative to the RFP expression.

	WT	siPAX7	enPAX7	sPAX7	IPAX7	PAX3
GFP $\geq$ RFP	9	0	4	4	5	3
GFP<RFP	5	5	9	2	4	2
No/little GFP	0	4	13	0	1	0
$\Sigma$	14	9	26	6	10	5

Table 4-3: **PAX7 knockdown and enPAX7 expression reduce canonical Wnt signaling.** Summary of embryos, visually categorized into three groups with different levels of canonical Wnt signaling. Embryos at HH stage 17, all electroporated with the TOP-dGFP construct. GFP expression indicates canonical Wnt signaling, RFP expression indicates electroporated cells. From the PAX7 expression modifications, the knock-down (siPAX7) showed the strongest reduction in canonical Wnt signaling, followed by the expression of the PAX7/ENGRAILED fusion protein (enPAX7). The long transactivation domain splice variant (IPAX7)

showed a tendency in reducing canonical Wnt signaling. Overexpression of the short transactivation domain splice variant (sPAX7) or PAX3 showed no impact on Wnt signaling. **WT**: Embryos electroporated with only the TOP-dGFP and 2A-lyn-Cherry plasmids, used as control group. **siPAX7**: Knock-down of PAX7 using the siPAX7-pSilencer1.0 plasmid. **enPAX7**: Expression of a PAX7/ENGRAILED fusion protein using the enPAX7-pMIW plasmid. **sPAX7** and **IPAX7**: Overexpression of the long or short transactivation domain splice variant of PAX7, using the sPAX7-pMES-ΔGFP or the IPAX7-pMES-ΔGFP plasmids. **PAX3**: Overexpression of PAX3 using the PAX3-pMIW plasmid.

Overall, GFP expression was lower than RFP expression, but both, the PAX7 knock down and the PAX7/ENGRAILED construct showed a strong tendency to further reduce the number of GFP positive cells (table 4-3), with more than 84% of the embryos having a lowered or absent GFP expression, with the reduction for both electroporations being significant with a  $p < 0.01$  in a two-sided Mann-Whitney-test using SPSS (table 4-4).

The long splice variant of PAX7 showed a similar, but weaker, non-significant effect, with half of all embryos electroporated showing a reduced or absent GFP expression (table 4-4).

Neither the short PAX7 splice variant, nor PAX3 showed a major impact on GFP expression compared to the wildtype (WT) embryos, only electroporated with the TOP-dGFP constructs (table 4-4).

	siPAX7-pSilencer1.0	enPAX7-pMIW	sPAX7-pMES-ΔGFP	IPAX7-pMES-ΔGFP	PAX3-pMIW
Mann-Whitney U	12.5	60.5	41	67	33.5
Wilcoxon W	117.5	165.5	62	172	138.5
Z	-3.442	-3.654	-0.1	-0.209	-0.166
Asymp. Sig. (2-tailed)	<.001	<.001	0.921	0.834	0.868
Exact Sig. [2*(1-tailed Sig.)]	<.001	<.001	.968	.886	.893

Table 4-4: **Significance testing of Top-dGFP experiments.** Results from five individual Mann-Whitney-U test using SPSS, comparing the individual PAX7 expression modification with wildtype embryos. Embryos electroporated with siPAX7-pSilencer and enPAX7-pMIW showed a significant reduction in canonical Wnt signaling activity in the two-sided Mann-Whitney U test. Detailed results/test statistics can be found in appendix 9.1.

In a few of the electroporated embryos, the rhombencephalon was electroporated alongside the targeted midbrain. Because of the lower number of embryos, especially “wildtype” embryos, no statistical analysis was performed. The effects observed were comparable to the effect seen in the midbrain, meaning a reduction in canonical Wnt signaling, when PAX7 is knocked down or the dominant

negative enPAX7 is being expressed. Interestingly, the overexpression of either PAX7 splice variant also resulted in a minor reduction, although a higher number of replicates is required for reliable statistical analysis.

	WT	siPAX7	enPAX7	sPAX7	IPAX7	PAX3
GFP $\cong$ RFP	4	0	0	0	3	2
GFP<RFP	0	0	6	2	3	0
No/little GFP	0	6	0	0	0	0
$\Sigma$	4	6	6	2	6	2

**Table 4-5: PAX7 knock-down reduces canonical Wnt signaling in the rhombencephalon.** Summary of embryos, visually categorized into three groups with different levels of canonical Wnt signaling. Embryos at HH stage 17, all electroporated with the TOP-dGFP construct. GFP expression indicates canonical Wnt signaling, RFP expression indicates electroporated cells. All PAX7 modifications showed a tendency to reduce canonical Wnt signaling, with PAX7 showing the strongest reduction by far. More replicates are required for a statistical analysis **WT**: Embryos electroporated with only the TOP-dGFP and 2A-lyn-Cherry plasmids, used as control group. **siPAX7**: Knock-down of PAX7 using the siPAX7-pSilencer1.0 plasmid. **enPAX7**: Overexpression of a PAX7/ENGRAILED fusion protein, inactivating the transcription of all genes that PAX7 binds in the promoter region. The enPAX7-pMIW plasmid was used. **sPAX7** and **IPAX7**: Overexpression of the long or short transactivation domain splice variant of PAX7, using the sPAX7-pMES- $\Delta$ GFP or the IPAX7-pMES- $\Delta$ GFP plasmids. **PAX3**: Overexpression of PAX3 using the PAX3-pMIW plasmid.

## 4.2 Detecting PAX7 and Wnt Signaling on RNA Level Using qPCR

For qPCR, two different systems were used, a traditional well-based StepOne Plus PCR cycler and a high-throughput chip-based Biomark system, that was used for analysis of single embryos.

A total of 15 qPCRs using the StepOne Plus cycler were performed. These runs differed in the modifications of the embryo, the tissue used (e.g. mes- or rhombencephalon) and the Hamburger and Hamilton stage of the embryos. In addition to these, some reactions on wild type midbrain tissue were performed, to assess the relative strength of expression of the two different transactivation domain splice variants at different stages of development.

An additional three chip-based qPCRs were run on the Biomark, allowing for the analysis of gene expression in individual embryos.

- 1<sup>st</sup> test run, 48.48 chip, non-exon-skipping primers, cNDA from mes- and rhombencephalon tissue, various electroporations and HH stages, cDNA loaded concentration adjusted

- 2<sup>nd</sup> test run, 48.48 chip, exon-skipping primers, cNDA from mes- and rhombencephalon tissue, various electroporations at HH stage 17, cDNA loaded concentration adjusted
- Final run, 96.96 chip, embryos at HH stage 17, exon-skipping primers, cNDA from midbrain tissue, electroporated with either pCAX or the siPAX7-pSilencer plasmid, cDNA loaded volume adjusted

## 4.2.1 qPCR Validation and Sample Preparation

As qPCR had not been done in our lab before, validating primers and developing RNA/cDNA isolation techniques presented a major task to be done, prior to measuring the impact of PAX7 modifications of canonical Wnt signaling.

### 4.2.1.1 RNA Isolation and cDNA Synthesis

#### 4.2.1.1.1 cDNA Synthesis for Chip-Based qPCR

The isolation of RNA from individual midbrain halves from chicken embryos at HH stage 17 presented itself as quite the challenge, as the amount of RNA isolated is extremely low. Several kits were tested first, always following the manufacturer's instructions, before settling for the SuperScript IV CellsDirect cDNA Synthesis kit from Thermo Fischer Scientific. Table 4-6 gives an overview of kits testes. The last two kits in the list directly synthesized cDNA, so RNA quantification was not applicable and the kits efficacy was instead tested using PCR.

Kit and Manufacturer	RNA isolated
RNeasy Plus Micro Kit, Qiagen	12µl à 3ng/µl (Qubit)
QIAzol/Maxtract/RNeasy, Qiagen	12µl à 3.5ng/µl (Qubit)
peqGOLD TRIfast (scaled down), Peqlab	10µl à 6.2ng/µl (Qubit)
Kit E6421, NEB	→direct cDNA, PCR worked
SuperScript IV CellsDirect cDNA Synthesis kit, Thermo	→direct cDNA, PCR worked, cheaper than E6421 from NEB

*Table 4-6: SuperScript IV CellsDirect cDNA Synthesis kit is the best kit for RNA isolation from midbrain halves. RNA isolated by various kits. Tissue from one halve of a midbrain from an embryo at HH stage 17 was used. The kits from NEB and Thermo Fischer Scientific directly synthesized cDNA from tissue, so the RNA isolated could not be quantified and the cDNA was tested using PCR instead.*

The CellsDirect kit reliably produced cDNA, directly from tissue. Unfortunately, during the first two runs on the Biomark system, with cDNA from this kit we learned, that the included DNase digest did not fully remove the gDNA, as the C<sub>q</sub>

values of the control without a reverse transcriptase in the master mix were not different from the  $C_q$  values of the actual samples (table 4-7).

Primer	$C_q$ no-RT control sample	Mean $C_q$ of cDNA 35 samples
Beta-actin-1	11.76	11.89
60 GAPDH 5'	8.37	8.77
60 Axin2	16.01	15.92

Table 4-7: **cDNA isolated using the CellsDirect kit also contains gDNA.** The no-RT control doesn't contain any cDNA, yet it has comparable  $C_q$  values to the other 35 samples containing cDNA. This indicates gDNA contamination and its amplification in the other samples.

The contamination with genomic DNA was validated using in conventional PCR and the 60Chr1Centromere (Cen1) primer (figure 4-4).

Further testing using PCR and gel electrophoresis revealed, as shown in figure 4-5, that mechanically lysing the midbrain tissue using

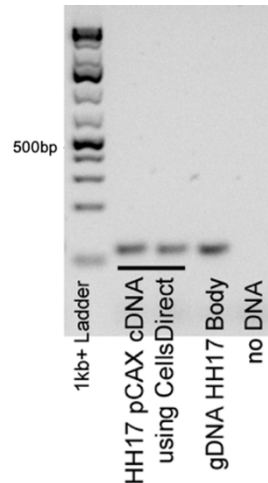


Figure 4-4: **gDNA contamination in cDNA isolated using the CellsDirect kit.** Electrophoresis from PCR using the Cen1 primers. Both cDNA samples isolated with the CellsDirect kit show a band around 104bp, like the one in the gDNA control, indicating contamination with genomic DNA.

using a small pestle reduced gDNA present in the cDNA. The DNase in a 40 $\mu$ l reaction also seemed to be at its digestive capacity when a single midbrain at HH stage 17 was used. More tissue, like older midbrains at HH stage 24 or multiple midbrain halves resulted in a higher concentration of genomic DNA, when tested with centromere primers using regular PCR and electrophoresis.

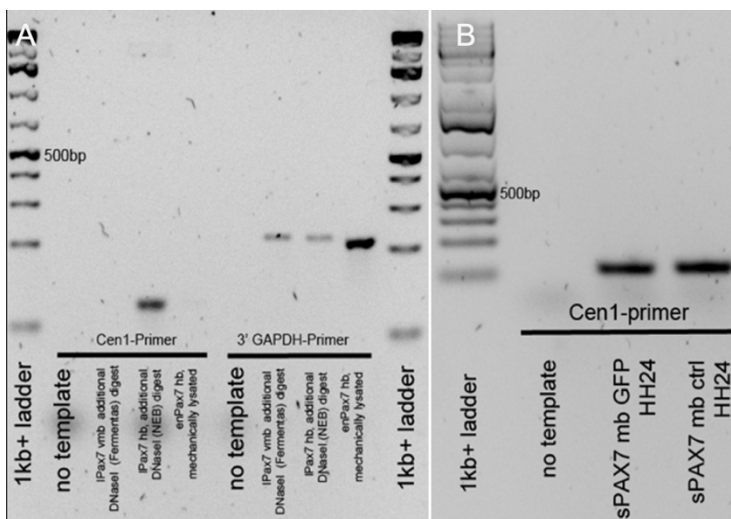
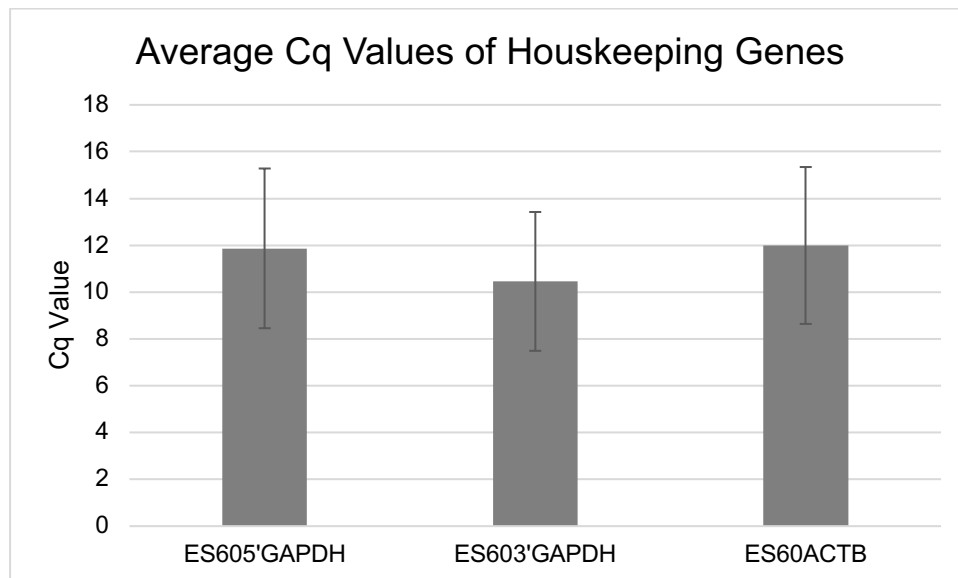


Figure 4-5: **Mechanic lysis reduces gDNA contamination.** Gel electrophoresis of PCR products using the Cen1 primer, amplifying gDNA. cDNA isolated using CellsDirect kit. **A:** cDNA isolated from ventral midbrain (vmb) and hindbrain (hb) tissue of one embryo at HH stage 17, transfected with IPAX7-pMES. Addition of DNaseI from Fermentas reduced and mechanical lysis gDNA contamination (amplified using the Cen1 primer). The DNaseI from NEB did not work. All three samples show cDNA isolation (GAPDH primer) **B:** Using larger midbrains at HH stage 24, the mechanical lysis failed to eliminate gDNA contamination.

The second test run for chip-based qPCR revealed another issue. Resulting from the way, the CellsDirect kit worked. As this kit skips the RNA isolation and directly synthesizes cDNA from cells, the amount of RNA used per reaction cannot be quantified, so photometric single strand DNA quantification had to be used instead.

As the concentration of cDNA, for the second test run, had been adjusted to 12ng per well, similar  $C_q$  values for the reference genes were expected. Looking at the highly expressed reference genes (figure 4-6), the standard deviation was around  $\pm 3 - 3.5$  cycles, which considering the exponentiality of PCR, results in a 64-128-fold concentration difference between the sample with the highest and the lowest  $C_q$  value.



*Figure 4-6: **High differences in cDNA concentration between samples.** Average of  $C_q$  values for reference genes from all samples tested in the second test run for chip-based qPCR. The high standard deviation indicates a 64-128-fold difference of template DNA present in the individual midbrain cDNA samples. Error bars indicate the standard deviation.*

This standard deviation did not change, when looking at electroporated and wildtype sides separately (table 4-8), indicating that the electroporation is not responsible for differences between  $C_q$  values, but is instead most likely caused by variance in cDNA present between the individual samples.

	ES605'GAPDH		ES603'GAPDH		ES60ACTB	
	Mean	SD	Mean	SD	Mean	SD
All samples	11.87	3.41	10.46	2.97	11.99	3.35
All electroporated side samples	11.81	3.35	10.35	2.91	11.80	2.98
All wildtype side samples	11.97	3.56	10.56	3.09	12.19	3.75

Table 4-8: **CDNA concentration and not electroporation caused high C<sub>q</sub> variances.** Means and standard deviations of C<sub>q</sub> values of reference genes, separately for electroporated and wildtype midbrain halves. The mean standard deviation are comparable between the different sides, showing no effect of electroporation, but instead indicating that the difference is caused by inconsistent cDNA concentration in the samples.

For the third and final run using the Biomark system, cDNA was also isolated using the Cells Direct kit. A total of 20 embryos were in the control group, being electroporated with pCAX plasmids and 24 embryos were in the PAX7 knock-down group, electroporated with the siPAX7-pSilencer1.0 construct. The cDNA samples were tested using both quantitative and regular PCR.

qPCR was used to get an approximate quantification of the cDNA present. 29 cDNA samples were selected at random to be analyzed. Using two cDNA samples (13.01.22 pCAX and enPAX7-pMIW, both dorsal midbrain control-side halves) from the second qPCR run on the Biomark as reference in combination with the ES60 3'GAPDH primers, the amount of cDNA present in the new samples could be estimated.

Most samples, except for the two samples from embryo number 6 in the PAX7 knock-down (siPAX7) group, showed similar cDNA concentrations (figure 4-7). Detailed C<sub>q</sub>-values can be found in appendix 9.2.2.1.

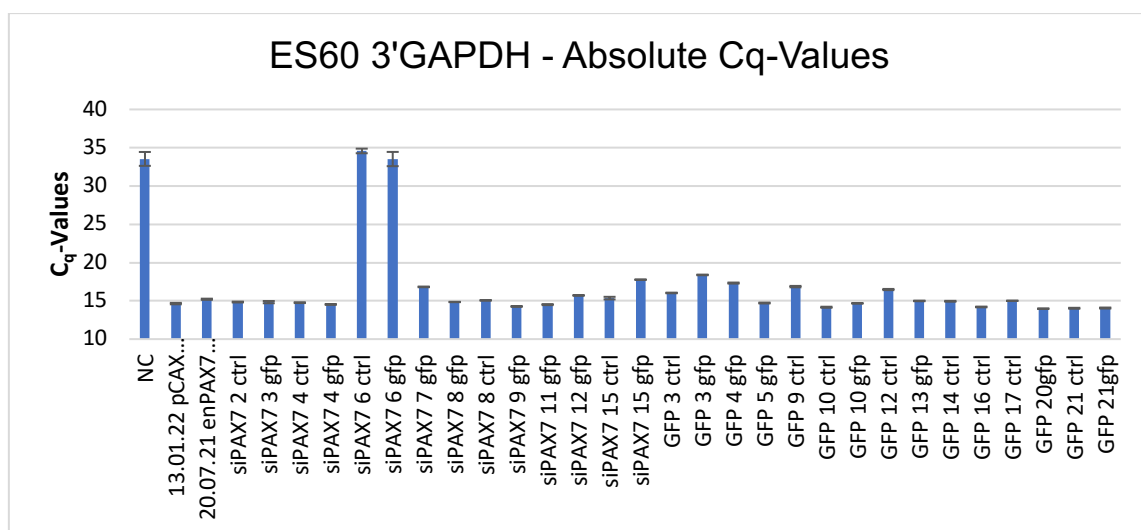
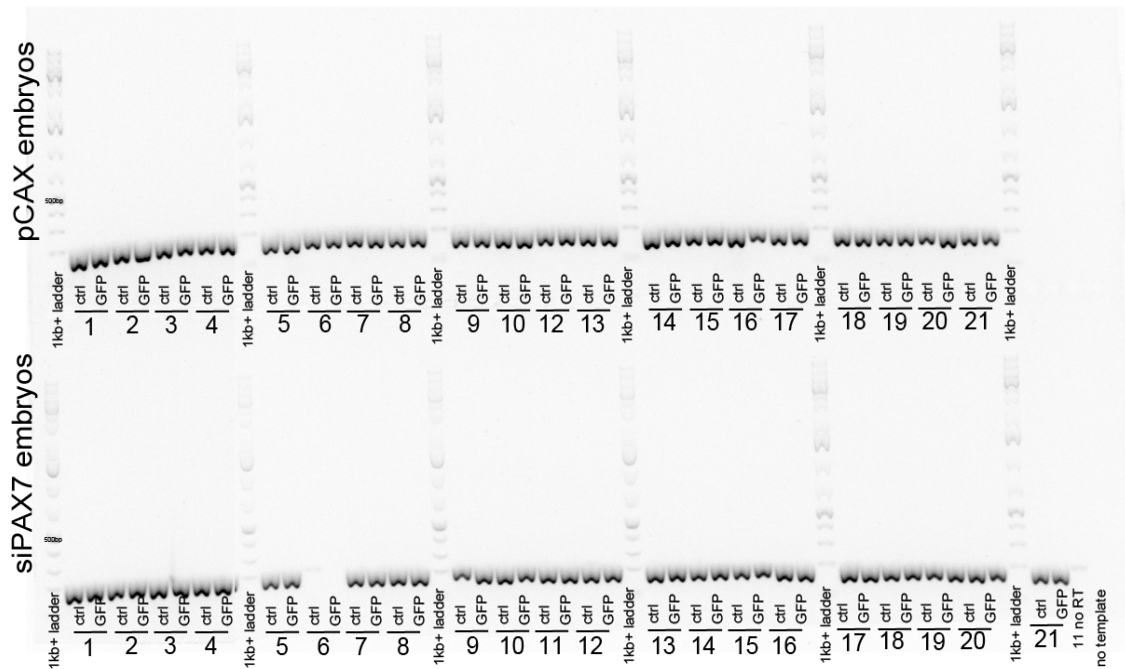


Figure 4-7: **Samples used for final chip-based qPCR have similar cDNA concentrations.** C<sub>q</sub>-values from GAPDH expression using ES60 3'GAPDH primers. Random selection of cDNA intended for 3<sup>rd</sup> Biomark experiment and two known good samples from 2<sup>nd</sup> experiment using the Biomark (pCAX and enPAX7-

*pMIW*). Most samples show similar  $C_q$ -values ( $\pm 2$  cycles), indicating a similar cDNA concentration. Samples 6 from embryo with *siPAX7-pSilencer1.0* show comparable  $C_q$  values to the no template (NC) control, indicating no cDNA present.

Since all samples tested, but the samples from embryo 6 in the PAX7 knock-down group, showed successful amplification, all samples intended for the Biomark were tested using regular PCR and gel electrophoresis (figure 4-15) with the same ES60 3'GAPDH primers, in search of other samples with no cDNA present.

#### ES60 3'GAPDH



**Figure 4-8: Most samples for the final Biomark run contain cDNA.** Gel electrophoresis from PCR using ES60 3'GAPDH primers. 1.5% gel, 100V, 60min. Expected fragment size: 196bp. cDNA samples intended for the 3<sup>rd</sup> experiment on the Biomark. All samples, except for embryo 6 in the PAX7 knock-down (*siPAX7*) group, show amplicons of the expected size, indicating successful cDNA synthesis.

As a result of these pre-tests all samples, except samples from embryo 6 in the PAX7 knock-down group, were analyzed using the Biomark system.

Knowing that the cDNA concentrations between samples were similar (figure 4-8), the same volume of each sample was used for the final run of chip-based qPCR.

This simplified approach resulted in overall slightly lower  $C_q$ -values compared to the second test run, but far more importantly in a lower variance between the samples. This is visible in the lower standard deviations (figure 4-9) between only

1.19 and 1.43 cycles (compared to 3 to 3.5 cycles in 2<sup>nd</sup> test run), indicating a more similar amount of cDNA used for each sample.

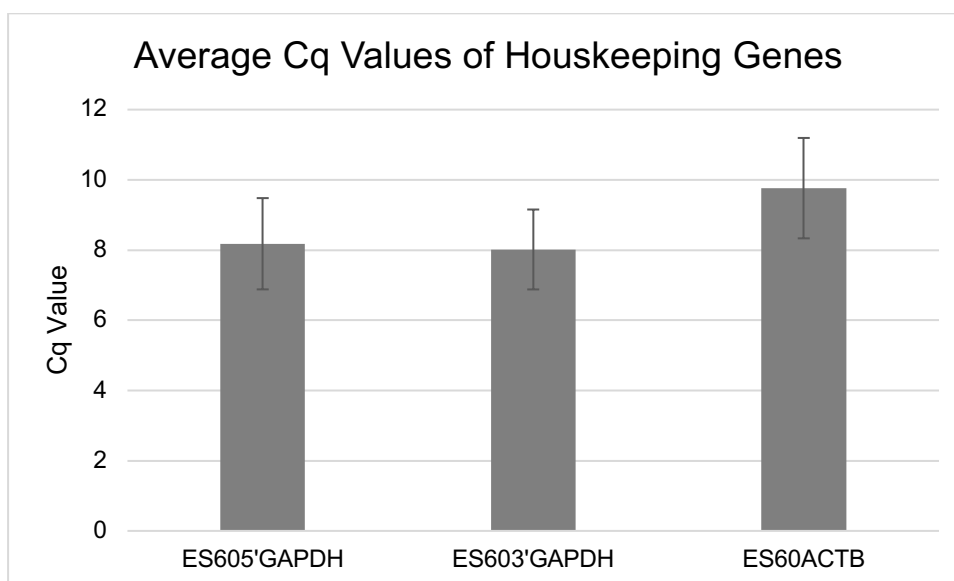


Figure 4-9: **Similar cDNA concentrations in samples used for final chip-based qPCR.** Average of the Cq-Values of the two ES60GAPDH primers and ES60ACTB primer. The relatively low standard deviation indicated by the error bars shows the overall low variance of cDNA concentration between the samples.

Comparing at the electroporated with the wildtype sides, no major difference for the means and standard deviations (table 4-9) can be seen. This indicates no impact on cDNA concentration by electroporation.

	ES605'GAPDH		ES603'GAPDH		ES60ACTB	
	Mean	SD	Mean	SD	Mean	SD
All samples	8.18	1.30	8.02	1.19	9.76	1.43
All electroporated side samples	8.34	1.37	8.16	1.09	9.86	1.21
All wildtype side samples	8.01	1.50	7.87	1.18	9.67	1.38

Table 4-9: **Electroporation has no impact on average reference gene expression in final Biomark run.** Means and standard deviations of C<sub>q</sub> values of reference genes, separately for electroporated and wildtype sides. The mean standard deviation is comparable between the different sides, showing no effect of electroporation and overall high consistency between samples.

#### 4.2.1.1.2 RNA Isolation and cDNA Synthesis for Well-Based qPCR

The RNA isolation using traditional phenol/chloroform precipitation from pooled had been established previously. All samples except one, had their RNA isolated using traditional phenol/chloroform precipitation.

This approach allowed for photometric RNA quantification and concentration adjusted loading of samples, reducing the amount of pre-testing required.

#### **4.2.1.2 Quality Control**

Depending on the method of RNA/cDNA isolation the RNA integrity (RIN) was measured using either qPCR or capillary electrophoresis. qPCR was used for samples intended for chip-based qPCR, whilst capillary electrophoresis was used for the RNA samples used in traditional well-based qPCR. A RIN >7 was considered to be acceptable.

##### **4.2.1.2.1 Good Sample Integrity for Chip-Based qPCR**

As the first test run on the Biomark showed amplification of genomic DNA residues, the  $C_q$  values obtained weren't analyzed.

For the second test run, the average  $\Delta C_{q_{3'-5'}} (GAPDH)$  was 1.41 cycles, with a standard deviation of 0.68 cycles, indicating a good RNA quality with a RIN>7. The  $\Delta C_{q_{3'-5'}}$  for the final Biomark run, using only embryos electroporated with pCAX and siPAX7-pSilencer, showed an even better  $\Delta C_{q_{3'-5'}} (GAPDH)$  average of 0.16 cycles and a standard deviation of 0.30 cycles across all embryos analyzed, indicating a high RNA integrity.

##### **4.2.1.2.2 Suboptimal RNA Integrity for Pooled Embryo Samples**

Photometric quantification showed that the yield of RNA varied, as expected with the number of embryos used and the HH stage. Many samples showed low quantities of RNA. Additionally, the measurements were skewed by both the 260/230 and 260/280 ratios being <1.8. These ratios indicate the presence of phenolic residue and protein contamination, both falsely increasing the concentration measured.

The RIN of this RNA, intended for well-based qPCR, was measured using capillary electrophoresis. Additionally, the QIAxcel electrophoresis device also measured RNA concentration.

Unfortunately, capillary electrophoresis had only just been made available towards the end of the project, when the qPCR had already been run, so in some instances no RIN could not be determined as not enough RNA remained. Additionally, some RNA samples had been stored at -20°C for over a year at the time of measuring, allowing for degradation to occur.

The first measurements using the QIAxcel resulted in low RIN for many samples. In this first run, 50ng RNA had been loaded per sample, but the device showed much lower RNA input (1-121µg) for most samples. For all samples with an RIN <7 a second measurement using 5µl of undiluted RNA was taken. This resulted in drastic uplifts for some samples, for example from 6.7 to 9.0 in case of the control side of pCAX electroporated midbrains at HH stage 17.

Tissue	n of embryos	Side	Concentration ng/µl (photometric)	260/280	260/230	Concentration ng/µl (capillary)	RIN (capillary)
MB HH stage 17 mixed 3x siPAX7-pSilencer1.0 <sup>a</sup> (= Batch 1)	8	GFP	53.2	2.1	-	-	-
		ctrl	69.2	2.1	-	40	8.1 <sup>b</sup>
MB HH stage 17 mixed 3x siPAX7-pSilencer1.0 (=Batch 2)	15	GFP	140	-	-	104	8.1 <sup>b</sup>
		ctrl	135	-	-	55	7.3 <sup>b</sup>
MB HH stage 17 siPAX7-pSilencer (= Batch 3)	13	GFP	30.8	1.80	0.55	89	9.0
		ctrl	31.2	1,86	0.60	121	8.4
MB HH stage 14 siPAX7-pSilencer	11	GFP	15	1.76	0.45	4	-
		ctrl	31	1.79	0.37	25	7.4
MB HH stage 17 sPAX7-pMES	15	GFP	86	1.87	-	12	6.5
		ctrl	148	1.61	-	18	6.1
MB HH stage 14 sPAX7-pMES	17	GFP	182	1.39	0.24	5	-
		ctrl	40	1.70	0.17	-	-
MB HH stage 17 iPAX7-pMES	16	GFP	143	1.47	0.24	14	5.9
		ctrl	80	1.43	0.52	33	5.8
MB HH stage 17 enPAX7-pMIW	14	GFP	70	1.65	0.74	15	6.6
		ctrl	72	1.47	0.46	6	7.1
MB HH stage 17 pCAX	13	GFP	96	1.63	1.57	17	7.6
		ctrl	87	1.56	0.71	15	6.7
HB HH stage 17 sPAX7-pMES	11	GFP	27	1.29	0.81	1	-
		ctrl	37	1.35	0.68	6	5.9
HB HH stage 14 sPAX7-pMES	12	GFP	40	1.32	0.28	6	-
		ctrl	102	1.29	0.37	2	6.3
HB HH stage 17 siPAX7-pSilencer1.0	17	GFP	78	1.43	0.68	4	5.9
		ctrl	51	1.31	0.43	4	5.8
HB HH stage 17 iPAX7-pMES	12	GFP	40.4	1.4	0.87	60	5.3
		ctrl	52.4	1.38	0.39	15	5.9
HB HH stage 17 enPAX7-pMIW	11	GFP	33	1.32	0.46	8	5.8
		ctrl	34	1.40	0.66	14	5.6

Table 4-10: **Low RNA yields correlate with low RNA integrity.** RIN (QIAxcel) and concentrations (QIAxcel + photometric) from RNA for qPCR on the StepOne Plus cycloer. The 260/280 and 260/230 ratios below 1.8

indicate contamination with both protein and phenol, resulting in a higher concentration measured at 260nm. A RIN <7 indicates degraded RNA and is not recommended for qPCR. The concentration measured photometrically was used for calculations for cDNA synthesis. The concentration measured using capillary electrophoresis should always be 50ng/μl, as based on photometric measurements, the same amount of RNA was loaded for all samples. <sup>a</sup>RNA isolated using Blirt Extract Me kit. All other samples isolated using phenol/chloroform isolation. More detailed overview of the individual batches can be found in table 4-16. <sup>b</sup> Results from first measurement with 50ng RNA loaded.

The RINs measured, at least for the RNA from mesencephalon tissue electroporated with siPAX7 constructs were good (>7). The other samples were in the range between 5 and 7, which is suboptimal for qPCR as the RNA was already moderately degraded.

#### 4.2.1.3 Primer Validation

Primers were validated in two steps, first testing their gen and cDNA specificity using PCR. In a second step, primer efficiency was validated using qPCR.

##### 4.2.1.3.1 Primers Show Specific Amplification

The testing for both gene and - if applicable - cDNA specificity was overall successful. All primers used in qPCR experiments passed these validations.

Primers were ordered and tested in multiple batches. The first batch of primers (figure 4-10) was tested on gDNA from a HH stage 17 body and cDNA from a HH stage 18 midbrain, both wildtype. All primers showed an amplicon on cDNA at the expected length, except the PAX3 primer, for which it took a second iteration (ES60PAX3-2) to amplify its target gene. (figure 4-11). No specific amplification on gDNA was detectable, except amplicons >1.5kb for both GAPDH primers.

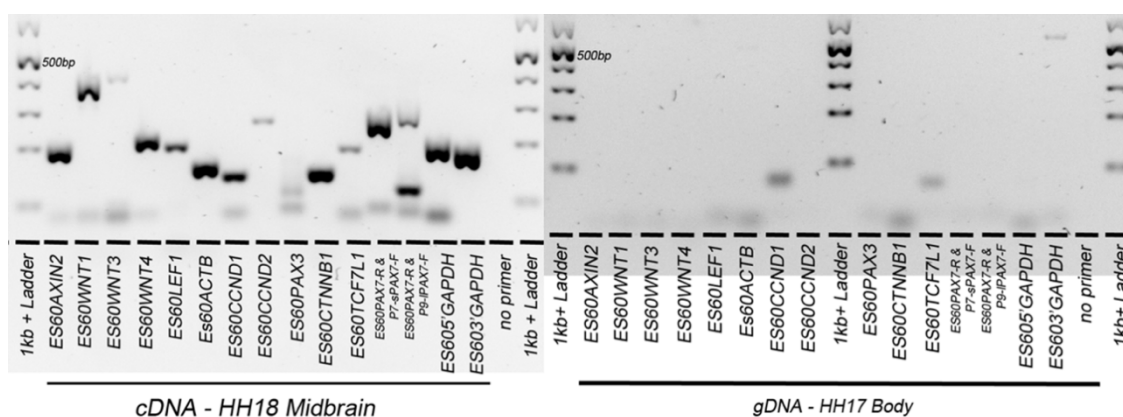


Figure 4-10: **Exon-skipping primers are specific and cDNA selective.** Side by side comparison of exon-spanning primers for qPCR using genomic and cDNA as template. Gel electrophoresis from conventional PCR. On cDNA all primers show amplification at the expected length, except for the ESPAX3 primer. Some primers, like the ES60PAX7-R/P9-IPAX7-F combination show additional bands <100bp, most likely primer dimers. Especially the strong band for the PAX7 primer did not re-appear in later qPCRs. Using genomic

DNA as template resulted in no specific amplification, as when cDNA was used as template, the bands <100bp are visible, most likely primer dimers.

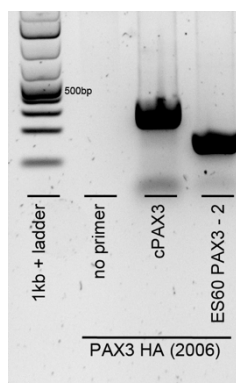


Figure 4-11: **The ES60PAX3-2 amplifies the intended PAX3 target gene.** PCR and gel electrophoresis. Plasmid containing a full-length PAX3 as template, old cPAX3 primer as positive control. The new ES60PAX3-2 primers show successful amplification at the expected length.

The second (figure 4-12) and third (figure 4-13) batch of primers, used for the final siPAX7-pSilencer1.0 experiment on the Biomark were tested using the same gDNA and a cDNA from the control side of a pCAX electroporated midbrain at HH stage 17. As expected, only the frizzled (FZD) primers showed amplification on the genomic DNA. The FZD5, DKK4, HES4 and TCF7L1-2 primers showed no amplification on cDNA and weren't used for further experiments.

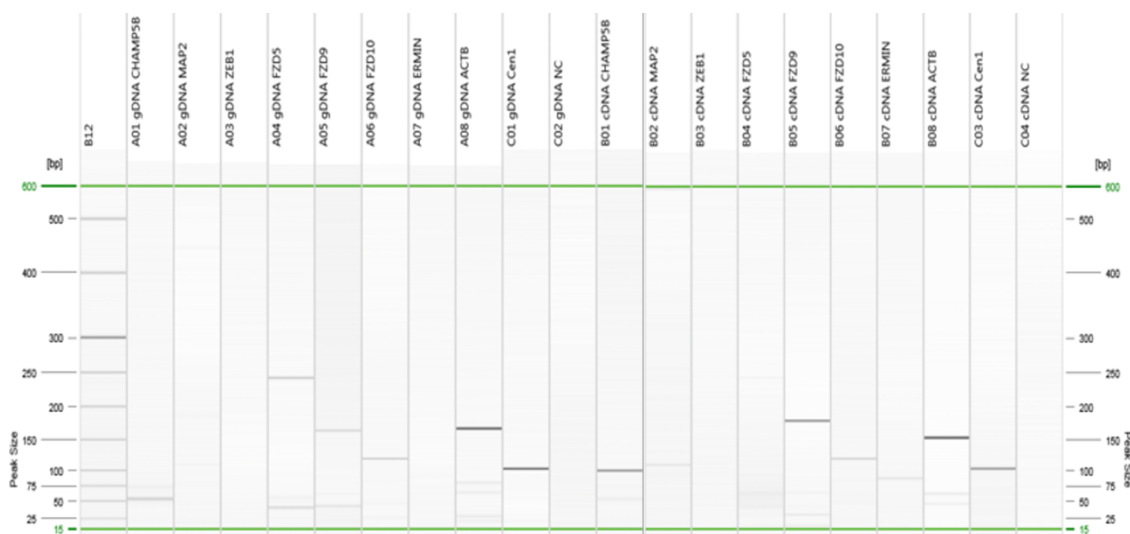
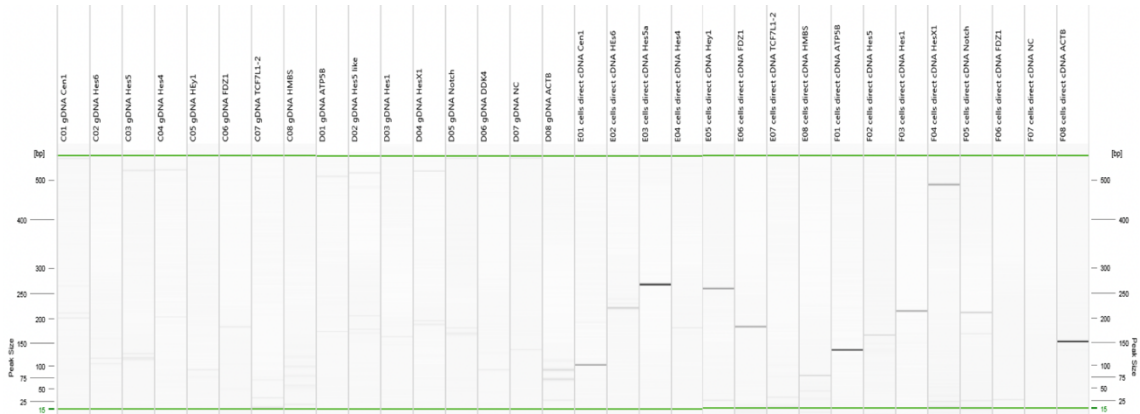


Figure 4-12: **Exon-skipping primers are specific and cDNA selective.** Side by side comparison of exon-spanning primers for qPCR using genomic and cDNA as template of potential off-target genes of the siPAX7-pSilencer1.0 construct and FZD receptors. The gDNA appears to contain some cDNA contamination, as the ES60ACTB (only labeled ACTB) and other primers also showed amplification on gDNA. The cDNA shows traces of gDNA presence (band around 100bp with the Cen1 primer). All primers produced a product of the expected size, when cDNA was used as template - except for the ES60ZEB1 and 60FZD5 primer, which were not used for later qPCR applications. Only genes used as labeling. All lanes – except for the FZD lanes – used exon-skipping primers.



**Figure 4-13: Exon-skipping primers are specific and cDNA selective.** Side by side comparison of exon-spanning primers for qPCR using genomic and cDNA as template of potential off-target genes of the siPAX7-pSilencer1.0 construct, FZD1 and diverse HES/NOTCH signaling pathway components. No specific amplification visible on the genomic DNA is visible, except for the FZD1 primer, which is to be expected as FZD genes don't contain any exons. The cDNA from the Cells Direct kit shows low levels of gDNA contamination, indicated by the weak band around 100bp with the Cen1 primer. ES60TCF7L1-2 and ES60HES4 failed to show amplification on gDNA and were excluded from further experiments

#### 4.2.1.3.2 PAX7 Primers Amplify Splice-Variants Specifically

The splice variant specific primers were not only tested on cDNA, but also with plasmid DNA containing the individual splice variants. Amplicons at the correct length could be observed for the reaction with the P7/ES60PAX7-R primer combination (specific for short TA splice variant of PAX7) with sPAX7-ΔGFP-pMES and P9/ES60PAX7-R primer combination (specific for long TA splice variant of PAX7) with IPAX7-ΔGFP-pMES (figure 4-14, lane 2 and lane 6). Interestingly, for the combination of P7 with the long splice variant plasmid and the combination of the P9 primer with the short splice variant plasmid, where no amplification was expected, an amplicon of larger size could be observed (figure 4-14, lane 3 and lane 5). This off target amplicon could also be replicated with the original P8 and P10 revers primers published by Mao et al. in 2009. Using different reaction buffers or MgCl<sub>2</sub> concentrations did not eliminate the off-target amplicons either. Fortunately, these amplicons did not appear in the qPCR products analyzed using capillary electrophoresis, where only singular amplicons at ~280bp or ~320bp could be observed.

The unexpected bands (figure 4-14) indicate either a contamination of the plasmid DNA with the other splice variant or some other unspecific binding in the gene or plasmid. The latter one seems more likely, as in the case of contamination a shorter amplicon would be expected.

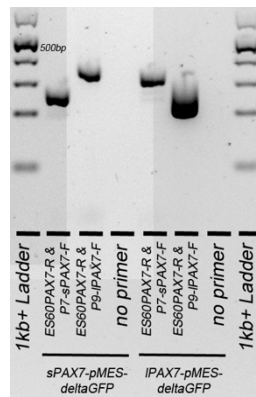


**Figure 4-14 PAX7 splice variant specific primers have off-target amplicons in the PAX7 gene.** PAX7 splice variant specific primers on plasmids containing specific PAX7 splice variants. Both primers show amplification on both splice variants, but in both cases the amplicons aren't the expected length, that the primer should produce. Later qPCR testing showed a strong preference of the primers for their intended splice variants.

To further determine the splice variant selectivity of the PAX7 splice variant primers, the same experiment was done using qPCR. Despite the high standard deviations, the P7/ES60PAX7-R primer combination showed over 10000 times stronger amplification (table 4-11) of the short splice variant compared with the long splice variant of PAX7. The P9/ES60PAX7-R primer combination showed an almost 50000 times stronger amplification (table 4-13) on its intended long splice variant.

	P7/ES60PAX7-R		P9/ES60PAX7-R	
	mean	SD	mean	SD
sPAX7-ΔGFP-pMES	9.318	1.548	22.717	0.884
IPAX7-ΔGFP-pMES	28.758	1.605	9.857	0.447
fold difference (correct SV over wrong SV)	10799		489438	

**Table 4-11: PAX7 splice variant specific primers are splice variant specific.** The ES60PAX7-R primer paired with either the P7 primer amplifying the short TA of PAX7 or the P9 primer amplifying the long PAX7 TA splice variant. The P7/ES60PAX7-R variant shows a more than 10000-fold preference for the intended short TA splice variant, whereas the P9/ES60PAX7-R combination shows almost a 490000-fold preference for the intended long PAX7 TA splice variant. Both primers amplify the intended splice variant with a high specificity.

Overall, the splice variant specific PAX7 primers can be considered to be specific for qPCR applications as they show:

- A strong preference for their intended splice variant when tested with plasmid DNA
- No off-target amplicons when tested using cDNA as template.

#### 4.2.1.3.3 Primers for Pooled-Embryo qPCR have Good Efficiency

Once the specificity of the primers was tested, their efficiency was determined using qPCR. The ES603'GAPDH, ES60ACTB, ES60YWATZ, ES60CTNNB1,

ES60AXIN2, ES60CCND1 as well as the P7/ES60PAX7-R and P7/ES60PAX7-R combinations, primer efficiency was assessed using the StepOne Plus cycler with cDNA from spinal cord of mixed wildtype embryos. All of the eight primers showed amplification with at least 5 of 6 of the cDNA concentrations tested (figure 4-15). All had an efficiency of between 98-105% (table 4-12) and were thus viable for qPCR (>90% and <110%).

RNA concentration [ng/μl]	Log conc.	ES60 ACTB	ES60 3GAPDH	ES60 YWATZ	ES60 CTNNB1	ES60 PAX7-r	P9/ES60 PAX7-R	ES60 AXIN2	ES60 CCND1
250	2,398		11,92	17,96	16,01	21,16	24,78	18,80	13,84
50	1,699	12,27	14,27	19,93	18,09	23,54	27,00	20,98	16,05
10	1,000	14,45	16,21	22,22	20,18	25,69	28,99	23,32	18,15
2	0,301	16,84	18,46	24,42	22,54	27,83	31,33	25,22	20,46
0,4	-0,398	19,03	20,85	26,78	24,80	30,37	34,03	27,92	23,00
0,08	-1,097	21,46	23,31	29,12	27,18	33,05		30,03	25,59
Slope		-3,288	-3,227	-3,212	-3,202	-3,355	-3,266	-3,224	-3,348
Efficiency [%]		<b>101,4</b>	<b>104,1</b>	<b>104,8</b>	<b>105,3</b>	<b>98,6</b>	<b>102,4</b>	<b>104,3</b>	<b>98,9</b>

Table 4-12: **Primers for pooled embryo qPCR show good efficiency.**  $C_q$  values obtained by qPCR on a dilution series of cDNA. The slope of the  $C_q$  values with the logarithmic values of the RNA concentration equivalents allow for the efficiency calculation. Efficiencies between 90 to 110% are acceptable for qPCR.

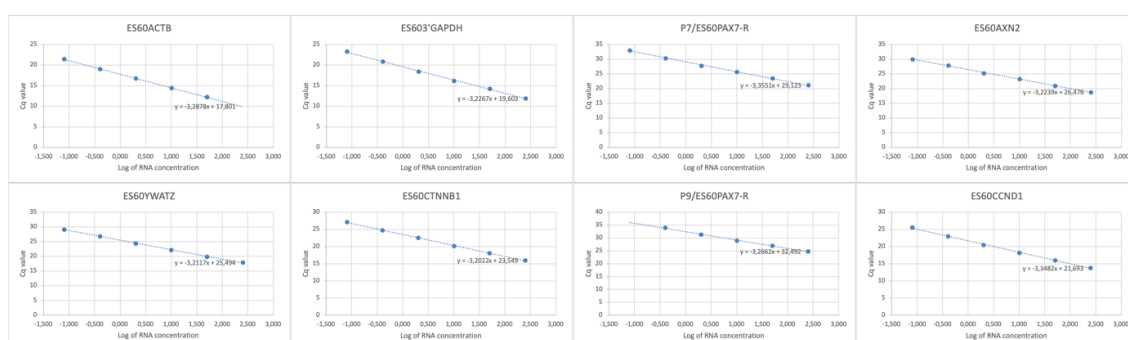


Figure 4-15: **Primers for pooled embryo qPCR show good efficiency.** Visualization of slopes used for efficiency calculation.  $C_q$  values and corresponding RNA amounts blotted.

#### 4.2.1.3.4 Primers for Single Embryo Analysis have too high Efficiency

In addition to the primer testing using the StepOne Plus cycler, all primers used for single embryo analysis were tested with the Biomark system on the same chip alongside the samples themselves. Prior to this primer specificity was assessed using conventional PCR (figures 4-10 to 4-14).

Using the Biomark with a 96.96 chip, all primers successfully amplifying cDNA, showed efficiencies higher than 110% (table 4-13). This means, that the cDNA

more than doubles with each amplification cycle and renders the results from the single embryo analysis invalid. The ES60WNT1, ES60WNT3A, ES60HESX1 and EGFP primers failed amplification in more than two dilution steps and were excluded from all further analysis.

Sample	Log conc.	ES60 ACTB	ES60 3'GAPD	ES60 5'GAPD	ES60 YWATZ	ES60 ATP5B	ES60 HMBS	ES60 AXIN2	ES60 WNT4	ES60 LEF1
1G pure	0.000	4.64	4.26	4.96	10.11	7.36	11.85	10.18	9.89	10.61
1G 1:5	-0.699	10.30	8.09	8.51	14.07	12.47	15.24	14.44	16.07	14.51
1G 1:25	-1.398	11.53	9.71	10.01	15.50	13.74	16.79	16.22	16.12	16.00
1G 1:125	-2.097	12.21	10.27	10.55	16.09	14.29	17.29	16.84	17.13	16.70
1G 1:625	-2.796	14.01	12.11	12.49	18.12	16.15	18.91	19.21	18.68	18.41
1G 1:3125	-3.495	14.78	12.67	13.07	19.25	17.17	20.25	19.30	21.32	19.15
Slope		-2.557	-2.235	-2.167	-2.390	-2.480	-2.189	-2.475	-2.699	-2.254
Efficiency [%]		<b>146.1</b>	<b>180.2</b>	<b>189.4</b>	<b>162.1</b>	<b>153.1</b>	<b>186.2</b>	<b>153.5</b>	<b>134.7</b>	<b>177.8</b>

Sample	Log conc.	ES60 CTNNB1	60 FZD1	60 FZD5	60 FZD9	60 FZD10	P7sPAX7-F/ES60 PAX7-R	P9 IPAX7-F/ES60 PAX7-R	ES60 PAX3-2	ES60 CCND1
1G pure	0.000	7.77	9.28	13.42	13.17	10.07	11.48	15.92	10.04	7.60
1G 1:5	-0.699	11.98	13.49	16.87	17.66	13.62	15.85	19.51	13.55	11.45
1G 1:25	-1.398	13.50	14.89	18.81	19.00	15.04	17.43	21.08	15.07	12.58
1G 1:125	-2.097	14.11	15.65	18.72	19.53	15.77	18.28	22.46	15.62	13.24
1G 1:625	-2.796	15.95	17.70	20.87	20.97	17.79	19.94		17.58	15.20
1G 1:3125	-3.495	16.49	18.25	21.06	22.23	18.40	20.29		18.27	15.56
Slope		-2.296	-2.380	-2.047	-2.278	-2.243	-2.337	-3.033	-2.201	-2.115
Efficiency [%]		<b>172.6</b>	<b>163.1</b>	<b>208.0</b>	<b>174.7</b>	<b>179.2</b>	<b>167.9</b>	<b>113.6</b>	<b>184.6</b>	<b>197.0</b>

Sample	Log conc.	ES60 NOTCH1	ES60 HES1	ES60 HESSA	ES60 HES5	ES60 HES6	ES60 HEY1	ES60 CHMP48	ES60 ERMN	ES60 MAP2
1G pure	0.000	12.91	13.06	10.79	10.40	13.60	11.41	8.91	16.29	13.31
1G 1:5	-0.699	16.40	17.08	15.29	14.73	17.37	14.90	12.35	19.47	16.96
1G 1:25	-1.398	17.58	18.59	16.95	16.40	18.73	16.40	13.77	21.43	18.68

1G 1:125	-2.097	18.14	19.31	17.56	17.06	19.61	17.11	14.24	22.00	18.86
1G 1:625	-2.796	15.79	20.90	19.59	18.85	22.17	19.57	16.35	23.78	20.85
1G 1:3125	-3.495	15.66	21.90	20.85	19.50	22.04	19.42	17.05		20.51
Slope		-0.510	-2.303	-2.609	-2.392	-2.348	-2.237	-2.173	-2.505	-1.956
Efficiency [%]		<b>9046.3</b>	<b>171.8</b>	<b>141.7</b>	<b>161.8</b>	<b>166.6</b>	<b>179.9</b>	<b>188.6</b>	<b>150.7</b>	<b>224.5</b>

*Table 4-13: Too high primer efficiencies for primers used for single embryo analysis on the Biomark qPCR system. cDNA from the midbrain of a HH-stage 17 embryo, electroporated with pCAX, only electroporate side used. All primers failed efficiency validation with efficiencies > 110%. In addition to this the primer combination P9 IPAX7-F/ES60-PAX7-R failed amplification in samples with dilutions >1:625.*

In search of the cause of these too high primer efficiencies a well-based qPCR using the StepOne plus system was performed.

The known good ES60ACTB primer was used with a fresh dilution series from the same cDNA used for efficiency testing on the Biomark system, alongside the Exo1-digested preamplification product, from the efficiency testing on the Biomark, that had been stored at -20°C.

Using the C<sub>q</sub>-values obtained this way, primer efficiencies were calculated, revealing a 94.9% (table 4-14) for the fresh dilution series, whereas the Exo1-digested pre-amplification product showed an efficiency of 139.6% (table 4-14). The efficiency of the newly done dilution series only being 6 percentage points off from the previously measured efficiency (table 4-12) indicates the cDNA isolated using the CellsDirect Kit not being the cause of the primer efficiencies being too high when using the Biomark system. As the efficiency obtained using the preamplification product (table 4-14) was in line with the efficiency result obtained using the Biomark system (table 4-13), the Biomark as a qPCR cyclor also wasn't the problem, leaving only the preamplification, the Exo1 digest or the dilution steps done prior to the preamplification as root cause, with the preamplification being the most likely culprit.

No further experiments on this issue were performed and the experiments using the Biomark system weren't re-run due to budgeted constrains.

Sample	Log conc.	New Dilution Series	Exo1-Digested Preamplification Product
pure	0.00	17.28	10.54
1:5	-0.70	19.85	16.38
1:25	-1.40	21.37	17.55
1:125	-2.10	25.35	17.90
1:625	-2.80	27.30	19.67
1:3125	-3.49	28.90	21.39
Slope		-3.45	-2.63
Efficiency [%]		94.93	139.63

Table 4-14: **Preamplification process caused too high primer efficiencies.** C<sub>q</sub>-values and primer efficiencies of the ES60ACTB primer. Both preamplification product from chip-based qPCR preparation and fresh dilution series using the same cDNA used as template. The resulting efficiencies are in both cases in line with previous results (table 4-13 and 4-14). This indicates the chip-based qPCR not causing the high efficiencies, leaving the preamplification/Exo-I digest as likely sources.

#### 4.2.2 Short TA Splice Variant of PAX7 is Dominant in the Mid-brain

cDNA synthesized by Ulrike Kohler from old, preexisting RNA samples (date of RNA isolation and number of biological replicates within each sample unknown) was used to assess expression of the two different PAX7 transactivation splice variants at different HH stages. As all samples were from wildtype tissue, only the ES603'GAPDH primer was used as reference gene, along with the P7- or P9/ES60PAX7-R primers, allowing for the direct import of standard deviations and  $\Delta C_q$  values from the StepOne software.

The quality of the qPCR was overall acceptable. The melt curves only showed singular peaks, the no template controls show no amplification, but the C<sub>q</sub> values are much higher than desired (table 4-15). Values of 8-10 cycles for the reference genes and 15-20 for PAX7 splice variants would be desirable, as lower cycle numbers typically result in lower standard deviations. This indicates low cDNA/RNA input and might also be the result of poor RNA quality because of prolonged storage at -20°C. For the short splice variant, at HH stage 23 in the dorsal midbrain, two wells failed to detect amplification, thus no standard deviation could be calculated.

Using the  $\Delta C_q$  values, at least for the samples from the dorsal midbrain, where PAX7 is primarily expressed, a lower expression of the long PAX7 splice variant can be observed, as indicated by the higher  $\Delta C_q$  values (table 4-15). The expression of the short splice variant seems to be constantly higher, between values of 7.7 to 9.4 cycles, compared to the 10-12.5 cycles of the long splice variant. The long splice variant shows a stronger change in expression, between the different HH stages, with a standard deviation of 1.13 cycles compared to the 0.65 cycles of the short splice variant. Overall, the expression of the long splice variant seems to be increasing from HH stage 17 to HH stage 29, with a decrease at HH stage 38, whilst the short splice variant is constantly highly expressed.

The  $\Delta C_q$  values from the whole midbrains show strong deviations between the technical replicates, making the results less reliable, but the overall trend of stronger expression of the short splice variant prevails.

	ES603' GAPDH		P9+ES60PAX7-R				P7+ES60PAX7-R			
	Mean	SD	Mean	SD	$\Delta C_q$	$\Delta C_q$ SD	Mean	SD	$\Delta C_q$	$\Delta C_q$ SD
dmb HH stage 17/18	19.31	0.11	31.82	0.58	12.50	0.59	28.21	0.45	8.90	0.47
dmb HH stage 23	18.04	0.13	28.66	0.11	10.62	0.18	25.72		7.67	
dmb HH stage 24	17.96	0.13	28.71	0.27	10.76	0.36	26.39	0.39	8.44	0.49
dmb HH stage 29	18.09	0.05	28.06	0.30	9.97	0.30	26.44	0.66	8.35	0.67
dmb HH stage 38	18.42	0.08	30.78	0.24	12.36	0.25	27.82	0.29	9.40	0.30
mb HH stage 17/18	19.28	0.29	32.59	1.36	13.31	1.39	30.09	1.69	10.81	2.09
mb HH stage 22/23	17.37	0.14	29.85	0.76	12.47	0.77	26.77	1.61	9.40	1.98
mb HH stage 35	20.78	0.10	31.09	0.28	10.31	0.48	30.46	0.23	9.68	0.40

Table 4-15: **The short TA domain splice variant of PAX7 shows higher expression in the midbrain.** In the dorsal midbrain (dmb), where PAX7 is primarily expressed, the short splice variant shows higher expression (lower  $\Delta C_q$  values) compared to the long splice variant. The high standard deviations for the results from the midbrain (mb) tissue don't allow for the same statement, but the means show a similar trend.

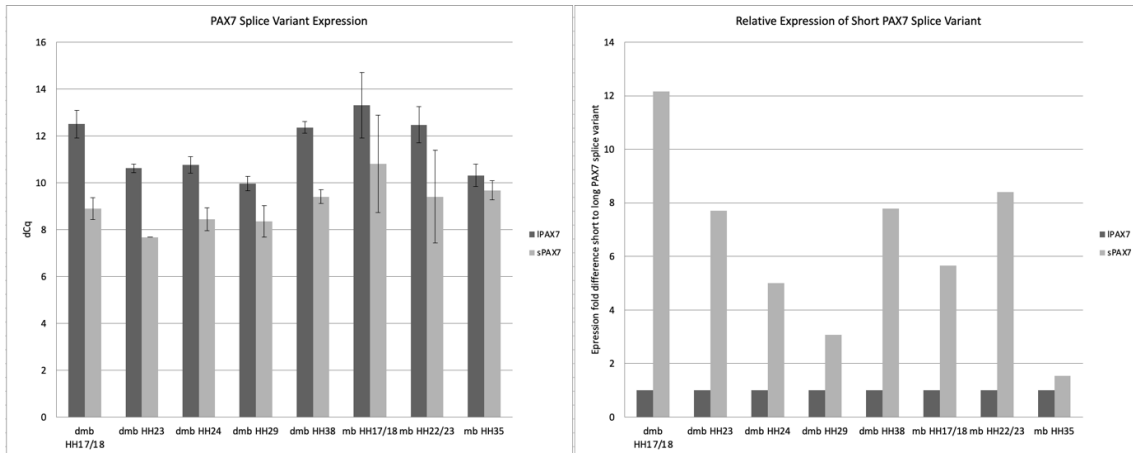


Figure 4-16: **Expression of PAX7 trans activation domain splice variants in the midbrain (mb) of wildtype chicken embryos between HH stage 17 and HH38.** Left side: absolute  $\Delta Cq$  values. Right side: fold change in expression of the short splice variant compared with the long splice variant. PAX7 is typically expressed in the dorsal midbrain (dmb) of chicken embryos. Here the short splice variant shows constant and stronger expression than the long splice variant. Error bars indicate standard deviation.

### 4.2.3 ddCq Expression Analysis of Pooled Embryos

Using the StepOne Plus cycler, qPCR was performed with one type of tissue, stage and plasmid electroporated per plate, but the results will be presented gene by gene, allowing for an easier comparison between the effects of the different electroporations.

In the following, the individual results will be presented in detail, a summary of all results can be found in chapter 4.2.3.6. The detailed presentation for each gene is accompanied by general expression statistics and quality control data for the individual runs.

Special attention was put on the PAX7 knock-down in the midbrain for embryos harvested at HH stage 17, as this was the expression modification known to show an impact on canonical Wnt signaling. Three individual badges of embryos were electroporated:

Batch Number	Plasmid	n	RNA Isolation Method
Batch 1	3x siPAX7 -pSilencer1.0 plasmid mix	8	Blirt Extract Me RNA Isolation Kit
Batch 2		15	Phenol/Chloroform Precipitation
Batch 3	siPAX7-pSi- lencer1.0	13	

Table 4-16: **Multiple PAX7 knock-downs in the midbrain.** Three batches of midbrain tissue with PAX7 knock-downs were prepared, differing in the plasmid(s), RNA isolation technique and number of embryos included. The 3x siPAX7-pSilencer1.0 plasmid mix consists of the three plasmids generated in chapter 4.4; the plasmid used for batch 3 was the plasmid generated by Li that had previously shown to reduce canonical Wnt signaling activity.

### 4.2.3.1 qPCR Quality

For most qPCR reactions run, the amplification and melting curves were examined per primer and for each plate individually, negative controls excluded. For 12 qPCRs from PAX7 expression modifications and the qPCR from embryos treated with LiCl, all melt curves showed singular clean peaks at comparable temperatures (figure 4-17).

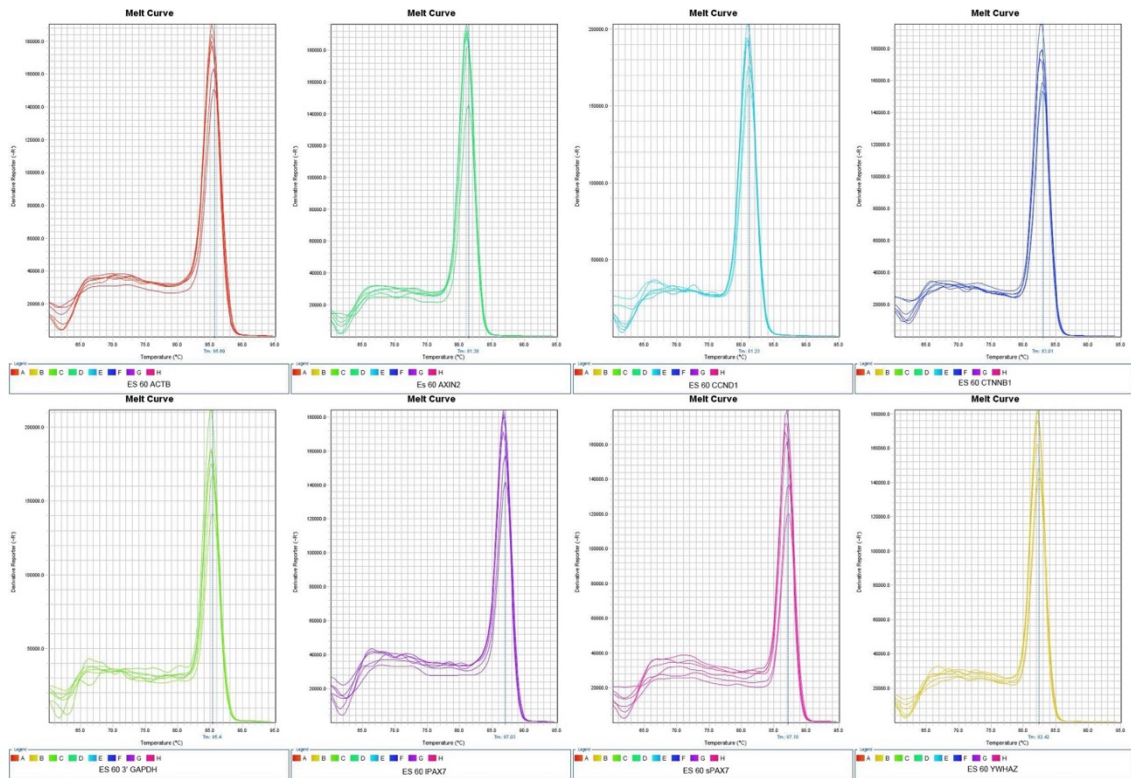


**Figure 4-17: Singular amplicon detected in all qPCRs**, exemplary shown for qPCR from HH stage 17 midbrain tissue, electroporated with the pCAX plasmid. All blots show singular sharp peaks, indicating only a singular amplicon being produced. Wells loaded with the same primer blotted together (excluding no template control), the peaks being at the same temperature indicate the same amplicon being produced in each well. P7/ES60PAX7-R is abbreviated as ES60sPAX7 and P9/ES60PAX7-R is abbreviated as ES60IPAX7, analog to the splice variant amplified.

Amplification curves had the expected sigmoid shape, except for the ES60CTNNB1 curves in the EnPAX7-pMIW electroporated midbrains, where

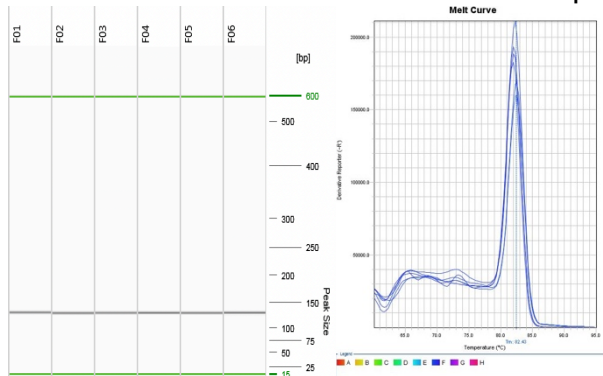


**Figure 4-18: qPCR quality control for samples with unexpected amplification curve shows only expected amplicon.** Capillary electrophoresis and meltcurve of the ES60CTNNB1 wells of the enPAX7-pMIW midbrain qPCR. Although initial background skewed the amplification curve, the PCR reaction only produced the expected 129bp amplicon and showed a singular peak in the meltcurve analysis. F01-F03: PCR products (using the ES60CTNNB1 primer) from the GFP-side of the enPAX7-pMIW electroporated embryos, F04-F06: PCR products from the corresponding control side.

strong initial background required manual tuning of the detection threshold. Using capillary electrophoresis, amplicon lengths were verified for all reactions on this plate (figure 4-18).

A total of one well of the P9/ES60PAX7-R, one well of ES60ACTB and three wells of ES603'GAPDH reactions were omitted from the analysis, as they showed strong (>2 cycles) deviation from their other technical replicates.

#### **4.2.3.2 Reference Gene Expression Unaffected by Electroporations**

All qPCRs, except for the PAX7 knock-down batch 2 run and the run using the siPAX7-pSilencer1.0 designed by Li in midbrains at HH stage 14 used ES603'GAPDH, ES60YWATZ and the ES60ACTB primers to detect them as reference genes. These two exceptions only used ES603'GAPDH primers.

The  $C_q$  values of the reference genes are, with the exceptions of PAX7 knock-down batch 2 and the HH stage 17 midbrains electroporated with sPAX7-pMES, much higher than desired, but still within validated range. This is most likely the result of low RNA input. This itself wasn't a problem, as all values were still within the area tested for primer efficiency, but it results in higher standard deviations. The standard deviations are acceptable, especially for the combined reference genes are mostly below 0.15 cycles.

For most treatments and stages, the  $C_q$  values of the different reference genes show similar  $C_q$ -value differences between the sides, not raising concerns about their expression being affected by the treatments (table 4-17). An exception to this is the HH stage 14 midbrain electroporated with sPAX7-pMES, where the ES603'GAPDH primer produces an inverse delta compared to the other two primer pairs. (Figure 4-19) As this only occurs in one of four tissues/stages treated with sPAX7-pMES, it is unclear, whether this is caused by the treatment or just biological/technical variance. For  $\Delta\Delta C_q$  analysis, the geometric mean was still used.

One ES60ACTB well of the batch 1 of the PAX7 knock-down in the midbrain at HH stage 17 was omitted. Same goes for ES603'GAPDH primer wells in the second run under the same conditions and for the runs with the siPAX7-pSilencer1.0 plasmid from Li on midbrain tissue (both at HH stage 14 and 17 (=batch 3)).

Stage and Region	Treatment	n	Side	ES60 ACTB		ES60 YWATZ		ES60 3'GAPDH		All Reference Genes	
				Mean	SD	Mean	SD	Mean	SD	Geo. Mean	SD
HH stage 17 Midbrain	3x siPAX7-pSi-lencer1.0; run 1	8	GFP	14.58	0.278	19.31	0.295	13.65	0.112	15.66	0.134
			ctrl.	16.72	0.067	20.76	0.772	14.09	0.261	16.97	0.236
	3x siPAX7-pSi-lencer1.0; run 2	15	GFP					9.28	0.047	9.28	0.047
			ctrl.					9.66	0.057	9.66	0.057
	siPAX7-pSi-lencer1.0	13	GFP	16.18	0.010	14.06	0.393	8.87	0.085	12.64	0.124
			ctrl.	15.95	0.020	13.68	0.115	7.16	0.028	11.60	0.036
	sPAX7-pMES	15	GFP	8.68	0.244	15.01	0.088	21.87	0.032	14.18	0.136
			ctrl.	8.58	0.094	15.04	0.010	21.73	0.020	14.10	0.052
	IPAX7-pMES	16	GFP	18.88	0.085	17.26	0.060	17.90	0.060	18.00	0.040
			ctrl.	18.89	0.045	16.09	0.180	17.83	0.067	17.57	0.071
	enPAX7-pMIW	14	GFP	16.24	0.071	18.87	0.039	15.76	0.103	16.90	0.046
			ctrl.	17.90	0.026	20.88	0.013	16.89	0.024	18.48	0.013
	pCAX	13	GFP	16.90	0.039	19.92	0.041	15.91	0.010	17.50	0.018
			ctrl.	16.90	0.034	19.80	0.059	15.88	0.025	17.45	0.023
HH stage 14 Hind-brain	siPAX7-pSi-lencer1.0	11	GFP					11.26	0.139	11.26	0.139
			ctrl.					10.96	0.001	10.96	0.001
sPAX7-pMES	17	GFP	21.65	0.034	23.91	0.030	18.41	0.065	21.20	0.029	
		ctrl.	17.94	0.037	21.49	0.047	20.88	0.038	20.04	0.023	
HH stage 17 Hind-brain	siPAX7-pSi-lencer1.0	17	GFP	16.98	0.041	20.18	0.075	16.35	0.077	17.76	0.038
			ctrl.	18.94	0.020	22.46	0.174	17.69	0.114	19.60	0.066
	sPAX7-pMES	11	GFP	20.62	0.286	24.84	0.092	19.89	0.070	21.68	0.107
			ctrl.	17.92	0.035	21.48	0.197	16.47	0.293	18.51	0.124
	IPAX7-pMES	12	GFP	18.96	0.025	22.13	0.055	16.87	0.041	19.20	0.024
			ctrl.	18.83	0.096	21.98	0.075	16.92	0.012	19.13	0.039
enPAX7-pMIW	11	GFP	19.17	0.077	22.88	0.017	17.66	0.074	19.79	0.039	
		ctrl.	18.83	0.057	23.46	0.063	16.95	0.029	19.56	0.029	
HH stage 14 Hind-brain	sPAX-pMES	12	GFP	18.74	0.279	22.80	0.076	18.69	0.202	19.99	0.125
			ctrl.	18.72	0.116	22.46	0.014	18.13	0.052	19.68	0.045
HH stage 24 Body	LiCl and NaCl	1	LiCl	15.43	0.031	19.92	0.042	15.45	0.077	16.81	0.032
			NaCl	15.62	0.102	19.70	0.051	15.31	0.020	16.76	0.040

**Table 4-17: Overview of  $C_q$  values, showing no impact of electroporation on reference gene expression. Only the overexpression of the short splice variant of PAX7 seemingly increased GAPDH expression compared to ACTB and YWATZ, but only in HH stage 14 midbrains.**

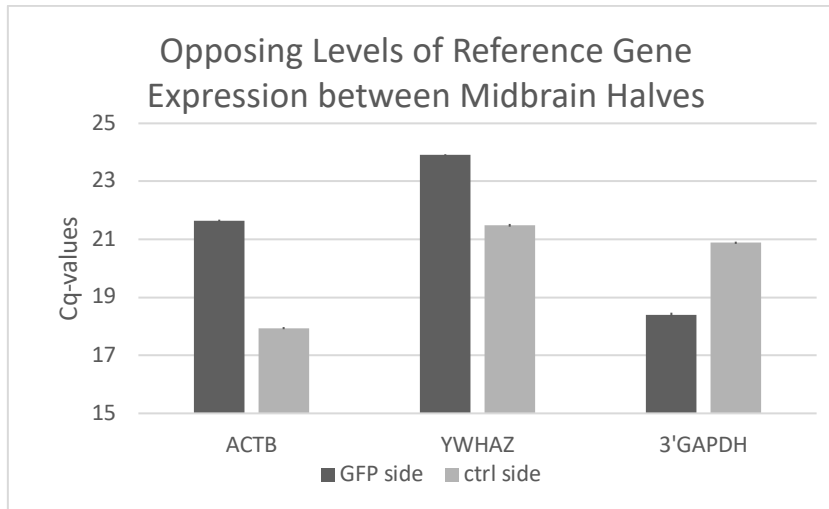


**Figure 4-19: Low RNA input likely caused false reference gene expression measurements.** Average  $C_q$  values of reference genes in qPCR from midbrain at HH stage 14 electroporated with sPAX7-pMES. The inverse expression levels of GAPDH compared to ACTB and YWHAZ, alongside the high  $C_q$  values indicate extremely low RNA input and reduce accuracy of results. Error bars (barely visible) indicate SD.

#### 4.2.3.3 PAX7 Expression Modifications Do Not Cause Expected Changes in PAX7 Expression

Expression analysis of the short and long transactivation domain splice variants was done using the same P7, P9 and ES60PAX7-R primer combinations as before, with P7 detecting the short, and P9 detecting the long splice variant. With average  $C_q$  values of ~25.6 cycles for the long and ~21.5 cycles for the short splice variant (appendix 9.2.1.1),  $C_q$  values are generally high, partly resulting in high standard deviations within the technical replicates, not allowing for conclusions about electroporation impacts on gene overexpression or knockdowns. All  $C_q$  values are still within validated range.

Overall expression of the short splice variant is stronger, with a  $\Delta C_q$  of 3.89 cycles over all tissues and stages, when only looking at the control sides, confirming the earlier findings, at least for HH stage 14 and HH stage 17.

##### 4.2.3.3.1 Midbrain

In the midbrain of embryos at HH stage 17, the electroporation of pCAX in 13 embryos resulted in a 1.039-fold increase in expression of the long PAX7 splice variant. Similar changes were observed for the short splice variant, with a 0.998 increase in expression. These results show, that the pCAX used as negative control did - as expected - not affect PAX7 gene expression (figure 4-20).

A reduction in expression of the long splice variant could only be achieved in one of three knockdown experiments. Batch 1 showed a 55.6% reduction of the expression of the long splice variant. The 40% reduction of expression of the short

splice variant in the same experiment can unfortunately not be considered valid and reliable, as it has a standard deviation of 0.633 cycles with an  $\Delta\Delta C_q$  value of only 0.74 cycles. The other two knockdown experiments show almost no impact on the expression of the short splice variant ( $\Delta\Delta C_q$  values of -0.09 cycles in both experiments), especially when considering the standard deviations of 0.205 cycles and 0.227 cycles. Batch 2 showed a similar picture for the long splice variant ( $\Delta\Delta C_q$  of -0.16 cycles, SD 0.446 cycles) and the run using batch 3 even resulted in a 1.42-fold increase of long PAX7 expression with a standard deviation of 0.146 cycles and an  $\Delta\Delta C_q$  value of -0.5 cycles, making it a measurable increase (figure 4-20).

Overexpression of the long PAX7 splice variant worked as intended and resulted in a 2.77-fold increase of the expression of the long splice variant PAX7. The expression of the short splice variant did also increase to, by 1.47-fold. For both increases, the standard deviations, from the base  $\Delta\Delta C_q$  values are decently low, with 0.089 cycles and 0.092 cycles respectively, making these results unlikely to be an error of measurement (figure 4-20).

Overexpression of the short splice variant, using the sPAX7-pMES plasmid did not affect the expression of the long splice variant, with a standard deviation of 0.156 cycles and a  $\Delta\Delta C_q$  value of 0.15. The expression of the short splice variant saw a minor reduction in expression, of at most 17%, but with a standard deviation of 0.196 cycles and a base  $\Delta\Delta C_q$  value of only 0.27 cycles, the reduction measured is to be taken with a grain of salt (figure 4-20).

The same is true for the overexpression of the enPAX7-pMIW construct, a construct that inhibits expression of all genes regulated by PAX7. Both the short and long splice variant show a minor reduction in their expression, of about 13-14%, which are to be considered valid measurements with standard deviations of 0.072 cycles ( $\Delta\Delta C_q$  0.22 cycles) for the short and 0.056 cycles ( $\Delta\Delta C_q$  0.21 cycles) for the long splice variant (figure 4-20).

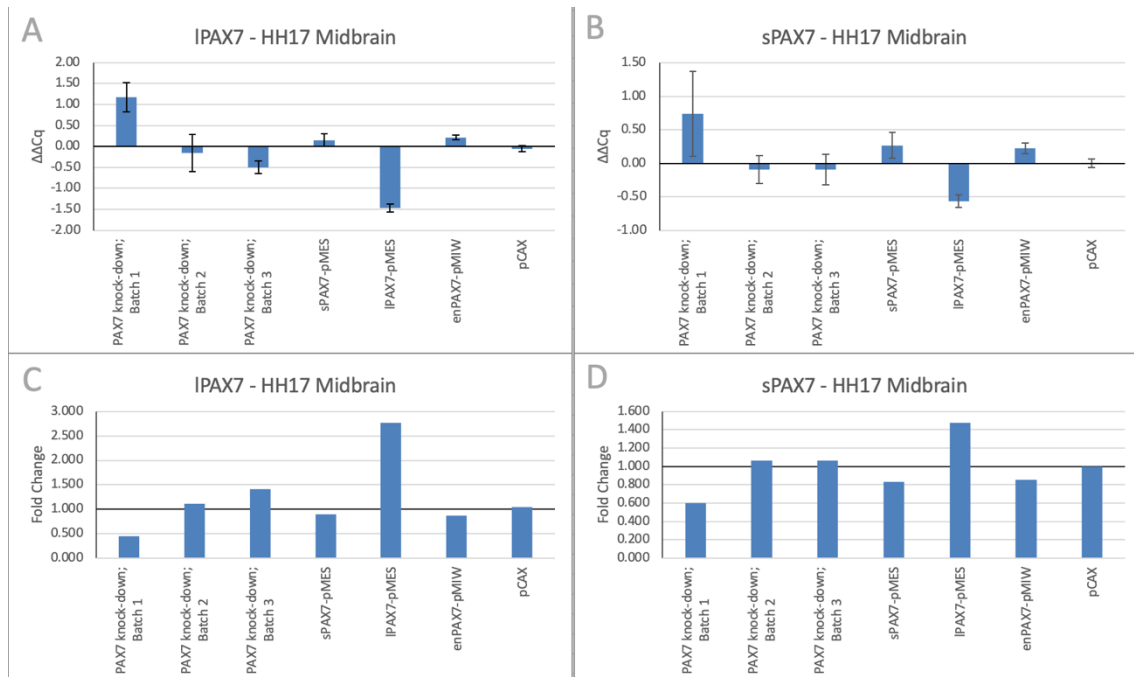


**Figure 4-20: Only overexpression of the long PAX7 splice variant resulted in the expected PAX7 expression changes. A and B:**  $\Delta\Delta C_q$  values with standard deviations (technical replicates). The baseline of 0 indicates no change from electroporation. Positive values show a reduction, negative values an increase of expression. **C and D:** Fold change, calculated from  $\Delta\Delta C_q$  values. The long splice variant (IPAX7, in **A and C**) is only strongly affected by its overexpression (IPAX7-pMES) and the first knockdown experiment using the 3x siPAX7-pSilencer1.0 construct. The short splice variant (sPAX7, in **B and D**) is also affected by long splice variant overexpression (IPAX7-pMES). Most other electroporations show only weak effects ( $\pm 10-15\%$ ) on expression and have relatively high standard deviations. The negative control (pCAX) doesn't affect either splice variant.

At HH stage 14 in the midbrain only samples were analyzed. The qPCR from the tissue of the 11 embryos electroporated with the siPAX7-pSilencer1.0 plasmid had standard deviations as high or higher than the  $\Delta\Delta C_q$  value itself for both PAX7 splice variants, not allowing for conclusions.

The overexpression of the short splice variant in a total of 17 embryos resulted in a strong reduction of the expression of both PAX7 splice variants. With a  $\Delta\Delta C_q$  value of 4.16 cycles and a standard deviation of only 0.180 cycles the reduction in expression for the long splice variant was much stronger than the reduction of the short splice variant with a  $\Delta\Delta C_q$  of 2.01 cycles and a standard deviation of 0.059 cycles. This results in a 75% expression reduction for the short and 94% expression reduction for the long splice variant (figure 4-21). As this sample was also the sample showing incongruent reference gene expression (figure 4-19), the validity of these results cannot be taken at face value.

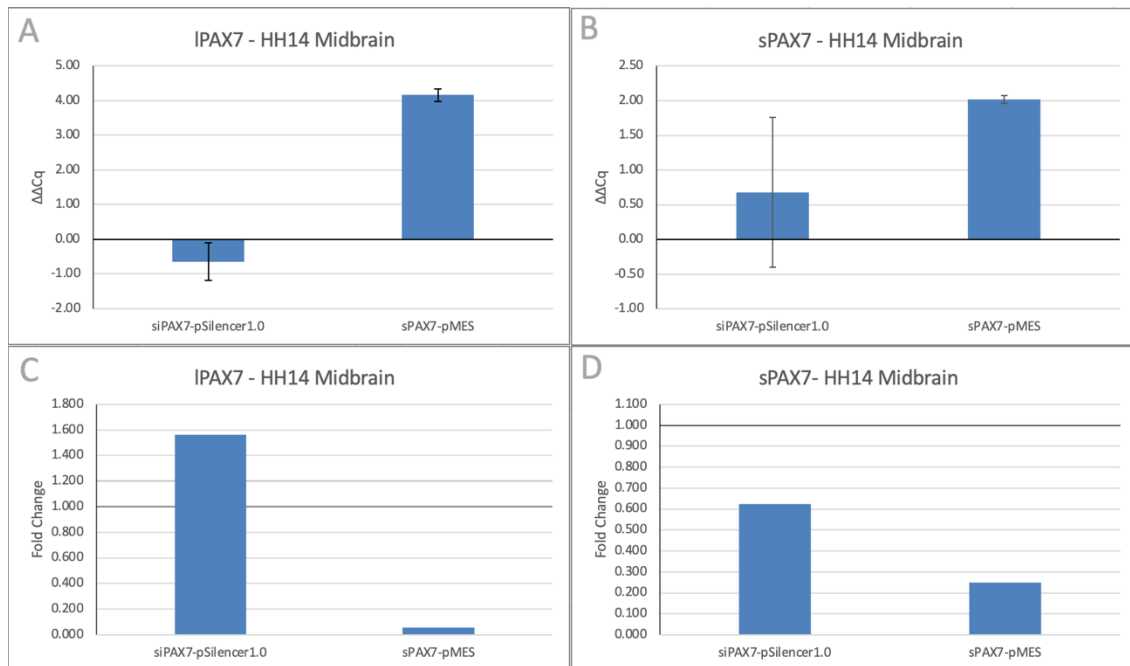


**Figure 4-21: Overexpression of the short PAX7 splice variant greatly reduces PAX7 expression in the midbrain at HH stage 14. A and B:**  $\Delta\Delta C_q$  values with standard deviations (technical replicates). The baseline of 0 indicates no change from electroporation. Positive values show a reduction, negative values an increase of expression. **C and D:** Fold change, calculated from  $\Delta\Delta C_q$  values. The high standard deviations from the qPCR with tissue electroporated with siPAX7-pSilencer1.0 don't allow for conclusions. The overexpression of the short splice variant using sPAX7-pMES resulted in a strong reduction of both the long (IPAX7, in **A** and **C**) and short (sPAX7, in **B** and **D**) splice variants of PAX7.

#### 4.2.3.3.2 Hindbrain

The knockdown of PAX7 resulted in a reduction in expression of both PAX7 splice variants in hindbrain tissue harvested at HH stage 17, but the reduction of the short splice variant was, with a  $\Delta\Delta C_q$  of only 0.2 cycles and a standard deviation of 0.114 cycles questionable. The long splice variant shows a reduction of 34%, with a  $\Delta\Delta C_q$  of 0.57 cycles and a standard deviation of 0.107 cycles (figure 4-22). Overexpressing the short PAX7 splice variant yields comparable results to the knock-down using the siPAX7 construct. Both short and long PAX7 splice variants show a reduced expression, but both are highly questionable with standard deviation from technical replicates being almost identical to the observed expression changes (IPAX7:  $\Delta\Delta C_q$  0.15 cycles, SD: 0.156 cycles, sPAX7:  $\Delta\Delta C_q$ : 0.27 cycles, SD: 0.196 cycles).

The overexpression of the long splice variant using IPAX7-pMES, resulted in an even lower expression of the long splice variant, with a  $\Delta\Delta C_q$  of 1.47 cycles and a standard deviation of 0.066 cycles. At the same time, the short splice variant

showed an increase in expression by 29% with  $\Delta\Delta C_q$  values of -3.7 cycles and a standard deviation of 0.057 cycles (figure 4-22).

The expression of the enPAX7-pMIW construct showed once again a reduction in the expression of both splice variants, but this time reducing expression of the short splice variant by 54% and of the long splice variant by 57%. With  $\Delta\Delta C_q$  values of 1.12 cycles for the short and 1.21 cycles for the long splice variant, and their standard deviations at 0.095 cycles and 0.104 cycles, respectively, the measured reduction is this time most likely not the result of imprecision.

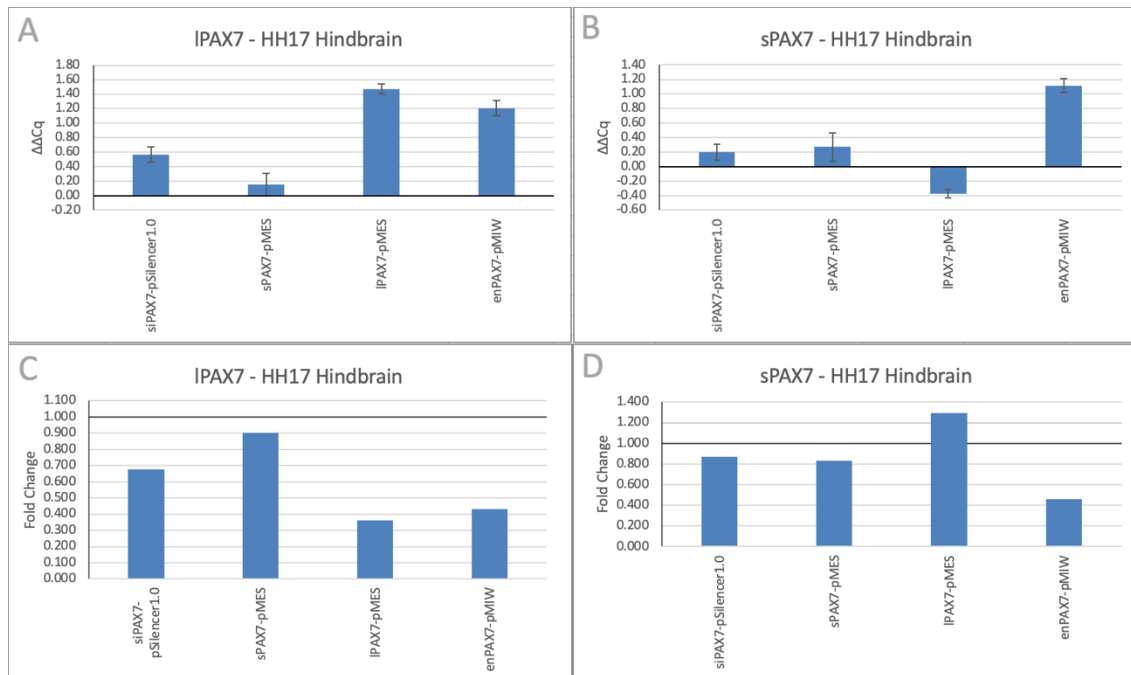


**Figure 4-22: PAX7 expression at HH stage 17 in the hindbrain is reduced by both PAX7 knock-down and overexpression. A and B:**  $\Delta\Delta C_q$  values with standard deviations (technical replicates). The baseline of 0 indicates no change from electroporation. Positive values show a reduction, negative values an increase of expression. **C and D:** Fold change, calculated from  $\Delta\Delta C_q$  values. All, siPAX7-pSilencer1.0, sPAX7-pMES, IPAX7-pMES and enPAX7-pMIW reduce expression of the long PAX7 splice variant (IPAX7, in **A and C**). Expression of the short splice variant (sPAX7, in **B and D**) is reduced by enPAX7-pMIW and increased by IPAX7-pMES overexpression. The knockdown using siPAX7-pSilencer1.0 shows weak reduction on the expression of the short splice variant, but the relative standard deviation is high, the same is true for the overexpression of the overexpression of the short PAX7 splice variant.

At HH stage 14 in the hindbrain, only short splice variant of PAX7 was overexpressed by electroporation. The overexpression resulted in a reduction of expression for both splice variants; the short splice variant showed a marginally stronger expression reduction compared to the long splice variant. Expression of the long variant was reduced by 26%, with  $\Delta\Delta C_q$  values of 0.45 cycles and a relatively high standard deviation of 0.281 cycles, compared to a  $\Delta\Delta C_q$  of 0.69 cycles and

a standard deviation of 0.141 cycles resulting in a 38% reduction of expression of the short PAX7 splice variant.

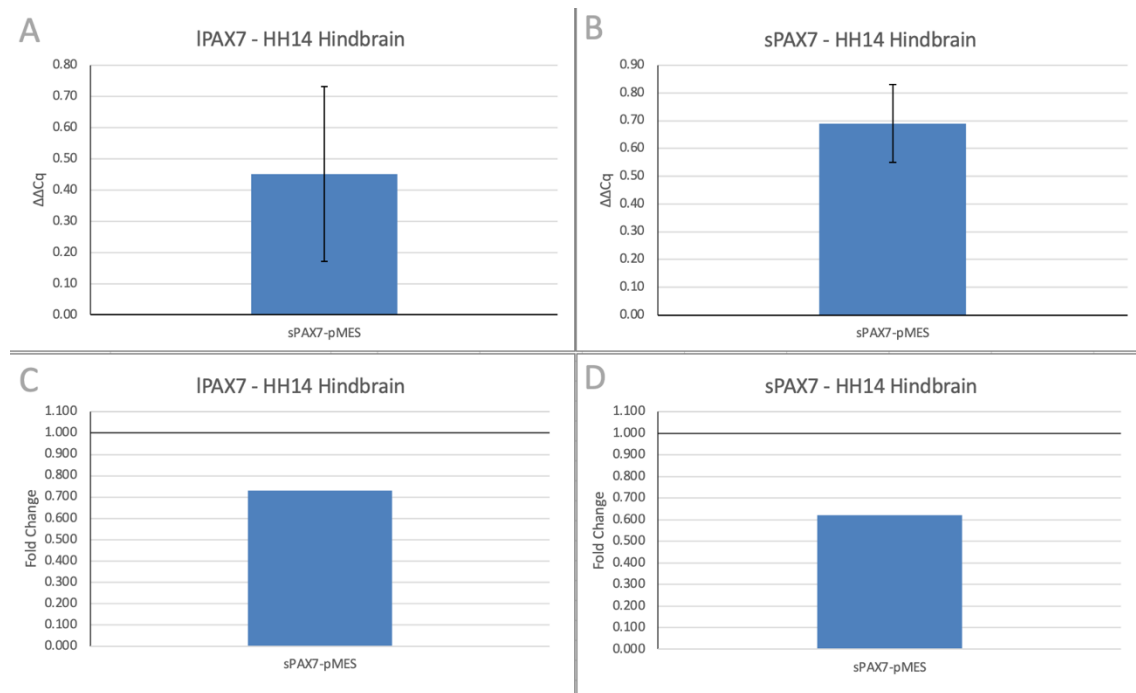


**Figure 4-23: Overexpression of the short PAX7 splice variant in the hindbrain at HH stage 14 reduces PAX7 expression.** **A and B:**  $\Delta\Delta C_q$  values with standard deviations (technical replicates). The baseline of 0 indicates no change from electroporation. Positive values show a reduction, negative values an increase of expression. **C and D:** Fold change, calculated from  $\Delta\Delta C_q$  values. Only overexpression of the short PAX7 splice variant was done, using the sPAX7-pMES plasmid. This resulted in a reduction of expression of 26% for the long splice variant (IPAX7, in **A and C**) and of 38% for the short splice variant (sPAX7, in **B and D**). The standard deviation for the  $\Delta\Delta C_q$  value of the long splice variant are relatively high, reducing confidence in the result.

#### 4.2.3.3.3 Summary of PAX7 Expression Changes

Summarizing the results for the PAX7 expression analysis, it can be concluded that in most cases, on an RNA level, the electroporations did not cause the expected effect. The knockdowns only resulted in a reduction of PAX7 (both splice variants) expression in half of the cases analyzed. Overexpression of the short splice variant always resulted in reduced expression of both PAX7 variants, overexpressing the long PAX7 splice variant always resulted in increased expression of the short splice variant, but only showed an increase of itself in one of the two brain regions analyzed.

#### 4.2.3.4 PAX7 Knock-Down Does Not Reduce Wnt Signaling on an RNA Level

The effect of PAX7 expression on canonical Wnt signaling on an RNA level was analyzed using the ES60AXIN2 primer and the ES60CTNNB1 primer. AXIN2 is

a feedback gene for Wnt signaling and commonly used to detect the activity of canonical Wnt signaling, with a higher expression of AXIN2 correlating with a higher Wnt signaling activity. (Lustig et al., 2002) The ES60CTNNB1 primer detects expression of CTNNB1 ( $\beta$ -catenin) and was selected as potential target for the PAX7/Wnt interaction, as PAX7 has been shown to bind upstream of the gene, potentially regulating gene expression.

AXIN2 showed a lower expression across all embryos, with  $C_q$  values averaging around 22.6 cycles compared to CTNNB1 at around 19.1 cycles average (detailed results in appendix 9.2.1.2). All  $C_q$  values are within validated primer range. The standard deviations from the  $\Delta C_q$  values of the technical replicates were good and mostly below 0.1 cycles, except for the PAX7 knock-down batch 1 at HH stage 17 midbrains and the PAX7 knock-down in midbrains at HH stage 14. The latter of the two had two wells with ES60AXIN2 failing to detect amplification and a strong variance between the wells with ES60CTNNB1 primers, most likely the result of low RNA input.

#### **4.2.3.4.1 Midbrain**

The electroporation with the pCAX plasmid, used as reference group, resulted in a change of both, AXIN2 and CTNNB1 expression by -10%, with  $\Delta\Delta C_q$  values of 0.15 cycles for AXIN2 and 0.16 cycles for CTNNB1, with standard deviations of 0.054 cycles and 0.044 cycles respectively (figure 4-24).

The knock-down of PAX7 expression shows mixed results. The first batch, using the 3x siPAX7-pSilencer1.0 mix resulted in a 49% reduction of AXIN2 expression, indicating a reduction in canonical Wnt signaling activity. The caveat is a high standard deviation of 0.588 cycles with a  $\Delta\Delta C_q$  value of 0.97 cycles, but still showing a measurable difference. The two other runs show the opposite effect on AXIN2 expression, with both, the second and third batch showing an increase in expression by approximately 50%, with much smaller standard deviations. This goes against the previous findings, that showed a reduction in canonical Wnt signaling activity using the TOP-dGFP reporter system. Looking at the expression of CTNNB1, the first batch with a PAX7 knock-down resulted in a strong 61% reduction of expression, this time with a lower standard deviation of 0.295 cycles and a  $\Delta\Delta C_q$  value of 1.34 cycles. The second batch using the same construct

resulted in functionally no change in CTNNB1 expression, especially when comparing it to the pCAX negative control. The third batch resulted in a 1.45-fold increase in CTNNB1 expression, with a  $\Delta\Delta C_q$  value of -0.51 cycles and a standard deviation of 0.154 cycles (figure 4-24).

The overexpression of the two transactivation domain splice variants of PAX7 resulted in a minor reduction of AXIN2 expression for the short and a strong increase for the long splice variant. The long splice variant increased AXIN2 expression 1.87-fold, whilst the short splice variant reduced expression by 26%, only slightly more change than seen from the negative control, especially when taking the standard deviation of 0.147 cycles with an  $\Delta\Delta C_q$  of only 0.43 cycles into consideration. The effect of the short splice variant on CTNNB1 expression shows similar results, with a 19% reduction in expression only barely surpassing the 10% reduction from the pCAX plasmid, whilst having an over three times higher standard deviation. The standard deviation for the long splice variants effect on CTNNB1 expression surpasses the base value of its  $\Delta\Delta C_q$ , not allowing for any meaningful interpretation (figure 4-24).

The PAX7/ENGRAILED construct, enPAX7-pMIW, that inhibits expression of all genes directly regulated by PAX7, shows a 21% reduction in CTNNB1 expression. At the same time canonical Wnt signaling seems to be slightly increased, as AXIN2 expression was 1.15-fold higher compared to the wildtype control side. The relatively low increase, with a  $\Delta\Delta C_q$  of only -0.15 cycles with its standard deviation of 0.054 cycles inspires much less confidence in the result, compared to the reduction of CTNNB1 expression with a  $\Delta\Delta C_q$  0.48 cycles and a standard deviation of 0.055 cycles (figure 4-24).

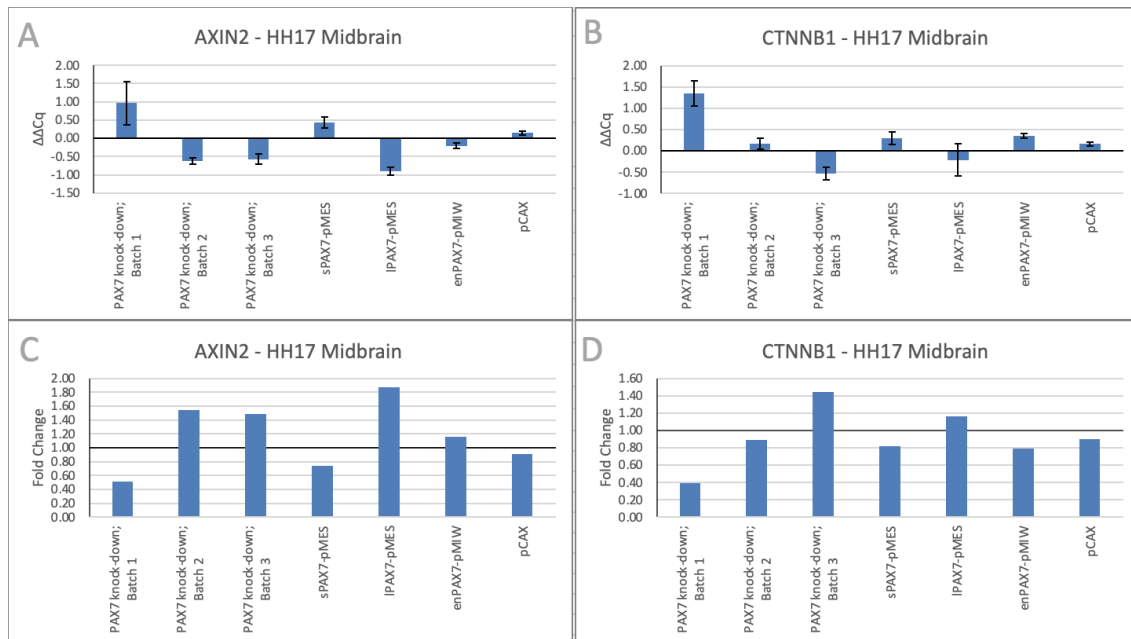


**Figure 4-24: The effects of PAX7 expression modifications on Wnt signaling in the midbrain are inconclusive. A and B**  $\Delta\Delta C_q$  values with standard deviations (technical replicates). The baseline of 0 indicates no change from electroporation. Positive values show a reduction, negative values an increase of expression. **C and D:** Fold change, calculated from  $\Delta\Delta C_q$  values. AXIN2 (**A and C**) expression correlates with canonical Wnt signaling activity and is reduce in one of three PAX7 knockdown experiments, whilst increased in the other two. Overexpression of the long splice variant also increased AXIN2 expression. CTNNB1 is the chicken's homologue of  $\beta$ -catenin (**B and D**), an essential component of Wnt signaling. Its expression is reduced in one of three PAX7 knockdown experiments and increased in another one whilst not being affected in the third. The negative control (pCAX) shows only a minor impact on both genes, the same goes for the short PAX7 splice variant and the PAX7/ENGRAILED fusion gene.

At HH stage 14 in the midbrain, only a knockdown of PAX7 and the overexpression of the short and more prominent splice variant were tested. Unfortunately, the standard deviations of the PAX7 knock-down sample are too high with some reactions completely failing amplification and not allowing for any meaningful interpretation of the results. The overexpression of the short splice variant of PAX7 resulted in a minor, 14% reduction of AXIN2 expression, but with a standard deviation of 0.103 cycles and a  $\Delta\Delta C_q$  of only 0.21 cycles, the validity of this result can be questioned. The 28% reduction on CTNNB1 expression on the other hand is much more reliable, with a  $\Delta\Delta C_q$  of 0.48 cycles and a standard deviation of 0.042 cycles. (figure 4-25, A and B)

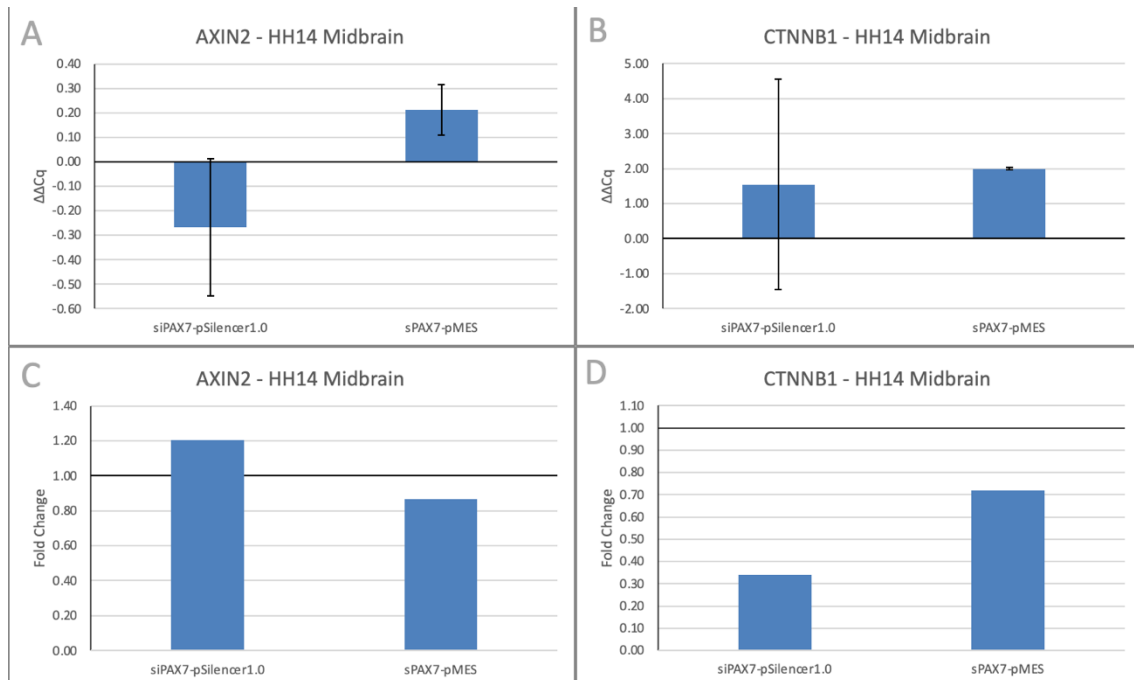


**Figure 4-25: No clear impact of PAX7 modifications on Wnt signaling in midbrains at HH stage 14. A and B:**  $\Delta\Delta C_q$  values with standard deviations (technical replicates). The baseline of 0 indicates no change from electroporation. Positive values show a reduction, negative values an increase of expression. **C and D:** Fold change, calculated from  $\Delta\Delta C_q$  values. The standard deviations of the PAX7 knockdown (siPAX7-pSilencer) are too high to allow for any conclusions. The overexpression of the short splice variant of the PAX7 transactivation domain (sPAX7-pMES) show a reduction in CTNNB1 ( $\beta$ -catenin expression, in **B and D**). AXIN2 expression (**A and C**), correlating with canonical Wnt signaling was not affected by electroporations.

#### 4.2.3.4.2 Hindbrain

In hindbrain at HH stage 17, AXIN2 expression changed overexpression of both PAX7 splice variants and the expression of the PAX7/ENGRAILED fusion protein. The knockdown of PAX7 only resulted in a minor reduction with relatively high standard deviation. The short splice variant and the enPAX7 fusion gene reduced AXIN2 expression, indicating a reduction in canonical Wnt signaling, with the short splice variant showing a stronger reduction of 56% compared to the 45% reduction caused by enPAX7. Overexpression of the long PAX7 variant resulted in a 47% increase in AXIN2 expression (figure 4-26 A and C).

Expression of CTNNB1 was reduced by both, PAX7 knock-downs and overexpressions. Although the overexpression of the long splice variant of PAX7 caused only a minor and questionable reduction with a  $\Delta\Delta C_q$  0.18 cycles and a standard deviation of 0.074 cycles. The knockdown using the siPAX7-pSilencer1.0 construct reduced CTNNB1 expression by 33%, overexpressing of the short PAX7 splice variant reduced CTNNB1 expression by 38%. The reduction caused by

short splice variant overexpression is with a  $\Delta\Delta C_q$  of 0.68 cycles was the strongest reduction seen for CTNNB1 in the hindbrain at HH stage 17 but also had the highest standard deviation of 0.26 cycles raising doubt about this result (figure 4-33 B and D).

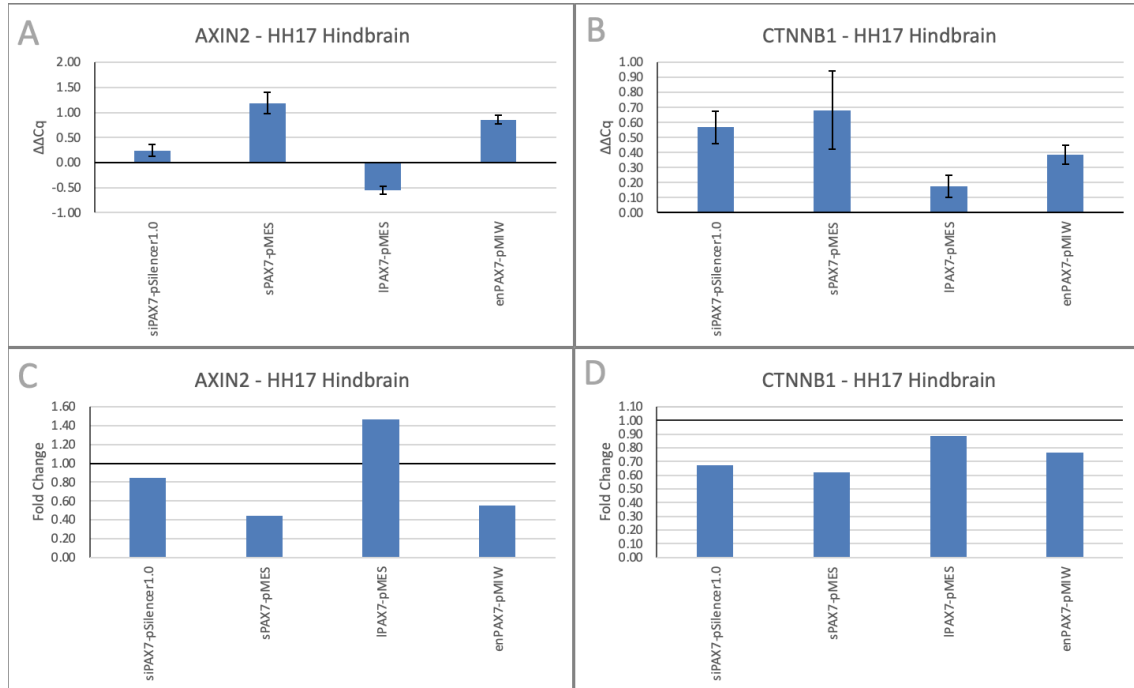


**Figure 4-26: Influence of PAX7 expression modifications on Wnt signaling in the hindbrain at HH stage 17. A and B:**  $\Delta\Delta C_q$  values with standard deviations (technical replicates). The baseline of 0 indicates no change from electroporation. Positive values show a reduction, negative values an increase of expression. **C and D:** Fold change, calculated from  $\Delta\Delta C_q$  values. The AXIN2 expression (**A and C**) correlates with canonical Wnt signaling activity and is reduced by overexpression of PAX7 with the short splice variant transactivation domain (sPAX7-pMES) and a fusion gene from PAX7 with the ENGRAILED transactivation domain (enPAX7-pMIW) that inhibits transcription of genes regulated by PAX7. Knockdown of PAX7, the overexpression of both splice variants and the PAX7/ENGRAILED fusion protein reduced, in varying strength, CTNNB1 ( $\beta$ -catenin, **B and D**) expression, an essential component of Wnt signaling.

Hindbrain tissue at HH stage 14 was only harvested from embryos in which the short PAX7 splice variant had been overexpressed. For CTNNB1 no change in expression could be detected. AXIN2 expression was reduced by 19%, but with a high standard deviation of 0.148 cycles and a  $\Delta\Delta C_q$  of only 0.31 cycles the measurement is not the most reliable, rendering the data unusable (figure 4-27).

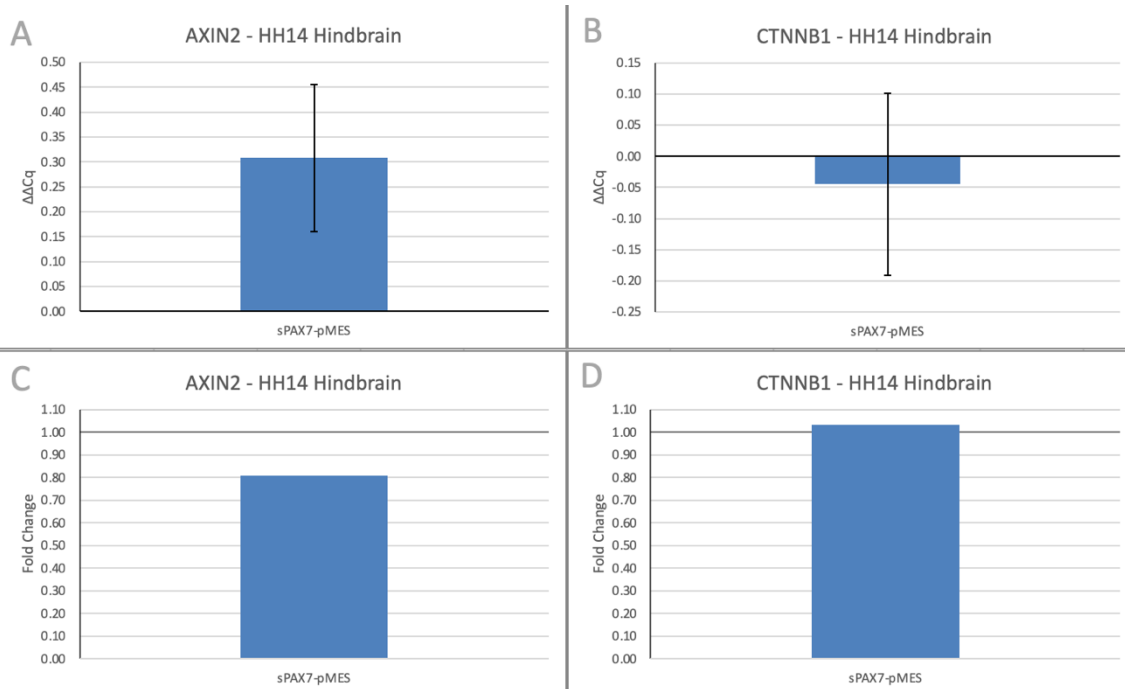


**Figure 4-27: Measurements of PAX7 overexpression impact on canonical Wnt signaling unusable. A and B:**  $\Delta\Delta C_q$  values with standard deviations (technical replicates). The baseline of 0 indicates no change from electroporation. Positive values show a reduction, negative values an increase of expression. **C and D:** Fold change, calculated from  $\Delta\Delta C_q$  values. Only the short splice variant of PAX7 electroporated. It shows no influence on CTNNB1 expression (**B and D**) and only a minor reduction in AXIN2 expression (**A and C**), both measurements show high standard deviations from the technical replicates.

#### 4.2.3.4.3 LiCl Positive Control

Additionally, to the experiments modifying PAX7 expression, the whole body of an embryo was incubated with LiCl, an unspecific activator of canonical Wnt signaling, to check whether an effect on AXIN2 expression could be detected. Unfortunately, the 14% increase in AXIN2 expression measured had a relatively high standard deviation from the measurements with 0.074 cycles when considering the  $\Delta\Delta C_q$  of only -0.19 cycles (figure 4-28). The impact on CTNNB1 expression was even smaller and had higher standard deviations.

Failing to detect a reliable increase in Wnt signaling induced by LiCl equals a failed positive control, putting all other results from detecting Wnt signaling through qPCR into question.

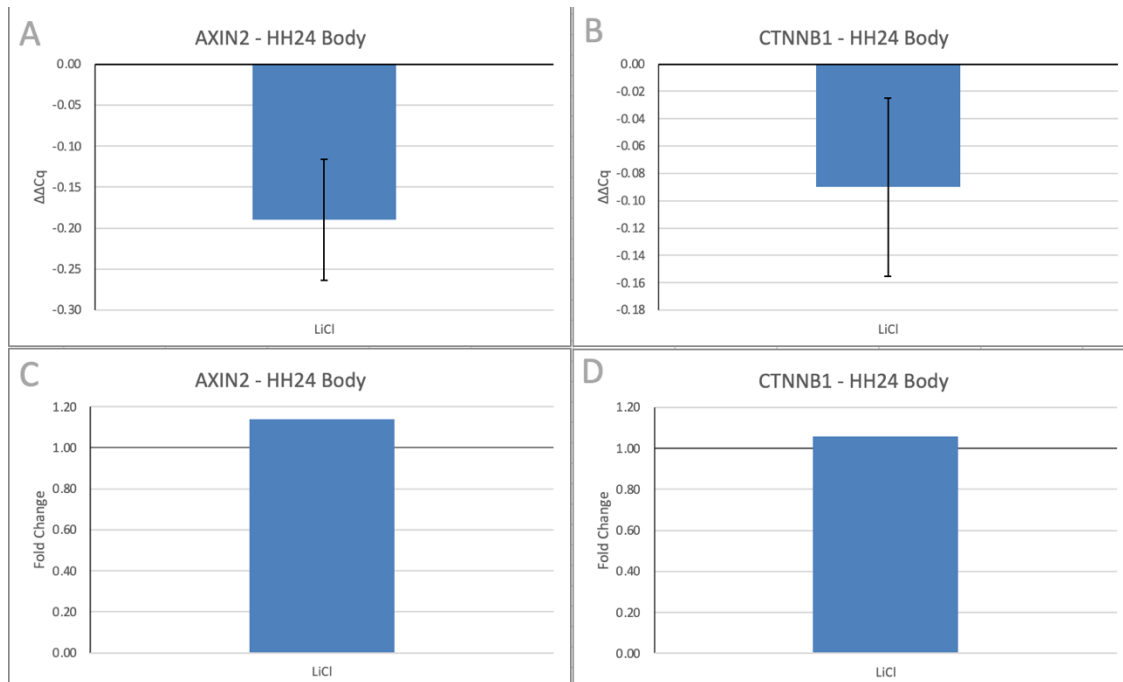


**Figure 4-28: LiCl does not show the expected increase in canonical Wnt signaling. A and B:**  $\Delta\Delta C_q$  values with standard deviations (technical replicates). The baseline of 0 indicates no change from electroporation. Positive values show a reduction, negative values an increase of expression. **C and D:** Fold change, calculated from  $\Delta\Delta C_q$  values. NaCl body was used as reference. Only one embryo was analyzed per treatment. Only neglectable changes in expression of AXIN2 (**A and C**) and CTNNB1 (**B and D**) were measured.

#### 4.2.3.4.4 Summary of Wnt Signaling Component Expression Changes

To summarize, the knockdowns of PAX7 expression in the midbrain (HH stage 14+17) resulted in an increase of AXIN2 expression in 3 of 4 experiments. Expression of CTNNB1 was reduced in 3 of 4 cases in the same experiments. The knock-down showed reduced expression for both genes.

Overexpression of the short splice variant resulted in reduced AXIN2 expression at HH stage 14 and HH stage 17 in both mid- and hindbrain. A reduction in expression can also be observed for CTNNB1 in the same samples, with the exception being tissue from hindbrain at HH stage 14, where its expression was unchanged by the electroporations.

The long PAX7 splice variant was only tested at HH stage 17. It showed reduction of AXIN2 expression in both mid- and hindbrain. CTNNB1 expression was unchanged in midbrain and showed reduced expression in the hindbrain

The reducing PAX7 transcriptional activity using the enPAX7 construct, only electroporated at HH stage 17, reduced expression of both CTNNB1 and AXIN2, except for AXIN2 in the midbrain, where a minor increase could be observed.

#### **4.2.3.5 Effect of PAX7 Expression Modifications on CCND1 Expression**

The last gene studied in pooled tissue analysis was cyclin D1 (CCND1). It promotes cells in the G1 phase of the cell cycle to enter the S phase and was used to check for the influence of PAX7 on cell proliferation.

CCND1 was overall the strongest expressed gene of interest across all tissues and electroporation, reflecting the high proliferation in the embryonic brain. It showed an average  $\Delta C_q$  of 18.25 cycles across all samples. The individual results were all within the range validated for the ES60CCND1 primers. The standard deviations from the technical replicates varied greatly between 0.808 cycles and 0.013 cycles (appendix 9.2.1.3).

CCND1 qPCRs weren't done for all stages and tissues as not enough RNA was available. It was chosen to confirm results from prior experiments on PAX7 and its influence on the cell cycle, which unfortunately could not be confirmed.

##### **4.2.3.5.1 Midbrain at HH Stage 17**

The expression of CCND1 in the midbrain at HH stage 17 did not change in the negative control, the sample with the short PAX7 overexpression or the PAX7/EN1 expression.

The knock-down experiments show, once again, very different effects between the three experiments. Batch 2 from the PAX7 knock-down experiments showed no impact on CCND1 expression. The first batch resulted in a 61% reduction of CCND1 expression, although be it with a high standard deviation of 0.295 cycles at a  $\Delta\Delta C_q$  of 1.34 cycles. On the other hand, the third batch resulted in a 1.65-fold increase in CCND1 expression, with a  $\Delta\Delta C_q$  of -0.72 cycles and a standard deviation of 0.149 cycles.

The only other electroporation that effected cyclin D1 expression was the long splice variant of PAX7. It increased CCND1 expression 1.56-fold equaling a  $\Delta\Delta C_q$  of -0.65 cycles with a standard deviation of 0.094 cycles.

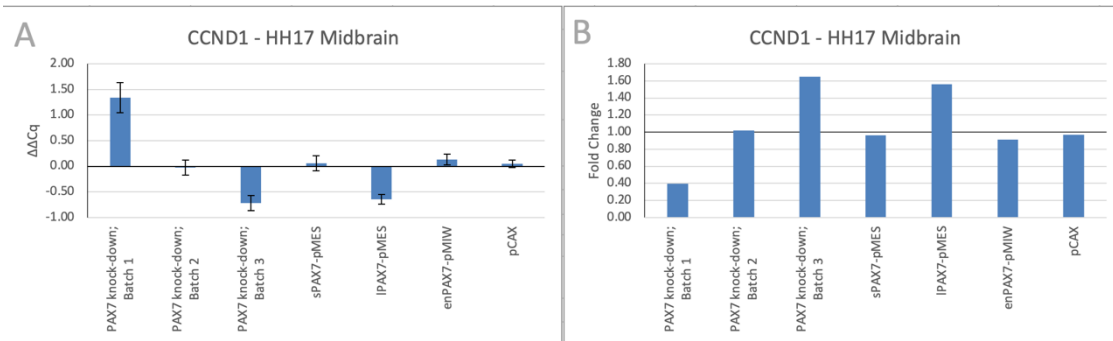


**Figure 4-29: Changes in CCND1 expression at HH stage 17 in the midbrain, resulting from PAX7 expression modifications.** **A:**  $\Delta\Delta C_q$  values with standard deviations (technical replicates). The baseline of 0 indicates no change from electroporation. Positive values show a reduction, negative values an increase of expression. **B:** Fold change, calculated from  $\Delta\Delta C_q$  values. The knockdown experiments of PAX7 (siPAX7-pSilencer1.0 constructs) resulted in every possible outcome: an increase, a reduction, and no change in expression – one possibility for each of the three batches tested. The overexpression of the long splice variant (IPAX7-pMES) also resulted in an increase in CCND1 expression.

#### 4.2.3.5.2 Mid- and Hindbrain at HH Stage 14

At HH stage 14 only tissue with the short splice variant overexpressed was harvested in mir- and hindbrain. In the hindbrain the overexpression had no impact. In the midbrain on the other hand a 93% reduction ( $\Delta\Delta C_q$ : 3.88 cycles, SD: 0.072 cycles) in CCND1 expression could be observed (figure 4-30). This strong change in expression stands as an outlier and requires further testing.

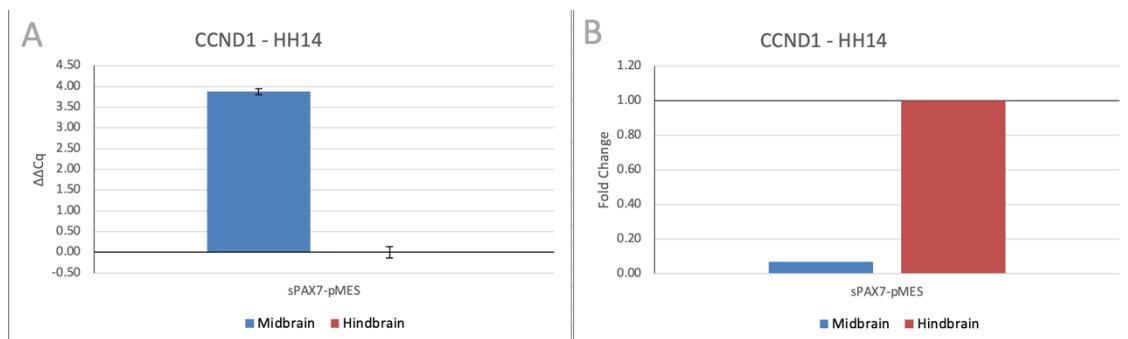


**Figure 4-30: Overexpression of the short PAX7 splice variant caused strong reduction in CCND1 expression.** **A:**  $\Delta\Delta C_q$  values with standard deviations (technical replicates). The baseline of 0 indicates no change from electroporation. Positive values show a reduction, negative values an increase of expression. **B:** Fold change, calculated from  $\Delta\Delta C_q$  values. In the hindbrain no effect on CCND1 expression could be observed, whilst the midbrain showed a strong reduction in expression. This reduction stands as an outlier and requires further investigation.

#### 4.2.3.5.3 Hindbrain at HH Stage 17

In the hindbrain at HH stage 17, both the overexpression of the long PAX7 splice variant as well as the knockdown of PAX7 resulted in a reduction of 11% and 20% respectively. In both instances the standard deviations were relatively high compared to the base  $\Delta\Delta C_q$  values. (figure 4-31)

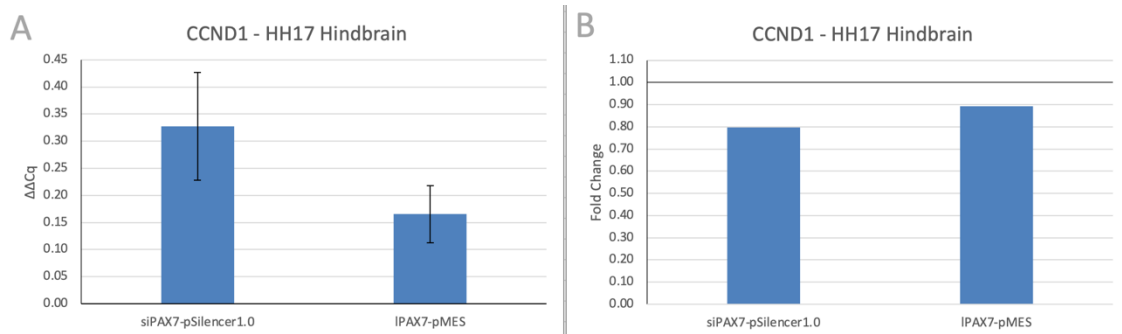


**Figure 4-31: PAX7 modifications do not meaningfully impact CCND1 expression in the hindbrain. A:**  $\Delta\Delta C_q$  values with standard deviations (technical replicates). The baseline of 0 indicates no change from electroporation. Positive values show a reduction, negative values an increase of expression. **B:** Fold change, calculated from  $\Delta\Delta C_q$  values. Although both, the knockdown using siPAX7-pSilencer1.0 and the overexpression of the long PAX7 splice variant, resulted in a small reduction in CCND1 expression, the validity of these results is questionable when looking at the relatively high standard deviations.

Taken together the results of the CCND1 expression analysis after PAX7 expression modification, no clear conclusions can be drawn. The observable effects are either opposing each other (siPAX7-pSilencer1.0 in midbrains at HH stage 17) or unreliable resulting from poor reference gene performance (sPAX7-pMES in midbrains at HH stage 14).

#### 4.2.3.6 Summary of Pooled Tissue qPCR

Since there were multiple batches of midbrain tissue at HH stage 17 transfected with plasmids knocking-down PAX7 expression, a comparative overview of the different expression changes is given in table 4-18. Batch 1 was the only batch showing strong suppression of PAX7 expression on an RNA level. It also showed a reduction in expression of AXIN2, CTNNB1 and CCND1.

Sample	n	Short PAX7 SV	Long PAX7 SV	AXIN2	CTNNB1	CCND1
Batch 1	8	(↓)	↓	↓	↓	↓
Batch 2	15	-	-	↑	-	-
Batch 2	13	-	↓	↑	↑	↑
PAX7/EN1	14	(↓)	-	(↑)	↓	-

**Table 4-18: Overview of Expression Changes from PAX7 knock-downs, detected in qPCR in pooled midbrain tissue at HH stage 17.** Batch 1 shows a reduction in expression for all five genes tested. Batch 2 and 3 did not show a comparable reduction in PAX7 expression. Both these batches also showed an increased expression of AXIN2, indicating increased canonical Wnt signaling activity, contradicting the findings of the *in vivo* experiments. Expression of the PAX7/EN1 fusion protein did not affect PAX7 expression on canonical Wnt signaling. ↑ increased expression, ↓ decreased expression, - expression unchanged. Brackets indicate weak changes compared to high standard deviations, rendering observed expression changes unreliable.

Analog to the overview for the PAX7 knock-down batches, a summary of expression changes resulting from PAX7 splice variant overexpression seen at HH stage 17 in the midbrain, is given in table 4-19.

Sample	n	Short PAX7 SV	Long PAX7 SV	AXIN2	CTNNB1	CCND1
NC	13	-	-	-	-	-
Short PAX7 SV	15	(↓)	-	↓	↓	-
Long PAX7 SV	16	↑	↑	↑	(↑)	↑

*Table 4-19: Overview of Expression Changes from PAX7 overexpressions, detected in qPCR in pooled midbrain tissue at HH stage 17. In the NC (pCAX) no major expression changes were observed. Overexpressions did not result in PAX7 expression increases. Overexpression of the short PAX7 splice variant resulted in reduced canonical Wnt signaling, whilst overexpression of the long splice variant resulted in an increase. ↑ increased expression, ↓ decreased expression, - expression unchanged. Brackets indicate weak changes compared to high standard deviations, rendering observed expression changes unreliable.*

Summarizing the results of all qPCRs using pooled tissue, no clear conclusions about the interactions between PAX7 and canonical Wnt signaling can be drawn.

- Overall, only minor changes in gene expression were observed. In combination with varying standard deviations result interpretation is difficult.
- The PAX7 expression modifications did not always cause the expected effects on PAX7 expression on an RNA level
- No clear pattern in expression in-/decreases for AXIN2 or CTNNB1 can be seen, as a result from PAX7 expression modifications
- CCND1 expression seems mostly unaffected by PAX7 expression modifications, and the few detectable changes are incoherent

Drawing conclusion about the transfections at other HH stages or in the hindbrain is not straight forward either. A table summarizing these results can be found in appendix 9.2.1.4.

#### **4.2.4 ddCq Expression Analysis of Tissue from Single Embryos**

Since the analysis of pooled tissue did not show a clear impact of the PAX7 knockdown on canonical Wnt signaling and as not all embryos with a PAX7 knock-down showed the phenotype with smaller midbrains or reduced canonical

Wnt signaling activity in the Top-dGFP experiments, we decided to analyze the cDNA of the embryos individually using a 96.96 chip qPCR using a Biomark system as it provided the required sample throughput.

A total of 44 embryos were analyzed, 20 control group embryos, being electroporated with the GFP expressing pCAX plasmid and 24 with a PAX7 knock-down group, electroporated with the siPAX7-pSilencer1.0 construct.

The expression of multiple genes was tested. Expression of the PAX7 splice variants, multiple components of canonical Wnt signaling and the expression of several HES genes was quantified. In addition to these genes, multiple potential off-target genes of the siPAX7-pSilencer1.0 plasmid, used for the knock-down, had their expression quantified. The latter was done to ensure that effects seen with this construct were in fact caused by the PAX7 knock-down and not the result of another gene getting knocked-down by accident.

#### **4.2.4.1 Disclaimer and Summary**

As shown in detail in chapter 4.2.1.3.4, primer efficiencies for this experiment were poor and did not meet best practice standards. Therefore, all results obtained cannot be taken as entirely valid, as  $C_q$ -values are heavily skewed.

No statistically significant changes in expression were detected (two sided tests,  $p < 0.05$ ) because of the PAX7 knock-down. Even when only embryos were included that showed at least a 50% reduction in expression of the short PAX7 splice variant (the long splice variant had only one sample with a >50% reduction in expression) in the knock-down group, no statistically significant changes could be observed (appendix 9.2.2.4)

Despite of all these limitations, the obtained data will be presented in detail in the following.

#### **4.2.4.2 Technical Summary and qPCR Performance**

From the 44 embryos analyzed, 6 were excluded. Two because amplification in with multiple primers failed and a further 4 embryos because the  $\Delta C_{q5'-3'}$  was larger than 1 cycle, indicating lower RIN. Three of the samples excluded because of lower RIN had all been prepared at least two years prior to the experiment itself, showing that cDNA degradation still occurs when samples are stored at -

20°C. This left 19 control and 18 PAX7 knock-down embryos for downstream analysis.

WNT1, WNT3a and HESX1 were excluded from the analysis as the primers targeting them failed to show amplification in most cDNA samples.

Using SPSS, the distribution of  $\Delta\Delta C_q$ -values was analyzed for normal distribution using the Kolmogorov-Smirnov test (appendix 9.2.2.3)

For all genes of interest that showed a normal distribution, the t-test for equality of means and the Lvene's test for equality of variances were performed. The latter showed a  $p > 0.05$  for all samples, confirming the equality of variances and allowing for the use of the t-test for equality of means. Individual results for Lvene's test can be found in appendix 9.2.2.3.

Gene expression differences that showed a skewed distribution in the Kolmogorov-Smirnov test had their changes in gene expression tested for statistical significance using the Mann-Whitney-U test.

#### **4.2.4.3 Reference Genes**

Six primer pairs were used to detect reference gene expression and normalize the expression of the other genes. Multiple genes were used, instead of just a singular gene, to minimize impact of electroporation on reference gene expression, as no data for reference gene expression stability in the chicken embryos midbrain has been published yet. All of them were exon spanning, thus only amplifying cDNA. The two primers that amplify GAPDH were also used to assure RNA integrity. Besides them, ACTB, YWATZ, ATP5B and HMBS primers were used. All these genes are either involved in cellular metabolism or cytoskeleton and have been shown to have stable expression in many tissues. For the  $\Delta\Delta C_q$  analysis, the geometric mean of the  $C_q$ -values of all six primers were used (table 4-20).

All  $C_q$ -values obtained were included in the analysis. Overall, the GAPDH primers produced the lowest  $C_q$ -values around 8 cycles, the ES60HMBS primer produced the highest  $C_q$ -values around 15 – 16 cycles. (table 4-20) The standard deviations for the individual triplicates averaged below 0.2 cycles (table 4-20 shows standard deviation across all samples) for all primers, indicating a high precision of the

measurements, even at higher cycle numbers. The individual results can be found in appendix 9.2.2.2.

	ES60ACTB	ES603'GAPDH	ES605'GAPDH	ES60YWATZ	ES60ATP5B	ES60HMBS	Geomean
mean	9.76	8.02	8.18	14.67	11.71	15.33	10.90
SD	1.43	1.14	1.30	1.38	1.33	1.23	1.29

Table 4-20: **Reference gene expression in qPCR with tissue from single embryos.** Averaged Cq values from all reactions off all embryos analyzed. The GAPDH primers show the lowest Cq Values, the ES60HMBS primer shows the highest Cq value.

#### 4.2.4.4 PAX7 and PAX3 Expression Not Affected by siPAX7-pSilencer1.0

The P7 sPAX7-F/ES60PAX7-R and P9 IPAX7-F/ES60PAX7-R primer pairs were used to detect the short and long PAX7 transactivation domain splice variants, respectively. The ES60PAX3-2 primer pair was used to detect PAX3, the PAX gene family member with the closest relation to PAX7. This was done to investigate a potential cross regulation. The ES60PAX3 primer as well as the primer pair amplifying the short PAX7 splice variant all embryos were included in the analysis. Five samples, in combination with the primer for the long PAX7 transactivation domain splice variant failed amplification and were excluded from the analysis. Two of these embryos were in the control group, one failed amplification on the GFP, the other on the wildtype side. The remaining 3 embryos were from the PAX7 knock-down group, with two of them failing amplification on the electroporated GFP side. These two embryos showed both showed an above average reduction in short PAX7 splice variant expression, with  $\Delta\Delta C_q$ -values of 1.29 and 1.70 cycles compared to the average in the knock-down group of 0.58 cycles (table 4-21). The results for all three genes showed a normal distribution, so t-tests were performed.

$\Delta\Delta C_q$ -Values	Group	N	Mean	Std. Deviation	Std. Error Mean
sPAX7	control	19	0.334	1.441	0.330
	PAX7 knock-down	18	0.578	0.827	0.195
IPAX7	control	17	-0.352	0.955	0.232
	PAX7 knock-down	15	0.158	0.746	0.193
PAX3	control	19	-0.026	0.461	0.106
	PAX7 knock-down	18	0.086	0.357	0.084

Table 4-21: **Group statistics for changes in expression (as  $\Delta\Delta C_q$ -values) of PAX3 and the two PAX7 trans activation domain splice variants.** Mean and standard deviation/error form biological replicates. Higher means indicate lower expression.

All genes revealed a wide spread of expression changes induced by the different transfections and only minor changes in the means between the two groups. Whilst the means for both PAX7 splice variants (figure 4-32) and PAX3 (figure 4-33) show a reduction in expression in the PAX7-knock-down group, the combination of high standard deviations and low mean differences, resulted in neither the t-test showing significant differences (for  $p > 0.05$ , two-sided) between the groups analyzed (table 4-22).

This indicates, that either the knock-down of PAX7 didn't work or can't be detected using this method.

	t-test for Equality of Means				
	t	Significance		Mean Difference	Std. Error Difference
		One-Sided p	Two-Sided p		
sPAX7	-0.627	0.267	0.535	-0.244	0.389
IPAX7	-1.665	0.053	0.106	-0.509	0.306
PAX3	-0.816	0.210	0.420	-0.111	0.136

Table 4-22: **Results from t-test for changes in expression of PAX3 and the two transactivation domain splice variants of PAX7.** The negative mean difference indicates a reduction in expression of both genes analyzed, although none of them is reduced significantly. Tests done using SPSS.

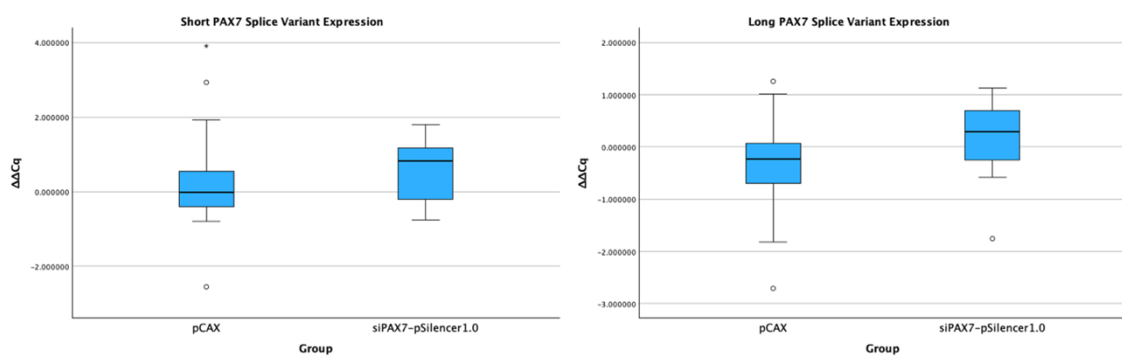


Figure 4-32: **PAX7 knock-down did not affect PAX7 expression.** Boxplots of  $\Delta\Delta C_q$  values for the long and short PAX7 trans activation domain splice variant expression changes, split between the reference (pCAX) and PAX7 knock-down n (siPAX7-pSilencer1.0) group. Although a difference in means, towards a lower PAX7 expression for both splice variants is visible, it is not significant (table 4-22). Whiskers mark the minimum/maximum value, circles and asterisks mark outliers.

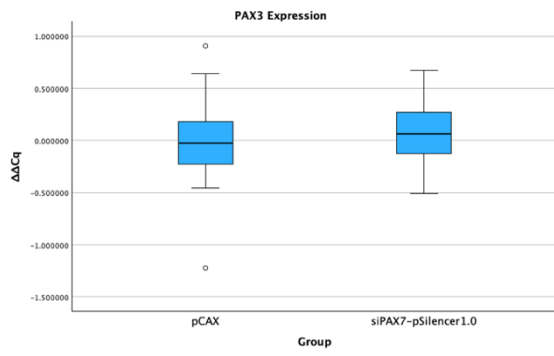


Figure 4-33: **PAX7 knock-down did not affect PAX3 expression.** Boxplots of  $\Delta\Delta C_q$  values for PAX3 expression change, split between the reference (pCAX) and PAX7 knock-down (siPAX7-pSilencer1.0) group. No significant change in expression could be detected (table 4-22). Whiskers mark the minimum/maximum value, circles mark outliers.

#### 4.2.4.5 Expression of Wnt Signaling Pathway Components Not Affected by siPAX7-pSilencer1.0

As in previous experiments, analyzing pooled embryos, AXIN2, the direct feedback gene for canonical Wnt signaling was analyzed as well as CTNNB1 ( $\beta$ -catenin), the suspected gene linking Wnt signaling with PAX7. To expand on these two genes, LEF1, a gene coding for a protein binding  $\beta$ -catenin in the nucleus and WNT4 coding for an activator of Wnt signaling were probed for expression changes. None of the reactions failed amplification, so all embryos were included in the analysis. The  $\Delta\Delta C_q$ -values obtained for AXIN2, LEF1 and WNT4 (table 4-23) showed no normal distribution, so Mann-Whitney-U tests instead of t-tests were performed.

$\Delta\Delta C_q$ -Values	Group	N	Mean	Std. Deviation	Std. Error Mean
AXIN2	control	19	0.022	1.016	0.233
	PAX7 knock-down	18	0.165	1.113	0.262
CTNNB1	control	19	0.021	0.326	0.075
	PAX7 knock-down	18	0.166	0.273	0.064
LEF1	control	19	-0.146	0.391	0.090
	PAX7 knock-down	18	-0.075	0.276	0.065
WNT4	control	18	0.165	1.113	0.262
	PAX7 knock-down	19	-0.146	0.391	0.090

Table 4-23: **Group statistics for changes in expression (as  $\Delta\Delta C_q$ -values) of canonical Wnt signaling components: AXIN2, CTNNB1, LEF1 and WNT4.** Mean and standard deviation/error form biological replicates. Higher means indicate lower expression, higher AXIN2 expression indicates higher canonical Wnt signaling activity.

Once again, the primers revealed a wide spread of expression changes for the individual embryos, but only minor differences in the means between the two

groups analyzed. Whilst all four genes analyzed showed a small reduction in expression, the large spread of individual results resulted in all reductions not being significant when tested. (two-sided t-test and Mann-Whitney-U test;  $p > 0.05$ ) (table 4-24 and 4-25 as well as figure 4-34 and 4-35)

	t-test for Equality of Means				
	t	Significance		Mean Difference	Std. Error Difference
		One-Sided p	Two-Sided p		
CTNNB1	-1.460	0.077	0.153	-0.145	0.099

Table 4-24: **Results from t-test for changes in expression of CTNNB1.** The negative mean difference indicates a reduction in expression of all genes analyzed, although not a significant one. Tests done using SPSS.

	Mann-Whitney U	Asymp. Sig. (2-tailed)	Exact Sig. [2*(1-tailed Sig.)]
AXIN2	169	0.952	0.964
WNT4	169	0.952	0.964
LEF1	171	1	1

Table 4-25: **Results from Mann-Whitney-U test for changes in expression of AXIN2, WNT4 and LEF1.** None of the genes tested show a significant change in expression because of the PAX7 knock-down. Tests done using SPSS.

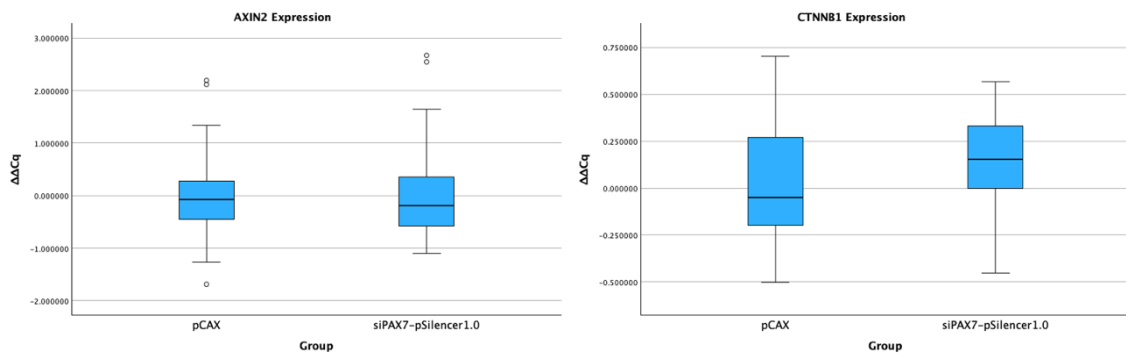


Figure 4-34: **PAX7 knock-down did not affect AXIN2 or CTNNB1 expression.** Boxplots of  $\Delta\Delta C_q$  values for AXIN2 and CTNNB1 expression changes, split between the reference (pCAX) and PAX7 knock-down n (siPAX7-pSilencer1.0) group. Although a difference in means, towards a lower CTNNB1 expression is visible, it is not significant (table 4-24 and 4-25). Whiskers mark the minimum/maximum value, circles mark outliers.

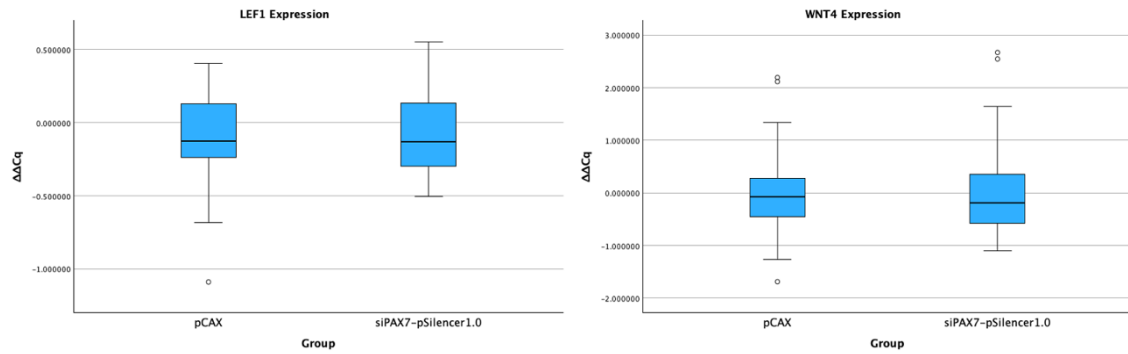


Figure 4-35: **PAX7 knock-down did not affect LEF1 or WNT4 expression.** Boxplots of  $\Delta\Delta C_q$  values for LEF1 and WNT4 expression changes, split between the reference (pCAX) and PAX7 knock-down *n* (siPAX7-pSilencer1.0) group. No significant changes in expression were detectable (table 4-25). Whiskers mark the minimum/maximum value, circles mark outliers.

#### 4.4.6.4 Frizzled Receptor Expression Not Affected by siPAX7-pSilencer1.0

Further expanding the set of genes tested directly involved in canonical Wnt signaling, the expression of the four primarily expressed frizzled receptors (FZD) receptors was tested. As none of the FZD genes in the chicken contain introns, the primers used weren't skipping from exon to exon and thus not cDNA specific, increasing background signal from genomic DNA. For FZD1 and FZD10 this didn't pose any problems, as both genes showed strong expression resulting in mean  $C_q$ -values  $\sim 7$ -8 cycles lower compared to the control sample without reverse transcription (no RT control) showing the amount of background signal from genomic DNA (table 4-26). For FZD5 and FZD9, both with a lower expression and lower  $C_q$ -value differences compared to the no RT control, this poses a problem, further difficulting the detection of expression changes (table 4-26).

Only the combination of the 60FZD5 primer and one embryo from the PAX7 knock-down group failed amplification and was excluded, all other data obtained was included in the analysis.

$C_q$ -Values	60 FZD1		60 FZD5		60 FZD9		60 FZD10	
	Mean	SD	Mean	SD	Mean	SD	Mean	SD
no RT control	21.73	0.95	21.29	1.14	22.10	0.43	20.46	0.89
all embryos	13.83	1.21	20.93	2.63	19.07	1.51	13.85	1.38

Table 4-26: **FZD receptor expression.** Comparison between  $C_q$ -values of the control sample without reverse transcriptase in the cDNA synthesis reaction to the mean of all samples included in the gene expression analysis. For FZD1 and FZD10 a strong expression allows for easy interpretation. The weak expression of FZD5 and FZD9, only a few cycles above the background from genomic DNA contamination makes detecting expression changes difficult.

$\Delta\Delta C_q$ -Values	Group	N	Mean	Std. Deviation	Std. Error Mean
FZD1	control	19	0.094	0.336	0.077
	PAX7 knock-down	18	-0.009	0.381	0.090
FZD5	control	19	0.669	3.647	0.837
	PAX7 knock-down	17	-0.918	3.349	0.812
FZD9	control	19	0.248	1.237	0.284
	PAX7 knock-down	18	-0.204	0.943	0.222
FZD10	control	19	-0.104	0.422	0.097
	PAX7 knock-down	18	0.045	0.360	0.085

Table 4-27: **Group statistics for changes in expression (as  $\Delta\Delta C_q$ -values) of frizzled receptors (FZD).** Mean and standard deviation/error form biological replicates. Higher means indicate lower gene expression.

For the overall strongly expressed FZD1 and FZD10 genes an overall low change in expression alongside a low spread between the individual embryos was observed indicating a stable expression between embryos and groups. FZD5 and FZD9 show higher alterations in expression between the two groups, but a high variance within the groups prevents the results from being statistically significant in the t-test and Mann-Whitney-U test (table 4-28 and 4-29 as well as figure 4-36 and 4-37).

	t-test for Equality of Means				
	t	Significance		Mean Difference	Std. Error Difference
		One-Sided p	Two-Sided p		
FZD1	0.873	0.194	0.389	0.103	0.118
FZD5	1.354	0.092	0.185	1.587	1.172
FZD10	-1.147	0.129	0.259	-0.148	0.129

Table 4-28: **Results from t-test for changes in expression of frizzled receptors (FZD).** Negative mean differences indicate a reduced level of gene expression, positive differences an increase in gene expression caused by the siPAX7-pSilencer1.0 plasmid. None of the expression level changes are significant ( $p > 0.05$ , two-sided t-test). Tests done using SPSS.

	Mann-Whitney U	Asymp. Sig. (2-tailed)	Exact Sig. [2*(1-tailed Sig.)]
FZD9	125	0.162	0.169

Table 4-29: **Results from Mann-Whitney-U test for changes in expression of FZD9.** The changes in expression resulting from PAX7 knock-down are insignificant. Test done using SPSS.

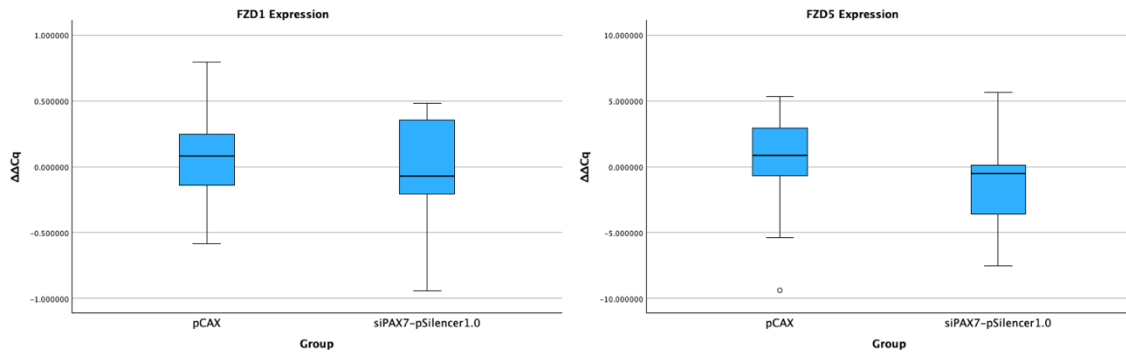


Figure 4-36: **PAX7 knock-down did not affect FZD1 or FZD5 expression.** Boxplots of  $\Delta\Delta C_q$  values for FZD1 and FZD5 expression changes, split between the reference (pCAX) and PAX7 knock-down n (siPAX7-pSilencer1.0) group. No significant changes in expression were detectable (table 4-28). Whiskers mark the minimum/maximum value, circles mark outliers.

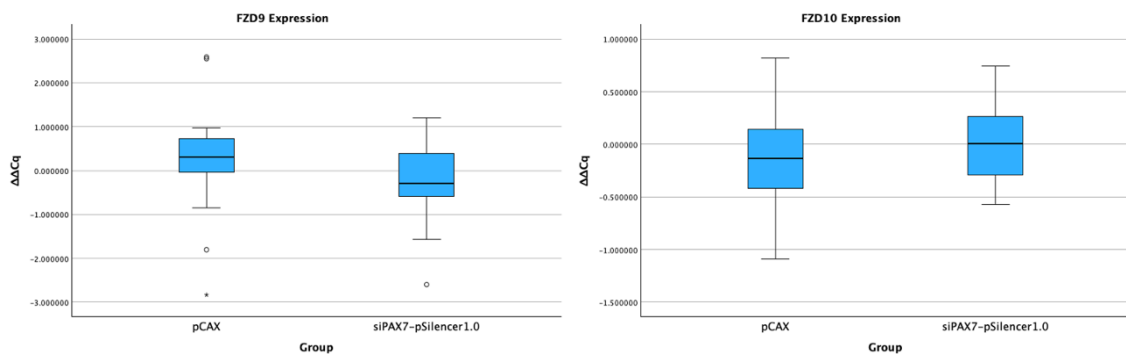


Figure 4-37: **PAX7 knock-down did not affect FZD9 or FZD10 expression.** Boxplots of  $\Delta\Delta C_q$  values for FZD9 and FZD10 expression changes, split between the reference (pCAX) and PAX7 knock-down n (siPAX7-pSilencer1.0) group. No significant changes in expression were detectable (table 4-28 and table 4-29). Whiskers mark the minimum/maximum value, circles mark outliers, stars extreme outliers (more than 1.5 interquartile ranges from box).

#### 4.2.4.6 Expression of Other Genes Active in Proliferating Cells Not Affected by siPAX7-pSilencer1.0

Widening the scope of genes, potentially affected by a knock-down of PAX7, multiple HES genes as well as NOTCH1, all involved in development of the midbrain and all expressed around HH stage 17, were probed for using exon spanning qPCR primers. All reactions showed successful amplification, so all were included in the statistical analysis (table 4-30).

$\Delta\Delta C_q$ -Values	Group	N	Mean	Std. Deviation	Std. Error Mean
NOTCH1	control	19	-0.535	1.494	0.343
	PAX7 knock-down	18	-0.425	1.413	0.333
HES1	control	19	-0.239	0.997	0.229
	PAX7 knock-down	18	-0.112	0.735	0.173
HES5A	control	19	-0.011	0.455	0.104
	PAX7 knock-down	18	0.228	0.635	0.150

HES5like	control	19	0.011	0.386	0.088
	PAX7 knock-down	18	0.203	0.309	0.073
HES6	control	18	0.094	0.668	0.158
	PAX7 knock-down	18	-0.186	0.691	0.163
HEY1	control	19	-0.076	0.296	0.068
	PAX7 knock-down	18	0.017	0.238	0.056

Table 4-30: **Group statistics for changes in expression (as  $\Delta\Delta C_q$ -values) of NOTCH 1 and multiple members of the HES gene family expressed in the midbrain at HH stage 17.** Mean and standard deviation/error form biological replicates. Higher means indicate lower gene expression.

The genes from the HES family show a non-significant reduction in expression caused by the siPAX7-pSilencer1.0 electroporation, except for HES6, where a non-significant increase can be observed. NOTCH1 also did not show a significant change in expression, although a minor reduction on the PAX7 knock-down side could be observed (table 4-31 and figures 4-38 to 4-40).

	t-test for Equality of Means				
	t	Significance		Mean Difference	Std. Error Difference
		One-Sided p	Two-Sided p		
NOTCH1	-0.231	0.409	0.819	-0.111	0.479
HES1	-0.439	0.332	0.664	-0.127	0.289
HES5A	-1.318	0.098	0.196	-0.238	0.181
HES5like	-1.665	0.052	0.105	-0.192	0.115
HES6	1.234	0.113	0.226	0.280	0.227
HEY1	-1.047	0.151	0.302	-0.093	0.089

Table 4-31: **Results from t-test for changes in expression of NOTCH and members of the HES gene family expressed in the midbrain at HH stage 17.** Negative mean differences indicate a reduced level of gene expression, positive differences an increase in gene expression caused by the siPAX7-pSilencer1.0 plasmid. None of the expression level changes are significant ( $p > 0.05$ , two-sided t-test). Tests done using SPSS.

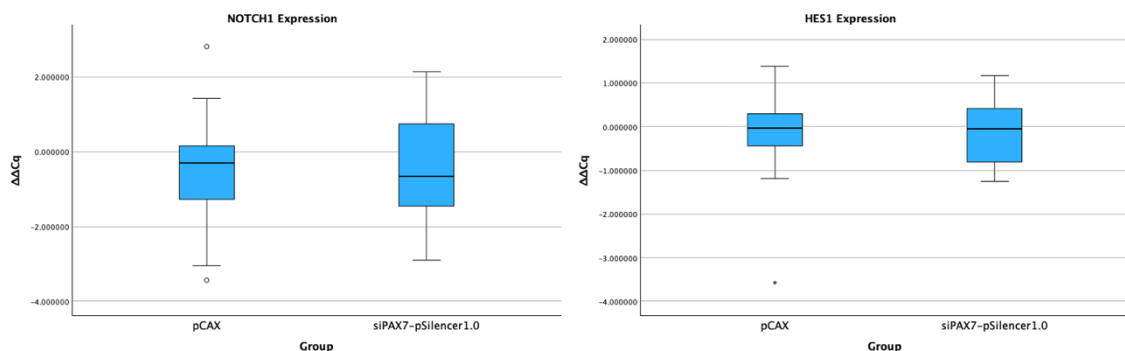


Figure 4-38: **PAX7 knock-down did not affect NOTCH1 or HES1 expression.** Boxplots of  $\Delta\Delta C_q$  values for NOTCH1 and HES1 expression changes, split between the reference (pCAX) and PAX7 knock-down n (siPAX7-pSilencer1.0) group. No significant changes in expression were detectable (table 4-31).

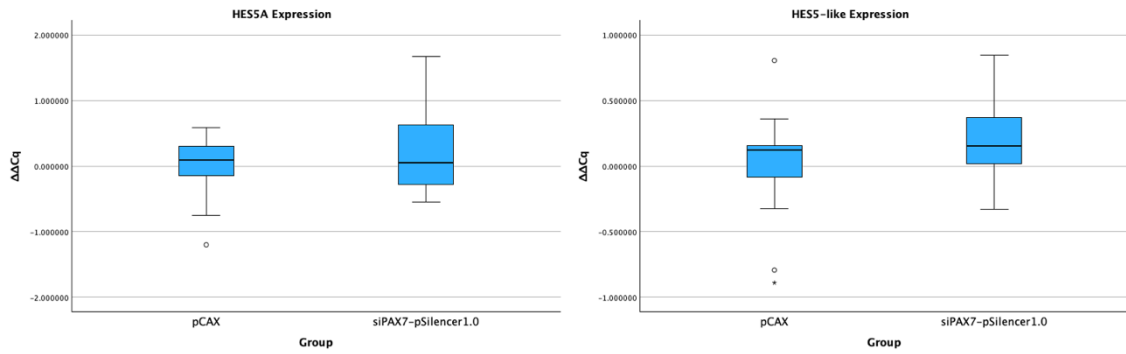


Figure 4-39: **PAX7 knock-down did not affect HES5A or HES5-like expression.** Boxplots of  $\Delta\Delta C_q$  values for HES5A and HES5-like expression changes, split between the reference (pCAX) and PAX7 knock-down *n* (siPAX7-pSilencer1.0) group. No significant changes in expression were detectable (table 4-31).

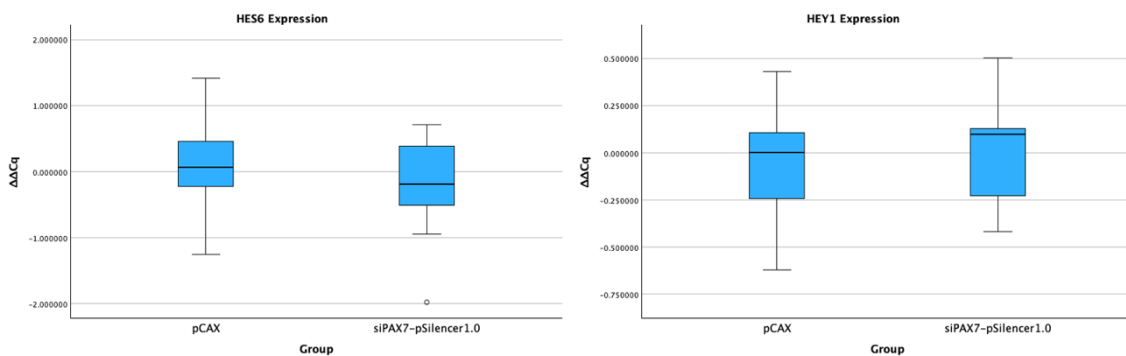


Figure 4-40: **PAX7 knock-down did not affect HES6 or HEY1 expression.** Boxplots of  $\Delta\Delta C_q$  values for HES6 and HEY1 expression changes, split between the reference (pCAX) and PAX7 knock-down *n* (siPAX7-pSilencer1.0) group. No significant changes in expression were detectable (table 4-31).

#### 4.2.4.7 Potential siPAX7-pSilencer1.0 off-Target Genes Expression not Affected by siPAX7-pSilencer1.0

As research using NCBI's BLAST tool revealed multiple genes besides PAX7 that could partially be bound and thus inhibited in translation by the siPAX7-pSilencer1.0 construct used for the PAX7 knock-down experiment, a small selection of genes expressed in the chicken midbrain during development were tested for expression alterations.

The ES60CHMP48, ES60ERMIN and ES60MAP2 primers showed decent amplification, all  $C_q$ -values obtained were analyzed, except for two embryos in the pCAX control group, that failed amplification when tested using the ES60ERMIN primers (table 4-32).

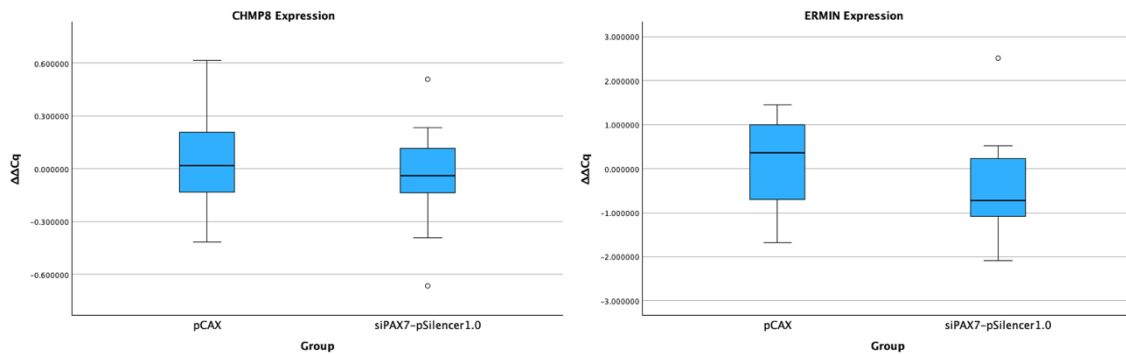
$\Delta\Delta C_q$ -Values	Group	N	Mean	Std. Deviation	Std. Error Mean
CHMP48	control	19	0.038	0.279	0.064
	PAX7 knock-down	18	-0.031	0.253	0.060
ERMIN	control	17	0.153	1.049	0.254
	PAX7 knock-down	18	-0.498	1.063	0.251
MAP2	control	19	-0.038	0.491	0.113
	PAX7 knock-down	18	0.125	0.384	0.091

Table 4-32: **Group statistics for changes in expression (as  $\Delta\Delta C_q$ -values) of potential off-target genes of the siPAX7-pSilencer1.0 construct.** Mean and standard deviation/error form biological replicates. Higher means indicate lower gene expression.

The minor changes in average expression in combination with large standard deviations, resulted in none of the expression changes observed in the PAX7 knock-down group being significantly different from the pCAX control group (on the standard  $p < 0.05$  significance level, if  $p < 0.1$  was to be considered significant, ERMIN would show a significant uplift in expression as a result of the siPAX7-pSilencer). This indicates that the siPAX7-pSilencer1.0 construct does not affect expression of the three potential off target genes tested (table 4-34 and figures 4-48 and 4-49).

	t-test for Equality of Means				
	t	Significance		Mean Difference	Std. Error Difference
		One-Sided p	Two-Sided p		
CHMP48	0.793	0.216	0.433	0.070	0.088
ERMIN	1.822	0.039	0.078	0.651	0.357
MAP2	-1.117	0.136	0.272	-0.163	0.146

Table 4-33: **Results from t-test for changes in expression potential off-target genes of the siPAX7-pSilencer1.0 construct.** Negative mean differences indicate a reduced level of gene expression, positive differences an increase in gene expression caused by the siPAX7-pSilencer1.0 plasmid. None of the expression level changes are significant. ( $p > 0.05$ , two-sided t-test). Tests done using SPSS.



**Figure 4-42: PAX7 knock-down did not affect CHMP48 or ERMIN expression.** Boxplots of  $\Delta\Delta C_q$  values for CHMP48 and ERMIN expression changes, split between the reference (pCAX) and PAX7 knock-down n (siPAX7-pSilencer1.0) group. No significant changes in expression on a  $p < 0.05$  level were detectable. If results with a  $p < 0.1$  were to be considered significant, ERMIN would show a significant uplift in expression because of the PAX7 knock-down (table 4-33).

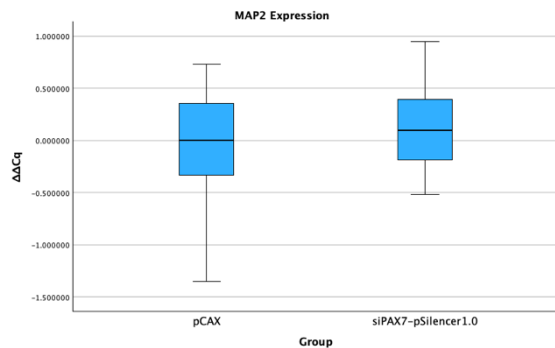


**Figure 4-41: PAX7 knock-down did not affect MAP2 expression.** Boxplots of  $\Delta\Delta C_q$  values for MAP2 expression changes, split between the reference (pCAX) and PAX7 knock-down (siPAX7-pSilencer1.0) group. No significant changes in expression were detectable (table 4-33).

## 4.3 Detecting PAX7 and Wnt Signaling on Protein Level Using Western Blot

As qPCR failed to detect the intended effects of the electroporations, Western blot was used to test whether changes in gene expression could be observed on protein level.

Protein from phenol-chloroform isolation was used for western blots detecting PAX7 and dephosphorylated active CTNNB1 ( $\beta$ -catenin). Like qPCR, antibodies were first validated using a dilution series from wildtype tissue.

### 4.3.1 Difficulties

Besides initial issues, with different electrophoresis chambers (for example the chamber from Biometra) and buffers, resulting in poor electrophoresis performance, quantification of proteins proved especially difficult.

For example, in initial testing, blots using 20 $\mu$ g of protein (1 $\mu$ g/ $\mu$ l and 6 $\mu$ g/ $\mu$ l measured using nanodrop) isolated from spinal cord resulted in no visible protein

in a ponceau stain, indicating falsely high photometric measurements. Dye based quantification using Qubit was tested – and showed unreliable results when testing measurement linearity using a dilution series. The issues with quantification primarily stemmed from low tissue input and solvents skewing the measurements. In the end, an approach analog to the qPCR from single embryos, the protein was simply directly loaded on the gels, skipping quantification. As once again midbrain halves with PAX7 expression modifications were to be compared with their corresponding wildtype midbrain halves, the amount of protein isolated and loaded should have been comparable. Minor differences in protein quantity could be adjusted for using whole protein normalization.

Unfortunately, the amount of protein isolated was in many cases too low to be detected using ponceau stain. For example, three of the 8 midbrain blots had no visible protein in the Ponceau stain. Despite that, PAX7 and active-CTNNB1 protein was detected using antibodies, and an attempt at normalization using the Revert 700 fluorescent whole protein stain was made.

#### **4.3.2 Validation of Antibodies for Western Blot**

The anti PAX7 antibody from DSHB, the anti  $\beta$ -catenin non-phospho(active) S45 antibody from Abcam and the anti active- $\beta$ -catenin (ABC, clone 8E7) antibody from Upstate were tested on blots ranging from 5-40 $\mu$ l protein extracted from midbrain of E6 embryos.

Blots were analyzed using Fiji, linear fits with forced  $y=0$  intersects were calculated using Excel. Major outliers were excluded. Table 4-37 shows averaged  $R^2$  values calculated.

For the anti PAX7 and the anti-non-phospho  $\beta$ -catenin antibody from Abcam, linear fits with  $R^2$  values over 0.9 could be generated, indicating good linearity between 5 $\mu$ l and 40 $\mu$ l of reference E6 midbrain protein. The anti-ABC antibody failed to produce such results, a linear fit was only successful on one blot, with poor  $R^2$  values indicating a poor fit (table 4-34).

A GAPDH antibody initially intended as loading control, produced multiple bands and was thus excluded from further testing and the Revert whole protein stain was instead used as loading control.

Anti PAX7, DSHB		Anti non-phospho $\beta$ -catenin, Abcam		Anti ABC, Upstate	
Range	R <sup>2</sup>	Range	R <sup>2</sup>	Range	R <sup>2</sup>
5-40 $\mu$ l	0.938	10-40 $\mu$ l	0.978	5-40 $\mu$ l	0.235
5-40 $\mu$ l	0.973	5-40 $\mu$ l	0.980		
5-40 $\mu$ l	0.969	5-40 $\mu$ l	0.912		
5-40 $\mu$ l*	0.978	5-40 $\mu$ l*	0.915		
average	0.965	average	0.946		

Table 4-34: **Anti PAX7 and Anti non-phospho  $\beta$ -catenin antibodies show linear scaling.** R<sup>2</sup> values from dilution series western blots to validate linearity of antibody signals. Both the anti PAX7 antibody and the anti-non-phospho  $\beta$ -catenin antibody from Abcam produce good linear fits with R<sup>2</sup> values >0.9. The Anti ABC antibody from Upstate showed poor performance and failed validation. \* staining on stripped blots.

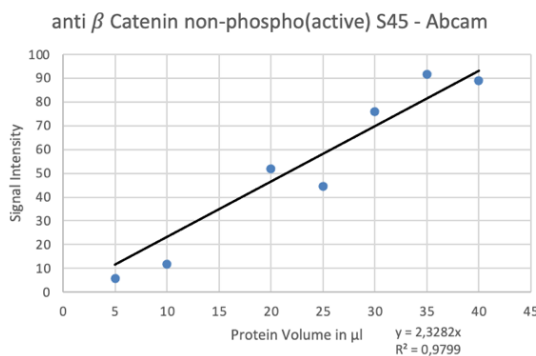


Figure 4-43: **Good correlation between signal intensity and loaded protein.** Exemplary blot with linear fit from western blot from antibody linearity testing using E6 wildtype midbrain tissue and anti-non-phospho  $\beta$ -catenin antibody from Abcam. The linear fit shows good linear correlation with an R<sup>2</sup> of 0.98.

### 4.3.3 Expression Analysis

For a total of 14 different protein samples western blot analysis was performed. 13 with modified PAX7 expression were from the same tissue samples as the RNA used for qPCR reactions (chapter 4.2.3). A positive control for canonical Wnt signaling activity was included, using protein isolated from LiCl (unspecific Wnt signaling activator) and NaCl (reference sample) treated embryos at HH stage.

#### 4.3.3.1 Summary

Resulting from the low protein input quantification of protein expression failed. Most of the obtained signals were outside of validated primer range and the measurement inaccuracies resulting from weak signals made drawing conclusions about the impact of the transfections impossible.

In the following, the results will still be briefly presented.

### 4.3.3.2 Whole Protein Stain

Quantification of protein isolated using phenol-chloroform preparation proved to be highly unreliable. Therefore, the assumption that both sides of the midbrain should yield comparable amounts of protein was made and equal volumes of protein were loaded for each side. A reference sample was loaded alongside the test samples, ensuring that the amount of protein detected was within validated range.

The whole protein stains using the Revert 700 Whole Protein Stain were analyzed using the Empiria software. The absolute signal intensities obtained cannot be compared across blotting membranes and antibodies as the Odyssey FC automatically adjusts acquisition settings depending on signal intensity.

Tis- sue	Stange	Plasmid	n	Relative Signal Intensities for Whole Protein Stain			
				GFP Side		Control Side	
				Rel. Mean	Rel. SD	Rel. Mean	Rel. SD
Midbrain	HH stage 17	PAX7 knock-down; Batch 2	15	0.85	0.338	0.57	0.142
		PAX7 knock-down; Batch 3	13	1.53	0.680	2.04	0.396
		sPAX7-pMES	15	0.12	0.102	0.10	0.034
		IPAX7-pMES	16	0.59	0.341	0.84	0.200
		enPAX7-pMIW	14	0.56	0.066	0.54	0.074
		pCAX	13				
	HH stage 14	siPAX7-pSilencer1.0	11	0.13	0.081	0.14	0.016
		sPAX7-pMES	17	0.29	0.102	0.36	0.010
Hindbrain	HH stage 17	siPAX7-pSilencer1.0	17	1.42	1.000	0.64	0.809
		sPAX7-pMES	11	0.06	0.103	0.14	0.082
		enPAX7-pMIW	11	0.11	0.660	0.00	0.481
	HH stage 14	sPAX7-pMES	12	2.99	1.741	2.53	1.992

*Table 4-35: Whole protein stain shows low protein input relative to loading control, in Western Blots. Sample protein loaded, relative to reference protein, calculated (from values in appendix 9.3) for better visualization and cross blot comparability.*

As shown in table 4-35, the relative signal intensity is below 1, which equals less than 10µl of reference E6 midbrain protein from antibody linearity testing. With a relative signal of 0.5 being the lower limit of validated signal ranges, more than half of the samples are bordering or are outside of validated ranges.

Overall, the amount of protein loaded, when comparing GFP and control sides is not too different, but extremely high standard deviations don't allow for more than vague statements (table 4-35, figure 4-44).

As expected, the sample using protein isolated from a whole embryo at HH stage 20, intended as positive control for canonical Wnt signaling showed much higher signal intensity, equaling a higher amount of protein loaded, whilst absolute standard deviations were comparable to samples from mid-/hindbrain (figure 4-45).

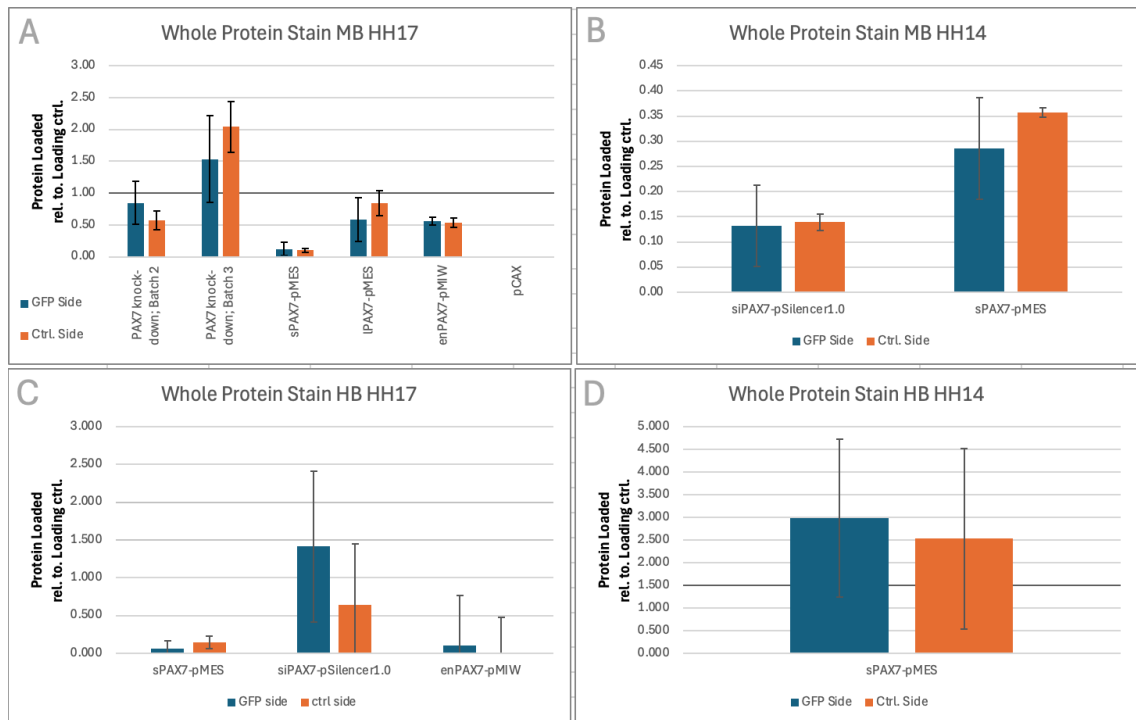


**Figure 4-45: Low amount of total protein loaded relative to E6 midbrain reference protein.** Protein loaded over all is low, standard deviations from technical replicates are high.

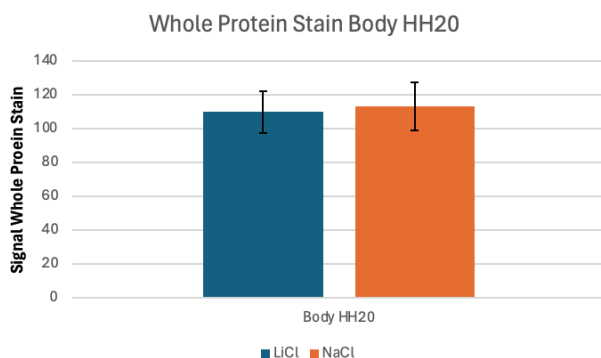


**Figure 4-44: Low standard deviations in whole protein stain for protein isolated from whole body at HH stage 20.** Revert 700 whole protein stain, absolute signal, thus Y-axis not comparable with figure 4-51. The standard deviation is much lower compared to the absolute signal because of more protein being loaded.

#### 4.3.3.3 Quantification of PAX7 Expression and Canonical Wnt Signaling on a Protein Level

The results show that the signals obtained from the transfected samples were much weaker compared to the signal from the E6 midbrain reference sample. Most signals from transfected samples did not reach 50% of reference sample signal (table 4-36 and 4-37), equaling the lower limit of validated primer range. Signal intensities outside of validated range cannot be interpreted reliably.

Tissue	Stage	Plasmid	n	Normalized Signal Intensities for PAX7				Reference E6 Mid-brain
				GFP Side		Control Side		
				Mean	SD	Mean	SD	
Midbrain	HH stage 17	PAX7 knock-down; Batch 2	15	0.50	0.168	0.37	0.098	1.21
		PAX7 knock-down; Batch 3	13	0.58	0.195	1.01	0.139	1.96
		sPAX7-pMES	15					0.05
		IPAX7-pMES	16	2.67	1.100	1.04	1.051	4.11
		enPAX7-pMIW	14	0.04	0.008	0.05	0.008	0.19
	pCAX	13						
	HH stage 14	siPAX7-pSilencer1.0	11	0.21	0.212	0.12	0.141	0.35
	sPAX7-pMES	17	0.11	0.163	0.05	0.009	0.05	
Hindbrain	HH stage 17	siPAX7-pSilencer1.0	17	0.12	0.022	0.09	0.041	1.18
		sPAX7-pMES	11	0.07	0.229	0.24	0.162	1.54
		IPAX7-pMES	12					
		enPAX7-pMIW	11	0.00	0.004	0.01	0.008	0.22
	HH stage 14	sPAX7-pMES	12	0.03	0.042	0.61	0.949	24.90

Table 4-36: **PAX7 protein quantification of mid- and hindbrain tissue.** Normalized signal intensities from PAX7 antibody. Averages and standard deviations from technical replicates. The signal intensities are blot specific and can't be compared across blots. Blank spots: no bands visible. Most samples produce a signal <50% of the reference signal and are thus below validated antibody range.

Tissue	Stage	Plasmid	n	Normalized Signal Intensities for non-phospho CTNNB1				Reference: E6 MB
				GFP Side		Control Side		
				Mean	SD	Mean	SD	
Midb		PAX7 knock-down; Batch 2	15	17.20	5.716	19.80	3.812	12.40

	HH stage 17	PAX7 knock-down; Batch 3	13	74.67	46.437	35.30	7.545	55.20
		sPAX7-pMES	15					1.29
		IPAX7-pMES	16	76.93	45.694	45.83	16.89 6	14.10
		enPAX7-pMIW	14	4.60	0.297	0.93	0.699	5.45
		pCAX	13					
	HH stage 14	siPAX7-pSi-lencer1.0	11	-0.74	2.753	0.07	2.731	3.61
		sPAX7-pMES	17	0.26	0.448	-0.39	0.754	0.50
Hindbrain	HH stage 17	siPAX7-pSi-lencer1.0	17	6.07	1.894	1.00	8.242	4.12
		sPAX7-pMES	11	-214.34	203.50 9	9.57	17.52 9	1.34
		IPAX7-pMES	12					
		enPAX7-pMIW	11	8.11	11.112	-0.24	1.447	1.54
	HH stage 14	sPAX7-pMES	12	1.20	1.690	0.37	0.395	2.48
Body	HH stage 20	LiCl/NaCl	1	0.79	0.358	0.92	0.268	

Table 4-37: **Canonical Wnt signaling activity quantifiable in a few protein samples.** Normalized non-phospho CTNNB1 signal from western blots. Averages and standard deviations from technical replicates. The signal intensities are blot specific and can't be compared across blots. Blank spots: no bands visible. The samples from midbrain at HH stage 17 mostly are within validated antibody range.

Independent of stage, brain region and electroporation not a single sample had both its brain sides within validated antibody range for the anti-PAX7 antibody whilst also having reasonable standard deviations. (figure 4-46)

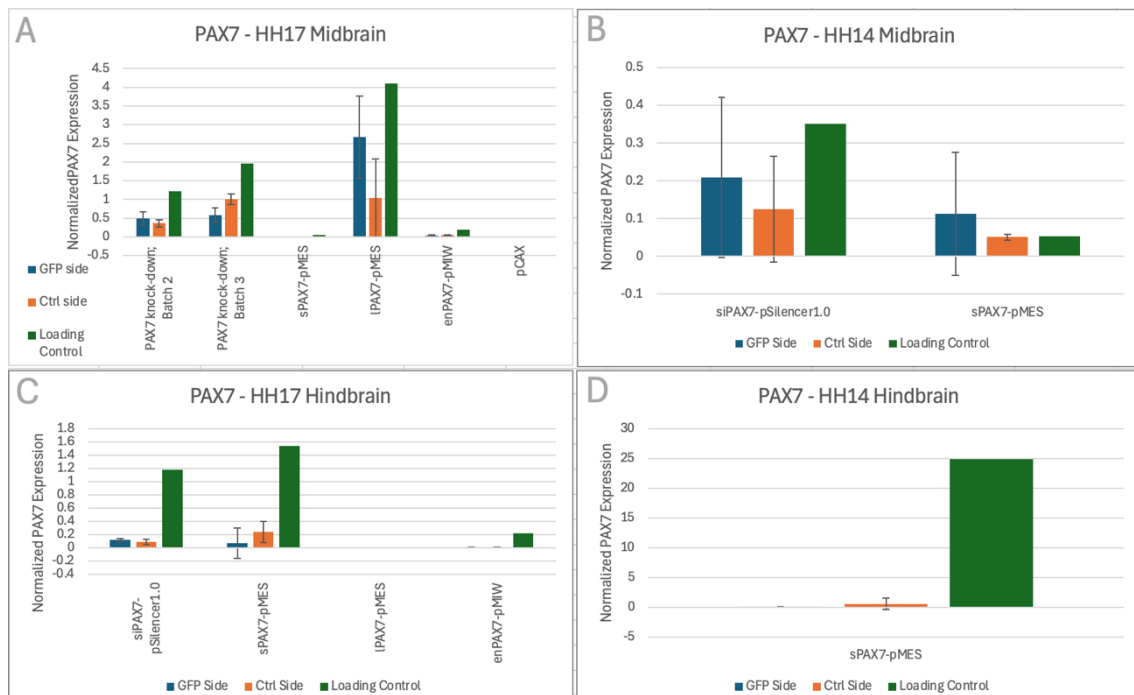


**Figure 4-46: PAX7 protein cannot be reliably quantified.** Western blot results using the PAX7 antibody from DSHB. Signal normalized to whole protein stain. Most signals are below validated antibody range (<50% of loading control). Standard deviations from technical replicates are too high, to allow for valid conclusions about changes in PAX7 detected. Protein harvested at: **A:** HH stage 17, midbrain tissue; **B:** HH stage 14, midbrain tissue; **C:** HH stage 17, hindbrain tissue; **D:** HH stage 14, hindbrain tissue.

The results from western blots stained using the non-phospho  $\beta$ -catenin antibody from Abcam look better compared to the results from PAX7 blots. The samples from the midbrain at HH stage 17 had mostly signal intensities within the validated range for antibody linearity. The spread between the individual measurements is still high resulting in high standard deviations. (figure 4-47)

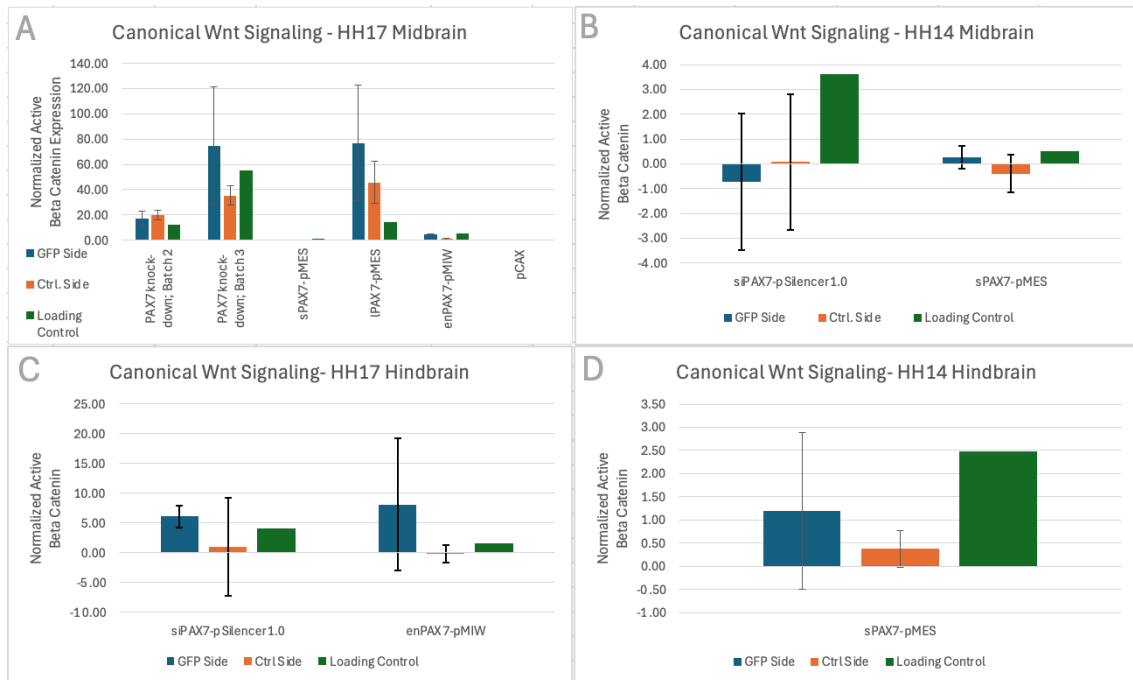


**Figure 4-47: High SDs undermine ability to draw conclusions about canonical Wnt signaling activity in HH stage 17 midbrain samples.** Results from western blot of midbrain tissue at HH stage 17 using the non-phospho  $\beta$ -catenin antibody from Abcam. Signal normalized to whole protein stain. Protein harvested at: **A:** HH stage 17, midbrain tissue; **B:** HH stage 14, midbrain tissue; **C:** HH stage 17, hindbrain tissue; **D:** HH stage 14, hindbrain tissue.

Samples from whole bodies at HH stage 20 treated with LiCl, intended as positive control for canonical Wnt signaling and tissue treated with an equimolar amount of NaCl as negative control were also tested using the non-phospho  $\beta$ -catenin antibody. Small changes in signal intensity and high standard deviations did not allow clear conclusions about CTTNB1 and Wnt signaling (figure 4-48). This positive control failing would put all other results using this antibody for quantification of canonical Wnt signaling in doubt, if they had shown significant differences in activity.

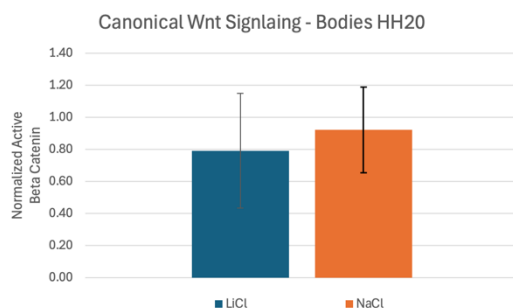


**Figure 4-48: Positive control does not show expected increase in canonical Wnt signaling activity.** Results from western blot of body tissue at HH stage 20 using the non-phospho  $\beta$ -catenin antibody from Abcam. Signal normalized to whole protein stain. High variance between measurements don't allow for conclusions about canonical Wnt signaling.

Summarizing, for the western blots using the Abcam non-phospho (active)  $\beta$ -catenin antibody, the same as for blots detecting PAX7 can be said. High

variance between the individual measurements and low signal intensity don't allow for reliable interpretation. Furthermore, the positive control failed detection of an increased canonical Wnt signaling activity.

## 4.4 New siRNA Constructs for PAX7

The original siRNA used to knock down PAX7 expression in the midbrain was designed by Naixin Li, a former member of the AG Wizenmann. In internal experiments, this siPAX7-pSilencer1.0 construct had shown to reduce the size of midbrains (Li) and a reduction of canonical Wnt signaling (Zeeb). Unfortunately, the sequence of this siRNA also showed some partial alignment with other chicken gene, for example ERMIN or MAP2, both expressed in the midbrain or neurons and involved in development. This, in combination with the fact, that nowadays a combination of multiple siRNAs injected simultaneously, is the preferred method of siRNA-based knock downs, a set of new siRNA-pSilencer1.0 constructs was generated.

### 4.4.1 Generation of New siPAX7 Plasmids

The pSilencer1.0 plasmid backbone was successfully extracted from the siPAX7-pSilencer plasmid using an EcoRI and Apal digest (figure 4-49).

The sense and antisense strands of the inserts were hybridized and then phosphorylated. DH5 $\alpha$  *E.coli* were transformed with ligated insert and plasmid. Using colony PCR and agarose electrophoresis the transformation success was controlled (figure 4-50).

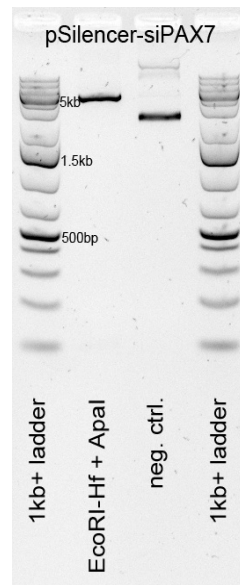


Figure 4-49: **Successful recovery of the pSilencer1.0 backbone.** Digest of siPAX7-pSilencer1.0 using EcoRI and Apal. 50ng per lane. The signal from the fragment cut from the plasmid is too weak (expected 66bp), but the difference with the negative control indicates successful digestion. The full length pSilencer1.0 plasmid has an expected size of 3.3kb.

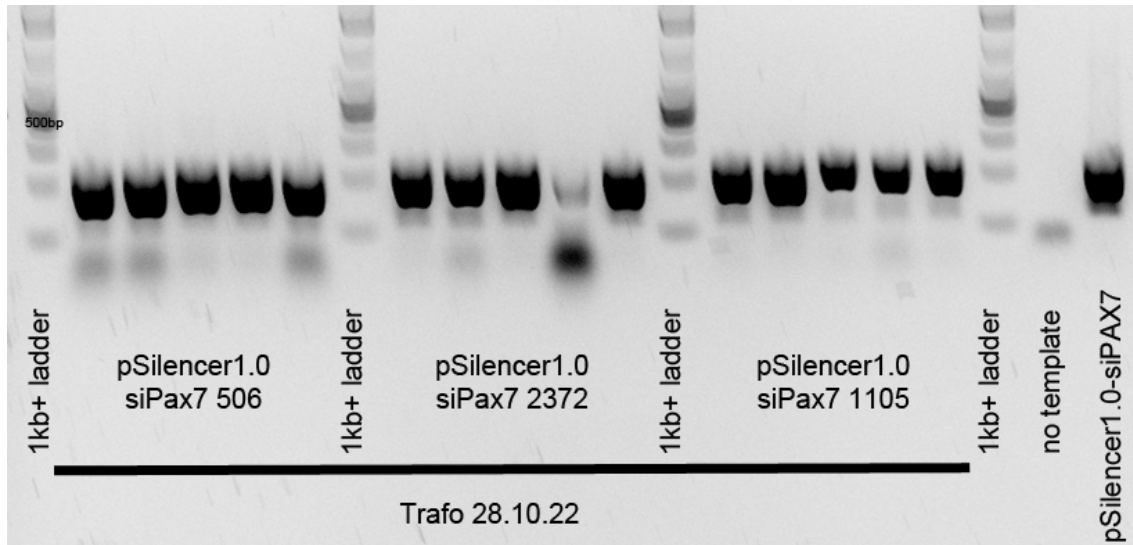


Figure 4-50: **Successful ligation and transformation of new siPAX7-pSilencer1.0 constructs.** Bands at 200bp indicate presence of pSilencer1.0 plasmid with insert. The siPAX7-pSilencer1.0 plasmid functioned as positive control. All colonies, except the 4th for the 2373 insert show a strong signal of the expected size, indicating successful ligation and transformation.

Sanger sequencing (figure 4-51) was used to confirm the presence of the desired inserts prior to the first in-ovo electroporations.

Wilbur-Lipman DNA Alignment  
 Ktuple: 3; Gap Penalty: 3; Window: 20

Seq1(1>1154)	Seq2(1>56)	Similarity	Gap	Gap
GKJ367_43253679_43253679	506.seq	Index	Number	Length
(48>103)	(1>56)	100.0	0	0

```

v50      v60      v70      v80      v90      v100
CTCC TC TGCAGG TACCAAG ATTC AAGAG ATC TTGG TACC TGCAGAGG ATTTTTT TAG
CTCC TC TGCAGG TACCAAG ATTC AAGAG ATC TTGG TACC TGCAGAGG ATTTTTT TAG
CTCC TC TGCAGG TACCAAG ATTC AAGAG ATC TTGG TACC TGCAGAGG ATTTTTT TAG
          ^10      ^20      ^30      ^40      ^50
Seq1(1>56)      Seq2(1>1163)      Similarity      Gap      Gap
2372.seq      GKJ368_43253686_43253686      Index      Number      Length
(1>56)      (47>102)      100.0      0      0
  
```

Seq1(1>56)	Seq2(1>1168)	Similarity	Gap	Gap
1105.seq	GKJ369_43253693_43253693	Index	Number	Length
(1>56)	(48>103)	100.0	0	0

```

v10      v20      v30      v40      v50
CGACC TATGG ACCAAAC ATATTC AAGAG ATATG TTGG TCC ATAGG TC TTTTTT TAG
CGACC TATGG ACCAAAC ATATTC AAGAG ATATG TTGG TCC ATAGG TC TTTTTT TAG
CGACC TATGG ACCAAAC ATATTC AAGAG ATATG TTGG TCC ATAGG TC TTTTTT TAG
          ^50      ^60      ^70      ^80      ^90      ^100
Seq1(1>56)      Seq2(1>1168)      Similarity      Gap      Gap
1105.seq      GKJ369_43253693_43253693      Index      Number      Length
(1>56)      (48>103)      100.0      0      0
  
```

Seq1(1>56)	Seq2(1>1168)	Similarity	Gap	Gap
1105.seq	GKJ369_43253693_43253693	Index	Number	Length
(1>56)	(48>103)	100.0	0	0

```

v10      v20      v30      v40      v50
CCCAAC TGCAGC ATTC AAC TTC AAGAG AGT TGAAT GC TGC GAG TTGG TTTTTT TAG
CCCAAC TGCAGC ATTC AAC TTC AAGAG AGT TGAAT GC TGC GAG TTGG TTTTTT TAG
CCCAAC TGCAGC ATTC AAC TTC AAGAG AGT TGAAT GC TGC GAG TTGG TTTTTT TAG
          ^50      ^60      ^70      ^80      ^90      ^100
  
```

Figure 4-51: **Successful generation of new siPAX7-pSilencer1.0 constructs.** Wilbur-Lipman alignment of the expected inserts with the sequencing results using DNASTAR MegAlign. The results show 100% base identity for the plasmids used for later PAX7 knockdown. From top to bottom: Insert 506; Insert 2373; Insert 1105. For better visibility, only the sequence of the 56bp sense strand of the insert shown.

#### 4.4.2 Size Reduction Caused by PAX7 Knock-Down

The newly generated plasmids were electroporated into the midbrain 11 chicken embryos, of which 8 were flat mounted at HH stage 17-18 as open book preparations and imaged. Using Fiji, the size of each midbrain half was measured and compared. The mean and standard deviation of the ratio of the areas were calculated (table 4-39). As no control group electroporated with only GFP expressing

plasmids was carried along and only n=8 embryos were measured, no significance could be tested, but past internal experiments had shown no impact on midbrain size when embryos were electroporated using only the pCAX plasmid.

Embryo ID	Side	Area [ $\mu\text{m}^2$ ]	GFP/Control	Mean of Ratios	SD of Ratios
22003	GFP	830732	0,996	0,983	0,120
	Control	834329			
22005	GFP	586449	0,915		
	Control	641097			
22007	GFP	418632	1,020		
	Control	410414			
22008	GFP	650298	0,902		
	Control	720840			
22010	GFP	537000	0,828		
	Control	648729			
22011	GFP	812690	1,215		
	Control	668848			
22012	GFP	812780	1,067		
	Control	761569			
22013	GFP	930115	0,923		
	Control	1007494			

Table 4-38: *PAX7 knock-down using the new siPAX7-pSilencer1.0 constructs does not reduce average midbrain size.* The comparison (through ratios) revealed only a 2% difference between both sides, indicating no effect of siPAX7 expression on midbrain size at HH stage 17-18 (n=8).

The new pSilencer1.0 plasmids did not show to reduce the average midbrain size, when compared to the unelectroporated side.

## 4.5 Antibody Testing for IHC

### 4.5.1 Detecting Canonical Wnt Signaling with IHC

The detection of canonical Wnt signaling activity, using the anti-active  $\beta$ -catenin antibody (ABC antibody) from Upstate, that only stains dephosphorylated, thus active CTNNB1, was another idea that was tested out. A total of over 40 of pre-existing cryosection slides were stained, some with 3M citric acid pretreatment (figure 4-52), some in combination with GFP stains and some with prolonged incubation times.

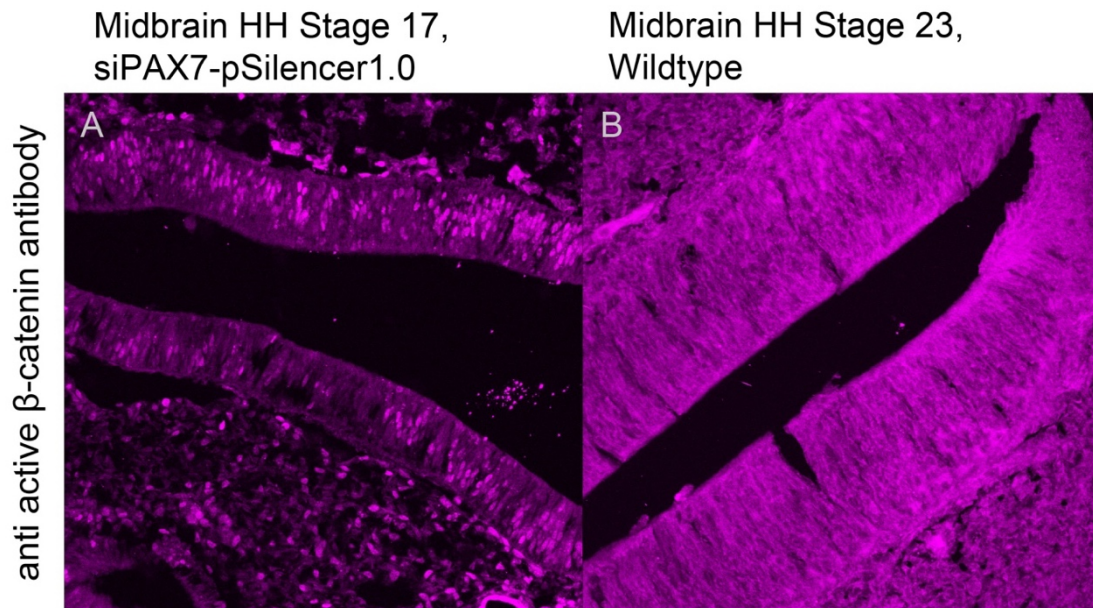
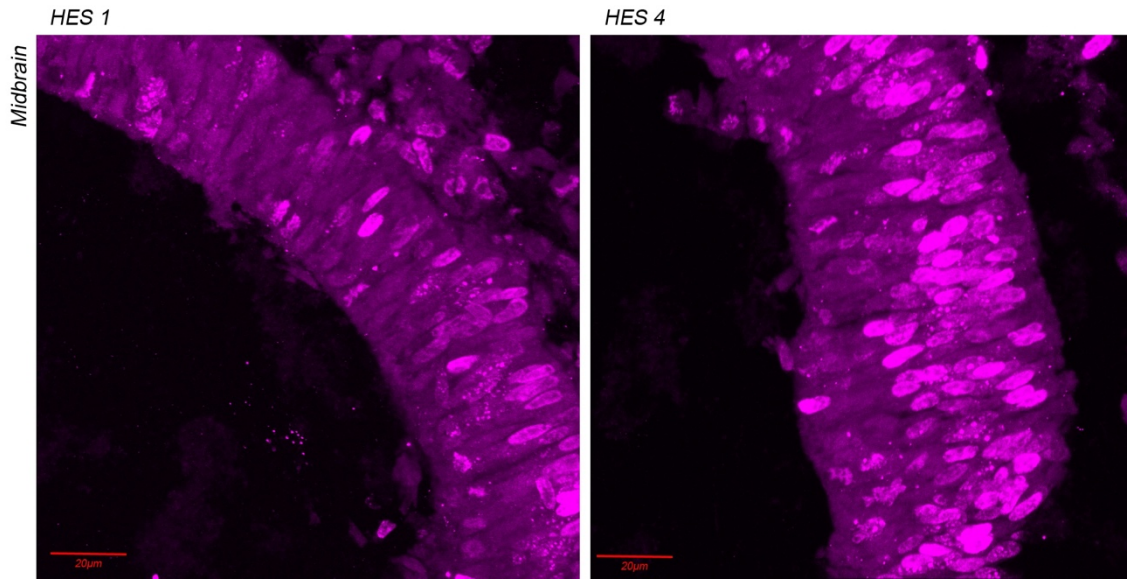


Figure 4-52: **IHC using the anti-active  $\beta$ -catenin antibody (ABC antibody) from Upstate.** Both slides underwent pretreatment in heated citric acid at pH 6. **A:** Neural epithelia of an embryo at HH stage 17 electroporated with the siPAX7-pSilencer1.0 plasmid. The antibody shows the expected nuclear staining, indicating active canonical Wnt signaling. **B:** Neural epithelia of a wildtype embryo at HH stage 23. The ABC antibody stained cytoskeletal CTNNB1. This staining pattern was the predominant when testing this antibody. It was not possible to determine the cause for the highly different patterns in staining, as the nuclear staining was not reproducible, so this approach was abandoned.

Overall, only two stains showed the specific nuclear staining, whilst the majority only showed cytoplasmic/cytoskeletal staining. Control sections, stained with DSHB's PAX7 antibody always worked, indicating that the issue was caused by the ABC primary antibody and not by other steps in the process.

#### 4.5.2 Detecting HES Genes Using IHC

Some initial testing using HES1 and HES4 primary antibodies from Santa Cruz Biotechnology was performed too and showed for the total of 4 stains done specific nuclear staining (figure 4-53), but as the intention for IHC experiments had been the probing for canonical Wnt signaling, further staining was abandoned in favor of western blotting.



**Figure 4-53: IHC using ant HES1 and anti HES4 antibodies on midbrain tissue.** Maximum intensity projection using LSM. Preexisting cryosection of midbrain tissue, HH stage unknown. The antibodies show clear nuclear staining, as expected. Scalebar at 20µm.

## 5 Discussion

The aim of this project was to investigate the influence of two PAX7 splice variants on the canonical Wnt signaling in the dorsal midbrain of chicken embryos. Firstly, it was possible to confirm, that in vivo, PAX7 and its transcription promoting activity is required for canonical Wnt signaling in the dorsal midbrain at HH stage 17. Secondly, the investigation of the effects of expression modifications of the two PAX7 splice variants on gene expression on an RNA level, did not give more insight into the different effects of the splice variants. However, these experiments showed that PAX7 expression is required for canonical Wnt signaling in the dorsal midbrain at HH stage 17, thus confirming the previous in vivo findings on an RNA level. The testing of the effects of PAX7 expression modifying transfections on a protein level with Western blot was unsuccessful, because of difficulties in protein isolation.

Taken together, it seems likely that PAX7 expression interacts with canonical Wnt signaling. Further experiments are required, to identify potential differences in the activities of the two PAX7 transactivation domain splice variants.

### 5.1 Impact of PAX7 Targeting Transfections in Vivo

#### 5.1.1 PAX7 is Required for Canonical Wnt Signaling in Vivo

Previous findings of Martin Zeeb (unpublished) could be confirmed. He had shown, using the same in vivo reporter gene assay, that the knock-down of PAX7 using siRNA reduced canonical Wnt signaling.

Expression of PAX7/ENGRAILED fusion construct (n=26) showed a reduction of canonical Wnt signaling comparable to the PAX7 knock-down (n=9). This indicates that the pro-transcriptional activity of PAX7 is essential for normal canonical Wnt signaling in the dorsal midbrain around HH stage 17.

No significant changes in canonical Wnt signaling could be observed, when over-expressing PAX7 splice variants (short PAX7 SV n=6, long PAX7 SV n=10) or PAX3 (n=5) in the dorsal midbrain. Since, the TOP-dGFP reporter can only detect whether canonical Wnt signaling is active, but not the strength of the activity. As canonical Wnt signaling is normally active in the dorsal midbrain, these findings

were not surprising. Interesting are the few examples in which ventral midbrain was electroporated with the short PAX7 splice variant. Here induction of canonical Wnt signaling was observable. Thus, a study in which the two PAX7 splice variants get ectopically expressed in ventral midbrain might be able to give some more insights into differences between the splice variants. These results confirm that PAX7 is required for normal canonical Wnt signaling in the dorsal midbrain.

In some embryos the hindbrain was transfected too. Like in midbrain, both the knock-down of PAX7 expression (n=6) as well as the repression of PAX7 target genes using the PAX7/ENGRAILED fusion protein (n=6) resulted in a reduction in canonical Wnt signaling. An interesting finding, potentially worth investigating was that the overexpression of either PAX7 splice variant seemed to also reduce canonical Wnt signaling activity *in vivo*, but not as strong as the PAX7 knock-down or the PAX7/ENGRAILED fusion protein did. Due to the low number of replicates no statistical analysis was performed. This result hints at a potential self-regulation of PAX7 expression or regulatory differences between the mid- and hindbrain and requires further investigation.

Canonical Wnt signaling was visualized in the dorsal midbrains of 70 chicken embryos using the TOP-dGFP vector (Dorsky et al., 2002). This allowed for the detection of cells with active canonical Wnt signaling with a fluorescence microscope. To achieve reproducibility and high statistical power, images were analyzed with Fiji. Unfortunately, the software was unable to differentiate between individual cells, resulting in highly varying results and high standard deviations. This was because most embryos were imaged using a binocular microscope with low magnification. Imaging with the LSM would have allowed for higher magnifications, resolving this issue. As the LSM available at the institute was old, it required 30-40min for a single image and its lasers quickly bleached the fluorescent proteins. This led to signal degradation while imaging and prevented re-imaging. Re-imaging was often required as the brains had to be flat-mounted, which made the adjustment of microscope settings difficult, as the tissue was thicker than the usual cryosections. Boosting signals by staining the fluorescent proteins with dye-coupled anti GFP or RFP antibodies had failed previously, as each antibody stained both green and red fluorescent proteins.

As software-based image analysis was unsuccessful, the expression of fluorescent proteins had to be categorized instead by visual inspection. This potentially introduced observer bias and weakened the statistical power, as different statistical tests had to be used.

As multiple vectors (up to 5) had to be electroporated at once, this experiment was more susceptible to electroporation related issues, as discussed in chapter 5.4.

The in vivo experiments sometimes showed differences between embryos within the same group, like for example in the enPAX7 group. Here 4 of 26 embryos showed no effect from transfection, whilst the others showed reduced canonical Wnt signaling. Electroporation related issues might explain the lack of effect seen. However, it could also be the result of cyclic gene expression. Cyclic gene expression is well known in the embryonic brain, for example in HES genes. In the hope to partially mitigate this issue by comparing transfected and un-transfected sides of the same embryos, other methods for detection of canonical Wnt signaling, like for example IHC and qPCR, were explored.

### **5.1.2 The Effects of the New siPAX7 Constructs Are Comparable to Old PAX7 Knock-Down in Vivo**

The siPAX7-pSilencer1.0 construct has a few known potential off target mRNAs it could potentially bind to, that weren't known when it was conceived. Thus, new siPAX7 constructs were designed and tested. Transfections in dorsal midbrain tissue showed a reduction in size in about 50% of the embryos at HH stage 17, a result comparable to the effects caused by the old siPAX7 (Li, 2007). In the in vivo experiments, using the canonical Wnt signaling reporter system, the new siPAX7 constructs showed the expected result and reduced canonical Wnt signaling. For the impact of the new constructs on gene expression, please see chapter 5.4 and 5.5.4.

In hindsight, it would have been more elegant to have a singular vector expressing all three siRNAs (Wang et al., 2006) as well as having a vector with a "scrambled" siRNA as a negative control vector, instead of using an entirely different plasmid as control (Fakhr et al., 2016).

## **5.2 Detection of Wnt Signaling on a Protein Level**

### **5.2.1 Detection of Wnt Signaling in Cryosections**

To detect canonical Wnt signaling, as well as PAX7 and various HES proteins cryosections of transfected midbrain tissue was stained using immunohistochemistry. This allowed for the comparison of the electroporated and unelectroporated brain sides in the same embryo. It also eliminated the need for transfections with multiple plasmids and allowed for the tracking of transfected cells using GFP. The issue of fluorescent protein bleaching was also eliminated, as only GFP was present, which could be re-stained. This enabled high resolution and high magnification imaging.

Since no commercially available antibodies for detection of canonical Wnt signaling were validated in chicken tissue an antibody targeting human  $\beta$ -catenin was tested. Chicken CTNNB1 is >99.6% identical to the human and mouse orthologs, especially in the domains involved in phosphorylation.

The anti-active  $\beta$ -catenin antibody (ABC antibody) from Upstate did not just bind the active form of CTNNB1, but also the inactive form involved in the cytoskeleton and cell-cell contacts, thus not only the nucleus but also the cytoskeleton was stained. Comparing these findings with published results revealed a lack of studies using this antibody in IHC. Just like the findings in chicken, most images showed primarily cytoskeletal staining and only a few stained nuclei (Staal et al., 2002, van Noort et al., 2002). Western blot seems to be the primary application for this antibody, with many papers listed in the vendors reference (Merck).

### **5.2.2 Detection of PAX7 and Canonical Wnt Signaling Using Western Blot**

Another approach for detection of changes in protein level is Western blotting. This technique allows for separate quantification of different proteins, like PAX7 and canonical Wnt signaling through dephosphorylated CTNNB1. The impact of PAX7 expression modifying transfections on PAX7 expression and canonical Wnt signaling on a protein level has not been tested and published so far.

Taken together, the results from the Western blots could not be interpreted. The Western blots were hindered by low protein isolation and the lack of reliable balancing of loaded protein between samples.

Embryonic tissue had to be pooled to obtain the required amounts of protein. The use of phenol-chloroform precipitation allowed for the simultaneous isolation of RNA and protein, allowing for parallel qPCR and Western blotting. This simultaneous analysis of transfection impacts would have been interesting, as it might have given insights into expression regulation and signal pathway interactions on an RNA and protein level. Unfortunately, this method resulted in low yield for both RNA and protein (see chapter 5.3.1). Additionally, none of the solvents used for protein resuspension allowed for quantification using the Qubit system.

The SDS electrophoresis procedure itself also proved difficult. In the end, a XCell SureLock Mini-Cell system produced decent gels.

The Pierce Fast Western Blot, Super Signal West Femto Mouse kit worked well, even when the used secondary anti mouse antibody was substituted with a anti rabbit antibody. In combination with the DSHB and PAX7 antibody and anti non-phospho  $\beta$ -catenin antibody from abcam, passing testing for specificity signal proportionality.

Instead of reference protein expression, the fluorescent Revert 700 total protein stain was used for normalization, which performed well in testing. This normalization was important, as the total protein could not be quantified prior to electrophoresis.

Unfortunately, total protein staining revealed large differences between the transfected and control samples in 5 of 13 blots. In addition to this, less than half of the blots had PAX7 or dephosphorylated CTNNB1 within validated detection range. This boiled down to overall low protein input and made drawing conclusions about protein levels impossible.

Further testing for the anti-non-phospho  $\beta$ -catenin antibody is required. The LiCl positive control, did not show the expected increase of canonical Wnt signaling. This could be because of technical difficulties, as in the other samples. Another possible explanation is a feedback mechanism, that could downregulate canonical Wnt signaling. This would not be atypical after 6h of strong chemical

activation. (Ikeda et al., 1998, Itoh et al., 1998, Lustig et al., 2002) Another explanation could be the detection of cytoskeletal CTNNB1, just as seen in IHC, resulting in high background signal. A negative control, with inhibited canonical Wnt signaling, would be important to rule out this potential issue. High background from unelectroporated cells within the tissue might remain an issue (see chapter 5.1, 5.3 and 5.4), even if enough protein were to be isolated. Fluorescence assisted cell sorting and protein isolation from the nucleus only might be possible approaches addressing these issues.

### **5.3 Influence of PAX7 Transfections on Gene Expression on an RNA Level**

A large part of this project was to establish a reliable qPCR protocol, that includes pre- and post-analytic procedures and quality controls.

Two types of qPCR workflows were established, one for pooled brain tissue and one for midbrain tissue from single embryos.

The first was for pooled tissue. Here, an RNA isolation protocol, including RIN measurements and cDNA synthesis were established, although there is room for improvements. Primers for qPCR on the StepOne were validated and the workflow was successfully established. The second qPCR approach was for extremely low tissue input from single midbrain halves. For this, a direct isolation of cDNA from tissue was established. This cDNA was then analyzed using chip-based qPCR on the Biomark system. Here, primer efficiency testing failed. Further testing and optimizations are required, until reliable results can be obtained. The qPCR experiments were focused on gene expression changes after transfections targeting PAX7 expression, including knock-down and overexpression. The expressions of the individual PAX7 splice variants were quantified, as well as various components of the Wnt signaling pathway. Furthermore, the changes in expression of select cell cycle genes, PAX3 and several HES genes were analyzed.

### **5.3.1 RNA Isolation for qPCR**

#### **5.3.1.1 RNA from Pooled Brain Tissue**

The RNA was isolated alongside protein using phenol-chloroform precipitation, suffering from the same yield problems as described in chapter 5.2 Furthermore, despite multiple washing steps, phenolic residues skewed photometric RNA quantification. This became evident in qPCR (highly different  $C_q$ -values for reference genes between samples) and RNA quantification through capillary electrophoresis.

The RNA integrity of most samples was poor. Only 8 of 22 samples had a RIN  $>7$  under best conditions. A RIN of  $<7$  indicates RNA degradation. RNA decay is a complex process and does not affect all mRNA equally. This reduces qPCR reliability. Since RIN measurements were taken 2-3 month after the RNA had already been tested using qPCR, the RIN then might have been better. In addition to this, it was observed that low RNA input reduced RIN. With the newer samples and the samples with more RNA having good RIN, it is likely, that the RIN for the other samples was good too, at the time of qPCR testing.

#### **5.3.1.2 RNA Isolation from Single Midbrain Halves**

It has been shown that not all embryos transfected with vectors targeting PAX7 develop the expected phenotype (Li, 2007). Transfections targeting PAX7 expression showed the strongest effect on midbrain size when done at HH stage 9-11. The size change itself was best observed 2-3 days after transfection. These size changes resulted from PAX7 influencing proliferation, especially at early stages. The larger number of cells produced early, later results in a larger midbrain. However, at HH stage 17 no or only minimal size changes are observable. So, the analysis of tissue from individual embryos theoretically allows the selection of tissues with the expected expressional changes, after quantification, thus reducing background. Theoretically, it could also allow for cyclic gene expression to be addressed. On the other hand, isolating RNA/cDNA from half of a dorsal midbrain at HH stage 17, an amount of tissue invisible without a microscope, was difficult and required new isolation methodology.

All approaches using traditional RNA extraction kits yielded too low for proper quantification. Kits that directly synthesized cDNA from tissue, optimized for

between 1-10000 cells worked well, if a tissue lysis step using a pestle was included. This additional lysis step successfully reduced gDNA residues, that could have caused falsely low  $C_q$ -values for the non-exon-skipping primers, like the FZD primers.

The approach of directly synthesizing cDNA did not allow to simply measure the RIN using the QIAxcel, as only RNA can be used for RIN measurement. It also, as qPCR testing revealed, didn't allow for quantification, with up to 128-fold differences in reference gene quantity between samples photometrically containing the same amount of ssDNA. This was most likely because of remaining genomic DNA. Dye based approaches, like Qubit also cannot differentiate between ssDNA and dsDNA, according to the manufacturer's manual, so equal volumes of cDNA were simply used for all qPCR reactions.

The issue of RIN was circumvented with two primer pairs, that amplify the opposing ends of the same gene. Identical  $C_q$ -values would then correspond to a perfect RNA integrity. A fix number for an acceptable  $C_q$  difference cannot be found in the literature, but a difference of up to one cycle is described as common, even in high RIN samples. Most cDNA obtained from single midbrain tissue was well within the one cycle difference, which is associated with high quality RNA samples. The average delta between the  $C_q$ -values for the 3'- and 5'-end primers in the final chip-based qPCR run was only 0.16 cycles, with a SD of 0.30 cycles. Absolute RIN could be theoretically determined by running a series of cDNA synthesized from RNA with different known RINs alongside the samples to be tested, if exact RIN numbers were desired. However, before this another issue with the chip-based qPCR needs to be resolved, as shown in the next chapter (chapter 5.4.3) (Ho-Pun-Cheung et al., 2009, Bustin et al., 2009).

An interesting finding, of the last run of chip-based qPCR was that the 6 samples of old cDNA, that were included from the previous test runs and had been stored at  $-20^{\circ}\text{C}$  for two years had a lower RIN with a  $\Delta C_q$  of 1.63 cycles. This confirmed that cDNA degradation took place at these temperatures.

### **5.3.2 Primer Validation for qPCR**

For reliable qPCR, the validation of primers is essential. All primers used were tested for specificity and efficiency using cDNA as template. In addition, melt

curve peaks were visually inspected, and some of the qPCR products were spot checked using capillary electrophoresis for production of the intended amplicon. The first set of primers was tested and discarded, as they also amplified residue gDNA. The use of exon skipping primers and the inclusion of mechanical tissue lysis, prior to the DNaseI digest, solved this issue.

The creation of PAX7 transactivation domain splice variant and cDNA specific primers was an issue. All primers tested showed unspecific amplification for the other splice variant, when tested on plasmid DNA containing the isolated PAX7 variants. In the end, the forward primers published by Mao et al. were combined with an own, exon skipping reverse primer. These primer pairs had an at least 10000 times stronger amplification on the targeted PAX7 variant, when tested on plasmid DNA using qPCR (Mao et al., 2008).

Primer efficiency testing with dilution series for the pooled tissue experiments was successful. The primer efficiency testing for single midbrain qPCR failed. Here, primers showed efficiencies of 135-200%, with one outlier at 9000%. All primers were well outside the 90-110% required for reliable qPCR.

High primer efficiencies are uncommon. Low efficiencies, often caused by transcription inhibitors that prevent the doubling of target DNA each cycle, are far more common. Further testing, with the intermediate products from the chip qPCR workflow, revealed that the issue was the pre-amplification procedure. The pre-amplified dilution series in combination with known good primers (ES60ACTB primers, 101% efficiency) produced a primer efficiency of 139%. It has been published that pre-amplifications of cDNA for the Biomark system can introduce a bias of  $C_q$  values (Korenkova et al., 2015). Interestingly, this usually occurs when higher numbers of pre-amplification cycles (>24 cycles, compared to the 12 cycles used here) are used. To mitigate the issue of improper primer efficiency and continue the use of the Biomark system for these experiments, further investigation into the exact source of this bias is required.

### 5.3.3 qPCR from Pooled Brain Tissue

#### 5.3.3.1 Reference Gene Expression Stability

The combination of the three used reference genes proved reliable. In 11 out of 14 pooled samples the transfection did not induce reference gene expression changes. Of the three other samples, two only had one reference gene quantified. The remaining sample (HH stage 14, midbrain, sPAX7-pMES) was an outlier. In it the GAPDH expression GFP side was much higher than expected. An error of measurement was unlikely, as the standard deviation from the technical replicates was in the same range as in the other measurements. As other samples (different HH-stages or brain regions) electroporated with the same plasmid did not show this behavior, it is up for speculation whether this is a stage and region-specific effect of the overexpression of the short PAX7 splice variant or whether it was an error, for example caused by contamination.

#### 5.3.3.2 PAX7 Expression in Wildtype Midbrain Tissue

Naixin Li showed a proliferation promoting function of the short transactivation domain splice variant of PAX7, resulting in larger midbrains (Li, 2007). The long splice variant was published as the dominant splice variant in satellite cells by Mao et al. in 2008. Kiona Lim, Ulrike Kohler and Annette Richter also showed the presence of the long splice variant in the midbrain (figure 5-1). Here, at HH stages below stage 29, the short splice variant was stronger expressed than the long splice variant.

The qPCR on wildtype tissue confirmed these results. In early HH stages, the short splice variant is the predominant one in the midbrain. The qPCRs also showed that the expression of the long splice variant in the midbrain increased from stage to stage.

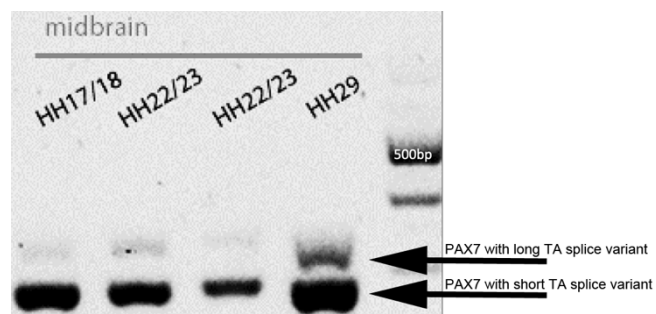


**Figure 5-1: The short PAX7 transactivation domain splice variant is the predominant one in the midbrain between HH stage 17 and 29.** Gel electrophoresis from PCR. Done by Ulrike Kohler and Kiona Lim in our lab, 2016.

These results raise the interesting question whether the long splice variant might become the predominant splice variant later in the development. Mao et al.

showed in their 2008 publication, that in muscle satellite cells, at later development stages, the long PAX7 splice variant is predominant. The youngest stages analyzed in this publication are around HH stage 24-35 (correlating to in-ovo day 7-9 in Mao et al.) and here, expression levels are only described as “almost the same everyday” (Mao et al., 2008) between the two splice variants. This does not allow for direct comparisons between their and our findings. So far, it seems like PAX7 undergoes a splice variant switch during development, that potentially coincides with a change in its transcriptional activity. In early stages, the short PAX7 splice variant promotes proliferation in the midbrain, which determines the later overall size of the midbrain. PAX7 (splice variant not known) it is also known to be expressed in distinct layers of the midbrain in later stages, where cells are differentiating and no longer proliferating (Kawakami et al., 1997a). Further investigation of the expression patterns of the different PAX7 splice variants, both in the midbrain at later developmental stages and in satellite cells or neural crest cells in earlier stages would be interesting.

### **5.3.3.3 Gene Expression Changes in Transfected Tissue**

The analysis of the impact of PAX7 expression modifications on canonical Wnt signaling with qPCR confirmed the in vivo findings. The PAX7 knock-down (2 of 6 samples) and the suppression of PAX7 pro-transcriptional activity (PAX7/ENGRAILED fusion gene, 2 of 2 samples) resulted in reduced canonical Wnt signaling and reduced CTNNB1 expression. Overexpression of the long PAX7 splice variant in the mid- and hindbrain resulted in increased expression of the short PAX7 splice variant and increase canonical Wnt signaling. Interestingly, when the long PAX7 splice variant was overexpressed, the expected increase in expression of the long PAX7 splice variant could only be observed in the midbrain, whilst in hindbrain the expression was reduced. This indicates regulatory differences in PAX7 expression between mid- and hindbrain.

Independent of stage and brain region, overexpression of the short PAX7 splice variant resulted in unchanged or mildly reduced expression levels of the individual PAX7 splice variants. Canonical Wnt signaling showed comparable minor reductions in activity.

Taken together, the expected changes in PAX7 expression could only be detected in 3 of 13 samples. This aligns with our previous unpublished findings. We could show, that PAX7 knock-downs reduced midbrain size and that overexpression of the short PAX7 splice variant increased midbrain size in vivo (Li, 2007). The effect of these PAX7 expression modification was strongest if transfections were done between HH stage 9-11. No or only minor changes in PAX7 expression could be detected at later stages on a protein level using IHC (Annette Richter, unpublished). Not being able to detect the expected changes could be the result of high background from untransfected cells/weak transfection or loss of transfected vector (see chapter 5.4). However, since changes in expression, both for the PAX7 splice variants and for AXIN2 are detectable, it is unlikely that the transfections did not cause an effect. Another possible explanation might be autoregulation. This hypothesis is supported by the differing effects seen when overexpressing the individual PAX7 splice variants. The long PAX7 splice variant was able to increase PAX7 expression, especially of the short splice variant. Overexpression of the short PAX7 splice variant on the other hand reduced PAX7 expression, also mainly of the short splice variant. It would have been expected, to be able to detect high levels of mRNA of the PAX7 splice variant that was being overexpressed. The vectors used for overexpression contained CMV enhancer and ACTB promoters, that provide strong and constant expression, that should not be affected by feedback mechanisms, as other regulatory elements were missing. Whilst epigenetic silencing of CVM promoters is possible, it has mostly been published to occur later after transfection (Brooks et al., 2004) and transient in-ovo transfections have been shown to be active for 72h (Momose et al., 1999). This either means, that the PAX7 mRNA from the vector was degraded at exceptionally high rates or that the transfection did not provide as much mRNA as expected, most likely resulting from low quantities of vector remaining. However, low quantities of vector would in turn again hint at poor transfection, as transfections should, as stated above, theoretically be active for up to 72h (Momose et al., 1999). Another possible explanation, for not being able to detect the mRNA transcribed from the vector could be poor cDNA synthesis. Poly-dT primers were used in revers transcription, so that only cDNA from mRNA was synthesized.

With the way, the pMES plasmids used for overexpression were designed, the reverse transcriptase had to first transcribe the EGFP gene and the IRIS site, before starting transcription of PAX7. This could have lowered reverse transcription efficiencies, resulting in lower detection in the qPCR. Further testing is needed to determine, whether poor transfection efficiencies, autoregulation or issues with the reverse transcription resulted in the unexpectedly low PAX7 RNA levels after overexpression of the short PAX7 splice variant. Here, it would be important to specifically detect the PAX7 mRNA produced by the transfection vector, independently from endogenous PAX7. Separate quantification could for example be achieved by using a primer pair binding in PAX7 and the IRES site or the EGFP primers. This would allow for statements on transfection efficiency and give more insight into the interactions between the endo- and exogenic PAX7.

Canonical Wnt signaling was detected using AXIN2, a known feedback gene (Lustig et al., 2002). CTNNB1 ( $\beta$ -catenin) is an essential signal transducer in canonical Wnt signaling. PAX7 is known to bind in its promoter region. This makes it a possible candidate for pathway crosstalk.

The qPCR experiments from pooled tissue confirm the *in vivo* findings of Martin Zeeb (unpublished). The pro-transcriptional activity of PAX7 seems to be required for canonical Wnt signaling, both in dorsal mid- and hindbrain. Overall, and independent from transfections, expression levels of both PAX7 splice variants correlate well with canonical Wnt signaling activity. Currently, there are no published result on PAX7 and canonical Wnt signaling interactions in the chicken midbrain. However, interactions in satellite cells have been studied. Here, PAX7 and canonical Wnt signaling seem to have a partially antagonistic role, with PAX7 promoting proliferation and WNTs blocking PAX7 in favor of cell differentiation (Hulin et al., 2016, Zhuang et al., 2014, Cui et al., 2019).

Our results differ from these publications. Satellite cells are, like the cells of the mid- and hindbrain derived from the neural plate. The different cell populations, different organisms and different stages of development could account for these differences. Some cooperative interactions of PAX7 and especially WNT3A have

been described (Pan et al., 2015). Changes in the regulatory effects caused by signaling systems during embryonic development are also not uncommon, so the interactions between PAX7 and canonical Wnt signaling might change from synergistic to antagonistic during development (Green et al., 2020).

To investigate the influence of PAX7 on cell cycle, the last gene analyzed was Cyclin-D1, encoded by CCND1. It is a well-known gene that depending on the level of expression and other co-factors either promotes proliferation or differentiation in neuronal progenitor cells. (Ratineau et al., 2002, Bienvenu et al., 2010) Expression of CCND1 did mostly correlate to PAX7 expression. This aligns with our previous results (Kira Wolff, unpublished).

For all stages, brain region and transfections – except for the PAX7 knock-down in the midbrain at HH stage 17 – only one batch of embryos was analyzed. Because of this lack of individually detected biological replicates and with the single midbrain tissue analysis failing, all findings are to be considered preliminary.

#### **5.3.3.3.1 Pooled Tissue from Dorsal Midbrain**

##### **HH Stage 17**

The dorsal midbrain at HH stage 17 was the primary stage and region of interest. Of the six samples analyzed (plus the pCAX control group), only one batch (1 of 3 batches) of PAX7 knock-downs and the overexpression of PAX7 showed the expected effects on PAX7 expression. The pCAX control showed only minor alterations in gene expression, that were used as baseline for expression changes induced by other transfections.

The PAX7 knock-down resulted in reduced expression of both PAX7 splice variants (long >> short SV), in the first batch of embryos transfected. A reduction in expression of AXIN2, CTNNB1 and CCND1 was also detected. This result supports the previous *in vivo* findings, that a PAX7 knock-down reduces canonical Wnt signaling (AXIN2). The other two batches of tissue with PAX7 knock-downs showed either no impact on PAX7 expression or even a weak increase in expression, with the expression of the other three genes tested showing minor and incoherent changes in expression.

The overexpression of the long PAX7 splice variant (1 of 1 batch) in the dorsal midbrain had the opposite effect, resulting in an increase in expression of all genes tested. This indicates that PAX7 overexpression can promote canonical Wnt signaling, a finding not observable in the *in vivo* experiments.

Overexpression of the short splice variant (1 of 1 batch) did not result in the expected increase in PAX7 expression, but mildly reduced AXIN2. As discussed previously, weak remaining effect from transfection or autoregulation might be causing the weak expression changes observed.

Expression of the PAX7/ENGRAILED fusion gene (1 of 1 batch) only showed a reduction in CTNNB1 expression. This potentially supports the hypothesis of PAX7 promoting CTNNB1 expression, whilst also antagonizing the hypothesis that PAX7 directly regulates its own transcription.

#### **HH Stage 14**

Gene expression quantification from the knock-down (1 of 1 batch) resulted in high standard deviations, most likely resulting from very low RNA input. No meaningful conclusions about expression changes could be drawn.

Interestingly, the overexpression of the short PAX7 splice variant (1 of 1 batch) resulted in the strongest reduction in PAX7 expression of all samples tested in qPCR. This would support the hypothesis of PAX7 regulating its own expression. In combination with the findings of the PAX7/ENGRAILED fusion protein not reducing PAX7 expression, this indicates an indirect feedback mechanism that regulates PAX7 expression, without PAX7 binding to its own promoter region. CTNNB1 showed a minor reduction in expression and AXIN2 expression was not affected. CCND1 expression was massively reduced (93% reduction). This reduction would fit the observed increase seen when PAX7 was knocked down (Kira Wolff). Interestingly, no other sample especially not the dorsal midbrain sample with the same electroporation, showed a comparable effect in CCND1 expression. These strong changes in expression could potentially fit in with previous findings, that the electroporations show their strongest impact on proliferation shortly after electroporation. There might also be other differences in expressional changes when comparing the effects of transfections between midbrain tissue harvested at HH stage 14 and 17, but as many expressional changes

observed were only minor and only one sample was tested in most instances, further testing is required.

#### **5.3.3.3.2 Hindbrain**

##### **HH Stage 17**

Overexpression of the long PAX7 splice variant (1 of 1 batch) increased expression of the short PAX7 splice variant, whilst expression of the long splice variant was reduced. Overexpression of the short splice variant (1 of 1 batch) mildly reduced expression of both splice variants. AXIN2 expression was increased by overexpression of the long PAX7 splice variant and reduced by the short PAX7 splice variant. The results for AXIN2 concur with the results seen in the midbrain at HH stage 17. The findings for PAX7 expression fit with the hypothesis, that especially the short PAX7 splice variant regulates its own expression.

The expression of the PAX7/ENGRAILED fusion gene (1 of 1 batch) resulted in the expression reduction of all genes tested. For the PAX7 expression regulation, the exact interactions remain unclear, but the hypothesis of the transcription promoting activities of PAX7 being required for canonical Wnt signaling are further reinforced by these results. The PAX7 knock-down (1 of 1 batch) did reduce or mildly reduce expression of all genes tested, fitting in nicely with the findings in the midbrain.

##### **HH Stage 14**

The knock-down failed to reduce PAX7 expression (1 of 1 batch) and for testing of other genes, insufficient amounts of RNA were isolated.

The overexpression of the short splice variant (1 of 1 batch) resulted in minor reductions of the expression of both PAX7 splice variants. This effect was comparable to the effects seen at HH stage 17. The expression of other genes was not altered in a relevant manner. The standard deviations were high for all genes, which was most likely the result of low RNA input, as seen in the overall high  $C_q$  values. Thus no conclusions could be made.

#### **5.3.4 Single Midbrain Tissue qPCR**

Whilst isolation of cDNA from single dorsal midbrain halves was successful, all primers failed efficiency testing. No reliable conclusions can be drawn about

potential impacts of PAX7 knock down on canonical Wnt signaling or any of the other genes tested.

Independent from this, even when the results were statistically analyzed, and even when only samples showing a reduced PAX7 expression were included, no significant changes in gene expression were observed.

From these results it remains unclear, whether there actually is no detectable change in expression caused by the PAX7 knock down or whether the primer efficiencies skewed the results too much for the changes to be detected.

The only gene showing a remotely significant change in expression ( $p=0.087$ ) was ERMIN. It is a potential off target gene of the siPAX7-pSilencer1.0 and involved in the cytoskeleton of neurons in the adult brain. Its expression in the chicken midbrain has not been described yet, but it is known to be expressed in the brain of mouse embryos until E 18 (Yue et al., 2014). This change in expression might be caused by chance ( $p=0.087 = 8.7\%$  chance), as the gene shows an increase in expression, instead of the expected decrease caused by RNA interference. It could also hint at the PAX7 knock-down inducing differentiation. However, this finding was accomplished with primers with skewed efficiencies, thus is not reliable anyways.

Three primers were excluded, as they failed successful amplification in many embryos. This is most likely explained by weak expression of their target genes at HH stage 17 in the midbrain. (Badde et al., 2005, Quinlan et al., 2009, Chapman et al., 2002)

Besides these difficulties, using volume adjusted cDNA loading worked well, with only 5% of sample being excluded for poor qPCR performance.

## **5.4 In-Ovo Electroporation**

This methodology allows for the easy introduction of one or multiple plasmids into the chicken embryo and it allows for the timing at which gene expression modifications come into effect. Furthermore, this technique allows for a wildtype control within the same embryo, as only one side receives the plasmid DNA. This reduces the impact of for example genetic or developmental differences between embryos, whilst also reducing the number of embryos needed. Expression of

fluorescent proteins allows for the tracking of transfected cells or as reporter genes. With the plasmids used for this thesis, transfections were transient, and the genomic DNA was not altered. Because of this, the experiments were only classified as S1 experiments, lowering lab safety requirements.

However, since none of the vectors used integrated into the genomic DNA and as most embryos were harvested 6 to 24h after electroporation, it was unclear how many cells were still affected by transfection. Theoretically, the number of cells/gene dose was halved with every cell division as they did not contain a eucaryotic replication origin. However, many publications showed effects on a protein level from transfection peaking 20h after electroporation and lasting for up to 72h (Momose et al., 1999, Nakamura and Funahashi, 2001). As the embryos were incubated for less than 24h at a maximum, effects from transfection should still be strong. The exact dose of vector initially received by the embryos was unknown, both from variation in electroporation efficiency and DNA concentration in the injection solution (Momose et al., 1999). The high DNA concentrations (over 1µg/µl) in the injection solution frequently precipitated, thus effectively lowering the DNA concentration. For several experiments (TOP-dGFP, all PAX7 knock-downs) multiple plasmids at once had to be electroporated. Whilst this has been shown to work (Veron et al., 2015, Itasaki et al., 1999, Huber et al., 2013, Momose et al., 1999), here the impact of the effects listed above was potentiated, as each plasmid was affected individually. This became obvious in the in vivo reporter gene experiments (chapter 4.1 and 5.1.1). Here cells only expressing the reporter gene (GFP) were observed, but the fluorescence signal for the cell being electroporated (RFP) was missing, thus not all plasmids electroporated were present. As the impact of transfection varied between embryos and batches and with several experiments not showing any effect from transfection (chapter 4.2.3.3 and 5.3.1), despite expressing the transfection reporter GFP, it is unclear how much of this can be attributed to the issue with the transfection methodology and how much is from biological effects. Vectors that can integrate into the genomic DNA are available and permanent knockouts using CRISPER-CAS have been published (Veron et al., 2015). Whilst the prolonged effects of these transfections would be interesting to study, they were not the aim of this project. The

plasmids used in this project had shown to increase and reduce midbrain size (Li, 2007) and to reduce canonical Wnt signaling (Martin Zeeb, unpublished).

## 6 Conclusion and Outlook

It was possible to confirm that the knock-down of PAX7 results in a reduction in canonical Wnt signaling activity in the chicken midbrain at HH stage 17 *in vivo*. Further it was possible to show, that the transcription promoting/enhancing capabilities of PAX7 are required for regular canonical Wnt signaling activity in the dorsal midbrain, as the repression of PAX7 transcriptional target genes also resulted in reduced canonical Wnt signaling.

To gain more insight in the interactions of the long and short PAX7 transactivation domain splice variants with canonical Wnt signaling qPCR and Western blots were performed.

Whilst the results from qPCR did partially support the *in vivo* findings, most of its results were inconclusive and the Western blots failed all together.

The primary issue with the experiments, was the acquisition of suitable RNA and protein from tissue with a sufficiently high number of transfected cells. In most qPCRs the expected modification of PAX7 gene expression could not be detected, but when PAX7 expression changes were detected, they supported the *in vivo* findings.

These preliminary findings need to be reproduced. To improve further experiments on the regulation of PAX7 splice variants, establishing PAX7 expression modifications as well as methods to quantify their activity are important. Furthermore, high transfection efficiencies are key. Stable modifications of PAX7 expression, that eliminate potential loss of transfection over time, could be tested. Tol2-transposase constructs (Sato et al., 2007) and CRISPR-CAS (Veron et al., 2015) have been published, however as these systems increase complexity it is debatable how big the activable improvements would be. Fluorescence Activated Cell Sorting (FACS) (Farley, 2013, Williams and Sauka-Spengler, 2021) or single cell RNA sequencing would be potential approaches to reduce background from untransfected cells, however both approaches are cost intensive.

The conventional qPCR, using cDNA from either single or pooled tissue was successfully established, but going forward, the combined isolation of RNA and

protein using a phenol-chloroform precipitation protocol cannot be recommended. Column-based RNA isolation proved more reliable and resulted in higher yield with lower contamination.

High throughput qPCR (Biomark system), for analysis tissue from individual embryos, requires further validation and testing, with the major problem being the amplification efficiency of the pre-amplification.

Western blots were unsuccessful due to low protein input. A different approach for protein isolation, for example an established RIPA protocol should be established. (Scharr et al., 2023) The anti  $\beta$ -catenin non-phospho(active) S45 antibody from abcam and the anti PAX7 antibody from DSHB worked well, but working positive and negative controls are required prior to further experimentation. Staining of active CTNNB1 in combination with DRAQ-5 nuclear staining in cryosections could also be retried. This would allow for the isolation of the signal from nuclear CTNNB1, the CTNNB1 that contributes to canonical Wnt signaling.

Based on my findings, the findings of Naixin Li, Annette Richter and Martin Zeeb, I propose, that with progressing developmental stages, PAX7 in the dorsal mid-brain undergoes a switch in splice variant expression. Initially the short transactivation domain splice variant of PAX7 promotes proliferation, whilst later, the long splice variant promotes differentiation by enabling canonical Wnt signaling. To test this hypothesis, and to verify the previous finding further experiments are required.

## 6.1 Zusammenfassung und Perspektiven

Es ist gelungen die vorbeschriebene Aktivitätsreduktion des kanonischen Wnt Signalwegs aufgrund eines PAX7 Knock-downs, im dorsalen Mittelhirn von Hühnerembryonen im HH Stadium 17, *in vivo* zu bestätigen. Des Weiteren ist es gelungen zu zeigen, dass die transkriptionsfördernden/-induzierenden Eigenschaften von PAX7 für eine normale Aktivität des kanonischen Wnt Signalwegs benötigt werden, da die Repression aller normalerweise von PAX7 induzierten Genen ebenfalls zu einer Reduktion der Aktivität des Wnt Signalwegs führte.

Um einen tieferen Einblick in die Interaktionen der verschiedenen, kurzen und langen PAX7 Transaktivierungsdomänenssplicevarianten zu bekommen, wurden qPCR und Western Blots durchgeführt.

Einige qPCR Ergebnisse bestätigten die Resultate der *in vivo* Versuche, jedoch war der Großteil der qPCR Ergebnisse uneindeutig und die Western Blots haben durch die Bank nicht funktioniert.

Das primäre Problem mit den qPCR und Western Blot Experimenten war die Gewinnung von ausreichenden Mengen an RNA und Protein aus Gewebe mit einer hohen Transfektionsrate. In den meisten qPCRs konnte die erwartete Modifikation der PAX7 Expression nicht nachgewiesen werden. In den Proben, in denen jedoch die erwarteten Modifikationen vorgefunden werden konnten, zeigten sich Veränderungen des kanonischen Wnt Signalwegs, welche denen der *in vivo* Experimenten entsprachen.

Es empfiehlt sich diese vorläufigen Ergebnisse zu wiederholen und zu verifizieren. Für weitere Versuche sollte der Fokus auf der Etablierung einer Transfektionsmethodik liegen, deren Effekt und Aktivität zuverlässig bestimmt werden kann. Hierbei ist insbesondere eine hohe Effizienz der Transfektionen wichtig. Stabile Transfektionen, welche den potenziellen Verlust der Transfektion über Zeit reduzieren könnten getestet werden. Tol2-transposase Konstrukte (Sato et al., 2007) und CRISPR-CAS (Veron et al., 2015) Knock-outs sind bereits publiziert worden. Hierbei kann jedoch über die Höhe des erzielbaren Verbesserungspotentials diskutiert werden, da diese Systeme die Komplexität der Versuche erhöhen. Des Weiteren könnten FACS (Fluorescence Activated Cell Sorting)

(Farley, 2013, Williams and Sauka-Spengler, 2021) oder Einzelzell RNA Sequenzierung genutzt werden, um das Hintergrundsignal von Zellen ohne Transfektion zu verringern. Beide Methoden sind jedoch kostenintensiv.

Die konventionelle qPCR auf dem StepOne Cycloer, mit cDNA von gepoolten Embryos, sowie cDNA von einzelnen Embryonen konnte erfolgreich etabliert werden. Für weitere Versuche an Gewebe von gepoolten Embryonen sollten zur RNA Isolation lieber säulchenbasierte Kits verwendet werden, da diese eine höher RNA Ausbeute zeigten, weniger gesundheitsschädliche Chemikalien verwenden. Die parallele Isolation von RNA und Proteinen zu geringen Ausbeuten und hohen Kontaminationsgraden der Proben führte.

Bei der Hochdurchsatz-qPCR auf dem Biomark System, für die Expressionsanalyse von Gewebe aus einzelnen Embryonen, sind weitere Validierungen und Test nötig, da die Primereffizienzen zu hoch sind. Das Problem hierbei liegt vermutlich in der Preamplifikation.

Die Western Blot Versuche sind durchweg gescheitert. Dies lag an zu geringen Mengen an isoliertem Protein. Eine effizientere Methode zur Proteinisolierung, welche auch die Messung der Gesamtproteinmenge vor der Elektrophorese ermöglicht, wäre von Vorteil. Beispielsweise das bereits etablierte RIPA-Protokoll wäre ein geeigneter Startpunkt für weitere Versuche. (Schar et al., 2023)

Der anti  $\beta$ -catenin non-phospho(active) S45 Antikörper von abcam, sowie der anti PAX7 Antikörper von DSHB haben insgesamt gut funktioniert. Für den  $\beta$ -catenin Antikörper wären für weitere Experimente jedoch funktionierende Positiv- und Negativkontrollen wichtig. Weitere IHC Versuche mit den anti non-phospho  $\beta$ -catenin Antikörpern in Kombination mit einer Zellkernfärbung durch DRAQ-5 auf Kryoschnitten könnten ebenfalls durchgeführt werden. Dies sollte es erlauben das tatsächliche Signal des kanonischen Wnt Signalweges vom zytoskeletalen Hintergrund zu isolieren.

Basierend auf meinen Ergebnissen sowie den Ergebnissen von Naixin Li, Anette Richter und Martin Zeeb, vermute ich, dass es während der Embryonalentwicklung im dorsalen Mittelhirn des Huhns zu einem Wechsel der Expression der

PAX7 Splicevarianten kommt. Zunächst wird die kurze Splicevariante der Transaktivierungsdomäne exprimiert, welche Proliferation fördert. Später dominiert dann die lange Splicevariante, welche über den Wnt Signalweg die Zelldifferenzierung fördert. Zur Überprüfung dieser Hypothese, sowie zur Bestätigung der bisherigen Ergebnisse sind jedoch weitere Versuche unumgänglich.

## 7 Erklärung zum Eigenanteil

Die Arbeit wurde am Institut für klinische Anatomie und Zellanalytik unter Betreuung von Prof. Dr. Stefan Liebau durchgeführt.

Die Konzeption der Studie erfolgte in Zusammenarbeit mit Dr. Andrea Wizenmann.

Die Versuche wurden von mir eigenständig durchgeführt. Die einzigen Ausnahmen hierbei stellten das Beladen und Bedienen des Biomark Cyclers sowie die Transfektionen der Embryonen dar. Letztere wurden durch Dr. Andrea Wizenmann durchgeführt. Der Biomark Cycler wurde von Sabine Conrad bedient. In einzelnen Versuchen wurden bereits vorhandene Gewebe und cDNA-Proben verwendet. Diese sind im Ergebnisteil kenntlich gemacht.

Die statistische Auswertung erfolgte eigenständig durch mich.

Zur Überprüfung von Rechtschreibung und Grammatik wurde das Microsoft Word für Mac verwendet.

Es wurden keine KI-Tools zur Erstellung dieser Arbeit genutzt.

Ich versichere, das Manuskript selbständig, unter Anleitung von Dr. Andrea Wizenmann, verfasst zu haben und keine weiteren als die von mir angegebenen Quellen verwendet zu haben.

Tübingen, den

## 8 References

- ALREFAEI, A. F., MUNSTERBERG, A. E. & WHEELER, G. N. 2020. FZD10 regulates cell proliferation and mediates Wnt1 induced neurogenesis in the developing spinal cord. *PLoS One*, 15, e0219721.
- ARCHER, T. C., JIN, J. & CASEY, E. S. 2011. Interaction of Sox1, Sox2, Sox3 and Oct4 during primary neurogenesis. *Dev Biol*, 350, 429-40.
- BADDE, A., BUMSTED-O'BRIEN, K. M. & SCHULTE, D. 2005. Chick receptor protein tyrosine phosphatase lambda/psi (cRPTPlambda/cRPTPsi) is dynamically expressed at the midbrain-hindbrain boundary and in the embryonic neural retina. *Gene Expr Patterns*, 5, 786-91.
- BAE, S., BESSHO, Y., HOJO, M. & KAGEYAMA, R. 2000. The bHLH gene Hes6, an inhibitor of Hes1, promotes neuronal differentiation. *Development*, 127, 2933-43.
- BASCH, M. L., BRONNER-FRASER, M. & GARCIA-CASTRO, M. I. 2006. Specification of the neural crest occurs during gastrulation and requires Pax7. *Nature*, 441, 218-22.
- BAYLY, R. D., NGO, M., AGLYAMOVA, G. V. & AGARWALA, S. 2007. Regulation of ventral midbrain patterning by Hedgehog signaling. *Development*, 134, 2115-24.
- BESSHO, Y., SAKATA, R., KOMATSU, S., SHIOTA, K., YAMADA, S. & KAGEYAMA, R. 2001. Dynamic expression and essential functions of Hes7 in somite segmentation. *Genes Dev*, 15, 2642-7.
- BIENVENU, F., JIRAWATNOTAI, S., ELIAS, J. E., MEYER, C. A., MIZERACKA, K., MARSON, A., FRAMPTON, G. M., COLE, M. F., ODOM, D. T., ODAJIMA, J., GENG, Y., ZAGOZDZON, A., JECROIS, M., YOUNG, R. A., LIU, X. S., CEPKO, C. L., GYGI, S. P. & SICINSKI, P. 2010. Transcriptional role of cyclin D1 in development revealed by a genetic-proteomic screen. *Nature*, 463, 374-8.
- BOETTGER, T., KNOETGEN, H., WITTLER, L. & KESSEL, M. 2001. The avian organizer. *Int J Dev Biol*, 45, 281-7.
- BRISCOE, J., SUSSEL, L., SERUP, P., HARTIGAN-O'CONNOR, D., JESSELL, T. M., RUBENSTEIN, J. L. & ERICSON, J. 1999. Homeobox gene Nkx2.2 and specification of neuronal identity by graded Sonic hedgehog signalling. *Nature*, 398, 622-7.
- BROOKS, A. R., HARKINS, R. N., WANG, P., QIAN, H. S., LIU, P. & RUBANYI, G. M. 2004. Transcriptional silencing is associated with extensive methylation of the CMV promoter following adenoviral gene delivery to muscle. *J Gene Med*, 6, 395-404.
- BUSCARLET, M., PERIN, A., LAING, A., BRICKMAN, J. M. & STIFANI, S. 2008. Inhibition of cortical neuron differentiation by Groucho/TLE1 requires interaction with WRPW, but not Eh1, repressor peptides. *J Biol Chem*, 283, 24881-8.
- BUSTIN, S. A., BENES, V., GARSON, J. A., HELLEMANS, J., HUGGETT, J., KUBISTA, M., MUELLER, R., NOLAN, T., PFAFFL, M. W., SHIPLEY, G. L., VANDESOMPELE, J. & WITTWER, C. T. 2009. The MIQE guidelines: minimum information for publication of quantitative real-time PCR experiments. *Clin Chem*, 55, 611-22.
- CATALA, M., TEILLET, M. A., DE ROBERTIS, E. M. & LE DOUARIN, M. L. 1996. A spinal cord fate map in the avian embryo: while regressing, Hensen's node lays down the notochord and floor plate thus joining the spinal cord lateral walls. *Development*, 122, 2599-610.

- CHAPMAN, S. C., SCHUBERT, F. R., SCHOENWOLF, G. C. & LUMSDEN, A. 2002. Analysis of spatial and temporal gene expression patterns in blastula and gastrula stage chick embryos. *Dev Biol*, 245, 187-99.
- CHI, N. & EPSTEIN, J. A. 2002. Getting your Pax straight: Pax proteins in development and disease. *Trends Genet*, 18, 41-7.
- CUI, S., LI, L., MUBAROKAH, S. N. & MEECH, R. 2019. Wnt/beta-catenin signaling induces the myomiRs miR-133b and miR-206 to suppress Pax7 and induce the myogenic differentiation program. *J Cell Biochem*, 120, 12740-12751.
- DADY, A., HAVIS, E., ESCRIOU, V., CATALA, M. & DUBAND, J. L. 2014. Junctional neurulation: a unique developmental program shaping a discrete region of the spinal cord highly susceptible to neural tube defects. *J Neurosci*, 34, 13208-21.
- DAVIS, R. J., D'CRUZ, C. M., LOVELL, M. A., BIEGEL, J. A. & BARR, F. G. 1994. Fusion of PAX7 to FKHR by the variant t(1;13)(p36;q14) translocation in alveolar rhabdomyosarcoma. *Cancer Res*, 54, 2869-72.
- DETRICK, R. J., DICKEY, D. & KINTNER, C. R. 1990. The effects of N-cadherin misexpression on morphogenesis in *Xenopus* embryos. *Neuron*, 4, 493-506.
- DOETZLHOFER, A., BASCH, M. L., OHYAMA, T., GESSLER, M., GROVES, A. K. & SEGIL, N. 2009. Hey2 regulation by FGF provides a Notch-independent mechanism for maintaining pillar cell fate in the organ of Corti. *Dev Cell*, 16, 58-69.
- DORSKY, R. I., SHELDAHL, L. C. & MOON, R. T. 2002. A transgenic Lef1/beta-catenin-dependent reporter is expressed in spatially restricted domains throughout zebrafish development. *Dev Biol*, 241, 229-37.
- DU, S., LAWRENCE, E. J., STRZELECKI, D., RAJPUT, P., XIA, S. J., GOTTESMAN, D. M. & BARR, F. G. 2005. Co-expression of alternatively spliced forms of PAX3, PAX7, PAX3-FKHR and PAX7-FKHR with distinct DNA binding and transactivation properties in rhabdomyosarcoma. *Int J Cancer*, 115, 85-92.
- EBERHARD, D., JIMENEZ, G., HEAVEY, B. & BUSSLINGER, M. 2000. Transcriptional repression by Pax5 (BSAP) through interaction with corepressors of the Groucho family. *EMBO J*, 19, 2292-303.
- ENZOKLOP. 2014. *Schematic drawing of the PCR cycle* [Online]. Wikimedia Commons. Available: [https://upload.wikimedia.org/wikipedia/commons/thumb/9/96/Polymerase\\_chain\\_reaction.svg/1600px-Polymerase\\_chain\\_reaction.svg.png?20201112132015](https://upload.wikimedia.org/wikipedia/commons/thumb/9/96/Polymerase_chain_reaction.svg/1600px-Polymerase_chain_reaction.svg.png?20201112132015) [Accessed 03/23 2024].
- FAKHR, E., ZARE, F. & TEIMOORI-TOOLABI, L. 2016. Precise and efficient siRNA design: a key point in competent gene silencing. *Cancer Gene Ther*, 23, 73-82.
- FARLEY, E. K. 2013. Gene transfer in developing chick embryos: in ovo electroporation. *Methods Mol Biol*, 1018, 141-50.
- FUJIMORI, T., MIYATANI, S. & TAKEICHI, M. 1990. Ectopic expression of N-cadherin perturbs histogenesis in *Xenopus* embryos. *Development*, 110, 97-104.
- GILBERT, M. J. B. A. S. F. 2020. *Developmental Biology* New York, Oxford University Press.
- GOULDING, M. D., CHALEPAKIS, G., DEUTSCH, U., ERSELIUS, J. R. & GRUSS, P. 1991. Pax-3, a novel murine DNA binding protein expressed during early neurogenesis. *Embo J*, 10, 1135-47.

- GREEN, D. G., WHITENER, A. E., MOHANTY, S., MISTRETTA, B., GUNARATNE, P., YEH, A. T. & LEKVEN, A. C. 2020. Wnt signaling regulates neural plate patterning in distinct temporal phases with dynamic transcriptional outputs. *Dev Biol*, 462, 152-164.
- HALEVY, O., PIESTUN, Y., ALLOUH, M. Z., ROSSER, B. W., RINKEVICH, Y., RESHEF, R., ROZENBOIM, I., WLEKLINSKI-LEE, M. & YABLONKA-REUVENI, Z. 2004. Pattern of Pax7 expression during myogenesis in the posthatch chicken establishes a model for satellite cell differentiation and renewal. *Dev Dyn*, 231, 489-502.
- HAMBURGER, V. & HAMILTON, H. L. 1951. A series of normal stages in the development of the chick embryo. *J Morphol*, 88, 49-92.
- HANKS, M., WURST, W., ANSON-CARTWRIGHT, L., AUERBACH, A. B. & JOYNER, A. L. 1995. Rescue of the En-1 mutant phenotype by replacement of En-1 with En-2 [see comments]. *Science*, 269, 679-82.
- HAYAT, R., MANZOOR, M. & HUSSAIN, A. 2022. Wnt signaling pathway: A comprehensive review. *Cell Biol Int*, 46, 863-877.
- HIRABAYASHI, Y., ITOH, Y., TABATA, H., NAKAJIMA, K., AKIYAMA, T., MASUYAMA, N. & GOTOH, Y. 2004. The Wnt/beta-catenin pathway directs neuronal differentiation of cortical neural precursor cells. *Development*, 131, 2791-801.
- HO-PUN-CHEUNG, A., BASCOUL-MOLLEVI, C., ASSEMAT, E., BOISSIERE-MICHOT, F., BIBEAU, F., CELLIER, D., YCHOU, M. & LOPEZ-CRAPEZ, E. 2009. Reverse transcription-quantitative polymerase chain reaction: description of a RIN-based algorithm for accurate data normalization. *BMC Mol Biol*, 10, 31.
- HUBER, C., PREM ANAND, A. A., MAUZ, M., KUNSTLE, P., HUPP, W., HIRT, B. & WIZENMANN, A. 2013. In ovo Expression of MicroRNA in Ventral Chick Midbrain. *J Vis Exp*.
- HUELSKEN, J. & BEHRENS, J. 2002. The Wnt signalling pathway. *J Cell Sci*, 115, 3977-8.
- HULIN, J. A., NGUYEN, T. D., CUI, S., MARRI, S., YU, R. T., DOWNES, M., EVANS, R. M., MAKARENKOVA, H. & MEECH, R. 2016. Barx2 and Pax7 Regulate Axin2 Expression in Myoblasts by Interaction with beta-Catenin and Chromatin Remodelling. *Stem Cells*, 34, 2169-82.
- IKEDA, S., KISHIDA, S., YAMAMOTO, H., MURAI, H., KOYAMA, S. & KIKUCHI, A. 1998. Axin, a negative regulator of the Wnt signaling pathway, forms a complex with GSK-3beta and beta-catenin and promotes GSK-3beta-dependent phosphorylation of beta-catenin. *EMBO J*, 17, 1371-84.
- INESTROSA, N. C. & VARELA-NALLAR, L. 2015. Wnt signalling in neuronal differentiation and development. *Cell Tissue Res*, 359, 215-23.
- ITASAKI, N., BEL-VIALAR, S. & KRUMLAUF, R. 1999. 'Shocking' developments in chick embryology: electroporation and in ovo gene expression. *Nat Cell Biol*, 1, E203-7.
- ITOH, K., KRUPNIK, V. E. & SOKOL, S. Y. 1998. Axis determination in *Xenopus* involves biochemical interactions of axin, glycogen synthase kinase 3 and beta-catenin. *Curr Biol*, 8, 591-4.
- JHO, E. H., ZHANG, T., DOMON, C., JOO, C. K., FREUND, J. N. & COSTANTINI, F. 2002. Wnt/beta-catenin/Tcf signaling induces the transcription of Axin2, a negative regulator of the signaling pathway. *Mol Cell Biol*, 22, 1172-83.

- KAGEYAMA, R., OHTSUKA, T. & KOBAYASHI, T. 2008. Roles of Hes genes in neural development. *Dev Growth Differ*, 50 Suppl 1, S97-103.
- KATANAEV, V. L. 2010. The Wnt/Frizzled GPCR signaling pathway. *Biochemistry (Mosc)*, 75, 1428-34.
- KAWAKAMI, A., KIMURA-KAWAKAMI, M., NOMURA, T. & FUJISAWA, H. 1997a. Distributions of PAX6 and PAX7 proteins suggest their involvement in both early and late phases of chick brain development. *Mech Dev*, 66, 119-30.
- KAWAKAMI, A., KIMURA-KAWAKAMI, M., NOMURA, T. & FUJISAWA, H. 1997b. Distributions of PAX6 and PAX7 proteins suggest their involvement in both early and late phases of chick brain development. *Mech Dev*, 66, 119-30.
- KIECKER, C. & NIEHRS, C. 2001. A morphogen gradient of Wnt/beta-catenin signalling regulates anteroposterior neural patterning in *Xenopus*. *Development*, 128, 4189-201.
- KOBAYASHI, T. & KAGEYAMA, R. 2014. Expression dynamics and functions of Hes factors in development and diseases. *Curr Top Dev Biol*, 110, 263-83.
- KORENKOVA, V., SCOTT, J., NOVOSADOVA, V., JINDRICOVA, M., LANGEROVA, L., SVEC, D., SIDOVA, M. & SJOBACK, R. 2015. Pre-amplification in the context of high-throughput qPCR gene expression experiment. *BMC Mol Biol*, 16, 5.
- KU, Y. C., RENAUD, N. A., VEILE, R. A., HELMS, C., VOELKER, C. C., WARCHOL, M. E. & LOVETT, M. 2014. The transcriptome of utricle hair cell regeneration in the avian inner ear. *J Neurosci*, 34, 3523-35.
- KUPHAL, S. & BOSSERHOFF, A. K. 2012. E-cadherin cell-cell communication in melanogenesis and during development of malignant melanoma. *Arch Biochem Biophys*, 524, 43-7.
- LI, N. 2007. *Dorso-ventral Differentiation and Specification of Mesencephalon in Early Chick Embryos*. Julius-Maximilians-Universität Würzburg.
- LI, N., HORNBRUCH, A., KLAFKE, R., KATZENBERGER, B. & WIZENMANN, A. 2005. Specification of dorsoventral polarity in the embryonic chick mesencephalon and its presumptive role in midbrain morphogenesis. *Dev Dyn*, 233, 907-20.
- LIEM, K. F., JR., JESSELL, T. M. & BRISCOE, J. 2000. Regulation of the neural patterning activity of sonic hedgehog by secreted BMP inhibitors expressed by notochord and somites. *Development*, 127, 4855-66.
- LU, W., YAMAMOTO, V., ORTEGA, B. & BALTIMORE, D. 2004. Mammalian ryk is a wnt coreceptor required for stimulation of neurite outgrowth. *Cell*, 119, 97-108.
- LUMSDEN, A. 2004. Segmentation and compartmentation in the early avian hindbrain. *Mech Dev*, 121, 1081-8.
- LUMSDEN, A. & KEYNES, R. 1989. Segmental patterns of neuronal development in the chick hindbrain. *Nature*, 337, 424-428.
- LUMSDEN, A. & KRUMLAUF, R. 1996. Patterning the vertebrate neuroaxis. *Science*, 274, 1109-1115.
- LUSTIG, B., JERCHOW, B., SACHS, M., WEILER, S., PIETSCH, T., KARSTEN, U., VAN DE WETERING, M., CLEVERS, H., SCHLAG, P. M., BIRCHMEIER, W. & BEHRENS, J. 2002. Negative feedback loop of Wnt signaling through upregulation of conductin/axin2 in colorectal and liver tumors. *Mol Cell Biol*, 22, 1184-93.

- MANSOURI, A., STOYKOVA, A., TORRES, M. & GRUSS, P. 1996. Dysgenesis of cephalic neural crest derivatives in Pax7<sup>-/-</sup> mutant mice. *Development*, 122, 831-8.
- MAO, C., HU, X. & LI, N. 2008. Identification and expression profile of a novel alternative splicing of Pax7 in chick skeletal muscle. *Poult Sci*, 87, 1919-25.
- MARSHALL, H., NONCHEV, S., SHAM, M. H., MUCHAMORE, I., LUMSDEN, A. & KRUMLAUF, R. 1992. Retinoic acid alters hindbrain *Hox* code and induces transformation of rhombomeres 2/3 into a 4/5 identity. *Nature*, 360, 737-741.
- MARTINEZ, S., WASSEF, M. & ALVARADO-MALLART, R. M. 1991. Induction of a mesencephalic phenotype in the 2-day-old chick prosencephalon is preceded by the early expression of the homeobox gene *en*. *Neuron*, 6, 971-81.
- MARTINEZ-LOPEZ, J. E., MORENO-BRAVO, J. A., MADRIGAL, M. P., MARTINEZ, S. & PUELLES, E. 2015. Mesencephalic basolateral domain specification is dependent on Sonic Hedgehog. *Front Neuroanat*, 9, 12.
- MAYRAN, A., PELLETIER, A. & DROUIN, J. 2015. Pax factors in transcription and epigenetic remodelling. *Semin Cell Dev Biol*, 44, 135-44.
- MERCK. *Anti-Active-β-Catenin (Anti-ABC) Antibody, clone 8E7* [Online]. Available: [https://www.merckmillipore.com/DE/de/product/Anti-Active-Catenin-Anti-ABC-Antibody-clone-8E7,MM\\_NF-05-665?ReferrerURL=https%3A%2F%2Fwww.google.com%2F#documentation](https://www.merckmillipore.com/DE/de/product/Anti-Active-Catenin-Anti-ABC-Antibody-clone-8E7,MM_NF-05-665?ReferrerURL=https%3A%2F%2Fwww.google.com%2F#documentation) [Accessed 02/16 2025].
- MÉSZÁROS, É. 2022. *How does qPCR work: SYBR® Green vs TaqMan®* [Online]. Integra. Available: <https://www.integra-biosciences.com/global/en/blog/article/how-does-qpcr-work-sybr-green-vs-taqman> [Accessed 02/21 2025].
- MEY, J. & THANOS, S. 2000. Development of the visual system of the chick. I. Cell differentiation and histogenesis. *Brain Res Brain Res Rev*, 32, 343-79.
- MOMOSE, T., TONEGAWA, A., TAKEUCHI, J., OGAWA, H., UMESONO, K. & YASUDA, K. 1999. Efficient targeting of gene expression in chick embryos by microelectroporation. *Dev Growth Differ*, 41, 335-44.
- MONTCOUQUIOL, M., CRENSHAW, E. B., 3RD & KELLEY, M. W. 2006. Noncanonical Wnt signaling and neural polarity. *Annu Rev Neurosci*, 29, 363-86.
- MORENO-BRAVO, J. A., MARTINEZ-LOPEZ, J. E. & PUELLES, E. 2012. Mesencephalic neuronal populations: new insights on the ventral differentiation programs. *Histol Histopathol*, 27, 1529-38.
- MUTCH, C. A., SCHULTE, J. D., OLSON, E. & CHENN, A. 2010. Beta-catenin signaling negatively regulates intermediate progenitor population numbers in the developing cortex. *PLoS One*, 5, e12376.
- NAKAMURA, H. & FUNAHASHI, J. 2001. Introduction of DNA into chick embryos by in ovo electroporation. *Methods*, 24, 43-8.
- NEW, D. A. 1959. The adhesive properties and expansion of the chick blastoderm. *J Embryol Exp Morphol*, 7, 146-64.
- NIWA, Y., MASAMIZU, Y., LIU, T., NAKAYAMA, R., DENG, C. X. & KAGEYAMA, R. 2007. The initiation and propagation of Hes7 oscillation are cooperatively regulated by Fgf and notch signaling in the somite segmentation clock. *Dev Cell*, 13, 298-304.

- OHTSUKA, T., ISHIBASHI, M., GRADWOHL, G., NAKANISHI, S., GUILLEMOT, F. & KAGEYAMA, R. 1999. Hes1 and Hes5 as notch effectors in mammalian neuronal differentiation. *EMBO J*, 18, 2196-207.
- OTTO, A., SCHMIDT, C. & PATEL, K. 2006. Pax3 and Pax7 expression and regulation in the avian embryo. *Anat Embryol (Berl)*, 211, 293-310.
- PAN, Y. C., WANG, X. W., TENG, H. F., WU, Y. J., CHANG, H. C. & CHEN, S. L. 2015. Wnt3a signal pathways activate MyoD expression by targeting cis-elements inside and outside its distal enhancer. *Biosci Rep*, 35.
- PLA, P. & MONSORO-BURQ, A. H. 2018. The neural border: Induction, specification and maturation of the territory that generates neural crest cells. *Dev Biol*, 444 Suppl 1, S36-S46.
- QUINLAN, R., GRAF, M., MASON, I., LUMSDEN, A. & KIECKER, C. 2009. Complex and dynamic patterns of Wnt pathway gene expression in the developing chick forebrain. *Neural Dev*, 4, 35.
- R. KAGEYAMA, J. H., AND T. OHTSUKA 2006. *Transcription Factors*, Weinheim, WILEY-VCH Verlag GmbH & Co. KGaA.
- RATINEAU, C., PETRY, M. W., MUTOH, H. & LEITER, A. B. 2002. Cyclin D1 represses the basic helix-loop-helix transcription factor, BETA2/NeuroD. *J Biol Chem*, 277, 8847-53.
- RAYA, A. & IZPISUA BELMONTE, J. C. 2004. Unveiling the establishment of left-right asymmetry in the chick embryo. *Mech Dev*, 121, 1043-54.
- SATO, Y., KASAI, T., NAKAGAWA, S., TANABE, K., WATANABE, T., KAWAKAMI, K. & TAKAHASHI, Y. 2007. Stable integration and conditional expression of electroporated transgenes in chicken embryos. *Dev Biol*, 305, 616-24.
- SCHARR, M., SCHERER, S., HIRT, B. & NECKEL, P. H. 2023. Dickkopf1 induces enteric neurogenesis and gliogenesis in vitro if apoptosis is evaded. *Commun Biol*, 6, 808.
- SCHOENWOLF, G. C. & DELONGO, J. 1980. Ultrastructure of secondary neurulation in the chick embryo. *Am J Anat*, 158, 43-63.
- SCHOENWOLF, G. C. & SMITH, J. L. 1990. Mechanisms of neurulation: traditional viewpoint and recent advances. 109, 243-270.
- SCHULE, S., STEIDL, S., PANITZ, S., COULIBALY, C., KALINKE, U., CICHUTEK, K. & SCHWEIZER, M. 2006. Selective gene transfer to T lymphocytes using coreceptor-specific [MLV(HIV)] pseudotype vectors in a transgenic mouse model. *Virology*, 351, 237-47.
- SHAW, T., BARR, F. G. & UREN, A. 2024. The PAX Genes: Roles in Development, Cancer, and Other Diseases. *Cancers (Basel)*, 16.
- SHAWLOT, W. & BEHRINGER, R. R. 1995. Requirement for LIM-1 in head-organizer function. *Nature*, 374, 425-430.
- SHENG, G. 2014. Day-1 chick development. *Dev Dyn*, 243, 357-67.
- SIMEONE, A., AVANTAGGIATO, V., MORONI, M. C., MAVILIO, F., ARRA, C., COTELLI, F., NIGRO, V. & ACAMPORA, D. 1995. Retinoic acid induces stage-specific antero-posterior transformation of rostral central nervous system. *Mech Dev*, 51, 83-98.
- SPRATT, N. T., JR. 1963. Role of the substratum, supracellular continuity, and differential growth in morphogenetic cell movements. *Dev Biol*, 6, 51-63.

- STAAL, F. J., VAN NOORT, M., STROUS, G. J. & CLEVERS, H. C. 2002. Wnt signals are transmitted through N-terminally dephosphorylated beta-catenin. *EMBO Rep*, 3, 63-8.
- TATEYA, T., IMAYOSHI, I., TATEYA, I., ITO, J. & KAGEYAMA, R. 2011. Cooperative functions of Hes/Hey genes in auditory hair cell and supporting cell development. *Dev Biol*, 352, 329-40.
- VAN NOORT, M., MEELDIJK, J., VAN DER ZEE, R., DESTREE, O. & CLEVERS, H. 2002. Wnt signaling controls the phosphorylation status of beta-catenin. *J Biol Chem*, 277, 17901-5.
- VERON, N., QU, Z., KIPEN, P. A., HIRST, C. E. & MARCELLE, C. 2015. CRISPR mediated somatic cell genome engineering in the chicken. *Dev Biol*, 407, 68-74.
- WALTHER, C., GUENET, J. L., SIMON, D., DEUTSCH, U., JOSTES, B., GOULDING, M. D., PLACHOV, D., BALLING, R. & GRUSS, P. 1991. Pax: a murine multigene family of paired box-containing genes. *Genomics*, 11, 424-34.
- WANG, S., SHI, Z., LIU, W., JULES, J. & FENG, X. 2006. Development and validation of vectors containing multiple siRNA expression cassettes for maximizing the efficiency of gene silencing. *BMC Biotechnol*, 6, 50.
- WEN, S., ZHU, H., LU, W., MITCHELL, L. E., SHAW, G. M., LAMMER, E. J. & FINNELL, R. H. 2010. Planar cell polarity pathway genes and risk for spina bifida. *Am J Med Genet A*, 152A, 299-304.
- WEN, Y., BI, P., LIU, W., ASAKURA, A., KELLER, C. & KUANG, S. 2012. Constitutive Notch activation upregulates Pax7 and promotes the self-renewal of skeletal muscle satellite cells. *Mol Cell Biol*, 32, 2300-11.
- WILLIAMS, R. M. & SAUKA-SPENGLER, T. 2021. Dissociation of chick embryonic tissue for FACS and preparation of isolated cells for genome-wide downstream assays. *STAR Protoc*, 2, 100414.
- WOLPERT, L. 1998. *Principles of Development*, London, Current Biology.
- YOSHIURA, S., OHTSUKA, T., TAKENAKA, Y., NAGAHARA, H., YOSHIKAWA, K. & KAGEYAMA, R. 2007. Ultradian oscillations of Stat, Smad, and Hes1 expression in response to serum. *Proc Natl Acad Sci U S A*, 104, 11292-7.
- YUE, F., CHENG, Y., BRESCHI, A., VIERSTRA, J., WU, W., RYBA, T., SANDSTROM, R., MA, Z., DAVIS, C., POPE, B. D., SHEN, Y., PERVOUCHINE, D. D., DJEBALI, S., THURMAN, R. E., KAUL, R., RYNES, E., KIRILUSHA, A., MARINOV, G. K., WILLIAMS, B. A., TROUT, D., AMRHEIN, H., FISHER-AYLOR, K., ANTOSHECHKIN, I., DESALVO, G., SEE, L. H., FASTUCA, M., DRENKOW, J., ZALESKI, C., DOBIN, A., PRIETO, P., LAGARDE, J., BUSSOTTI, G., TANZER, A., DENAS, O., LI, K., BENDER, M. A., ZHANG, M., BYRON, R., GROUDINE, M. T., MCCLEARY, D., PHAM, L., YE, Z., KUANG, S., EDSALL, L., WU, Y. C., RASMUSSEN, M. D., BANSAL, M. S., KELLIS, M., KELLER, C. A., MORRISSEY, C. S., MISHRA, T., JAIN, D., DOGAN, N., HARRIS, R. S., CAYTING, P., KAWLI, T., BOYLE, A. P., EUSKIRCHEN, G., KUNDAJE, A., LIN, S., LIN, Y., JANSEN, C., MALLADI, V. S., CLINE, M. S., ERICKSON, D. T., KIRKUP, V. M., LEARNED, K., SLOAN, C. A., ROSENBLOOM, K. R., LACERDA DE SOUSA, B., BEAL, K., PIGNATELLI, M., FLICEK, P., LIAN, J., KAHVECI, T., LEE, D., KENT, W. J., RAMALHO SANTOS, M., HERRERO, J., NOTREDAME, C., JOHNSON, A., VONG, S., LEE, K., BATES, D., NERI, F., DIEGEL, M., CANFIELD, T., SABO, P. J., WILKEN, M. S., REH, T. A., GISTE, E.,

- SHAFER, A., KUTYAVIN, T., HAUGEN, E., DUNN, D., REYNOLDS, A. P., NEPH, S., HUMBERT, R., HANSEN, R. S., DE BRUIJN, M., et al. 2014. A comparative encyclopedia of DNA elements in the mouse genome. *Nature*, 515, 355-64.
- ZHU, X. J., YUAN, X., WANG, M., FANG, Y., LIU, Y., ZHANG, X., YANG, X., LI, Y., LI, J., LI, F., DAI, Z. M., QIU, M., ZHANG, Z. & ZHANG, Z. 2017. A Wnt/Notch/Pax7 signaling network supports tissue integrity in tongue development. *J Biol Chem*, 292, 9409-9419.
- ZHUANG, L., HULIN, J. A., GROMOVA, A., TRAN NGUYEN, T. D., YU, R. T., LIDDLE, C., DOWNES, M., EVANS, R. M., MAKARENKOVA, H. P. & MEECH, R. 2014. Barx2 and Pax7 have antagonistic functions in regulation of wnt signaling and satellite cell differentiation. *Stem Cells*, 32, 1661-73.
- ZIMAN, M. R. & KAY, P. H. 1998. Differential expression of four alternate Pax7 paired box transcripts is influenced by organ- and strain-specific factors in adult mice. *Gene*, 217, 77-81.
- ZIMMERMAN, L. B., DE JESUS-ESCOBAR, J. M. & HARLAND, R. M. 1996. The Spemann organizer signal noggin binds and inactivates bone morphogenetic protein 4. *Cell*, 86, 599-606.

## 9 Appendix

### 9.1 Canonical Wnt Signaling in Vivo

The manual categorizations of canonical Wnt signaling were statistically analyzed using Mann-Whitney tests with SPSS.

#### 9.1.1 PAX7 Knock-Down

Ranks				
	electroporation	N	Mean Rank	Sum of Ranks
effect	WT	14	8.39	117.50
	siPAX7-pSilencer1.0	9	17.61	158.50
	Total	23		

Table 9-1: Ranks from Mann-Whitney test for canonical Wnt signaling of in vivo PAX7 knock-down experiments.

Test Statistics	
	effect
Mann-Whitney U	12.500
Wilcoxon W	117.500
Z	-3.442
Asymp. Sig. (2-tailed)	<.001
Exact Sig. [2*(1-tailed Sig.)]	<.001

Table 9-2: Results of Mann-Whitney test show significant reduction of canonical Wnt signaling, when PAX7 is knocked-down.

#### 9.1.2 enPAX7

Ranks				
	electroporation	N	Mean Rank	Sum of Ranks
effect	WT	14	11.82	165.50
	enPAX7-pMIW	26	25.17	654.50
	Total	40		

Table 9-3: Ranks from Mann-Whitney test for canonical Wnt signaling of in vivo experiments when PAX7 pro-transcriptional activity is suppressed.

Test Statistics	
	effect
Mann-Whitney U	60.500
Wilcoxon W	165.500
Z	-3.654
Asymp. Sig. (2-tailed)	<.001
Exact Sig. [2*(1-tailed Sig.)]	<.001

Table 9-4: Results of Mann-Whitney test show significant reduction of canonical Wnt signaling, when the pro-transcriptional activity of PAX7 is blocked.

### 9.1.3 Overexpression Short PAX7 SV

Ranks				
	electroporation	N	Mean Rank	Sum of Ranks
effect	WT	14	10.57	148.00
	sPAX7-pMES-ΔGFP	6	10.33	62.00
	Total	20		

Table 9-5: Ranks from Mann-Whitney test for canonical Wnt signaling of in vivo experiments with the overexpressed short PAX7 splice variant.

Test Statistics	
	effect
Mann-Whitney U	41.000
Wilcoxon W	62.000
Z	-.100
Asymp. Sig. (2-tailed)	.921
Exact Sig. [2*(1-tailed Sig.)]	.968 <sup>b</sup>

Table 9-6: Results of Mann-Whitney test show no significant change of canonical Wnt signaling, when the short PAX7 splice variant is overexpressed.

### 9.1.4 Overexpression Long PAX7 SV

Ranks				
	electroporation	N	Mean Rank	Sum of Ranks
effect	WT	14	12.29	172.00
	IPAX7-pMES-ΔGFP	10	12.80	128.00
	Total	24		

Table 9-7: Ranks from Mann-Whitney test for canonical Wnt signaling of in vivo experiments with the overexpressed long PAX7 splice variant.

Test Statistics	
	effect
Mann-Whitney U	67.000
Wilcoxon W	172.000
Z	-.209
Asymp. Sig. (2-tailed)	.834
Exact Sig. [2*(1-tailed Sig.)]	.886

Table 9-8: Results of Mann-Whitney test show no significant change of canonical Wnt signaling, when the long PAX7 splice variant is overexpressed.

### 9.1.5 Overexpression PAX3

Ranks				
	electroporation	N	Mean Rank	Sum of Ranks
effect	WT	14	9.89	138.50
	PAX3-pMIW	5	10.30	51.50
	Total	19		

Table 9-9: Ranks from Mann-Whitney test for canonical Wnt signaling of in vivo experiments with overexpressed PAX3.

Test Statistics	
	effect
Mann-Whitney U	33.500
Wilcoxon W	138.500
Z	-.166
Asymp. Sig. (2-tailed)	.868
Exact Sig. [2*(1-tailed Sig.)]	.893

Table 9-10: Results of Mann-Whitney test show no significant change of canonical Wnt signaling, when the PAX3 is overexpressed.

## 9.2 Detailed qPCR Results

### 9.2.1 qPCR from Pooled Brain Tissue

In the following, tables containing both averaged  $C_q$ -values or  $\Delta\Delta C_q$ -values for the individual genes and samples can be found.

#### 9.2.1.1 PAX7 Expression

Stage and Region	Treatment	n	Side	P9/ES60PAX7-R		P7/ES60PAX7-R	
				$C_q$	SD	$C_q$	SD
HH stage 17 Midbrain	3x siPAX7-pSilencer1.0; run 1	8	GFP side	23.84	0.054	20.73	0.017
			control side	23.98	0.217	21.30	0.572
	3x siPAX7-pSilencer1.0; run 2	15	GFP side	17.67	0.353	17.33	0.171
			control side	18.22	0.263	17.81	0.085
	siPAX7-pSilencer1.0	13	GFP side	25.45	0.066	14.68	0.162
			control side	24.91	0.012	13.73	0.091
	sPAX7-pMES	15	GFP side	25.91	0.008	15.53	0.128
			control side	25.68	0.056	15.19	0.028
	IPAX7-pMES	16	GFP side	24.94	0.031	23.88	0.035
			control side	25.97	0.022	24.01	0.026
	enPAX7-pMIW	14	GFP side	24.57	0.010	21.58	0.030
			control side	25.94	0.013	22.94	0.014
	pCAX	13	GFP side	24.93	0.052	21.90	0.041
			control side	24.93	0.040	21.85	0.040
HH stage 14 Midbrain	siPAX7-pSilencer1.0	11	GFP side	26.32	0.020	22.22	0.048
			control side	26.67	0.279	21.24	0.605
	sPAX7-pMES	17	GFP side	27.94	0.145	23.92	0.016
			control side	22.63	0.099	20.75	0.043
HH stage 17 Hind-brain	siPAX7-pSilencer1.0	17	GFP side	27.75	0.175	23.26	0.081
			control side	29.67	0.106	24.89	0.023
	sPAX7-pMES	11	GFP side	27.94	0.145	23.92	0.016
			control side	22.63	0.099	20.75	0.043
	IPAX7-pMES	12	GFP side	25.79	0.040	23.94	0.013
			control side	24.24	0.024	24.24	0.031
	enPAX7-pMIW	11	GFP side	30.36	0.089	25.39	0.054
			control side	28.93	0.025	24.06	0.062

HH stage 14 Hind-brain	sPAX7-pMES	12	GFP side	29.67	0.243	25.92	0.004
			control side	28.91	0.045	24.92	0.048

Table 9-11:  $C_q$  values of PAX7 splice variants from pooled tissue qPCR. Mean and standard deviation (SD) of technical replicates from  $C_q$  values obtained. The P9/ES60PAX7-R primer pair detects the long, the P7/ES60PAX7-R primer pair detects the short splice variant of the PAX7 transactivation domain. The side electroporated is labeled as GFP side, the unelectroporated wildtype side is labeled control side. (n=number of embryos)

Stage and Region	Treatment	n	P9/ES60PAX7-R			P7/ES60PAX7-R		
			$\Delta\Delta C_q$	SD	Fold Change	$\Delta\Delta C_q$	SD	Fold Change
HH stage 17 Midbrain	3x siPAX7-pSilencer1.0; run 1	8	1.17	0.352	0.444	0.74	0.633	0.600
	3x siPAX7-pSilencer1.0; run 2	15	-0.16	0.446	1.117	-0.09	0.205	1.065
	siPAX7-pSilencer1.0	13	-0.50	0.146	1.415	-0.09	0.227	1.064
	sPAX7-pMES	15	0.15	0.156	0.900	0.27	0.196	0.830
	IPAX7-pMES	16	-1.47	0.089	2.770	-0.56	0.092	1.478
	enPAX7-pMIW	14	0.21	0.056	0.865	0.22	0.074	0.856
	pCAX	13	-0.05	0.072	1.039	0.00	0.064	0.998
HH stage 14 Midbrain	siPAX7-pSilencer1.0	11	-0.64	0.541	1.563	0.68	1.078	0.625
	sPAX7-pMES	17	4.16	0.180	0.056	2.01	0.059	0.247
HH stage 17 Hind-brain	siPAX7-pSilencer1.0	17	0.57	0.107	0.675	0.20	0.114	0.872
	sPAX7-pMES	11	0.15	0.156	0.900	0.27	0.196	0.830
	IPAX7-pMES	12	1.47	0.066	0.360	-0.37	0.057	1.294
	enPAX7-pMIW	11	1.21	0.104	0.433	1.12	0.095	0.461
HH stage 14 Hind-brain	sPAX7-pMES	12	0.45	0.281	0.732	0.69	0.141	0.620

Table 9-12:  $\Delta\Delta C_q$  values and fold change of PAX7 splice variants, from pooled tissue qPCR, always comparing the side electroporated with a PAX7 construct with the corresponding control sides from the same embryos. (n number of embryos, SD standard deviation of technical replicates)

### 9.2.1.2 AXIN2/CTNNB1 Expression

Stage and Region	Treatment	n	Side	ES60AXIN2		ES60CTNNB1	
				$C_q$	SD	$C_q$	SD
HH stage 17 Midbrain	3x siPAX7-pSilencer1.0; run 1	8	GFP side	19.87	0.088	17.05	0.081
			control side	20.22	0.514	17.02	0.083
	3x siPAX7-pSilencer1.0; run 2	15	GFP side	21.91	0.024	12.53	0.099
			control side	22.92	0.013	12.76	0.033
	siPAX7-pSilencer1.0	13	GFP side	21.34	0.040	15.92	0.082
			control side	20.88	0.031	15.42	0.016
	sPAX7-pMES	15	GFP side	21.43	0.019	19.88	0.017
			control side	20.92	0.007	19.51	0.030
	IPAX7-pMES	16	GFP side	22.88	0.025	15.11	0.342
			control side	23.35	0.066	14.89	0.138
	enPAX7-pMIW	14	GFP side	20.09	0.031	18.97	0.005
			control side	21.88	0.004	20.21	0.016
	pCAX	13	GFP side	21.94	0.020	18.93	0.023
			control side	21.74	0.041	18.72	0.023

HH stage 14 Mid-brain	siPAX7-pSi-lencer1.0	11	GFP side	20.95	0.082	20.89	0.051
			control side	20.92		19.04	1.736
	sPAX7-pMES	17	GFP side	24.93	0.034	23.92	0.015
			control side	23.56	0.090	22.29	0.011
HH stage 17 Hindbrain	siPAX7-pSi-lencer1.0	17	GFP side	22.87	0.040	19.64	0.075
			control side	24.47	0.080	20.91	0.003
	sPAX7-pMES	11	GFP side	26.87	0.028	23.88	0.071
			control side	22.51	0.139	20.03	0.189
	IPAX7-pMES	12	GFP side	23.40	0.045	20.90	0.021
			control side	23.88	0.043	20.66	0.055
enPAX7-pMIW	11	GFP side	25.34	0.039	21.64	0.037	
		control side	24.26	0.062	21.03	0.007	
HH stage 14 Hindbrain	sPAX7-pMES	12	GFP side	24.97	0.028	22.21	0.059
			control side	24.35	0.060	21.95	0.017
HH stage 24 Body	LiCl and NaCl	1	LiCl	21.55	0.041	18.72	0.029
			NaCl	21.69	0.033	18.76	0.027

Table 9-13:  $C_q$  values of *AXIN2* and *CTNNB1* from pooled tissue qPCR. Mean and standard deviation (SD) of technical replicates from  $C_q$  values obtained. The ES60AXIN2 primer detects *AXIN2*, a feedback gene for canonical Wnt signaling, the ES60CTTNB1 primer detects *CTNNB1* ( $\beta$ -catenin), an essential component of Wnt signaling. The side electroporated is labeled as GFP side, the unelectroporated wildtype side is labeled control side. ( $n$ =number of embryos)

Stage and Region	Treatment	n	ES60AXIN2			ES60CTNNB1		
			$\Delta\Delta C_q$	SD	Fold Change	$\Delta\Delta C_q$	SD	Fold Change
HH stage 17 Midbrain	3x siPAX7-pSilencer1.0; run 1	8	0.97	0.588	0.51	1.34	0.295	0.39
	3x siPAX7-pSilencer1.0; run 2	15	-0.62	0.078	1.54	0.16	0.127	0.89
	siPAX7-pSilencer1.0	13	-0.57	0.139	1.49	-0.53	0.154	1.45
	sPAX7-pMES	15	0.43	0.147	0.74	0.30	0.149	0.81
	IPAX7-pMES	16	-0.90	0.107	1.87	-0.22	0.377	1.16
	enPAX7-pMIW	14	-0.21	0.072	1.15	0.35	0.055	0.79
	pCAX	13	0.15	0.054	0.90	0.16	0.044	0.90
HH stage 14 Midbrain	siPAX7-pSilencer1.0	11	-0.27	0.279	1.20	1.55	3.017	0.34
	sPAX7-pMES	17	0.21	0.103	0.86	0.48	0.042	0.72
HH stage 17 Hindbrain	old siPAX7-pSilencer1.0	17	0.24	0.117	0.85	0.57	0.107	0.67
	sPAX7-pMES	11	1.19	0.217	0.44	0.68	0.260	0.62
	IPAX7-pMES	12	-0.56	0.077	1.47	0.18	0.074	0.88
	enPAX7-pMIW	11	0.86	0.088	0.55	0.39	0.061	0.77
HH stage 14 Hindbrain	sPAX7-pMES	12	0.31	0.148	0.81	-0.04	0.146	1.03
HH stage 24 Body	LiCl and NaCl	1	-0.19	0.074	1.140	-0.09	0.065	1.06

Table 9-14:  $\Delta\Delta C_q$  values and fold change of *AXIN2* and *CTNNB1*, from pooled tissue qPCR, always comparing the side electroporated with a PAX7 construct with the corresponding control sides from the same embryos. The body used at HH stage 24 for the LiCl experiment was compared to a same stage body treated with NaCl in equimolar amounts. ( $n$  number of embryos, SD standard deviation of technical replicates)

### 9.2.1.3 CCND1 Expression

Stage and Region	Treatment	n	Side	ES60CCND1	
				C <sub>q</sub>	SD
HH stage 17 Midbrain	3x siPAX7-pSilencer1.0; run 1	8	GFP side	13.14	0.190
			control side	14.32	0.808
	3x siPAX7-pSilencer1.0; run 2	15	GFP side	19.07	0.051
			control side	19.49	0.120
	siPAX7-pSilencer1.0	13	GFP side	15.63	0.060
			control side	15.31	0.041
	sPAX7-pMES	15	GFP side	15.57	0.013
			control side	15.44	0.018
	IPAX7-pMES	16	GFP side	17.77	0.048
			control side	17.98	0.021
	enPAX7-pMIW	14	GFP side	19.04	0.051
			control side	20.49	0.018
	pCAX	13	GFP side	19.53	0.063
			control side	19.44	0.013
HH stage 14 Midbrain	siPAX7-pSilencer1.0	11	GFP side		
			control side		
	sPAX7-pMES	17	GFP side	20.49	0.035
			control side	15.46	0.051
HH stage 17 Hind-brain	siPAX7-pSilencer1.0	17	GFP side	20.40	0.041
			control side	21.91	0.048
	sPAX7-pMES	11	GFP side		
			control side		
	IPAX7-pMES	12	GFP side	21.18	0.021
			control side	20.95	0.015
	enPAX7-pMIW	11	GFP side		
			control side		
HH stage 14 Hind-brain	sPAX7-pMES	12	GFP side	19.56	0.010
			control side	19.26	0.025

Table 9-15: **C<sub>q</sub> values of CCND1 from pooled tissue qPCR.** Mean and standard deviation (SD) of technical replicates from C<sub>q</sub> values obtained. CCND1 is a gene promoting the S phase of the cell cycle and a marker for proliferation. The side electroporated is labeled as GFP side, the unelectroporated wildtype side is labeled control side. (n=number of embryos)

Stage and Region	Treatment	n	ES60CCND1		
			$\Delta\Delta C_q$	SD	Fold Change
HH stage 17 Midbrain	3x siPAX7-pSilencer1.0; run 1	8	1.34	0.295	0.39
	3x siPAX7-pSilencer1.0; run 2	15	-0.03	0.150	1.02
	siPAX7-pSilencer1.0	13	-0.72	0.149	1.65
	sPAX7-pMES	15	0.06	0.147	0.96
	IPAX7-pMES	16	-0.64	0.096	1.56
	enPAX7-pMIW	14	0.13	0.105	0.91
	pCAX	13	0.05	0.070	0.97

HH stage 14 Midbrain	siPAX7-pSilencer1.0	11			
	sPAX7-pMES	17	3.88	0.072	0.07
HH stage 17 Hind- brain	siPAX7-pSilencer1.0	17	0.33	0.099	0.80
	sPAX7-pMES	11			
	IPAX7-pMES	12	0.17	0.052	0.89
	enPAX7-pMIW	11			
HH stage 14 Hind- brain	sPAX7-pMES	12	0.00	0.135	1.00

Table 9-16:  $\Delta\Delta C_q$  values and fold change of *CCND1*, from pooled tissue qPCR, always comparing the side electroporated with a PAX7 construct with the corresponding control sides from the same embryos. (n number of embryos, SD standard deviation of technical replicates).

#### 9.2.1.4 Overview Pooled Brain Tissue qPCR

HH stage & Tissue	Sample	n	Short PAX7 SV	Long PAX7 SV	AXIN2	CTNNB1	CCND1	
Midbrain HH stage 17	NC	13	-	-	-	-	-	
	Short PAX7 SV	15	(↓)	-	↓	↓	-	
	Long PAX7 SV	16	↑	↑	↑	(↑)	↑	
	PAX7 knock- down	Batch 1	8	(↓)	↓	↓	↓	↓
		Batch 2	15	-	-	↑	-	-
		Batch 3	13	-	↓	↑	↑	↑
	PAX7/EN1	14	(↓)	-	(↑)	↓	-	
Midbrain HH stage 14	PAX7 knock- down		-	-	-	-	x	
	Short PAX7 SV		↓	↓	-	↓	↓↓↓	
Hindbrain HH stage 17	PAX7 knock- down		(↓)	↓	(↓)	↓		
	Short PAX7 SV		(↓)	(↓)	↓	(↓)	↓	
	Long PAX7 SV		↑	↓	↑	-	(↓)	
	PAX7/EN1		↓	↓	↓	↓		
Hind- brain HH stage 14	Short PAX7 SV		(↓)	-	-	-	-	

Table 9-17: **Overview of Expression Changes detected in qPCR in pooled brain tissue.** Expression changes overall were minor. Not all samples tested showed the expected change in PAX7 expression. Gene expression for other genes varied. Overall, it seems like the pro-transcriptional activity of PAX7 is required for canonical Wnt signaling. ↑ increased expression, ↓ decreased expression, - expression unchanged. Brackets indicate weak changes compared to high standard deviations, rendering observed expression changes unreliable.

## 9.2.2 qPCR from Midbrain Tissue of Single Embryos

### 9.2.2.1 Sample Concentration Pre-Testing

Sample	ES603'GAPDH	
	Mean	SD
No template control	33.54	0.91
13.01.22 pCAX dmb ctrl	14.64	0.09
20.07.21 enPAX7 dmb ctrl	15.21	0.08
siPAX7 2 ctrl	14.84	0.05
siPAX7 3 gfp	14.83	0.15
siPAX7 4 ctrl	14.77	0.05
siPAX7 4 gfp	14.53	0.05
siPAX7 6 ctrl	34.58*	0.30
siPAX7 6 gfp	33.52*	0.93
siPAX7 7 gfp	16.82	0.04
siPAX7 8 gfp	14.85	0.02
siPAX7 8 ctrl	15.06	0.03
siPAX7 9 gfp	14.27	0.06
siPAX7 11 gfp	14.51	0.07
siPAX7 12 gfp	15.71	0.03
siPAX7 15 ctrl	15.36	0.17
siPAX7 15 gfp	17.77	0.04
GFP 3 ctrl	16.03	0.04
GFP 3 gfp	18.39	0.04
GFP 4 gfp	17.32	0.07
GFP 5 gfp	14.72	0.06
GFP 9 ctrl	16.86	0.09
GFP 10 ctrl	14.17	0.07
GFP 10 gfp	14.67	0.05
GFP 12 ctrl	16.48	0.08
GFP 13 gfp	14.99	0.04
GFP 14 ctrl	14.94	0.06
GFP 16 ctrl	14.20	0.05
GFP 17 ctrl	15.01	0.01
GFP 20gfp	13.98	0.02
GFP 21 ctrl	14.03	0.06
GFP 21gfp	14.06	0.06

Table 9-18: **cDNA quantity comparable in most samples intended for final Biomark qPCR.** qPCR using cDNA isolated from individual dorsal midbrain halves. ES603'GAPDH primers were used. Samples marked with an **asterisk** did not contain cDNA, as  $C_q$ -values equal the no template control.

### 9.2.2.2 $C_q$ -Values from Single Midbrain Tissue qPCR

Tissue isolated from individual midbrain had its gene expression of multiple genes tested using qPCR on the Biomark system. The  $C_q$ -value averages of the individual triplicates can be found in the following tables, alongside their standard deviations. Samples from a control group, electroporated with the only GFP expressing pCAX vector were compared to a group with a PAX7 knock-down using the siPAX7-pSilencer1.0 vector designed by Li. A no template control and a control with tissue, but without reverse transcriptase were carried along.

	Sample	ES60 ACTB			Sample	ES60 ACTB	
		Average	SD			Average	SD
Dilution Series for Efficiency Testing	1G pure	4.64	0.298	PAX7 knock-down Group (siPAX7-pSilencer1.0 transfected)	1G	10.31	0.248
	1G 1:5	10.30	0.077		1C	8.85	0.156
	1G 1:25	11.53	0.176		2G	9.05	0.223
	1G 1:125	12.21	0.114		2C	9.57	0.128
	1G 1:625	14.01	0.082		3G	9.28	0.183
	1G 1:3125	14.78	0.099		3C	9.52	0.073
Control Group (pCAX transfected)	1G	10.24	0.119		4G	9.04	0.048
	1C	9.13	0.026		4C	9.17	0.145
	2G	9.80	0.059		5G	10.76	0.133
	2C	10.75	0.155		5C	10.32	0.082
	3G	13.35	0.205		6G	22.79	1.703
	3C	12.40	0.228		6C	21.83	1.021
	4G	11.31	0.054		7G	11.65	0.177
	4C	13.62	0.183		7C	10.86	0.200
	5G	8.61	0.120		8G	8.69	0.157
	5C	8.58	0.057		8C	9.11	0.170
	6G	10.62	0.058		9G	8.61	0.111
	6C	10.56	0.099		9C	8.73	0.152
	7G	10.18	0.109		10G	10.29	0.058
	7C	8.67	0.073		10C	9.29	0.008
	8G	12.68	0.158		11G	8.05	0.123
	8C	12.93	0.238		11C	10.20	0.052
	9G	11.43	0.021		12G	10.03	0.159
	9C	12.58	0.090		12C	9.54	0.067
	10G	9.51	0.139	13G	10.26	0.152	
	10C	8.15	0.170	13C	9.96	0.090	
	12G	8.96	0.144	14G	9.35	0.087	
	12C	6.31	0.093	14C	10.86	0.085	
	13G	9.07	0.096	15G	12.56	0.094	
	13C	8.41	0.068	15C	11.80	0.072	
14G	10.46	0.081	16G	8.36	0.079		
14C	9.36	0.068	16C	8.94	0.172		
15G	8.54	0.168	17G	9.32	0.044		
15C	8.85	0.207	17C	9.45	0.131		
16G	7.99	0.150	18G	10.75	0.055		
16C	8.84	0.173	18C	10.85	0.132		
17G	11.13	0.122	19G	11.42	0.100		
17C	10.62	0.155	19C	10.10	0.186		
18G	6.92	0.126	20G	9.95	0.029		
18C	673.88	563.124	20C	9.47	0.059		
19G	7.47	0.078	21G	10.91	0.086		
19C	7.75	0.103	21C	9.59	0.087		
20G	7.77	0.112	22G	13.08	0.273		
20C	7.99	0.034	22C	13.08	0.031		
21G	7.62	0.078	23G	13.22	0.069		
21C	8.00	0.103	23C	18.90	0.354		
Controls	no Template	999.00	0.000	24G	16.41	0.306	
	no RT	348.88	563.021	24C	11.83	0.065	

Table 9-19: qPCR results from single midbrain tissue for ACTB expression. This genes expression was used as a reference gene. Failed amplifications were encoded as 999 cycles, so all three-digit values were excluded from analysis. Samples with G are from transfected, samples with C from the untransfected brain sides.

	Sample	ES60 3'GAPDH			Sample	ES60 3'GAPDH	
		Average	SD			Average	SD
Dilution Series for Efficiency Testing	1G pure	4.26	0.046	PAX7 knock-down Group (siPAX7-pSilencer1.0 transfected)	1G	7.56	0.089
	1G 1:5	8.09	0.033		1C	6.94	0.036
	1G 1:25	9.71	0.102		2G	7.54	0.083
	1G 1:125	10.27	0.064		2C	7.74	0.090
	1G 1:625	12.11	0.052		3G	7.56	0.044
	1G 1:3125	12.67	0.080		3C	7.27	0.051
Control Group (pCAX transfected)	1G	8.44	0.038		4G	7.52	0.147
	1C	7.26	0.074		4C	7.55	0.069
	2G	7.91	0.095		5G	8.96	0.101
	2C	7.94	0.032		5C	8.80	0.063
	3G	11.42	0.109		6G	22.16	0.253
	3C	9.88	0.026		6C	999.00	0.000
	4G	9.79	0.046		7G	9.22	0.055
	4C	11.97	0.094		7C	8.77	0.079
	5G	7.26	0.118		8G	7.24	0.106
	5C	7.69	0.039		8C	7.62	0.064
	6G	9.23	0.166		9G	7.08	0.131
	6C	8.61	0.034		9C	7.26	0.051
	7G	8.84	0.074		10G	9.05	0.085
	7C	7.22	0.094		10C	7.35	0.065
	8G	9.93	0.048		11G	7.20	0.071
	8C	10.38	0.051		11C	8.27	0.048
	9G	9.77	0.070		12G	8.81	0.052
	9C	10.03	0.060		12C	7.57	0.030
	10G	7.03	0.028	13G	7.92	0.090	
	10C	6.76	0.108	13C	7.89	0.055	
	12G	7.96	0.037	14G	7.86	0.033	
	12C	5.83	0.059	14C	8.83	0.091	
	13G	7.78	0.023	15G	10.09	0.011	
	13C	7.20	0.038	15C	9.68	0.052	
14G	8.93	0.044	16G	7.21	0.056		
14C	7.51	0.091	16C	7.42	0.013		
15G	7.12	0.056	17G	7.70	0.043		
15C	7.45	0.097	17C	8.31	0.132		
16G	7.08	0.048	18G	8.80	0.124		
16C	7.14	0.024	18C	8.62	0.071		
17G	8.18	0.045	19G	8.67	0.058		
17C	7.87	0.016	19C	7.73	0.006		
18G	6.22	0.096	20G	7.89	0.078		
18C	999.00	0.000	20C	7.15	0.048		
19G	6.55	0.036	21G	8.99	0.014		
19C	6.44	0.185	21C	7.49	0.047		
20G	6.46	0.061	22G	8.93	0.090		
20C	6.78	0.083	22C	9.14	0.025		
21G	6.69	0.061	23G	11.53	0.096		
21C	6.97	0.029	23C	16.58	0.160		
Controls	no Template	999.00	0.000	24G	15.63	0.088	
	no RT	673.27	564.188	24C	9.56	0.096	

Table 9-20: qPCR results from single midbrain tissue for the expression of the 3'-domain of GAPDH. This expression was used as a reference gene and for RIN measurement. Failed amplifications were encoded as 999 cycles, so all three-digit values were excluded from analysis. Samples with G are from transfected, samples with C from the untransfected brain sides.

	Sample	ES60 5'GAPDH			Sample	ES60 5'GAPDH	
		Average	SD			Average	SD
Dilution Series for Efficiency Testing	1G pure	4.96	0.063	PAX7 knock-down Group (siPAX7-pSilencer1.0 transfected)	1G	7.90	0.127
	1G 1:5	8.51	0.070		1C	7.24	0.216
	1G 1:25	10.01	0.041		2G	7.64	0.113
	1G 1:125	10.55	0.099		2C	7.91	0.097
	1G 1:625	12.49	0.105		3G	7.63	0.084
	1G 1:3125	13.07	0.113		3C	7.56	0.037
Control Group (pCAX transfected)	1G	8.72	0.130		4G	7.78	0.138
	1C	7.09	0.164		4C	7.59	0.157
	2G	7.76	0.139		5G	9.42	0.089
	2C	8.15	0.098		5C	8.77	0.123
	3G	11.76	0.147		6G	999.00	0.000
	3C	9.81	0.068		6C	999.00	0.000
	4G	9.48	0.102		7G	9.48	0.074
	4C	12.85	0.325		7C	8.88	0.194
	5G	7.20	0.198		8G	7.69	0.027
	5C	7.40	0.046		8C	7.85	0.108
	6G	9.35	0.197		9G	7.46	0.230
	6C	8.84	0.127		9C	7.46	0.116
	7G	8.84	0.171		10G	9.30	0.271
	7C	7.15	0.096		10C	7.65	0.211
	8G	10.01	0.224		11G	6.94	0.060
	8C	10.71	0.181		11C	9.28	0.200
	9G	10.09	0.128		12G	8.93	0.169
	9C	10.41	0.111		12C	7.35	0.115
	10G	7.29	0.097	13G	7.96	0.089	
	10C	6.45	0.019	13C	8.38	0.045	
	12G	7.97	0.229	14G	8.09	0.053	
	12C	5.50	0.125	14C	9.58	0.043	
	13G	7.81	0.062	15G	11.21	0.180	
	13C	7.11	0.137	15C	10.87	0.129	
	14G	9.47	0.070	16G	7.31	0.147	
	14C	7.60	0.070	16C	7.83	0.091	
	15G	7.06	0.058	17G	8.15	0.142	
	15C	7.45	0.190	17C	8.52	0.123	
	16G	7.00	0.045	18G	9.48	0.212	
	16C	7.09	0.138	18C	9.29	0.213	
17G	8.18	0.174	19G	9.59	0.178		
17C	7.98	0.075	19C	8.30	0.120		
18G	5.86	0.119	20G	8.30	0.111		
18C	350.27	561.815	20C	7.68	0.120		
19G	6.20	0.106	21G	9.76	0.072		
19C	6.28	0.144	21C	7.63	0.023		
20G	6.35	0.040	22G	10.17	0.161		
20C	6.57	0.200	22C	10.38	0.129		
21G	6.37	0.110	23G	12.84	0.159		
21C	6.65	0.275	23C	17.88	0.196		
Controls	no Template	999.00	0.000	24G	18.16	0.147	
	no RT	999.00	0.000	24C	11.73	0.128	

Table 9-21: qPCR results from single midbrain tissue for the expression of the 5'-domain of GAPDH. This expression was used as a reference gene and for RIN measurement. Failed amplifications were encoded as 999 cycles, so all three-digit values were excluded from analysis. Samples with G are from transfected, samples with C from the untransfected brain sides.

	Sample	ES60 YWATZ			Sample	ES60 YWATZ	
		Average	SD			Average	SD
Dilution Series for Efficiency Testing	1G pure	10.11	0.011	PAX7 knock-down Group (siPAX7-pSilencer1.0 transfected)	1G	14.30	0.206
	1G 1:5	14.07	0.226		1C	13.40	0.202
	1G 1:25	15.50	0.372		2G	13.91	0.145
	1G 1:125	16.09	0.224		2C	14.40	0.092
	1G 1:625	18.12	0.294		3G	14.18	0.097
	1G 1:3125	19.25	0.220		3C	14.11	0.139
Control Group (pCAX transfected)	1G	14.22	0.219		4G	14.03	0.159
	1C	13.19	0.322		4C	13.86	0.170
	2G	14.54	0.210		5G	15.76	0.186
	2C	15.25	0.167		5C	15.54	0.191
	3G	17.44	0.403		6G	999.00	0.000
	3C	16.43	0.031		6C	674.46	562.116
	4G	16.23	0.116		7G	16.02	0.399
	4C	18.58	0.056		7C	15.77	0.107
	5G	13.50	0.236		8G	13.60	0.216
	5C	13.51	0.086		8C	14.16	0.151
	6G	16.45	0.225		9G	14.28	0.180
	6C	15.74	0.262		9C	13.67	0.233
	7G	14.92	0.254		10G	15.21	0.151
	7C	13.62	0.318		10C	14.49	0.254
	8G	16.97	0.226		11G	12.87	0.213
	8C	17.39	0.244		11C	15.56	0.111
	9G	16.92	0.162		12G	15.16	0.300
	9C	17.64	0.224		12C	14.58	0.111
	10G	13.79	0.311	13G	14.57	0.173	
	10C	12.84	0.183	13C	14.50	0.259	
	12G	14.15	0.227	14G	14.68	0.211	
	12C	11.74	0.205	14C	15.94	0.274	
	13G	13.84	0.131	15G	18.13	0.381	
	13C	13.74	0.286	15C	17.31	0.248	
14G	15.31	0.088	16G	13.45	0.228		
14C	14.62	0.284	16C	13.77	0.112		
15G	13.49	0.212	17G	14.69	0.130		
15C	14.20	0.109	17C	14.36	0.292		
16G	13.09	0.247	18G	15.57	0.131		
16C	13.76	0.087	18C	15.31	0.349		
17G	17.45	0.055	19G	15.74	0.292		
17C	17.39	0.327	19C	14.55	0.266		
18G	12.21	0.179	20G	14.20	0.090		
18C	999.00	0.000	20C	13.38	0.155		
19G	12.77	0.170	21G	15.67	0.216		
19C	13.18	0.075	21C	14.59	0.075		
20G	13.01	0.165	22G	18.69	0.192		
20C	13.17	0.169	22C	18.30	0.586		
21G	12.82	0.255	23G	17.39	0.553		
21C	13.11	0.242	23C	21.57	0.482		
Controls	no Template	348.40	563.437	24G	19.99	0.280	
	no RT	999.00	0.000	24C	16.10	0.128	

Table 9-22: qPCR results from single midbrain tissue for the YWATZ expression. This genes expression was used as a reference gene. Failed amplifications were encoded as 999 cycles, so all three-digit values were excluded from analysis. Samples with G are from transfected, samples with C from the untransfected brain sides.

	Sample	ES60 ATP5B			Sample	ES60 ATP5B	
		Average	SD			Average	SD
Dilution Series for Efficiency Testing	1G pure	7.36	0.059	PAX7 knock-down Group (siPAX7-pSilencer1.0 transfected)	1G	11.93	0.124
	1G 1:5	12.47	0.209		1C	10.93	0.142
	1G 1:25	13.74	0.089		2G	10.92	0.107
	1G 1:125	14.29	0.105		2C	11.31	0.055
	1G 1:625	16.15	0.065		3G	10.70	0.061
	1G 1:3125	17.17	0.311		3C	10.64	0.098
Control Group (pCAX transfected)	1G	12.50	0.070		4G	10.71	0.020
	1C	11.55	0.111		4C	11.06	0.043
	2G	12.49	0.148		5G	12.17	0.076
	2C	13.05	0.081		5C	11.93	0.148
	3G	15.32	0.202		6G	23.91	1.374
	3C	14.04	0.188		6C	21.04	0.320
	4G	14.23	0.098		7G	13.32	0.091
	4C	15.60	0.314		7C	12.51	0.218
	5G	10.74	0.088		8G	10.97	0.069
	5C	11.03	0.107		8C	11.18	0.122
	6G	12.35	0.117		9G	10.23	0.086
	6C	11.96	0.088		9C	10.16	0.067
	7G	12.30	0.053		10G	12.57	0.174
	7C	11.00	0.054		10C	11.22	0.117
	8G	13.68	0.194		11G	10.33	0.040
	8C	13.48	0.161		11C	11.26	0.153
	9G	12.52	0.159		12G	12.21	0.118
	9C	13.80	0.084		12C	11.73	0.068
	10G	11.45	0.143	13G	12.43	0.118	
	10C	10.79	0.049	13C	11.94	0.030	
	12G	11.06	0.162	14G	11.63	0.075	
	12C	8.99	0.058	14C	12.69	0.110	
	13G	10.63	0.110	15G	14.24	0.156	
	13C	10.08	0.171	15C	13.49	0.080	
14G	12.14	0.050	16G	10.79	0.075		
14C	10.94	0.093	16C	10.86	0.056		
15G	10.31	0.178	17G	11.26	0.027		
15C	10.66	0.121	17C	11.80	0.092		
16G	10.03	0.042	18G	12.35	0.118		
16C	11.10	0.147	18C	12.88	0.137		
17G	13.27	0.221	19G	13.51	0.177		
17C	13.17	0.200	19C	12.35	0.144		
18G	9.73	0.048	20G	12.11	0.205		
18C	23.57	0.770	20C	11.26	0.093		
19G	9.58	0.059	21G	12.96	0.076		
19C	9.44	0.080	21C	12.11	0.117		
20G	9.98	0.030	22G	13.90	0.155		
20C	10.03	0.071	22C	13.76	0.065		
21G	9.90	0.074	23G	14.83	0.085		
21C	10.24	0.142	23C	21.51	0.701		
Controls	no Template	24.04	1.147	24G	17.94	0.250	
	no RT	22.93	2.056	24C	13.58	0.063	

Table 9-23: qPCR results from single midbrain tissue for the ATP5b expression. This genes expression was used as a reference gene. Failed amplifications were encoded as 999 cycles, so all three-digit values were excluded from analysis. Samples with G are from transfected, samples with C from the untransfected brain sides.

Sample	ES60 HMBS
--------	-----------

Sample	ES60 HMBS
--------	-----------

		Average	SD			Average	SD
Dilution Series for Efficiency Testing	1G pure	11.85	0.078	PAX7 knock-down Group (siPAX7-pSilencer1.0 transfected)	1G	14.49	0.090
	1G 1:5	15.24	0.118		1C	14.30	0.199
	1G 1:25	16.79	0.183		2G	14.79	0.331
	1G 1:125	17.29	0.246		2C	15.12	0.144
	1G 1:625	18.91	0.343		3G	15.09	0.164
	1G 1:3125	20.25	0.383		3C	15.04	0.063
Control Group (pCAX transfected)	1G	15.57	0.196		4G	14.64	0.192
	1C	14.26	0.095		4C	14.92	0.146
	2G	15.81	0.067		5G	16.35	0.287
	2C	16.49	0.248		5C	16.52	0.101
	3G	18.34	0.199		6G	22.62	0.438
	3C	16.99	0.060		6C	20.81	0.210
	4G	15.91	0.166		7G	15.93	0.091
	4C	19.27	0.579		7C	15.67	0.184
	5G	14.48	0.110		8G	14.73	0.076
	5C	14.28	0.125		8C	14.93	0.254
	6G	16.49	0.243		9G	14.71	0.224
	6C	16.06	0.354		9C	14.61	0.029
	7G	15.67	0.403		10G	16.10	0.310
	7C	14.74	0.224		10C	15.13	0.175
	8G	17.93	0.537		11G	14.03	0.182
	8C	18.29	0.359		11C	15.06	0.109
	9G	16.45	0.061		12G	15.49	0.430
	9C	17.61	0.063		12C	14.91	0.131
	10G	14.46	0.221		13G	15.39	0.081
	10C	13.78	0.143		13C	15.19	0.197
	12G	14.82	0.258		14G	15.20	0.195
	12C	12.77	0.162		14C	16.10	0.212
	13G	14.59	0.256		15G	18.43	0.305
	13C	14.28	0.050		15C	17.64	0.550
	14G	16.08	0.162		16G	14.27	0.061
	14C	15.13	0.203		16C	14.44	0.078
	15G	14.26	0.252		17G	15.71	0.184
	15C	14.59	0.209		17C	15.41	0.144
	16G	13.94	0.130		18G	16.08	0.251
	16C	14.16	0.081		18C	16.15	0.027
17G	17.25	0.227	19G		16.35	0.146	
17C	16.86	0.161	19C		15.23	0.276	
18G	13.01	0.152	20G		15.18	0.160	
18C	23.41	0.933	20C		14.52	0.078	
19G	13.54	0.161	21G		16.38	0.196	
19C	13.85	0.140	21C		15.66	0.096	
20G	13.63	0.083	22G		18.27	0.059	
20C	14.12	0.232	22C		17.86	0.170	
21G	13.51	0.188	23G		18.22	0.171	
21C	13.73	0.093	23C		22.56	1.172	
Controls	no Template	23.99	0.958		24G	20.12	0.230
	no RT	23.48	1.484		24C	17.57	0.170

Table 9-24: **qPCR results from single midbrain tissue for HMBS expression.** This genes expression was used as a reference gene. Failed amplifications were encoded as 999 cycles, so all three-digit values were excluded from analysis. Samples with G are from transfected, samples with C from the untransfected brain sides.

Sample	ES60 AXIN2	
	Average	SD

Sample	ES60 AXIN2	
	Average	SD

Dilution Series for Efficiency Testing	1G pure	10.18	0.068	PAX7 knock-down Group (siPAX7-pSilencer1.0 transfected)	1G	14.39	0.117
	1G 1:5	14.44	0.154		1C	13.55	0.095
	1G 1:25	16.22	0.132		2G	14.17	0.108
	1G 1:125	16.84	0.170		2C	14.51	0.103
	1G 1:625	19.21	0.344		3G	14.58	0.056
	1G 1:3125	19.30	0.200		3C	14.32	0.113
	Control Group (pCAX transfected)	1G	14.74		0.092	4G	14.12
1C		13.41	0.067		4C	14.33	0.066
2G		15.29	0.066		5G	15.96	0.071
2C		15.18	0.039		5C	15.68	0.127
3G		17.52	0.164		6G	999.00	0.000
3C		15.71	0.098		6C	999.00	0.000
4G		15.78	0.120		7G	15.49	0.046
4C		17.25	0.266		7C	14.26	0.023
5G		14.22	0.040		8G	14.06	0.114
5C		14.63	0.073		8C	14.04	0.028
6G		16.18	0.128		9G	13.99	0.083
6C		15.82	0.113		9C	13.98	0.093
7G		15.45	0.200		10G	15.45	0.089
7C		14.26	0.049		10C	14.74	0.174
8G		16.70	0.399		11G	13.95	0.077
8C		17.53	0.241		11C	15.17	0.158
9G		15.88	0.013		12G	15.30	0.222
9C		16.57	0.114		12C	14.59	0.039
10G		14.12	0.029		13G	15.14	0.065
10C		13.70	0.046		13C	14.74	0.174
12G		14.55	0.051		14G	14.48	0.015
12C	12.21	0.097	14C		15.26	0.075	
13G	14.05	0.091	15G	17.22	0.112		
13C	14.11	0.085	15C	17.08	0.100		
14G	14.61	0.084	16G	13.47	0.044		
14C	14.76	0.047	16C	13.91	0.093		
15G	13.33	0.081	17G	14.55	0.074		
15C	14.24	0.080	17C	14.73	0.121		
16G	13.39	0.132	18G	15.45	0.085		
16C	13.58	0.049	18C	15.14	0.019		
17G	14.31	0.080	19G	15.01	0.109		
17C	14.11	0.141	19C	14.49	0.023		
18G	12.53	0.016	20G	14.48	0.072		
18C	999.00	0.000	20C	13.57	0.029		
19G	12.88	0.112	21G	15.37	0.131		
19C	13.10	0.070	21C	14.75	0.038		
20G	12.99	0.057	22G	17.16	0.454		
20C	13.41	0.029	22C	17.80	0.221		
21G	12.99	0.019	23G	17.61	0.107		
21C	13.26	0.074	23C	22.92	1.572		
Controls	no Template	999.00	0.000	24G	21.65	1.968	
	no RT	999.00	0.000	24C	15.86	0.113	

Table 9-25: **qPCR results from single midbrain tissue for AXIN2 expression.** This genes expression was used to detect canonical Wnt signaling. Failed amplifications were encoded as 999 cycles, so all three-digit values were excluded from analysis. Samples with G are from transfected, samples with C from the untransfected brain sides.

	Sample	ES60 WNT1			Sample	ES60 WNT1	
		Average	SD			Average	SD
Dilution Series for Efficiency Testing	1G pure	19.88	0.548	PAX7 knock-down Group (siPAX7-pSilencer1.0 transfected)	1G	25.50	0.684
	1G 1:5	349.18	562.764		1C	22.30	0.535
	1G 1:25	24.83	1.113		2G	24.11	0.509
	1G 1:125	674.49	562.063		2C	22.72	1.179
	1G 1:625	674.58	561.914		3G	21.02	0.141
	1G 1:3125	999.00	0.000		3C	21.50	0.641
Control Group (pCAX transfected)	1G	25.48	0.215		4G	21.97	0.331
	1C	21.19	0.714		4C	22.36	0.135
	2G	23.72	0.367		5G	21.10	0.243
	2C	23.55	1.271		5C	22.91	1.179
	3G	348.77	563.121		6G	999.00	0.000
	3C	25.16	1.503		6C	999.00	0.000
	4G	24.04	2.585		7G	23.96	1.437
	4C	999.00	0.000		7C	20.97	0.932
	5G	21.00	0.537		8G	21.97	0.825
	5C	22.79	1.356		8C	20.77	0.440
	6G	22.91	0.923		9G	20.96	0.162
	6C	21.57	0.368		9C	22.21	0.923
	7G	23.76	0.899		10G	23.08	0.670
	7C	21.47	0.824		10C	25.19	1.311
	8G	350.38	561.724		11G	21.57	0.683
	8C	24.71	0.693		11C	23.32	1.170
	9G	21.31	0.244		12G	21.19	0.339
	9C	674.60	561.886		12C	21.88	0.977
	10G	21.96	0.448	13G	349.12	562.812	
	10C	21.03	0.742	13C	22.97	1.023	
	12G	21.89	0.579	14G	22.85	0.371	
	12C	18.67	0.229	14C	26.06	2.542	
	13G	20.30	0.194	15G	23.75	0.715	
	13C	22.09	0.772	15C	24.15	1.698	
14G	22.26	0.500	16G	21.03	0.864		
14C	25.06	0.845	16C	23.49	2.891		
15G	19.27	0.074	17G	21.69	0.838		
15C	23.37	1.568	17C	22.83	1.642		
16G	20.51	0.281	18G	348.41	563.429		
16C	20.89	0.599	18C	22.92	0.753		
17G	348.78	563.107	19G	350.13	561.939		
17C	21.22	0.499	19C	23.10	1.474		
18G	19.73	0.348	20G	23.82	0.912		
18C	999.00	0.000	20C	21.65	0.358		
19G	19.34	0.319	21G	24.75	1.725		
19C	20.74	0.700	21C	22.26	0.651		
20G	20.73	0.128	22G	675.16	560.914		
20C	20.33	0.551	22C	25.93	2.306		
21G	19.44	0.473	23G	999.00	0.000		
21C	20.91	0.785	23C	999.00	0.000		
Controls	no Template	999.00	0.000	24G	674.42	562.191	
	no RT	999.00	0.000	24C	675.56	560.223	

Table 9-26: qPCR results from single midbrain tissue for WNT1 expression. This gene is part of the Wnt signaling pathway. Failed amplifications were encoded as 999 cycles, so all three-digit values were excluded from analysis. Samples with G are from transfected, samples with C from the untransfected brain sides.

	Sample	ES60 WNT3A			Sample	ES60 WNT3A	
		Average	SD			Average	SD
Dilution Series for Efficiency Testing	1G pure	674.45	562.144	PAX7 knock-down Group (siPAX7-pSilencer1.0 transfected)	1G	674.25	562.488
	1G 1:5	674.98	561.223		1C	673.15	564.391
	1G 1:25	349.46	562.521		2G	674.55	561.966
	1G 1:125	675.66	560.048		2C	349.95	562.096
	1G 1:625	999.00	0.000		3G	350.28	561.809
	1G 1:3125	999.00	0.000		3C	999.00	0.000
Control Group (pCAX transfected)	1G	999.00	0.000		4G	675.43	560.435
	1C	350.53	561.595		4C	999.00	0.000
	2G	674.96	561.253		5G	999.00	0.000
	2C	675.16	560.915		5C	999.00	0.000
	3G	674.40	562.218		6G	999.00	0.000
	3C	674.05	562.822		6C	999.00	0.000
	4G	999.00	0.000		7G	350.46	561.652
	4C	999.00	0.000		7C	350.98	561.205
	5G	674.89	561.368		8G	674.56	561.940
	5C	348.93	562.981		8C	673.62	563.579
	6G	999.00	0.000		9G	350.55	561.572
	6C	349.10	562.834		9C	674.12	562.716
	7G	674.91	561.339		10G	675.22	560.798
	7C	349.53	562.461		10C	674.18	562.606
	8G	999.00	0.000		11G	999.00	0.000
	8C	999.00	0.000		11C	999.00	0.000
	9G	999.00	0.000		12G	675.23	560.780
	9C	999.00	0.000		12C	351.67	560.605
	10G	350.49	561.625	13G	675.18	560.874	
	10C	350.73	561.416	13C	675.52	560.281	
	12G	675.19	560.855	14G	26.68	2.156	
	12C	349.71	562.304	14C	999.00	0.000	
	13G	351.80	560.493	15G	999.00	0.000	
	13C	674.16	562.643	15C	999.00	0.000	
14G	999.00	0.000	16G	25.59	3.222		
14C	674.96	561.252	16C	25.41	2.897		
15G	349.77	562.246	17G	673.68	563.465		
15C	350.17	561.900	17C	351.28	560.941		
16G	349.20	562.746	18G	674.18	562.597		
16C	348.30	563.521	18C	999.00	0.000		
17G	673.46	563.847	19G	674.69	561.723		
17C	27.01	1.234	19C	25.98	2.292		
18G	24.13	2.229	20G	674.15	562.651		
18C	999.00	0.000	20C	999.00	0.000		
19G	22.41	0.227	21G	999.00	0.000		
19C	23.94	0.467	21C	348.85	563.049		
20G	23.17	1.626	22G	24.39	1.432		
20C	673.05	564.566	22C	349.42	562.559		
21G	23.51	1.793	23G	999.00	0.000		
21C	25.95	2.171	23C	999.00	0.000		
Controls	no Template	999.00	0.000	24G	674.17	562.615	
	no RT	999.00	0.000	24C	999.00	0.000	

Table 9-27: qPCR results from single midbrain tissue for WNT3a expression. This gene is part of the Wnt signaling pathway, but it was excluded from the analysis as too many amplifications failed due to low expression. Samples with G are from transfected, samples with C from the untransfected brain sides.

	Sample	ES60 WNT4			Sample	ES60 WNT4	
		Average	SD			Average	SD
Dilution Series for Efficiency Testing	1G pure	9.89	0.036	PAX7 knock-down Group (siPAX7-pSilencer1.0 transfected)	1G	15.99	0.336
	1G 1:5	16.07	0.129		1C	13.51	0.094
	1G 1:25	16.12	0.088		2G	13.07	0.225
	1G 1:125	17.13	0.162		2C	13.52	0.054
	1G 1:625	18.68	0.450		3G	12.87	0.072
	1G 1:3125	21.32	0.463		3C	13.10	0.126
Control Group (pCAX transfected)	1G	15.62	0.177		4G	13.07	0.045
	1C	14.43	0.150		4C	13.43	0.097
	2G	15.20	0.008		5G	13.87	0.096
	2C	16.11	0.175		5C	13.22	0.049
	3G	17.69	0.091		6G	999.00	0.000
	3C	15.88	0.197		6C	999.00	0.000
	4G	18.30	0.514		7G	18.24	0.475
	4C	18.66	0.456		7C	15.01	0.130
	5G	13.02	0.032		8G	12.13	0.061
	5C	13.69	0.071		8C	12.43	0.064
	6G	14.50	0.040		9G	11.74	0.092
	6C	14.35	0.216		9C	12.29	0.131
	7G	13.71	0.024		10G	12.90	0.096
	7C	12.36	0.041		10C	12.65	0.052
	8G	15.37	0.180		11G	11.85	0.078
	8C	15.63	0.207		11C	13.28	0.175
	9G	14.58	0.006		12G	14.23	0.186
	9C	16.58	0.179		12C	14.14	0.128
	10G	15.51	0.125	13G	16.66	0.228	
	10C	12.59	0.044	13C	14.05	0.055	
	12G	12.22	0.042	14G	13.28	0.094	
	12C	11.49	0.106	14C	14.84	0.139	
	13G	12.54	0.027	15G	16.03	0.163	
	13C	11.83	0.113	15C	16.65	0.118	
14G	15.20	0.157	16G	12.18	0.057		
14C	15.15	0.085	16C	12.80	0.050		
15G	13.26	0.140	17G	13.08	0.075		
15C	14.26	0.252	17C	13.37	0.061		
16G	14.72	0.303	18G	14.39	0.142		
16C	15.42	0.231	18C	15.34	0.064		
17G	16.15	0.193	19G	18.21	0.359		
17C	14.53	0.147	19C	16.99	0.250		
18G	12.29	0.028	20G	16.41	0.055		
18C	999.00	0.000	20C	14.59	0.053		
19G	12.25	0.040	21G	14.38	0.075		
19C	11.70	0.079	21C	13.59	0.034		
20G	11.46	0.043	22G	17.01	0.046		
20C	11.74	0.096	22C	16.70	0.087		
21G	11.37	0.052	23G	17.88	0.088		
21C	11.74	0.070	23C	347.93	563.847		
Controls	no Template	675.23	560.779	24G	22.12	1.480	
	no RT	999.00	0.000	24C	16.20	0.034	

Table 9-28: qPCR results from single midbrain tissue for WNT4 expression. This gene is part of the Wnt signaling pathway. Failed amplifications were encoded as 999 cycles, so all three-digit values were excluded from analysis. Samples with G are from transfected, samples with C from the untransfected brain sides.

	Sample	ES60 LEF1			Sample	ES60 LEF1	
		Average	SD			Average	SD
Dilution Series for Efficiency Testing	1G pure	10.61	0.095	PAX7 knock-down Group (siPAX7-pSilencer1.0 transfected)	1G	14.51	0.137
	1G 1:5	14.51	0.122		1C	13.86	0.147
	1G 1:25	16.00	0.091		2G	13.95	0.050
	1G 1:125	16.70	0.027		2C	14.45	0.085
	1G 1:625	18.41	0.140		3G	14.44	0.129
	1G 1:3125	19.15	0.220		3C	14.58	0.167
Control Group (pCAX transfected)	1G	14.98	0.154		4G	14.48	0.137
	1C	13.51	0.157		4C	14.22	0.112
	2G	14.91	0.096		5G	16.77	0.227
	2C	16.08	0.142		5C	16.26	0.276
	3G	18.56	0.421		6G	999.00	0.000
	3C	16.74	0.084		6C	999.00	0.000
	4G	16.32	0.220		7G	15.88	0.081
	4C	19.55	0.597		7C	15.83	0.132
	5G	13.66	0.156		8G	14.12	0.123
	5C	13.77	0.115		8C	14.37	0.108
	6G	15.88	0.173		9G	14.22	0.066
	6C	15.48	0.097		9C	14.03	0.087
	7G	15.15	0.320		10G	16.05	0.157
	7C	13.82	0.049		10C	14.83	0.014
	8G	18.83	0.301		11G	13.28	0.086
	8C	18.78	0.276		11C	15.44	0.222
	9G	15.81	0.042		12G	15.39	0.138
	9C	16.78	0.127		12C	14.31	0.231
	10G	13.91	0.101	13G	14.75	0.205	
	10C	13.23	0.098	13C	14.67	0.040	
	12G	14.04	0.154	14G	14.63	0.083	
	12C	11.90	0.055	14C	16.18	0.326	
	13G	14.05	0.114	15G	20.73	0.360	
	13C	13.67	0.020	15C	18.61	0.097	
14G	15.67	0.136	16G	13.56	0.008		
14C	14.96	0.132	16C	14.00	0.060		
15G	14.03	0.069	17G	14.93	0.195		
15C	14.16	0.062	17C	14.63	0.135		
16G	13.41	0.169	18G	15.85	0.266		
16C	13.67	0.102	18C	16.06	0.069		
17G	16.63	0.165	19G	15.65	0.088		
17C	17.44	0.109	19C	14.75	0.099		
18G	12.20	0.087	20G	14.32	0.066		
18C	999.00	0.000	20C	13.93	0.080		
19G	12.63	0.141	21G	15.93	0.116		
19C	12.93	0.060	21C	14.96	0.173		
20G	12.98	0.032	22G	18.32	0.201		
20C	13.27	0.088	22C	18.53	0.188		
21G	12.95	0.155	23G	17.64	0.047		
21C	13.33	0.126	23C	999.00	0.000		
Controls	no Template	999.00	0.000	24G	22.50	1.103	
	no RT	999.00	0.000	24C	17.42	0.084	

Table 9-29: qPCR results from single midbrain tissue for LEF1 expression. This gene is part of the Wnt signaling pathway. Failed amplifications were encoded as 999 cycles, so all three-digit values were excluded from analysis. Samples with G are from transfected, samples with C from the untransfected brain sides.

	Sample	ES60 CTNNB1			Sample	ES60 CTNNB1	
		Average	SD			Average	SD
Dilution Series for Efficiency Testing	1G pure	7.77	0.048	PAX7 knock-down Group (siPAX7-pSilencer1.0 transfected)	1G	11.28	0.103
	1G 1:5	11.98	0.029		1C	10.44	0.106
	1G 1:25	13.50	0.058		2G	11.04	0.054
	1G 1:125	14.11	0.189		2C	11.53	0.066
	1G 1:625	15.95	0.179		3G	11.72	0.029
	1G 1:3125	16.49	0.104		3C	11.75	0.078
Control Group (pCAX transfected)	1G	12.37	0.038		4G	11.54	0.105
	1C	10.70	0.114		4C	11.45	0.030
	2G	12.11	0.070		5G	13.54	0.043
	2C	12.58	0.084		5C	12.90	0.059
	3G	15.85	0.232		6G	999.00	0.000
	3C	13.73	0.095		6C	999.00	0.000
	4G	13.75	0.046		7G	13.34	0.198
	4C	16.51	0.341		7C	12.29	0.103
	5G	10.35	0.040		8G	11.82	0.054
	5C	10.88	0.074		8C	11.58	0.170
	6G	13.77	0.057		9G	11.67	0.147
	6C	13.29	0.104		9C	11.32	0.028
	7G	12.45	0.087		10G	13.35	0.197
	7C	11.00	0.065		10C	12.01	0.030
	8G	14.31	0.203		11G	10.73	0.030
	8C	14.84	0.100		11C	12.64	0.155
	9G	13.92	0.152		12G	12.59	0.136
	9C	14.26	0.079		12C	11.34	0.099
	10G	10.85	0.060		13G	11.75	0.156
	10C	10.25	0.119		13C	11.63	0.068
	12G	11.75	0.061		14G	12.12	0.044
	12C	8.91	0.038		14C	12.88	0.031
	13G	11.19	0.109		15G	16.14	0.073
	13C	11.15	0.007		15C	15.49	0.240
	14G	12.26	0.079	16G	11.16	0.050	
	14C	11.02	0.090	16C	11.40	0.059	
	15G	10.33	0.029	17G	12.05	0.079	
	15C	10.92	0.075	17C	12.14	0.044	
	16G	9.87	0.040	18G	13.40	0.130	
	16C	9.90	0.120	18C	13.19	0.163	
17G	13.00	0.082	19G	12.76	0.053		
17C	13.07	0.082	19C	12.01	0.098		
18G	9.38	0.120	20G	11.75	0.027		
18C	999.00	0.000	20C	10.47	0.064		
19G	9.73	0.131	21G	13.70	0.047		
19C	9.90	0.035	21C	12.36	0.036		
20G	10.33	0.054	22G	15.44	0.116		
20C	10.43	0.058	22C	15.11	0.169		
21G	9.88	0.065	23G	16.20	0.086		
21C	10.20	0.051	23C	21.22	0.594		
Controls	no Template	999.00	0.000	24G	19.76	0.124	
	no RT	999.00	0.000	24C	14.66	0.050	

Table 9-30: qPCR results from single midbrain tissue for CTNNB1 expression. This gene is part of the Wnt signaling pathway. Failed amplifications were encoded as 999 cycles, so all three-digit values were excluded from analysis. Samples with G are from transfected, samples with C from the untransfected brain sides.

	Sample	60 FZD1			Sample	60 FZD1	
		Average	SD			Average	SD
Dilution Series for Efficiency Testing	1G pure	9.28	0.051	PAX7 knock-down Group (siPAX7-pSilencer1.0 transfected)	1G	13.13	0.055
	1G 1:5	13.49	0.058		1C	12.48	0.050
	1G 1:25	14.89	0.051		2G	13.09	0.113
	1G 1:125	15.65	0.051		2C	13.59	0.049
	1G 1:625	17.70	0.135		3G	13.27	0.103
	1G 1:3125	18.25	0.291		3C	13.41	0.020
Control Group (pCAX transfected)	1G	13.70	0.053		4G	13.17	0.033
	1C	12.75	0.064		4C	12.87	0.104
	2G	13.61	0.046		5G	15.03	0.084
	2C	14.22	0.111		5C	14.31	0.049
	3G	16.02	0.196		6G	999.00	0.000
	3C	15.18	0.199		6C	999.00	0.000
	4G	15.06	0.097		7G	15.02	0.219
	4C	17.81	0.222		7C	14.92	0.084
	5G	12.55	0.036		8G	13.59	0.067
	5C	12.47	0.051		8C	13.99	0.091
	6G	14.69	0.185		9G	13.56	0.119
	6C	14.19	0.083		9C	13.60	0.061
	7G	14.37	0.080		10G	15.11	0.220
	7C	12.92	0.040		10C	13.72	0.086
	8G	15.61	0.176		11G	12.32	0.099
	8C	15.77	0.059		11C	14.52	0.205
	9G	15.42	0.069		12G	14.33	0.052
	9C	15.81	0.101		12C	13.12	0.057
	10G	12.94	0.162	13G	13.19	0.155	
	10C	11.97	0.046	13C	14.06	0.097	
	12G	13.36	0.030	14G	13.94	0.052	
	12C	11.06	0.078	14C	15.47	0.084	
	13G	13.64	0.152	15G	16.99	0.264	
	13C	12.84	0.085	15C	16.74	0.199	
14G	15.21	0.048	16G	12.65	0.042		
14C	13.27	0.079	16C	13.12	0.138		
15G	13.25	0.089	17G	14.34	0.076		
15C	12.86	0.004	17C	14.19	0.047		
16G	12.48	0.011	18G	15.28	0.249		
16C	12.86	0.032	18C	14.79	0.044		
17G	14.83	0.039	19G	15.30	0.111		
17C	14.71	0.158	19C	13.81	0.052		
18G	11.70	0.103	20G	13.79	0.118		
18C	999.00	0.000	20C	13.45	0.070		
19G	11.80	0.089	21G	15.84	0.117		
19C	12.08	0.022	21C	14.00	0.081		
20G	12.35	0.060	22G	16.31	0.138		
20C	12.35	0.126	22C	16.08	0.142		
21G	12.56	0.050	23G	17.63	0.126		
21C	12.42	0.106	23C	22.95	0.842		
Controls	no Template	999.00	0.000	24G	20.27	0.563	
	no RT	21.73	0.952	24C	15.16	0.131	

Table 9-31: qPCR results from single midbrain tissue for FZD1 expression. This gene is part of the Wnt signaling pathway. Failed amplifications were encoded as 999 cycles, so all three-digit values were excluded from analysis. Samples with G are from transfected, samples with C from the untransfected brain sides.

	Sample	60 FZD5			Sample	60 FZD5	
		Average	SD			Average	SD
Dilution Series for Efficiency Testing	1G pure	13.42	0.091	PAX7 knock-down Group (siPAX7-pSilencer1.0 transfected)	1G	23.22	2.216
	1G 1:5	16.87	0.184		1C	23.36	1.532
	1G 1:25	18.81	0.285		2G	21.85	0.279
	1G 1:125	18.72	0.095		2C	22.07	0.553
	1G 1:625	20.87	0.114		3G	21.64	0.818
	1G 1:3125	21.06	0.352		3C	22.33	1.326
Control Group (pCAX transfected)	1G	16.86	0.289		4G	22.18	1.286
	1C	21.00	0.948		4C	25.83	4.077
	2G	17.53	0.320		5G	22.93	1.358
	2C	27.42	0.338		5C	23.53	2.496
	3G	24.61	0.743		6G	25.77	1.630
	3C	20.28	0.267		6C	24.45	0.665
	4G	22.99	0.737		7G	20.99	1.490
	4C	22.40	2.037		7C	24.83	0.895
	5G	18.90	0.142		8G	18.53	0.303
	5C	20.20	0.594		8C	23.51	2.082
	6G	20.53	0.383		9G	15.80	0.131
	6C	21.37	0.402		9C	23.27	3.726
	7G	19.06	0.782		10G	24.24	0.204
	7C	20.02	0.897		10C	18.21	0.288
	8G	23.51	0.891		11G	21.06	1.077
	8C	24.07	2.881		11C	17.42	0.293
	9G	22.33	1.525		12G	24.23	1.370
	9C	21.11	0.631		12C	23.52	3.303
	10G	22.50	1.443	13G	23.52	1.438	
	10C	19.41	0.786	13C	23.31	1.082	
	12G	19.41	0.784	14G	22.19	0.963	
	12C	16.75	0.243	14C	21.50	0.666	
	13G	22.76	0.635	15G	24.10	0.429	
	13C	16.85	0.290	15C	23.57	1.960	
14G	23.33	2.027	16G	22.14	0.842		
14C	16.93	0.312	16C	16.84	0.121		
15G	20.82	0.763	17G	18.71	0.092		
15C	20.35	0.392	17C	348.01	563.776		
16G	20.25	0.461	18G	20.21	0.443		
16C	18.21	0.222	18C	19.98	0.477		
17G	22.94	0.979	19G	18.27	0.256		
17C	17.78	0.296	19C	17.10	0.175		
18G	18.84	0.954	20G	18.69	0.438		
18C	25.59	2.240	20C	22.79	1.048		
19G	18.71	0.565	21G	22.72	0.861		
19C	15.83	0.197	21C	21.83	1.458		
20G	16.69	0.109	22G	16.96	0.025		
20C	16.81	0.070	22C	16.99	0.335		
21G	19.66	0.608	23G	351.97	560.347		
21C	19.74	0.234	23C	999.00	0.000		
Controls	no Template	25.32	1.046	24G	674.88	561.388	
	no RT	21.29	1.138	24C	21.30	0.595	

Table 9-32: qPCR results from single midbrain tissue for FZD5 expression. This gene is part of the Wnt signaling pathway. Failed amplifications were encoded as 999 cycles, so all three-digit values were excluded from analysis. Samples with G are from transfected, samples with C from the untransfected brain sides.

	Sample	60 FZD9			Sample	60 FZD9	
		Average	SD			Average	SD
Dilution Series for Efficiency Testing	1G pure	13.17	0.072	PAX7 knock-down Group (siPAX7-pSilencer1.0 transfected)	1G	19.72	0.046
	1G 1:5	17.66	0.291		1C	18.97	0.380
	1G 1:25	19.00	0.331		2G	19.05	0.287
	1G 1:125	19.53	0.088		2C	19.28	0.120
	1G 1:625	20.97	0.609		3G	18.93	0.115
	1G 1:3125	22.23	0.912		3C	19.64	0.133
Control Group (pCAX transfected)	1G	17.88	0.012		4G	18.75	0.277
	1C	18.42	0.205		4C	19.10	0.224
	2G	17.68	0.218		5G	20.60	0.461
	2C	21.03	0.495		5C	19.90	0.239
	3G	21.99	0.638		6G	999.00	0.000
	3C	20.22	0.333		6C	674.97	561.245
	4G	20.35	0.243		7G	21.88	0.874
	4C	22.42	0.221		7C	20.59	0.150
	5G	18.09	0.180		8G	18.38	0.138
	5C	18.01	0.248		8C	19.24	0.309
	6G	19.79	0.332		9G	16.68	0.137
	6C	19.24	0.306		9C	19.26	0.211
	7G	19.22	0.301		10G	20.43	0.658
	7C	18.56	0.251		10C	18.03	0.142
	8G	21.29	0.277		11G	17.31	0.333
	8C	21.69	0.648		11C	18.35	0.097
	9G	20.35	0.154		12G	19.76	0.154
	9C	20.52	0.522		12C	19.32	0.344
	10G	18.84	0.050	13G	19.45	0.235	
	10C	17.73	0.049	13C	19.66	0.181	
	12G	18.39	0.146	14G	18.89	0.475	
	12C	15.63	0.061	14C	20.79	0.332	
	13G	18.67	0.497	15G	23.54	1.251	
	13C	17.15	0.237	15C	22.43	1.106	
14G	20.99	0.210	16G	17.88	0.155		
14C	17.07	0.185	16C	17.02	0.126		
15G	18.30	0.094	17G	18.67	0.397		
15C	18.73	0.133	17C	19.51	0.427		
16G	18.34	0.082	18G	19.57	0.514		
16C	17.97	0.185	18C	20.15	0.326		
17G	21.30	0.306	19G	19.53	0.620		
17C	18.46	0.173	19C	17.99	0.060		
18G	16.54	0.215	20G	18.91	0.290		
18C	999.00	0.000	20C	19.77	0.291		
19G	16.72	0.105	21G	22.23	0.951		
19C	15.91	0.063	21C	19.90	0.253		
20G	16.21	0.285	22G	18.44	0.172		
20C	16.38	0.151	22C	18.87	0.243		
21G	17.00	0.226	23G	21.21	0.368		
21C	17.40	0.416	23C	999.00	0.000		
Controls	no Template	999.00	0.000	24G	348.97	562.946	
	no RT	22.10	0.433	24C	21.57	0.660	

Table 9-33: qPCR results from single midbrain tissue for FZD9 expression. This gene is part of the Wnt signaling pathway. Failed amplifications were encoded as 999 cycles, so all three-digit values were excluded from analysis. Samples with G are from transfected, samples with C from the untransfected brain sides.

	Sample	60 FZD10			Sample	60 FZD10	
		Average	SD			Average	SD
Dilution Series for Efficiency Testing	1G pure	10.07	0.086	PAX7 knock-down Group (siPAX7-pSilencer1.0 transfected)	1G	13.71	0.175
	1G 1:5	13.62	0.056		1C	12.68	0.103
	1G 1:25	15.04	0.051		2G	13.34	0.074
	1G 1:125	15.77	0.116		2C	13.72	0.072
	1G 1:625	17.79	0.075		3G	13.41	0.076
	1G 1:3125	18.40	0.055		3C	13.66	0.061
Control Group (pCAX transfected)	1G	13.96	0.148		4G	13.49	0.035
	1C	12.56	0.062		4C	13.12	0.055
	2G	13.78	0.061		5G	15.59	0.067
	2C	14.47	0.085		5C	15.04	0.107
	3G	17.22	0.451		6G	351.90	560.402
	3C	14.98	0.072		6C	347.85	563.911
	4G	15.46	0.092		7G	14.80	0.119
	4C	18.52	0.136		7C	13.50	0.039
	5G	12.39	0.108		8G	13.52	0.044
	5C	12.69	0.021		8C	13.39	0.181
	6G	14.97	0.067		9G	13.28	0.021
	6C	14.58	0.063		9C	13.82	0.105
	7G	14.00	0.081		10G	15.25	0.295
	7C	13.02	0.013		10C	14.32	0.007
	8G	15.91	0.072		11G	12.74	0.077
	8C	16.40	0.248		11C	14.62	0.162
	9G	15.67	0.164		12G	14.26	0.044
	9C	16.41	0.062		12C	13.29	0.049
	10G	12.86	0.040	13G	14.00	0.050	
	10C	11.90	0.100	13C	13.81	0.111	
	12G	13.49	0.084	14G	13.71	0.012	
12C	10.73	0.041	14C	15.30	0.149		
13G	13.14	0.081	15G	18.70	0.489		
13C	13.07	0.106	15C	18.22	0.358		
14G	14.12	0.113	16G	12.66	0.023		
14C	13.89	0.057	16C	13.14	0.027		
15G	12.35	0.087	17G	13.88	0.126		
15C	13.19	0.040	17C	13.88	0.166		
16G	12.08	0.053	18G	15.24	0.063		
16C	12.49	0.069	18C	14.68	0.053		
17G	15.85	0.136	19G	14.65	0.149		
17C	15.22	0.130	19C	13.74	0.141		
18G	11.07	0.077	20G	13.65	0.096		
18C	350.27	561.821	20C	13.03	0.037		
19G	11.45	0.047	21G	15.36	0.126		
19C	11.94	0.012	21C	13.99	0.111		
20G	11.92	0.044	22G	16.19	0.069		
20C	12.34	0.083	22C	16.46	0.122		
21G	11.88	0.063	23G	16.72	0.196		
21C	11.94	0.082	23C	20.86	0.385		
Controls	no Template	673.67	563.489	24G	20.38	0.240	
	no RT	20.46	0.887	24C	15.62	0.022	

Table 9-34: qPCR results from single midbrain tissue for FZD10 expression. This gene is part of the Wnt signaling pathway. Failed amplifications were encoded as 999 cycles, so all three-digit values were excluded from analysis. Samples with G are from transfected, samples with C from the untransfected brain sides.

	Sample	P7sPAX7-F/ ES60 PAX7-R			Sample	P7sPAX7-F/ ES60 PAX7-R	
		Average	SD			Average	SD
Dilution Series for Efficiency Testing	1G pure	11.48	0.048	PAX7 knock-down Group (siPAX7-pSilencer1.0 transfected)	1G	14.80	0.128
	1G 1:5	15.85	0.215		1C	14.13	0.219
	1G 1:25	17.43	0.137		2G	14.72	0.132
	1G 1:125	18.28	0.452		2C	15.26	0.011
	1G 1:625	19.94	0.547		3G	15.22	0.251
	1G 1:3125	20.29	0.491		3C	15.04	0.228
Control Group (pCAX transfected)	1G	16.13	0.044		4G	15.44	0.215
	1C	14.21	0.116		4C	15.25	0.248
	2G	15.54	0.225		5G	17.69	0.388
	2C	15.21	0.044		5C	16.41	0.210
	3G	20.39	0.980		6G	674.24	562.495
	3C	16.49	0.124		6C	673.94	563.018
	4G	17.36	0.104		7G	16.71	0.313
	4C	19.91	0.629		7C	14.92	0.168
	5G	13.46	0.056		8G	15.60	0.219
	5C	14.19	0.189		8C	14.53	0.210
	6G	16.29	0.144		9G	15.00	0.015
	6C	15.95	0.161		9C	15.20	0.494
	7G	15.79	0.217		10G	17.70	0.100
	7C	14.22	0.144		10C	16.01	0.053
	8G	17.15	0.039		11G	15.00	0.117
	8C	17.44	0.606		11C	17.09	0.138
	9G	16.62	0.126		12G	15.95	0.043
	9C	17.42	0.357		12C	14.53	0.123
	10G	14.06	0.027	13G	15.60	0.376	
	10C	13.61	0.025	13C	14.65	0.117	
	12G	15.38	0.145	14G	15.10	0.280	
12C	12.45	0.042	14C	15.86	0.235		
13G	14.52	0.128	15G	18.17	0.514		
13C	14.71	0.078	15C	17.52	0.133		
14G	15.28	0.043	16G	14.53	0.139		
14C	14.90	0.101	16C	14.83	0.103		
15G	13.65	0.094	17G	14.91	0.072		
15C	14.30	0.109	17C	15.53	0.167		
16G	13.39	0.151	18G	16.78	0.020		
16C	13.41	0.046	18C	16.64	0.446		
17G	14.91	0.129	19G	16.67	0.331		
17C	14.28	0.123	19C	15.50	0.186		
18G	12.94	0.160	20G	15.25	0.284		
18C	999.00	0.000	20C	14.16	0.115		
19G	13.20	0.146	21G	16.69	0.178		
19C	13.50	0.122	21C	15.54	0.087		
20G	13.21	0.053	22G	18.71	0.192		
20C	13.70	0.176	22C	18.46	0.442		
21G	13.47	0.104	23G	19.01	0.334		
21C	13.58	0.207	23C	347.93	563.847		
Controls	no Template	674.05	562.825	24G	21.08	0.926	
	no RT	999.00	0.000	24C	17.33	0.426	

Table 9-35: qPCR results from single midbrain tissue for short PAX7 splice variant expression. This gene was the primary focus of this study. Failed amplifications were encoded as 999 cycles, so all three-digit values were excluded from analysis. Samples with G are from transfected, samples with C from the untransfected brain sides.

	Sample	P9 IPAX7-F/ ES60 PAX7-R			Sample	P9 IPAX7-F/ ES60 PAX7-R	
		Average	SD			Average	SD
Dilution Series for Efficiency Testing	1G pure	15.92	0.190	PAX7 knock-down Group (siPAX7-pSilencer1.0 transfected)	1G	18.38	0.088
	1G 1:5	19.51	0.481		1C	17.79	0.483
	1G 1:25	21.08	1.171		2G	18.82	0.469
	1G 1:125	22.46	0.715		2C	19.52	0.619
	1G 1:625	350.23	561.852		3G	19.12	0.225
	1G 1:3125	999.00	0.000		3C	18.75	0.275
Control Group (pCAX transfected)	1G	21.11	0.298		4G	19.44	0.253
	1C	18.59	0.153		4C	19.57	0.601
	2G	19.35	0.796		5G	999.00	0.000
	2C	22.58	1.436		5C	21.14	0.981
	3G	348.58	563.283		6G	999.00	0.000
	3C	20.95	0.402		6C	999.00	0.000
	4G	22.29	0.932		7G	20.98	1.257
	4C	674.03	562.872		7C	347.24	564.440
	5G	16.76	0.162		8G	19.87	0.338
	5C	18.10	0.816		8C	19.24	0.265
	6G	19.99	0.543		9G	19.27	0.597
	6C	19.46	0.665		9C	19.82	0.847
	7G	19.63	0.446		10G	350.07	561.989
	7C	18.37	0.659		10C	20.94	0.812
	8G	21.79	0.382		11G	19.46	0.180
	8C	22.08	1.218		11C	21.50	0.332
	9G	21.23	0.725		12G	20.05	0.987
	9C	21.00	0.388		12C	18.20	0.340
	10G	17.56	0.419	13G	19.45	0.198	
	10C	16.97	0.210	13C	18.25	0.473	
	12G	18.50	0.678	14G	18.53	0.443	
12C	16.10	0.190	14C	19.53	0.340		
13G	18.15	0.216	15G	673.29	564.139		
13C	19.42	0.771	15C	21.09	1.238		
14G	19.97	0.410	16G	18.51	0.108		
14C	18.96	0.453	16C	18.56	0.288		
15G	17.45	0.011	17G	19.49	0.538		
15C	17.85	0.503	17C	19.99	0.769		
16G	17.38	0.181	18G	21.09	0.683		
16C	17.39	0.102	18C	20.72	1.099		
17G	18.41	0.183	19G	21.76	0.952		
17C	19.06	0.303	19C	19.60	0.176		
18G	16.36	0.203	20G	19.31	0.177		
18C	999.00	0.000	20C	18.13	0.461		
19G	16.70	0.275	21G	20.55	0.752		
19C	17.26	0.486	21C	20.89	2.130		
20G	16.34	0.273	22G	21.00	1.070		
20C	17.29	0.047	22C	20.14	0.347		
21G	16.73	0.124	23G	21.73	0.607		
21C	17.31	0.057	23C	673.34	564.068		
Controls	no Template	999.00	0.000	24G	22.86	0.674	
	no RT	673.98	562.947	24C	18.96	0.358	

Table 9-36: **qPCR results from single midbrain tissue for long PAX7 splice variant expression.** This gene was the primary focus of this study. Failed amplifications were encoded as 999 cycles, so all three-digit values were excluded from analysis. Samples with G are from transfected, samples with C from the untransfected brain sides.

	Sample	ES60 PAX3-2			Sample	ES60 PAX3-2	
		Average	SD			Average	SD
Dilution Series for Efficiency Testing	1G pure	10.04	0.062	PAX7 knock-down Group (siPAX7-pSilencer1.0 transfected)	1G	13.46	0.102
	1G 1:5	13.55	0.053		1C	12.70	0.120
	1G 1:25	15.07	0.140		2G	12.98	0.094
	1G 1:125	15.62	0.080		2C	13.54	0.090
	1G 1:625	17.58	0.419		3G	13.44	0.076
	1G 1:3125	18.27	0.221		3C	13.34	0.054
Control Group (pCAX transfected)	1G	13.75	0.050		4G	13.78	0.029
	1C	12.15	0.110		4C	13.17	0.031
	2G	13.18	0.073		5G	14.97	0.078
	2C	13.51	0.134		5C	14.74	0.180
	3G	16.16	0.177		6G	23.06	0.528
	3C	14.37	0.082		6C	674.01	562.899
	4G	15.23	0.124		7G	14.18	0.138
	4C	17.59	0.280		7C	13.35	0.044
	5G	11.64	0.065		8G	13.29	0.027
	5C	11.67	0.098		8C	12.95	0.031
	6G	14.86	0.166		9G	13.36	0.161
	6C	14.56	0.076		9C	13.20	0.200
	7G	13.83	0.020		10G	15.68	0.190
	7C	12.79	0.106		10C	14.25	0.105
	8G	14.87	0.134		11G	12.31	0.032
	8C	15.35	0.048		11C	14.47	0.070
	9G	15.26	0.075		12G	13.82	0.229
	9C	15.39	0.049		12C	13.20	0.030
	10G	12.01	0.102		13G	13.60	0.098
	10C	11.63	0.131		13C	13.39	0.094
	12G	13.73	0.093		14G	13.34	0.020
	12C	10.40	0.048		14C	14.40	0.128
	13G	12.76	0.072		15G	16.29	0.156
	13C	12.65	0.048		15C	15.70	0.141
	14G	13.17	0.106	16G	12.49	0.096	
	14C	13.07	0.084	16C	12.91	0.077	
	15G	11.98	0.079	17G	13.97	0.114	
	15C	12.40	0.022	17C	13.58	0.137	
16G	11.29	0.011	18G	15.06	0.147		
16C	11.78	0.023	18C	14.58	0.077		
17G	13.25	0.148	19G	13.92	0.106		
17C	13.05	0.060	19C	13.22	0.061		
18G	10.69	0.061	20G	13.09	0.088		
18C	999.00	0.000	20C	12.51	0.120		
19G	11.17	0.097	21G	14.81	0.147		
19C	11.54	0.056	21C	13.80	0.117		
20G	11.55	0.085	22G	16.54	0.135		
20C	11.98	0.114	22C	16.52	0.049		
21G	11.41	0.059	23G	15.29	0.161		
21C	11.55	0.060	23C	22.24	1.552		
Controls	no Template	673.94	563.028	24G	18.26	0.075	
	no RT	24.26	4.018	24C	15.08	0.192	

Table 9-37: qPCR results from single midbrain tissue for PAX3 expression. This gene is a close relative to PAX7. Failed amplifications were encoded as 999 cycles, so all three-digit values were excluded from analysis. Samples with G are from transfected, samples with C from the untransfected brain sides.

	Sample	ES60 CCND1			Sample	ES60 CCND1	
		Average	SD			Average	SD
Dilution Series for Efficiency Testing	1G pure	7.60	0.031	PAX7 knock-down Group (siPAX7-pSilencer1.0 transfected)	1G	11.21	0.053
	1G 1:5	11.45	0.103		1C	10.54	0.104
	1G 1:25	12.58	0.117		2G	10.46	0.103
	1G 1:125	13.24	0.054		2C	11.01	0.018
	1G 1:625	15.20	0.158		3G	10.60	0.049
	1G 1:3125	15.56	0.117		3C	11.06	0.026
Control Group (pCAX transfected)	1G	11.56	0.085		4G	10.86	0.022
	1C	10.35	0.031		4C	10.75	0.114
	2G	11.88	0.119		5G	12.63	0.006
	2C	12.29	0.088		5C	12.02	0.087
	3G	14.76	0.124		6G	23.93	0.983
	3C	13.06	0.119		6C	25.23	2.206
	4G	13.32	0.078		7G	13.10	0.121
	4C	16.66	0.089		7C	12.91	0.080
	5G	10.53	0.082		8G	10.04	0.061
	5C	10.72	0.014		8C	10.49	0.102
	6G	12.18	0.048		9G	10.05	0.097
	6C	11.98	0.108		9C	10.06	0.089
	7G	11.92	0.035		10G	11.61	0.078
	7C	10.25	0.037		10C	10.58	0.085
	8G	13.42	0.125		11G	9.60	0.017
	8C	14.01	0.103		11C	11.64	0.149
	9G	12.64	0.071		12G	11.65	0.112
	9C	13.34	0.117		12C	10.41	0.061
	10G	10.66	0.048	13G	11.23	0.064	
	10C	9.94	0.083	13C	11.51	0.046	
	12G	10.46	0.095	14G	11.09	0.059	
12C	8.54	0.056	14C	12.65	0.105		
13G	10.22	0.106	15G	14.15	0.143		
13C	9.75	0.118	15C	14.08	0.078		
14G	12.19	0.092	16G	10.03	0.026		
14C	10.69	0.003	16C	10.51	0.020		
15G	9.85	0.040	17G	11.05	0.101		
15C	10.09	0.075	17C	11.06	0.036		
16G	9.93	0.059	18G	11.96	0.077		
16C	10.11	0.061	18C	12.00	0.079		
17G	11.93	0.097	19G	12.72	0.005		
17C	11.87	0.028	19C	11.46	0.174		
18G	8.84	0.070	20G	10.89	0.054		
18C	23.40	0.652	20C	10.47	0.064		
19G	8.70	0.081	21G	12.06	0.048		
19C	8.91	0.021	21C	10.87	0.042		
20G	9.31	0.070	22G	14.33	0.125		
20C	9.40	0.016	22C	14.25	0.185		
21G	8.96	0.118	23G	14.99	0.131		
21C	9.13	0.032	23C	20.47	0.093		
Controls	no Template	348.74	563.143	24G	18.58	0.256	
	no RT	22.71	0.557	24C	13.71	0.033	

Table 9-38: qPCR results from single midbrain tissue for CCND1 expression. This gene is involved in cell cycle regulation. Failed amplifications were encoded as 999 cycles, so all three-digit values were excluded from analysis. Samples with G are from transfected, samples with C from the untransfected brain sides.

	Sample	EGFP			Sample	EGFP	
		Average	SD			Average	SD
Dilution Series for Efficiency Testing	1G pure	17.36	0.182	PAX7 knock-down Group (siPAX7-pSilencer1.0 transfected)	1G	16.62	0.142
	1G 1:5	21.30	0.999		1C	347.76	563.988
	1G 1:25	999.00	0.000		2G	19.21	0.356
	1G 1:125	999.00	0.000		2C	22.62	0.849
	1G 1:625	999.00	0.000		3G	15.72	0.100
	1G 1:3125	673.70	563.434		3C	347.93	563.841
Control Group (pCAX transfected)	1G	21.48	0.320		4G	17.84	0.438
	1C	21.18	0.894		4C	21.02	0.645
	2G	15.68	0.155		5G	14.99	0.135
	2C	674.56	561.947		5C	20.72	1.396
	3G	20.66	0.285		6G	999.00	0.000
	3C	21.86	1.339		6C	999.00	0.000
	4G	19.23	0.881		7G	17.62	0.241
	4C	999.00	0.000		7C	19.61	1.454
	5G	14.73	0.049		8G	18.27	0.501
	5C	999.00	0.000		8C	20.96	1.502
	6G	16.27	0.160		9G	14.35	0.073
	6C	999.00	0.000		9C	347.98	563.798
	7G	16.92	0.460		10G	22.55	0.837
	7C	347.99	563.793		10C	21.62	0.668
	8G	21.12	0.922		11G	15.33	0.139
	8C	349.14	562.791		11C	673.82	563.230
	9G	20.98	0.391		12G	16.13	0.353
	9C	999.00	0.000		12C	347.30	564.389
	10G	20.55	0.271		13G	16.94	0.144
	10C	999.00	0.000		13C	20.72	0.454
	12G	16.65	0.069		14G	14.65	0.129
	12C	18.55	0.362		14C	21.27	0.201
	13G	12.91	0.110		15G	16.67	0.252
	13C	347.89	563.876		15C	347.08	564.577
	14G	999.00	0.000	16G	15.86	0.165	
	14C	349.74	562.279	16C	999.00	0.000	
	15G	999.00	0.000	17G	15.36	0.137	
	15C	999.00	0.000	17C	348.77	563.118	
16G	999.00	0.000	18G	19.49	0.400		
16C	675.22	560.796	18C	675.12	560.972		
17G	15.77	0.071	19G	16.62	0.279		
17C	17.65	0.139	19C	673.21	564.288		
18G	16.09	0.233	20G	14.73	0.071		
18C	999.00	0.000	20C	673.73	563.390		
19G	14.56	0.190	21G	17.03	0.071		
19C	15.20	0.167	21C	19.94	0.153		
20G	14.08	0.086	22G	14.47	0.079		
20C	14.24	0.121	22C	20.72	0.612		
21G	13.19	0.121	23G	20.62	0.609		
21C	19.02	0.637	23C	999.00	0.000		
Controls	no Template	999.00	0.000	24G	673.85	563.180	
	no RT	999.00	0.000	24C	347.60	564.130	

Table 9-39: qPCR results from single midbrain tissue for EGFP expression. This gene was intended as indicator for transfection efficiency but excluded from analysis due to too many transfected samples not showing amplification. Samples with G are from transfected, samples with C from the untransfected brain sides.

	Sample	ES60 HESX1			Sample	ES60 HESX1	
		Average	SD			Average	SD
Dilution Series for Efficiency Testing	1G pure	17.49	0.286	PAX7 knock-down Group (siPAX7-pSilencer1.0 transfected)	1G	19.64	0.966
	1G 1:5	21.51	0.223		1C	19.42	0.114
	1G 1:25	347.61	564.116		2G	20.26	0.542
	1G 1:125	23.37	0.420		2C	20.26	0.112
	1G 1:625	673.35	564.050		3G	20.66	1.256
	1G 1:3125	999.00	0.000		3C	19.13	0.983
Control Group (pCAX transfected)	1G	25.35	4.157		4G	20.00	0.748
	1C	19.21	0.804		4C	20.36	1.565
	2G	20.87	0.476		5G	23.18	4.688
	2C	20.88	1.030		5C	19.47	0.215
	3G	24.75	2.290		6G	999.00	0.000
	3C	22.41	1.718		6C	28.29	0.498
	4G	21.99	1.032		7G	21.84	1.694
	4C	22.93	2.964		7C	22.52	0.513
	5G	20.59	1.226		8G	22.18	1.509
	5C	20.26	1.145		8C	19.83	0.930
	6G	22.88	1.062		9G	20.73	1.542
	6C	20.80	1.018		9C	19.42	0.608
	7G	347.75	564.003		10G	24.52	2.559
	7C	19.81	0.622		10C	20.81	0.421
	8G	21.64	0.993		11G	18.94	0.236
	8C	347.96	563.816		11C	23.48	0.488
	9G	24.74	2.865		12G	22.15	0.730
	9C	347.69	564.047		12C	22.58	1.373
	10G	20.54	0.533	13G	21.73	1.548	
	10C	18.72	0.269	13C	20.56	0.379	
	12G	19.92	0.440	14G	20.35	1.234	
	12C	17.71	0.220	14C	20.44	0.665	
	13G	20.35	0.460	15G	348.05	563.743	
	13C	20.00	0.810	15C	347.71	564.031	
14G	21.49	0.628	16G	19.68	0.980		
14C	20.26	1.272	16C	20.61	0.903		
15G	19.40	0.502	17G	347.41	564.297		
15C	19.80	0.260	17C	21.11	0.776		
16G	19.88	0.525	18G	348.05	563.743		
16C	19.76	0.808	18C	22.79	0.729		
17G	27.82	0.093	19G	347.80	563.953		
17C	348.46	563.389	19C	21.24	0.654		
18G	17.97	0.362	20G	20.48	0.356		
18C	28.21	0.714	20C	20.59	0.518		
19G	18.01	0.335	21G	20.98	0.579		
19C	18.56	0.717	21C	21.89	0.664		
20G	18.92	0.385	22G	673.31	564.106		
20C	19.35	0.090	22C	347.71	564.035		
21G	18.05	0.381	23G	999.00	0.000		
21C	18.27	0.728	23C	999.00	0.000		
Controls	no Template	352.11	560.223	24G	999.00	0.000	
	no RT	351.59	560.678	24C	21.05	0.534	

Table 9-40: qPCR results from single midbrain tissue for HESX1 expression. This gene was excluded from analysis due to too many transfected samples not showing amplification. Samples with G are from transfected, samples with C from the untransfected brain sides.

	Sample	ES60 NOTCH1			Sample	ES60 NOTCH1	
		Average	SD			Average	SD
Dilution Series for Efficiency Testing	1G pure	12.91	0.041	PAX7 knock-down Group (siPAX7-pSilencer1.0 transfected)	1G	14.54	0.181
	1G 1:5	16.40	0.091		1C	14.86	0.123
	1G 1:25	17.58	0.288		2G	15.46	0.166
	1G 1:125	18.14	0.181		2C	15.08	0.170
	1G 1:625	15.79	0.192		3G	14.86	0.110
	1G 1:3125	15.66	0.115		3C	15.24	0.084
Control Group (pCAX transfected)	1G	16.72	0.299		4G	14.69	0.208
	1C	15.15	0.190		4C	14.79	0.034
	2G	16.58	0.012		5G	14.47	0.050
	2C	15.96	0.231		5C	15.05	0.402
	3G	14.45	0.059		6G	14.86	0.260
	3C	16.08	0.123		6C	14.19	0.194
	4G	14.55	0.181		7G	13.01	0.128
	4C	14.28	0.102		7C	14.25	0.126
	5G	15.82	0.093		8G	15.59	0.234
	5C	14.55	0.034		8C	14.88	0.080
	6G	15.10	0.090		9G	17.27	0.242
	6C	14.85	0.148		9C	15.69	0.262
	7G	16.32	0.315		10G	14.22	0.181
	7C	16.09	0.297		10C	15.78	0.135
	8G	14.51	0.138		11G	15.51	0.050
	8C	15.17	0.332		11C	16.33	0.349
	9G	14.25	0.238		12G	14.36	0.405
	9C	15.31	0.242		12C	14.58	0.098
	10G	14.72	0.199	13G	14.63	0.141	
	10C	14.84	0.092	13C	14.44	0.087	
	12G	15.33	0.070	14G	14.41	0.100	
	12C	14.09	0.147	14C	14.36	0.227	
	13G	15.12	0.130	15G	14.29	0.226	
	13C	15.86	0.144	15C	14.49	0.212	
14G	14.67	0.083	16G	14.76	0.176		
14C	16.78	0.280	16C	16.56	0.206		
15G	14.65	0.231	17G	17.20	0.120		
15C	15.05	0.262	17C	15.31	0.213		
16G	14.32	0.098	18G	15.38	0.306		
16C	15.20	0.243	18C	14.95	0.215		
17G	14.46	0.044	19G	15.34	0.156		
17C	16.24	0.067	19C	15.70	0.068		
18G	14.42	0.093	20G	15.32	0.123		
18C	14.14	0.153	20C	16.87	0.102		
19G	14.47	0.096	21G	15.55	0.086		
19C	16.22	0.157	21C	15.43	0.286		
20G	15.56	0.138	22G	17.39	0.543		
20C	16.11	0.014	22C	18.30	0.229		
21G	15.08	0.058	23G	17.14	0.262		
21C	14.88	0.058	23C	18.65	0.188		
Controls	no Template	14.41	0.062	24G	17.10	0.148	
	no RT	15.57	0.216	24C	19.65	0.440	

Table 9-41: qPCR results from single midbrain tissue for NOTCH1 expression. Failed amplifications were encoded as 999 cycles, so all three-digit values were excluded from analysis. Samples with G are from transfected, samples with C from the untransfected brain sides.

	Sample	ES60 HES1			Sample	ES60 HES1	
		Average	SD			Average	SD
Dilution Series for Efficiency Testing	1G pure	13.06	0.072	PAX7 knock-down Group (siPAX7-pSilencer1.0 transfected)	1G	17.48	0.036
	1G 1:5	17.08	0.281		1C	16.54	0.116
	1G 1:25	18.59	0.356		2G	16.57	0.245
	1G 1:125	19.31	0.189		2C	16.73	0.112
	1G 1:625	20.90	0.725		3G	16.34	0.249
	1G 1:3125	21.90	0.620		3C	16.62	0.166
Control Group (pCAX transfected)	1G	17.39	0.210		4G	17.30	0.133
	1C	16.55	0.012		4C	16.20	0.081
	2G	17.02	0.183		5G	17.95	0.108
	2C	17.80	0.342		5C	17.23	0.055
	3G	18.61	0.302		6G	999.00	0.000
	3C	17.63	0.072		6C	674.83	561.474
	4G	18.52	0.427		7G	18.12	0.622
	4C	24.64	1.299		7C	17.49	0.181
	5G	16.48	0.253		8G	15.62	0.196
	5C	15.26	0.041		8C	16.82	0.230
	6G	17.74	0.392		9G	15.86	0.211
	6C	17.28	0.284		9C	16.07	0.167
	7G	18.00	0.122		10G	16.60	0.143
	7C	16.49	0.139		10C	16.48	0.214
	8G	19.27	0.357		11G	15.67	0.074
	8C	19.26	0.777		11C	18.28	0.069
	9G	17.41	0.036		12G	17.16	0.186
	9C	19.04	0.086		12C	16.38	0.179
	10G	16.11	0.027	13G	16.69	0.220	
	10C	14.86	0.109	13C	17.87	0.461	
	12G	15.23	0.007	14G	15.73	0.142	
	12C	14.00	0.091	14C	17.80	0.132	
	13G	16.46	0.096	15G	19.88	0.374	
	13C	15.50	0.111	15C	19.91	0.781	
14G	17.99	0.433	16G	15.36	0.123		
14C	17.46	0.203	16C	16.74	0.106		
15G	16.48	0.280	17G	17.00	0.465		
15C	16.74	0.215	17C	16.70	0.025		
16G	15.90	0.150	18G	18.70	0.555		
16C	16.63	0.126	18C	17.54	0.236		
17G	15.85	0.128	19G	18.76	0.576		
17C	14.95	0.142	19C	17.02	0.245		
18G	14.64	0.071	20G	16.81	0.200		
18C	999.00	0.000	20C	16.50	0.299		
19G	14.74	0.067	21G	18.03	0.171		
19C	15.16	0.049	21C	16.51	0.291		
20G	14.93	0.071	22G	20.64	0.410		
20C	15.22	0.059	22C	19.81	0.293		
21G	14.67	0.077	23G	20.79	0.999		
21C	14.74	0.085	23C	999.00	0.000		
Controls	no Template	999.00	0.000	24G	999.00	0.000	
	no RT	999.00	0.000	24C	19.67	0.605	

Table 9-42: qPCR results from single midbrain tissue for HES1 expression. This gene belongs to the family of Hes genes. Failed amplifications were encoded as 999 cycles, so all three-digit values were excluded from analysis. Samples with G are from transfected, samples with C from the untransfected brain sides.

	Sample	ES60 HES5A			Sample	ES60 HES5A	
		Average	SD			Average	SD
Dilution Series for Efficiency Testing	1G pure	10.79	0.019	PAX7 knock-down Group (siPAX7-pSilencer1.0 transfected)	1G	14.39	0.064
	1G 1:5	15.29	0.172		1C	13.27	0.091
	1G 1:25	16.95	0.221		2G	13.87	0.062
	1G 1:125	17.56	0.275		2C	14.43	0.104
	1G 1:625	19.59	0.292		3G	14.19	0.061
	1G 1:3125	20.85	1.149		3C	14.51	0.087
Control Group (pCAX transfected)	1G	15.47	0.048		4G	14.58	0.060
	1C	14.21	0.039		4C	14.30	0.098
	2G	14.31	0.050		5G	15.97	0.064
	2C	14.95	0.046		5C	15.59	0.060
	3G	18.79	0.464		6G	26.27	0.302
	3C	16.87	0.167		6C	25.37	0.140
	4G	17.73	0.416		7G	16.67	0.124
	4C	21.47	0.554		7C	14.44	0.083
	5G	11.99	0.046		8G	15.83	0.110
	5C	12.06	0.045		8C	15.51	0.146
	6G	16.44	0.110		9G	15.38	0.144
	6C	15.84	0.339		9C	14.73	0.206
	7G	16.74	0.170		10G	16.48	0.047
	7C	15.39	0.126		10C	15.68	0.108
	8G	16.45	0.051		11G	13.11	0.051
	8C	17.36	0.365		11C	15.94	0.328
	9G	18.06	0.088		12G	15.67	0.133
	9C	18.26	0.292		12C	14.69	0.038
	10G	13.09	0.055	13G	14.58	0.057	
	10C	12.20	0.097	13C	14.80	0.195	
	12G	14.18	0.082	14G	15.78	0.086	
	12C	11.36	0.097	14C	17.34	0.224	
	13G	14.25	0.095	15G	20.80	0.197	
	13C	13.50	0.059	15C	20.09	0.328	
14G	15.13	0.122	16G	13.71	0.101		
14C	13.35	0.065	16C	14.29	0.130		
15G	12.99	0.112	17G	16.03	0.123		
15C	13.53	0.044	17C	15.01	0.106		
16G	11.88	0.019	18G	16.85	0.156		
16C	12.25	0.068	18C	16.84	0.107		
17G	17.47	0.134	19G	15.66	0.135		
17C	17.93	0.287	19C	14.30	0.127		
18G	11.65	0.037	20G	14.20	0.026		
18C	25.77	1.810	20C	13.78	0.051		
19G	11.98	0.026	21G	18.22	0.296		
19C	12.45	0.078	21C	15.56	0.037		
20G	12.72	0.057	22G	18.37	0.045		
20C	12.85	0.038	22C	18.68	0.192		
21G	12.53	0.046	23G	18.26	0.298		
21C	12.44	0.064	23C	999.00	0.000		
Controls	no Template	26.31	0.720	24G	22.54	1.066	
	no RT	27.53	0.489	24C	15.13	0.095	

Table 9-43: qPCR results from single midbrain tissue for HES5a expression. This gene belongs to the family of Hes genes. Failed amplifications were encoded as 999 cycles, so all three-digit values were excluded from analysis. Samples with G are from transfected, samples with C from the untransfected brain sides.

	Sample	ES60 HES5 like			Sample	ES60 HES5 like	
		Average	SD			Average	SD
Dilution Series for Efficiency Testing	1G pure	10.40	0.041		1G	14.11	0.108
	1G 1:5	14.73	0.057		1C	13.19	0.092
	1G 1:25	16.40	0.190		2G	14.17	0.039
	1G 1:125	17.06	0.185		2C	14.75	0.116
	1G 1:625	18.85	0.499		3G	14.38	0.060
	1G 1:3125	19.50	0.149		3C	14.65	0.061
Control Group (pCAX transfected)	1G	15.31	0.097	PAX7 knock-down Group (siPAX7-pSilencer1.0 transfected)	4G	14.60	0.034
	1C	13.92	0.066		4C	14.50	0.104
	2G	15.26	0.038		5G	16.74	0.145
	2C	15.81	0.061		5C	16.40	0.058
	3G	18.26	0.098		6G	999.00	0.000
	3C	16.69	0.133		6C	999.00	0.000
	4G	17.20	0.200		7G	16.81	0.267
	4C	20.54	0.273		7C	15.56	0.081
	5G	12.85	0.028		8G	15.17	0.091
	5C	12.85	0.063		8C	15.13	0.075
	6G	15.89	0.126		9G	14.52	0.054
	6C	15.68	0.068		9C	14.24	0.062
	7G	16.01	0.273		10G	16.10	0.112
	7C	14.39	0.062		10C	14.83	0.026
	8G	16.92	0.264		11G	13.83	0.089
	8C	16.97	0.188		11C	16.10	0.294
	9G	17.72	0.268		12G	15.67	0.251
	9C	17.69	0.107		12C	14.47	0.097
	10G	13.20	0.122		13G	14.34	0.081
	10C	12.72	0.046		13C	14.25	0.162
	12G	14.47	0.068		14G	14.81	0.054
	12C	11.69	0.064		14C	16.07	0.085
	13G	14.26	0.064		15G	19.98	0.648
	13C	13.79	0.105		15C	19.95	0.263
	14G	15.25	0.097		16G	13.93	0.023
	14C	13.79	0.068		16C	14.19	0.100
	15G	13.01	0.078		17G	15.57	0.121
	15C	13.49	0.065		17C	14.98	0.103
	16G	12.62	0.082		18G	16.75	0.188
	16C	12.93	0.100		18C	16.06	0.053
	17G	17.81	0.322		19G	15.68	0.057
	17C	18.41	0.238		19C	14.22	0.042
18G	12.02	0.039	20G	14.36	0.072		
18C	999.00	0.000	20C	13.50	0.066		
19G	12.38	0.061	21G	17.39	0.291		
19C	12.51	0.099	21C	15.59	0.208		
20G	12.87	0.036	22G	17.70	0.186		
20C	12.89	0.089	22C	17.47	0.265		
21G	12.83	0.078	23G	17.50	0.225		
21C	13.00	0.020	23C	23.33	0.776		
Controls	no Template	999.00	0.000	24G	19.58	0.218	
	no RT	675.57	560.197	24C	15.74	0.089	

Table 9-44: qPCR results from single midbrain tissue for HES5-like expression. This gene belongs to the family of Hes genes. Failed amplifications were encoded as 999 cycles, so all three-digit values were excluded from analysis. Samples with G are from transfected, samples with C from the untransfected brain sides.

	Sample	ES60 HES6			Sample	ES60 HES6	
		Average	SD			Average	SD
Dilution Series for Efficiency Testing	1G pure	13.60	0.048		1G	17.65	0.086
	1G 1:5	17.37	0.407		1C	16.78	0.134
	1G 1:25	18.73	0.099		2G	17.88	0.107
	1G 1:125	19.61	0.277		2C	18.25	0.186
	1G 1:625	22.17	1.362		3G	17.10	0.158
	1G 1:3125	22.04	0.781		3C	17.55	0.108
Control Group (pCAX transfected)	1G	17.78	0.412	PAX7 knock-down Group (siPAX7-pSilencer1.0 transfected)	4G	17.67	0.219
	1C	16.73	0.085		4C	17.01	0.124
	2G	16.76	0.219		5G	18.78	0.080
	2C	17.90	0.238		5C	18.69	0.519
	3G	19.08	0.177		6G	999.00	0.000
	3C	18.92	0.217		6C	674.45	562.130
	4G	20.41	0.548		7G	19.49	0.113
	4C	348.32	563.508		7C	19.88	0.457
	5G	16.92	0.265		8G	17.55	0.324
	5C	15.66	0.155		8C	18.30	0.323
	6G	20.32	0.683		9G	18.17	0.207
	6C	19.01	0.305		9C	17.75	0.152
	7G	19.30	0.391		10G	17.42	0.261
	7C	17.85	0.183		10C	16.90	0.063
	8G	18.61	0.218		11G	15.81	0.181
	8C	18.80	0.527		11C	17.89	0.330
	9G	19.99	0.894		12G	18.09	0.171
	9C	21.44	1.002		12C	17.63	0.187
	10G	16.61	0.025		13G	17.06	0.179
	10C	16.02	0.069		13C	18.97	0.134
	12G	18.09	0.348		14G	17.34	0.191
	12C	14.76	0.096		14C	18.75	0.369
	13G	17.11	0.175		15G	19.83	0.331
	13C	16.11	0.159		15C	20.50	0.033
	14G	18.60	0.248		16G	16.04	0.258
	14C	16.85	0.150		16C	16.96	0.021
	15G	16.70	0.237		17G	19.10	0.240
	15C	16.33	0.167		17C	18.64	0.154
	16G	15.56	0.087		18G	20.20	0.480
	16C	15.91	0.140		18C	19.48	0.493
	17G	19.47	0.122		19G	18.83	0.050
	17C	19.41	0.292		19C	17.01	0.086
18G	15.20	0.132	20G	17.73	0.073		
18C	351.97	560.342	20C	17.06	0.284		
19G	15.25	0.159	21G	20.19	0.331		
19C	16.01	0.058	21C	19.11	0.102		
20G	16.22	0.151	22G	19.60	0.568		
20C	16.47	0.097	22C	19.64	0.647		
21G	15.80	0.162	23G	22.79	0.638		
21C	15.64	0.136	23C	999.00	0.000		
Controls	no Template	999.00	0.000	24G	349.07	562.856	
	no RT	675.28	560.703	24C	18.93	0.283	

Table 9-45: qPCR results from single midbrain tissue for HES6 expression. This gene belongs to the family of Hes genes. Failed amplifications were encoded as 999 cycles, so all three-digit values were excluded from analysis. Samples with G are from transfected, samples with C from the untransfected brain sides.

	Sample	ES60 HEY1			Sample	ES60 HEY1	
		Average	SD			Average	SD
Dilution Series for Efficiency Testing	1G pure	11.41	0.004	PAX7 knock-down Group (siPAX7-pSilencer1.0 transfected)	1G	15.08	0.136
	1G 1:5	14.90	0.210		1C	13.99	0.182
	1G 1:25	16.40	0.125		2G	14.50	0.070
	1G 1:125	17.11	0.162		2C	15.09	0.109
	1G 1:625	19.57	0.085		3G	14.77	0.057
	1G 1:3125	19.42	0.439		3C	15.03	0.076
Control Group (pCAX transfected)	1G	15.46	0.080		4G	14.78	0.157
	1C	14.12	0.152		4C	14.79	0.203
	2G	14.48	0.149		5G	15.95	0.066
	2C	15.13	0.131		5C	15.45	0.047
	3G	17.97	0.303		6G	351.01	561.179
	3C	16.49	0.182		6C	351.05	561.142
	4G	16.21	0.195		7G	15.51	0.091
	4C	19.38	0.455		7C	15.24	0.046
	5G	14.22	0.176		8G	14.83	0.100
	5C	14.13	0.046		8C	15.25	0.245
	6G	16.18	0.351		9G	14.50	0.145
	6C	15.28	0.116		9C	14.89	0.174
	7G	16.00	0.115		10G	16.48	0.075
	7C	14.65	0.052		10C	15.03	0.132
	8G	17.04	0.103		11G	13.96	0.071
	8C	17.37	0.478		11C	16.01	0.222
	9G	15.92	0.234		12G	16.05	0.111
	9C	16.93	0.203		12C	14.99	0.127
	10G	14.40	0.036	13G	15.38	0.093	
	10C	13.59	0.131	13C	15.06	0.041	
	12G	15.17	0.130	14G	15.05	0.250	
12C	12.52	0.120	14C	16.20	0.152		
13G	14.81	0.265	15G	17.30	0.511		
13C	14.76	0.132	15C	17.02	0.107		
14G	15.55	0.093	16G	14.29	0.131		
14C	14.83	0.038	16C	14.50	0.111		
15G	13.70	0.040	17G	15.14	0.106		
15C	14.35	0.162	17C	15.27	0.122		
16G	13.33	0.111	18G	16.30	0.104		
16C	13.94	0.106	18C	15.79	0.201		
17G	15.17	0.113	19G	15.78	0.095		
17C	14.76	0.059	19C	14.81	0.072		
18G	13.04	0.127	20G	15.05	0.067		
18C	999.00	0.000	20C	14.37	0.069		
19G	13.11	0.048	21G	16.42	0.246		
19C	13.56	0.040	21C	14.91	0.342		
20G	13.63	0.136	22G	18.69	0.510		
20C	13.79	0.051	22C	19.12	0.190		
21G	13.70	0.155	23G	18.32	0.327		
21C	13.77	0.185	23C	349.59	562.406		
Controls	no Template	674.16	562.647	24G	22.37	0.431	
	no RT	350.82	561.343	24C	17.85	0.235	

Table 9-46: qPCR results from single midbrain tissue for HEY1 expression. This gene belongs to the family of Hes genes. Failed amplifications were encoded as 999 cycles, so all three-digit values were excluded from analysis. Samples with G are from transfected, samples with C from the untransfected brain sides.

	Sample	ES60 CHMP48			Sample	ES60 CHMP48	
		Average	SD			Average	SD
Dilution Series for Efficiency Testing	1G pure	8.91	0.092	PAX7 knock-down Group (siPAX7-pSilencer1.0 transfected)	1G	12.09	0.155
	1G 1:5	12.35	0.080		1C	11.38	0.147
	1G 1:25	13.77	0.094		2G	11.89	0.190
	1G 1:125	14.24	0.189		2C	12.30	0.152
	1G 1:625	16.35	0.140		3G	12.47	0.095
	1G 1:3125	17.05	0.101		3C	12.26	0.130
Control Group (pCAX transfected)	1G	12.68	0.067		4G	12.35	0.022
	1C	11.50	0.063		4C	12.29	0.113
	2G	12.92	0.027		5G	13.89	0.121
	2C	13.24	0.085		5C	13.67	0.123
	3G	15.75	0.242		6G	999.00	0.000
	3C	13.99	0.058		6C	999.00	0.000
	4G	14.46	0.043		7G	14.11	0.181
	4C	16.39	0.304		7C	13.74	0.172
	5G	11.67	0.100		8G	12.08	0.101
	5C	11.88	0.051		8C	12.33	0.091
	6G	13.68	0.121		9G	11.93	0.119
	6C	13.13	0.066		9C	12.01	0.052
	7G	13.10	0.078		10G	13.59	0.185
	7C	11.72	0.085		10C	12.45	0.060
	8G	15.13	0.206		11G	11.66	0.054
	8C	15.01	0.101		11C	12.61	0.109
	9G	13.72	0.050		12G	13.20	0.135
	9C	14.48	0.073		12C	12.24	0.091
	10G	11.64	0.063	13G	12.59	0.048	
	10C	11.24	0.063	13C	12.29	0.042	
	12G	12.36	0.073	14G	12.59	0.035	
12C	10.18	0.057	14C	13.33	0.046		
13G	12.08	0.053	15G	16.22	0.164		
13C	11.72	0.090	15C	15.40	0.195		
14G	13.13	0.136	16G	11.56	0.048		
14C	11.93	0.083	16C	11.75	0.063		
15G	11.56	0.069	17G	12.45	0.096		
15C	11.82	0.099	17C	12.75	0.029		
16G	11.12	0.147	18G	13.51	0.091		
16C	11.28	0.066	18C	13.40	0.053		
17G	14.04	0.132	19G	13.23	0.140		
17C	14.17	0.118	19C	12.42	0.070		
18G	10.57	0.122	20G	12.22	0.064		
18C	348.40	563.438	20C	11.55	0.016		
19G	10.86	0.065	21G	13.57	0.126		
19C	10.87	0.031	21C	12.82	0.035		
20G	11.07	0.049	22G	14.42	0.174		
20C	11.11	0.068	22C	14.34	0.243		
21G	10.80	0.107	23G	16.00	0.205		
21C	11.26	0.063	23C	22.12	0.763		
Controls	no Template	999.00	0.000	24G	19.03	0.297	
	no RT	999.00	0.000	24C	15.23	0.133	

Table 9-47: qPCR results from single midbrain tissue for CHMP48 expression. This gene was a potential off target gene of the PAX7 knock-down. Failed amplifications were encoded as 999 cycles, so all three-digit values were excluded from analysis. Samples with G are from transfected, samples with C from the untransfected brain sides.

	Sample	ES60 ERMN			Sample	ES60 ERMN	
		Average	SD			Average	SD
Dilution Series for Efficiency Testing	1G pure	16.29	0.028	PAX7 knock-down Group (siPAX7-pSilencer1.0 transfected)	1G	19.45	0.440
	1G 1:5	19.47	0.185		1C	19.49	0.241
	1G 1:25	21.43	0.616		2G	19.18	0.718
	1G 1:125	22.00	0.633		2C	20.23	0.446
	1G 1:625	23.78	0.281		3G	19.50	0.544
	1G 1:3125	673.76	563.338		3C	20.24	0.088
Control Group (pCAX transfected)	1G	19.98	0.346		4G	20.13	0.622
	1C	20.01	0.511		4C	19.95	0.394
	2G	19.78	1.023		5G	21.50	1.141
	2C	21.98	0.799		5C	21.98	0.519
	3G	21.78	0.758		6G	26.85	1.967
	3C	21.06	0.795		6C	999.00	0.000
	4G	22.14	0.196		7G	25.37	2.663
	4C	349.79	562.229		7C	22.30	0.112
	5G	19.82	0.453		8G	19.00	0.341
	5C	18.99	0.535		8C	20.40	0.316
	6G	21.75	1.091		9G	18.84	0.343
	6C	21.21	0.616		9C	19.44	0.303
	7G	22.18	0.889		10G	19.41	0.110
	7C	20.33	0.436		10C	19.69	0.205
	8G	350.10	561.970		11G	19.18	0.306
	8C	22.43	0.513		11C	20.09	0.270
	9G	20.98	0.676		12G	20.85	0.599
	9C	23.22	2.108		12C	21.68	0.718
	10G	20.13	0.296	13G	19.51	0.272	
	10C	17.95	0.392	13C	21.54	0.179	
	12G	18.89	0.075	14G	19.89	0.814	
12C	17.54	0.288	14C	21.97	0.509		
13G	21.15	0.732	15G	22.38	0.991		
13C	19.88	0.503	15C	348.45	563.392		
14G	22.06	0.877	16G	19.00	0.295		
14C	19.78	0.166	16C	19.63	0.236		
15G	21.33	0.709	17G	20.92	0.078		
15C	21.41	0.576	17C	21.45	1.494		
16G	21.50	1.302	18G	21.28	0.800		
16C	20.51	0.701	18C	20.75	0.099		
17G	22.86	0.765	19G	21.79	0.170		
17C	21.58	0.585	19C	20.09	0.896		
18G	18.70	0.361	20G	20.87	0.148		
18C	351.16	561.049	20C	21.46	0.423		
19G	18.70	0.288	21G	21.88	0.500		
19C	19.13	0.099	21C	20.16	0.254		
20G	18.52	0.646	22G	22.50	2.048		
20C	18.15	0.151	22C	21.58	0.589		
21G	19.01	0.185	23G	347.54	564.184		
21C	18.06	0.036	23C	999.00	0.000		
Controls	no Template	350.86	561.305	24G	999.00	0.000	
	no RT	351.27	560.953	24C	21.99	0.885	

Table 9-48: qPCR results from single midbrain tissue for ERMN expression. This gene was a potential off target gene of the PAX7 knock-down. Failed amplifications were encoded as 999 cycles, so all three-digit values were excluded from analysis. Samples with G are from transfected, samples with C from the untransfected brain sides.

	Sample	ES60 MAP2			Sample	ES60 MAP2	
		Average	SD			Average	SD
Dilution Series for Efficiency Testing	1G pure	13.31	0.173	PAX7 knock-down Group (siPAX7-pSilencer1.0 transfected)	1G	15.93	0.213
	1G 1:5	16.96	0.025		1C	15.34	0.053
	1G 1:25	18.68	0.053		2G	16.34	0.339
	1G 1:125	18.86	0.083		2C	16.62	0.054
	1G 1:625	20.85	0.596		3G	16.44	0.104
	1G 1:3125	20.51	0.161		3C	16.56	0.064
Control Group (pCAX transfected)	1G	17.29	0.176		4G	16.78	0.182
	1C	15.28	0.062		4C	16.25	0.108
	2G	16.51	0.056		5G	18.40	0.224
	2C	16.47	0.078		5C	17.98	0.151
	3G	18.90	0.255		6G	999.00	0.000
	3C	17.07	0.087		6C	999.00	0.000
	4G	17.88	0.146		7G	18.13	0.356
	4C	20.55	0.430		7C	17.17	0.293
	5G	15.55	0.068		8G	16.28	0.199
	5C	15.52	0.095		8C	16.15	0.227
	6G	17.86	0.107		9G	16.68	0.096
	6C	16.97	0.044		9C	16.64	0.093
	7G	17.17	0.099		10G	18.21	0.220
	7C	16.04	0.148		10C	17.11	0.185
	8G	17.73	0.189		11G	15.69	0.147
	8C	18.08	0.178		11C	18.41	0.254
	9G	17.75	0.127		12G	17.03	0.093
	9C	18.67	0.436		12C	15.78	0.158
	10G	16.02	0.109	13G	16.42	0.201	
	10C	15.11	0.173	13C	16.87	0.052	
	12G	16.67	0.179	14G	16.36	0.196	
	12C	14.20	0.103	14C	17.28	0.204	
	13G	16.37	0.051	15G	19.66	0.303	
	13C	16.48	0.187	15C	18.57	0.212	
	14G	17.03	0.179	16G	15.70	0.076	
	14C	17.06	0.088	16C	16.41	0.028	
	15G	15.49	0.099	17G	17.24	0.254	
	15C	16.32	0.116	17C	16.92	0.021	
	16G	15.56	0.264	18G	18.30	0.087	
	16C	15.67	0.104	18C	17.35	0.044	
17G	17.45	0.131	19G	17.38	0.107		
17C	17.46	0.194	19C	16.35	0.142		
18G	14.34	0.029	20G	16.45	0.140		
18C	999.00	0.000	20C	15.72	0.033		
19G	14.56	0.207	21G	18.30	0.179		
19C	15.04	0.100	21C	16.76	0.123		
20G	15.31	0.205	22G	21.52	0.108		
20C	15.73	0.079	22C	21.15	0.517		
21G	14.79	0.100	23G	20.51	0.374		
21C	14.75	0.142	23C	999.00	0.000		
Controls	no Template	999.00	0.000	24G	22.11	0.500	
	no RT	674.34	562.325	24C	19.47	0.208	

Table 9-49: qPCR results from single midbrain tissue for MAP2 expression. This gene was a potential off target gene of the PAX7 knock-down. Failed amplifications were encoded as 999 cycles, so all three-digit values were excluded from analysis. Samples with G are from transfected, samples with C from the untransfected brain sides.

### 9.2.2.3 Results from Statistical Analysis of all Samples

Tests of Normality				
	Group	Kolmogorov-Smirnov		
		Statistic	n	Sig.
AXIN2	pCAX	.202	16	.082
	siPAX7-pSilencer1.0	.305	14	<.001
WNT4	pCAX	.202	16	.082
	siPAX7-pSilencer1.0	.305	14	<.001
LEF1	pCAX	.231	16	.022
	siPAX7-pSilencer1.0	.143	14	.200*
CTNNB1	pCAX	.154	16	.200*
	siPAX7-pSilencer1.0	.109	14	.200*
FZD1	pCAX	.120	16	.200*
	siPAX7-pSilencer1.0	.167	14	.200*
FZD5	pCAX	.157	16	.200*
	siPAX7-pSilencer1.0	.225	14	.053
FZD9	pCAX	.214	16	.048
	siPAX7-pSilencer1.0	.195	14	.155
FZD10	pCAX	.146	16	.200*
	siPAX7-pSilencer1.0	.122	14	.200*
sPAX7	pCAX	.205	16	.070
	siPAX7-pSilencer1.0	.188	14	.193
IPAX7	pCAX	.160	16	.200*
	siPAX7-pSilencer1.0	.175	14	.200*
PAX3	pCAX	.144	16	.200*
	siPAX7-pSilencer1.0	.130	14	.200*
CCND1	pCAX	.163	16	.200*
	siPAX7-pSilencer1.0	.129	14	.200*
NOTCH1	pCAX	.126	16	.200*
	siPAX7-pSilencer1.0	.190	14	.183
HES1	pCAX	.090	16	.200*
	siPAX7-pSilencer1.0	.112	14	.200*
HES5A	pCAX	.151	16	.200*
	siPAX7-pSilencer1.0	.176	14	.200*
HES5like	pCAX	.184	16	.151
	siPAX7-pSilencer1.0	.122	14	.200*
HES6	pCAX	.110	16	.200*
	siPAX7-pSilencer1.0	.194	14	.162
HEY1	pCAX	.111	16	.200*
	siPAX7-pSilencer1.0	.132	14	.200*
CHMP48	pCAX	.104	16	.200*
	siPAX7-pSilencer1.0	.171	14	.200*
ERMIN	pCAX	.167	16	.200*
	siPAX7-pSilencer1.0	.141	14	.200*
MAP2	pCAX	.116	16	.200*
	siPAX7-pSilencer1.0	.109	14	.200*

Table 9-50: Results from testing of normal distribution of samples with the Kolmogorov-Smirnov test in SPSS. All samples show normal distribution (Sig. >0.05), except for AXIN2, WNT4, LEF1 and FZD9. For these samples Mann-Whitney tests were done, the other genes with normal distribution were tested for significance of changes seen using t-tests. **Asterisk:** This is a lower bound of the true significance.

	Levene's Test for Equality of Variances	
	F	Sig.
AXIN2	0.256	0.616
WNT4	0.256	0.616
LEF1	0.804	0.376
CTNNB1	0.496	0.486
FZD1	0.381	0.541
FZD5	0.11	0.743
FZD9	0.102	0.752
FZD10	0.092	0.763
sPAX7	1.127	0.296
IPAX7	0.276	0.603
PAX3	0.329	0.57
CCND1	0.038	0.847
NOTCH1	0.068	0.795
HES1	0.035	0.854
HES5A	2.07	0.159
HES5like	0.213	0.648
HES6	0.005	0.945
HEY1	1.007	0.323
CHMP48	0.712	0.405
ERMIN	0.271	0.606
MAP2	0.626	0.434

Table 9-51: **Results from Leven's test show equal variances of all genes with normal distribution, if all samples are included in the analysis. This allows for the statistically more powerful use of t-test results for equal variances, as shown in chapter 4.2.4**

#### 9.2.2.4 Results from Statistical Analysis of Samples with Reduced PAX7 Expression

In addition to the analysis of all samples, a statistical analysis of the embryos with a larger than 50% reduction in expression of the short PAX7 splice variant was done. It, like the full analysis did not show any significant expression changes.

Group Statistics					
	Group	N	Mean	Std. Deviation	Std. Error Mean
sPAX7	pCAX	19	0.33	1.440	0.330
	siPAX7-pSilencer1.0	8	1.34	0.275	0.098
IPAX7	pCAX	17	-0.35	0.954	0.232
	siPAX7-pSilencer1.0	5	0.31	1.170	0.523
PAX3	pCAX	19	-0.03	0.461	0.106
	siPAX7-pSilencer1.0	8	-0.05	0.388	0.137
CTNNB1	pCAX	19	0.02	0.326	0.075
	siPAX7-pSilencer1.0	8	0.22	0.363	0.128
FZD1	pCAX	19	0.09	0.336	0.077

	siPAX7-pSilencer1.0	8	0.07	0.346	0.122
FZD5	pCAX	19	0.67	3.647	0.837
	siPAX7-pSilencer1.0	8	-1.36	3.219	1.138
FZD10	pCAX	19	-0.10	0.422	0.097
	siPAX7-pSilencer1.0	8	0.08	0.386	0.136
NOTCH1	pCAX	19	-0.54	1.494	0.343
	siPAX7-pSilencer1.0	8	-1.35	1.162	0.411
HES1	pCAX	19	-0.24	0.997	0.229
	siPAX7-pSilencer1.0	8	-0.19	0.613	0.217
HES5A	pCAX	19	-0.01	0.455	0.104
	siPAX7-pSilencer1.0	8	0.38	0.761	0.269
HES5like	pCAX	19	0.01	0.386	0.088
	siPAX7-pSilencer1.0	8	0.26	0.236	0.083
HES6	pCAX	18	0.09	0.668	0.158
	siPAX7-pSilencer1.0	8	-0.33	0.486	0.172
HEY1	pCAX	19	-0.08	0.296	0.068
	siPAX7-pSilencer1.0	8	-0.02	0.176	0.062
CHMP48	pCAX	19	0.04	0.279	0.064
	siPAX7-pSilencer1.0	8	-0.19	0.244	0.086
ERMIN	pCAX	17	0.15	1.049	0.254
	siPAX7-pSilencer1.0	8	-0.40	1.441	0.510
MAP2	pCAX	19	-0.04	0.491	0.113
	siPAX7-pSilencer1.0	8	0.13	0.256	0.090

Table 9-52: Group statistics from SPSS for single brain tissue samples with normal distribution that showed reduced PAX7 expression. t-tests were performed for these samples.

Ranks				
	Group	N	Mean Rank	Sum of Ranks
AXIN2	pCAX	19	13.68	260
	siPAX7-pSilencer1.0	8	14.75	118
	Total	27		
WNT4	pCAX	19	13.68	260
	siPAX7-pSilencer1.0	8	14.75	118
	Total	27		
LEF1	pCAX	19	14.42	274
	siPAX7-pSilencer1.0	8	13	104
	Total	27		
FZD9	pCAX	19	13.95	265
	siPAX7-pSilencer1.0	8	14.13	113
	Total	27		

Table 9-53: Group statistics from SPSS for single brain tissue samples without normal distribution that showed reduced PAX7 expression. Mann-Whitney-tests were performed for these samples.

Independent Samples Test						
		Levene's Test for Equality of Variances		t-test for Equality of Means		
		F	Sig.	t	Significance	
					One-Sided p	Two-Sided p
sPAX7	Equal variances assumed	4.465	0.045	-1.93	0.033	0.065
	Equal variances not assumed			-2.906	0.004	0.008
IPAX7	Equal variances assumed	0.209	0.652	-1.29	0.106	0.212
	Equal variances not assumed			-1.149	0.148	0.297
PAX3	Equal variances assumed	0.083	0.776	0.129	0.449	0.899
	Equal variances not assumed			0.138	0.446	0.892
CTNNB1	Equal variances assumed	0.23	0.635	-1.378	0.09	0.18
	Equal variances not assumed			-1.317	0.106	0.212
FZD1	Equal variances assumed	0.054	0.819	0.189	0.426	0.852
	Equal variances not assumed			0.187	0.427	0.855
FZD5	Equal variances assumed	0.051	0.824	1.362	0.093	0.185
	Equal variances not assumed			1.436	0.086	0.172
FZD10	Equal variances assumed	0.016	0.9	-1.046	0.153	0.306
	Equal variances not assumed			-1.086	0.148	0.295
NOTCH1	Equal variances assumed	0.736	0.399	1.377	0.09	0.181
	Equal variances not assumed			1.528	0.072	0.145
HES1	Equal variances assumed	0.268	0.609	-0.125	0.451	0.902
	Equal variances not assumed			-0.152	0.441	0.881
HES5A	Equal variances assumed	3.978	0.057	-1.64	0.057	0.114
	Equal variances not assumed			-1.336	0.107	0.214
HES5like	Equal variances assumed	1.052	0.315	-1.693	0.051	0.103
	Equal variances not assumed			-2.055	0.026	0.052
HES6	Equal variances assumed	1.34	0.258	1.616	0.06	0.119
	Equal variances not assumed			1.828	0.042	0.084
HEY1	Equal variances assumed	2.502	0.126	-0.534	0.299	0.598

	Equal variances not assumed			-0.654	0.26	0.52
CHMP48	Equal variances assumed	0.48	0.495	1.969	0.03	0.06
	Equal variances not assumed			2.084	0.027	0.055
ERMIN	Equal variances assumed	0.877	0.359	1.101	0.141	0.282
	Equal variances not assumed			0.98	0.174	0.349
MAP2	Equal variances assumed	2.456	0.13	-0.901	0.188	0.376
	Equal variances not assumed			-1.152	0.131	0.261

Table 9-54: **Results from t-test of single midbrain samples with reduced PAX7 expression.** The Leven's test shows that all genes, except for the short PAX7 splice variant have equal variances. The short PAX7 splice variant is also the only gene showing significant expression changes compared to the control group, which is not surprising as only samples showing a reduced expression of this gene were included in the analysis.

Test Statistics				
	AXIN2	WNT4	LEF1	FZD9
Mann-Whitney U	70	70	68	75
Asymp. Sig. (2-tailed)	0.75	0.75	0.671	0.958
Exact Sig. [2*(1-tailed Sig.)]	0.775	0.775	0.696	0.979

Table 9-55: **Results from Mann-Whitney test of single midbrain samples with reduced PAX7 expression.** None of the genes tested show significant changes in expression.

### 9.3 Protein Expression Analysis

Tissue	Stage	Plasmid	n	Absolute Signal Intensities for Whole Protein Stain				
				GFP Side		Control Side		Reference E6 Mid-brain
				Mean	SD	Mean	SD	
Midbrain	HH stage 17	3x siPAX7-pSilencer1.0	15	71.23	28.418	48.27	11.935	84.20
		siPAX7-pSilencer1.0	13	58.77	26.043	78.20	15.174	38.30
		sPAX7-pMES	15	9.81	8.021	8.14	2.650	78.90
		IPAX7-pMES	16	39.36	22.817	56.47	13.419	67.00
		enPAX7-pMIW	14	37.28	4.380	35.60	4.903	66.50
		pCAX	13					
	HH stage 14	siPAX7-pSilencer1.0	11	16.19	9.943	17.10	1.916	123.00
	sPAX7-pMES	17	22.97	8.165	28.70	0.794	80.40	
Hindbrain	HH stage 17	siPAX7-pSilencer1.0	17	17.55	12.398	7.96	10.033	12.40
		sPAX7-pMES	11	3.01	4.998	6.95	3.956	48.50
		IPAX7-pMES	12	12.25	4.874	9.51	3.957	
		enPAX7-pMIW	11	1.21	7.459	-0.03	5.434	11.30

	HH stage 14	sPAX7-pMES	12	14.42	8.409	12.22	9.619	4.83
Body	HH stage 20	LiCl/NaCl	1	110.02	12.340	112.70	14.240	

Table 9-56: **Intensities of whole protein stain on Western Blots.** Average and standard deviation (SD) from protein triplicates loaded, detected using Revert 700 Whole Protein Stain. The signal intensities are blot specific and can't be compared across blots. 10µl of protein from antibody linearity testing loaded as reference alongside. For the IPAX7-pMES HH stage 17 hindbrain and the whole body blots no E6 midbrain reference sample was loaded